

# **Alkali-Metal-Mediated Cleave and Capture Chemistry**

**Donna Louise Ramsay**

A thesis submitted to the Department of Pure and Applied Chemistry, University  
of Strathclyde, in part fulfilment of the requirements for the degree of Doctor of  
Philosophy

September 2015

This thesis is the result of the author's original research. It has been composed by the author and has not been previously submitted for examination which has led to the award of a degree.

The copyright of this thesis belongs to the author under the terms of the United Kingdom Copyright Acts as qualified by University of Strathclyde Regulation 3.50. Due acknowledgement must always be made of the use of any material contained in, or derived from, this thesis.

Signed:

Date:

*For My Grandparents*

*James, John, Katie and Louise*

## Acknowledgements

---

While there are many people who deserve personal thanks for their contribution to this project, the person who made this PhD possible for me and in fact convinced me to do it in the first place is Prof. Robert Mulvey. Taking me into his small group he supported me from the start, a support that never once dwindled in three and a half years. His never-ending encouragement, especially in times when things weren't going as planned, and his constant availability day or night was invaluable. I thank him for letting me be a part of his group for these few short years and for being such a great boss!

Dr Stuart Robertson played a major role in my PhD study, beginning with the task of training me in the lab, through to performing the X-ray crystallographic analysis for all of my structures on top of many very helpful and productive discussions both in meetings and informal conversations in front of the NMR computer. The other academics in the group, Prof. Eva Hevia and Dr Charlie O'Hara also deserve a massive thank you for their insight and helpful discussions on the work detailed in this thesis.

By far the people that had the biggest influence on my time within the group are the other PhD students and postdocs that worked beside me on a daily basis. With too many to name and at the risk of missing someone, I would like to thank each and every one of them collectively for making the group such an enjoyable place to work, both in the lab and on our unforgettable trips to places like Rothesay. To name a select few: Sarah started the PhD with me and I could not have asked for a better friend to go through the process with - she made writing our first year reports much more enjoyable! Though unfortunately she is not finishing with me, she will continue to be a very special friend and I have lovely memories of our time together in the group. Although I have only known Marina for a few years now, I couldn't imagine not having her in my life! I especially miss not seeing her on a daily basis anymore but know I have made a true friend for life. A special mention should also be given to Sam and Jenni for being such good friends and although I have now left Sam as the sole PhD student of the Mulvey group I have no doubt she will do great! Elaine also needs a special

acknowledgement for her contribution to the aluminium work detailed in Chapter 3. During the PhD I also had the pleasure of mentoring two undergraduate students Gary and Adele, both of whom were incredibly hardworking and a pleasure to work with.

Janie-Anne also deserves a massive thank you for her behind the scenes hard work to ensure the lab ran smoothly on a day to day basis, as well as her never-ending patience in dealing with requests for all sorts from both labs!

Turning away from the university, I would not be where I am today if it wasn't for my mum and dad. They have supported me my whole life in everything I have done and all that I have I owe to them. Though they know nothing about chemistry they have supported me immensely throughout this PhD in a way no one else could, encouraging and reassuring me through every presentation and exam, down to the writing of this thesis. I could not ask for better parents and thank them for being such selfless, loving and caring people.

Last, but by no means least, is my boyfriend Sean. Moving in together shortly after starting our PhDs, he has been incredibly supportive and understanding of the time and effort I have had to put into this project over the past three and a half years. Completing his PhD at the same time, we even managed to survive writing our theses together! He has made this whole process, especially the writing, much easier and always keeps me smiling.

## Abstract

---

Whilst metallation, a fundamental reaction in synthetic chemistry, is well established with mono-metallic organolithium reagents, recently a second generation of bimetallic reagents has been gathering momentum, evading some of the limitations associated with organolithium reagents. This study extends the current research in this area of synergic bimetallic chemistry and reports the synthesis and characterisation of new compounds from reactions of bases with different substrates, as well as detailed studies of the starting reagents.

A new method for synthesising the utility organoamidolithium reagent LiTMP by way of a transmetallation reaction between  $t\text{BuLi}$  and  $\text{Zn}(\text{TMP})_2$  is described. This realised a new crystalline polymorph of LiTMP in the cyclotrimer  $(\text{LiTMP})_3$  **2.1**.

Remarkably an interrogation of the two most popular aluminating reagents “ $\text{LiTMP}\cdot\text{Al}(i\text{Bu})_3$ ” **3.1** and “ $\text{LiTMP}\cdot\text{Al}(\text{TMP})(i\text{Bu})_2$ ” **3.2** established that **3.1** is not a single species as previously reported but in fact a complex mixture of five distinct species all in equilibria with each other. Additionally it was discovered that the modus operandi of both reagents is a two-step lithiation – trans-metal-trapping protocol, and not by direct alumination.

The pharmacologically relevant amine DMPEA was studied with a range of bimetallic base mixtures. Post metallation and subsequent  $\beta$ -elimination the  $\text{NMe}_2$  fragment was captured in three different crystalline compounds:  $[\text{TMEDA}\cdot\text{Na}(\text{TMP})(\text{NMe}_2)\text{Zn}(t\text{Bu})]$  **4.2**,  $[\text{PMDETA}\cdot\text{Li}(\text{NMe}_2)\text{Zn}(t\text{Bu})_2]$  **4.3** and  $[\text{THF}\cdot\text{Li}(\text{TMP})(\text{NMe}_2)\text{Al}(i\text{Bu})_2]$  **4.4**. The first crystal structure where DMPEA is bonded to a metal has also been revealed in  $[\text{DMPEA}\cdot\text{Li}(\text{TMP})\text{Zn}(\text{Me})_2]$  **4.5**.

Probing ferrocene with bimetallic mixtures afforded a range of mono- and di-deprotonated products depending on the stoichiometry used. Both zincations in  $\text{TMEDA}\cdot\text{Na}(\mu\text{-TMP})[\mu\text{-}(\text{C}_5\text{H}_4)\text{Fe}(\text{C}_5\text{H}_5)]\text{Zn}(t\text{Bu})$  **5.1** and  $[\text{TMEDA}\cdot\text{Na}(\mu\text{-TMP})\text{Zn}(t\text{Bu})_2(\text{C}_5\text{H}_4)_2\text{Fe}]$  **5.2** and aluminations in  $\text{THF}\cdot\text{Li}(\mu\text{-TMP})[\mu\text{-}(\text{C}_5\text{H}_4)\text{Fe}(\text{C}_5\text{H}_5)]\text{Al}(i\text{Bu})_2$  **5.4**,  $[\text{THF}\cdot\text{Li}(\mu\text{-TMP})\text{Al}(i\text{Bu})_2]_2(\text{C}_5\text{H}_4)_2\text{Fe}$  **5.5**,  $[\text{TMP}(\text{H})\cdot\text{Li}(\mu\text{-TMP})\text{Al}(i\text{Bu})_2]_2(\text{C}_5\text{H}_4)_2\text{Fe}$  **5.6** and

TMP(H)·Li(TMP)[(C<sub>5</sub>H<sub>4</sub>)Fe(C<sub>5</sub>H<sub>5</sub>)]Al(<sup>t</sup>Bu)<sub>2</sub> **5.7** were possible. The zinc system also provided the novel ferrocenophane type structure [{Fe(C<sub>5</sub>H<sub>4</sub>)<sub>2</sub>}]<sub>2</sub>{Na<sub>2</sub>Zn<sub>2</sub>(<sup>t</sup>Bu)<sub>2</sub>·(THF)<sub>6</sub>}] **5.8**, as well as hints of a possible polymetallated product.

### Publications in Peer Reviewed Journals

- [1] A. R. Kennedy, R. E. Mulvey, **D. L. Ramsay**, S. D. Robertson, Heterobimetallic Metallation Studies of N,N-Dimethylphenylethylamine (DMPEA) : Benzylic C-H bond Cleavage/Dimethylamino Capture or Intact DMPEA Complex, *Dalton Transactions*, **2015**, *44*, 5875.
- [2] W. Clegg, E. Crosbie, S. H. Dale, E. Hevia, G. W. Honeyman, A. R. Kennedy, R. E. Mulvey, **D. L. Ramsay**, S. D. Robertson, Structurally Defined Zincated and Aluminated Complexes of Ferrocene made by Alkali-Metal-Synergistic Syntheses, *Organometallics*, **2015**, *34*, 2580.
- [3] D. R. Armstrong, E. Crosbie, E. Hevia, R. E. Mulvey, **D. L. Ramsay**, S. D. Robertson, TMP (2,2,6,6-Tetramethylpiperidide)-Aluminate Bases: Lithium-Mediated Aluminatation or Lithiation/Alkylaluminium-Trapping Reagents?, *Chemical Science*, **2014**, *5*, 3031.
- [4] E. Hevia, A. R. Kennedy, R. E. Mulvey, **D. L. Ramsay**, S. D. Robertson, Concealed Cyclotrimeric Polymorph of Lithium 2,2,6,6-Tetramethylpiperidide Unconcealed: X-ray Crystallographic and NMR Spectroscopic Studies, *Chemistry – A European Journal*, **2013**, *19*, 14069.



## Conference Presentations (Oral)

- [5] E. Hevia, R. E. Mulvey, **D. L. Ramsay**, S. D. Robertson, Lithium TMP-Aluminate Reagents: Lithium Bases or Aluminium Bases?, *WestChem Research Day*, University of Strathclyde, Glasgow, **2014**. [Prize for best oral presentation]
- [6] E. Hevia, A. R. Kennedy, R. E. Mulvey, **D. L. Ramsay**, S. D. Robertson, Utility Amide Lithium TMP and Its Role in Cleave and Capture Chemistry, *Universities of Scotland Inorganic Conference (USIC-47)*, University of Edinburgh, Edinburgh, **2013**. [Prize for best oral presentation]
- [7] E. Hevia, A. R. Kennedy, R. E. Mulvey, **D. L. Ramsay**, S. D. Robertson, Utility Amide Lithium TMP and Its Role in Cleave and Capture Chemistry, *University of Strathclyde Inorganic Section Meeting*, West Brewery, Glasgow, **2013**.

## Conference Presentations (Poster)

- [8] E. Hevia, R. E. Mulvey, **D. L. Ramsay**, S. D. Robertson, Cleave and Capture in Heterobimetallic Main Group Chemistry, *Universities of Scotland Inorganic Conference (USIC-48)*, University of Glasgow, Glasgow, **2014**.
- [9] E. Hevia, R. E. Mulvey, **D. L. Ramsay**, S. D. Robertson, Cleave and Capture Chemistry in Heterobimetallic Main Group Chemistry, *245<sup>th</sup> American Chemical Society National Meeting*, New Orleans, USA, Paper ID 19915, **2013**.

## Abbreviations

---

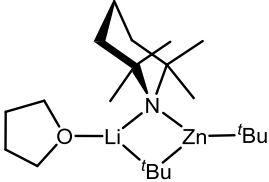
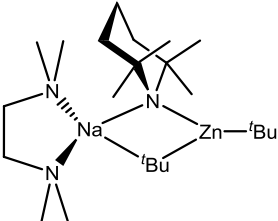
<b>AMMAI</b>	Alkali-Metal-Mediated Aluminatation
<b>AMMM</b>	Alkali-Metal-Mediated Metallation
<b>AMMMg</b>	Alkali-Metal-Mediated Magnesiatio
<b>AMMZn</b>	Alkali-Metal-Mediated Zincation
<b>BuLi</b>	<i>n</i> -butyllithium
<b><sup>i</sup>Bu</b>	<i>iso</i> -butyl
<b><sup>n</sup>Bu</b>	<i>normal</i> -butyl
<b><sup>t</sup>Bu</b>	<i>tertiary</i> -butyl
<b>CIP</b>	Contacted Ion-Pair
<b>CIPE</b>	Complex-Induced Proximity Effect
<b>COSY</b>	Correlation Spectroscopy
<b>Cp</b>	cyclopentadiene anion (C <sub>5</sub> H <sub>5</sub> ) <sup>-</sup>
<b>CSD</b>	Cambridge Structural Database
<b>DA</b>	diisopropylamide
<b>Dipp</b>	2,6-diisopropylphenyl
<b>DFT</b>	Density Functional Theory
<b>DME</b>	1,2-dimethoxyethane
<b>DMG</b>	Directed Metallating Group
<b>DMPEA</b>	<i>N,N</i> -dimethylphenylethylamine
<b>DoM</b>	Directed <i>ortho</i> -Metallation
<b>DOSY</b>	Diffusion Ordered Spectroscopy
<b>Et</b>	ethyl
<b>FLP</b>	Frustrated Lewis Pair
<b>HMDS</b>	1,1,1,3,3,3-hexamethyldisilazide
<b>HMPA</b>	hexamethylphosphoramide
<b>HMQC</b>	Heteronuclear Multiple Quantum Correlation
<b>HOESY</b>	Heteronuclear Overhauser Effect Spectroscopy

<b>HSQC</b>	Heteronuclear Single Quantum Correlation
<b>LDA</b>	lithium diisopropylamide
<b>LIC-KOR</b>	Superbasic mixture of alkyllithium/potassium alkoxide
<b>LiNK</b>	Mixture of BuLi/KO <sup>t</sup> Bu/TMP(H)
<b>MDAE</b>	1-methoxy-2-dimethylaminoethane
<b>Me</b>	methyl
<b>Me<sub>4</sub>AEE</b>	bis[2-( <i>N,N</i> -dimethylamino)ethyl]ether
<b>Me<sub>2</sub>TFA</b>	<i>N,N</i> -dimethyltetrahydrofurfurylamine
<b>Me<sub>6</sub>-TREN</b>	tris[2-(dimethylamino)ethyl]amine
<b>MOM</b>	methoxymethylether group
<b>MW</b>	molecular weight
<b>NHC</b>	N-heterocyclic carbene
<b>NMR</b>	Nuclear Magnetic Resonance
<b>Ph</b>	phenyl
<b>PMDETA</b>	<i>N,N,N',N'',N'''</i> -pentamethyldiethylenetriamine
<b>PMP</b>	2,2,4,6,6-pentamethylpiperidide
<b>ppm</b>	parts per millions
<b><sup>i</sup>Pr</b>	<i>iso</i> -propyl
<b>SSIP</b>	Solvent-Separated Ion-Pair
<b>TCI</b>	Tokyo Chemical Industry UK Ltd.
<b>THF</b>	tetrahydrofuran
<b>TMEDA</b>	<i>N,N,N',N'</i> -tetramethylcyclohexane-1,2-diamine
<b>TMEDA</b>	<i>N,N,N',N'</i> -tetramethylethylenediamine
<b>TMP</b>	2,2,6,6-tetramethylpiperidide
<b>TMP(H)</b>	2,2,6,6-tetramethylpiperidine
<b>TMS</b>	tetramethylsilane
<b>TOCSY</b>	Total Correlated Spectroscopy

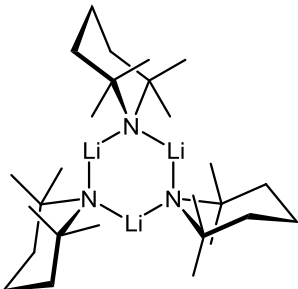
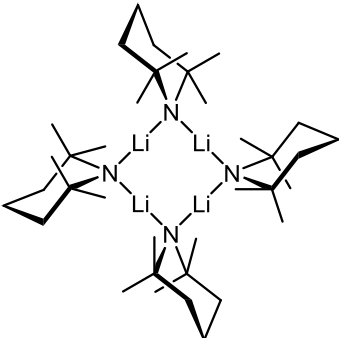
<b>TREN</b>	tris(2-aminoethyl)amine
<b>TTHP</b>	2,2,6-trimethyl-1,2,3,4-tetrahydropyridide
<b>TVA</b>	Thermal Volatilisation Analysis
<b>UK</b>	United Kingdom

## List of Numbered Compounds

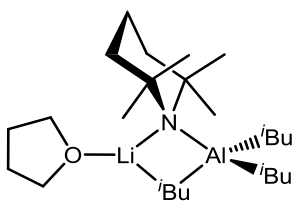
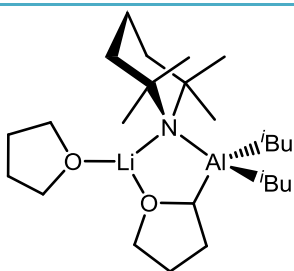
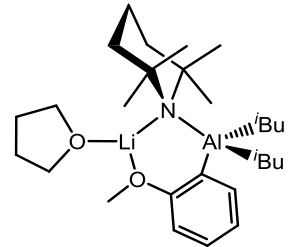
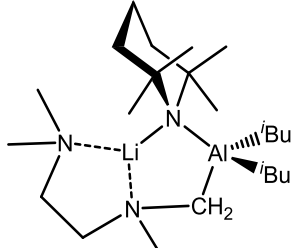
### Chapter 1

Compound number	Structure/formula
1.1	$\text{Li}^+[\text{Zn}(\text{TMP})(\text{tBu})_2]^-$
1.2	
1.3	

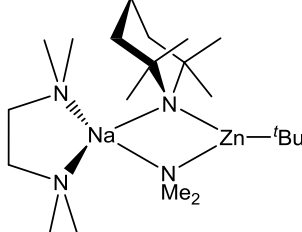
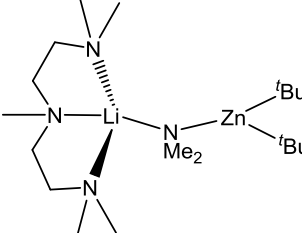
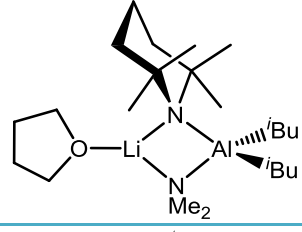
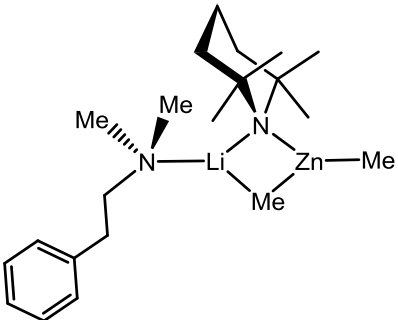
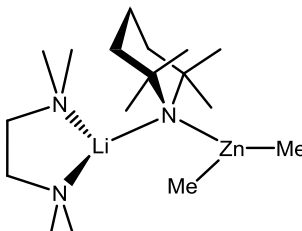
### Chapter 2

Compound number	Structure/formula
2.1	
2.2	

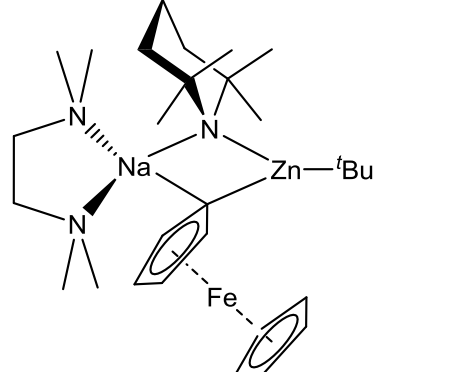
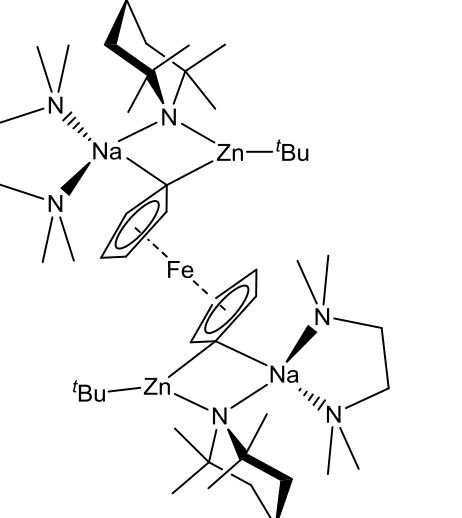
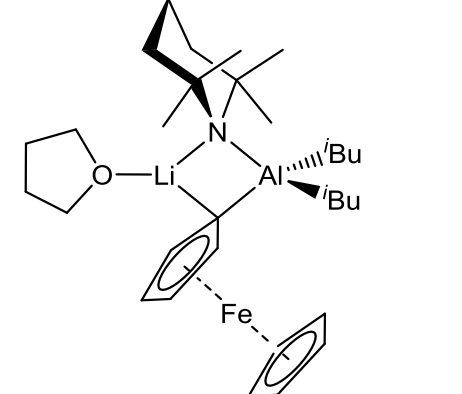
## Chapter 3

Compound number	Structure/formula
3.1	$\text{LiTMP}\cdot\text{Al}(i\text{Bu})_3$
3.1·THF	
3.2	$\text{LiTMP}\cdot\text{Al}(\text{TMP})(i\text{Bu})_2$
3.1·(THF) <sub>4</sub>	$[\{\text{Li}(\text{THF})_4\}^+\{\text{Al}(\text{TMP})(i\text{Bu})_3\}^-]$
3.2·(THF) <sub>4</sub>	$[\{\text{Li}(\text{THF})_4\}^+\{\text{Al}(\text{TMP})_2(i\text{Bu})_2\}^-]$
3.3	$[\{\text{Li}(\text{THF})_4\}^+\{\text{Al}(i\text{Bu})_4\}^-]$
3.4	
3.5	
3.6	

## Chapter 4

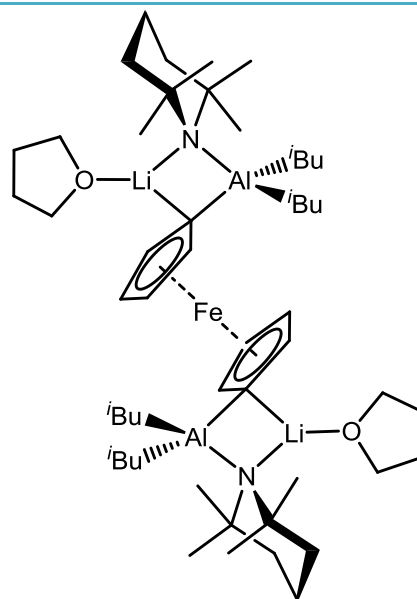
Compound number	Structure/formula
4.1	[PMDETA·Li(TMP)Zn( <sup>t</sup> Bu) <sub>2</sub> ]
4.2	
4.3	
4.4	
4.5	
4.6	

# Chapter 5

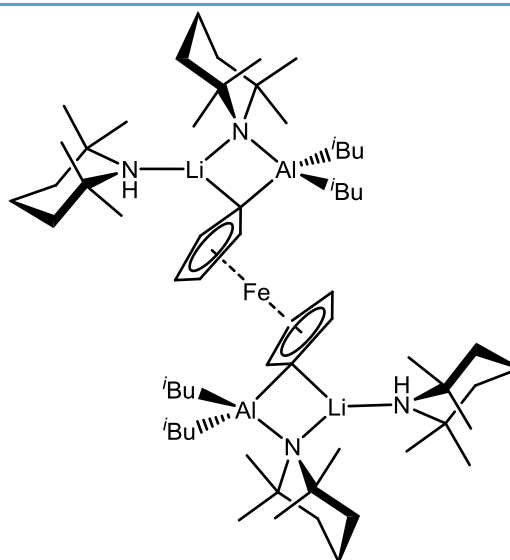
Compound number	Structure/formula
5.1	
5.2	
5.3	<p>suspected tetrazincated ferrocene (formula as yet unknown)</p>
5.4	



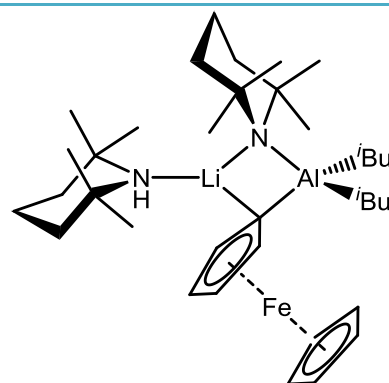
5.5



5.6



5.7



5.8

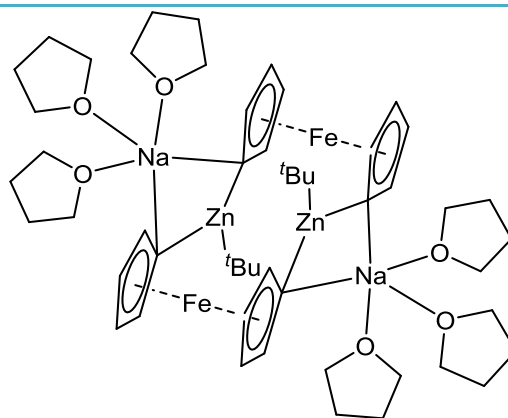


# Table of Contents

---

Acknowledgements	iv
Abstract	vi
Publications	viii
Abbreviations	x
List of Numbered Compounds	xiii
Table of Contents	xix

## **1. An Introduction to Polar Organometallic and Metallation Chemistry** 1

1.1 An Introduction to Metallation	2
1.2 Conventional Metallating Agents	3
1.2.1 Organolithium Reagents	3
1.2.2 Alternative Organometallic Reagents	18
1.3 Heterobimetallic Metallating Agents	22
1.3.1 Mixed Alkali Metal Reagents	24
1.3.2 Mixed Metal Reagents	26
1.3.3 The Lithium Chloride Salt Effect	40
1.3.4 Turbo-Grignard Reagents and their Hauser Base Equivalents	41
1.3.5 Recent Developments in Main Group Catalysis	44
1.4 Bibliography	52

## **2. Concealed Cyclotrimeric Polymorph of Lithium 2,2,6,6-Tetramethylpiperide Unconcealed** 58

2.1 Aims	59
2.2 Introduction	60
2.2.1 Structural Considerations	63
2.3 Results and Discussion	65
2.3.1 Synthesis and Crystallisation	65
2.3.2 X-ray Crystallographic Studies	67
2.3.3 NMR Spectroscopic Studies	70
2.3.4 Reflections on Previous Theoretical Calculations	76
2.3.5 Relevance to Reactivity and Structural Design	77
2.4 Conclusions	78
2.5 Future Work	79
2.6 Experimental	80
2.7 Bibliography	83

## **3. TMP-Aluminate Bases: Lithium-Mediated Aluminatation or Lithiation – Alkylaluminium-Trapping Reagents?** 86

3.1 Aims	87
3.2 Introduction	88
3.3 Results and Discussion	95
3.3.1 Has the Active Base of 3.1 been Crystallographically Characterised?	95
3.3.2 <i>In Situ</i> 3.1 versus Crystalline 3.1·THF: Comparative Reactivity Studies with Anisole	103
3.3.3 Towards Solving the Puzzle of “LiTMP·Al(TMP)( <i>t</i> Bu) <sub>2</sub> ”	108

3.3.4 Re-evaluating the Composition and Active Base Component of <i>In Situ</i> 3.1 in THF Solution	125
3.3.5 Theoretical Calculations	133
3.4 Conclusions	137
3.5 Future Work	140
3.6 Experimental	141
3.7 Bibliography	145
<b>4. Heterobimetallic Metallation Studies of <i>N,N</i>-Dimethylphenylethylamine</b>	<b>148</b>
4.1 Aims	149
4.2 Introduction	150
4.3 Results and Discussion	153
4.3.1 AMMM Reactions with DMPEA and Characterisation of “Captured Products”	154
4.3.2 Mechanistic Implications	167
4.3.3 Capture of the Whole Parent Amine, DMPEA	172
4.3.4 Is [DMPEA·Li(TMP)Zn(Me) <sub>2</sub> ] a Pre-Metallation Complex?	181
4.4 Conclusions	182
4.5 Future Work	182
4.6 Experimental	184
4.7 Bibliography	188
<b>5. Structurally Defined Zincated and Aluminated Complexes of Ferrocene made by Alkali-Metal-Synergistic Syntheses</b>	<b>192</b>
5.1 Aims	193
5.2 Introduction	194
5.3 Results and Discussion	199
5.3.1 Studies of Sodium Zincate TMEDA·Na(μ-TMP)(μ- <i>t</i> Bu)Zn( <i>t</i> Bu)	199
5.3.2 Ferrocene Metallation by Lithium Aluminate “LiAl(TMP) <sub>2</sub> <i>t</i> Bu <sub>2</sub> ”	206
5.4 Conclusions	217
5.5 Future Work	219
5.6 Experimental	221
5.7 Bibliography	229
<b>6. General Conclusions</b>	<b>233</b>
6.1 General Conclusions	234
6.2 Bibliography	237
<b>7. General Experimental Techniques</b>	<b>238</b>
7.1 Schlenk Techniques	239
7.2 Glove Box	240
7.3 Solvent Purification	241
7.4 NMR Solvent Purification	242

<b>7.5</b> Purification of Hygroscopic Liquids	242
<b>7.6</b> Commercial Reagents Used	243
<b>7.7</b> Standardisation of Organolithium Reagents	243
<b>7.8</b> Preparation of Common Starting Materials	244
<b>7.8.1</b> Preparation and Isolation of <i>n</i> BuNa	244
<b>7.8.2</b> Preparation and Isolation of <i>t</i> Bu <sub>2</sub> Zn	245
<b>7.9</b> Instrumentation for Compound Characterisation	246
<b>7.9.1</b> Nuclear Magnetic Resonance (NMR) Spectroscopy	246
<b>7.9.2</b> Elemental Microanalysis	246
<b>7.10</b> X-Ray Crystallographic Studies	247
<b>7.11</b> Bibliography	248

## **Chapter 1**

# **An Introduction to Polar Organometallic and Metallation Chemistry**

## 1.1 An Introduction to Metallation

Ask any scientist to justify their research and you will undoubtedly be given an account of why their chosen area of study is especially worthy of their expertise. In the case of organometallic chemistry, and more specifically metallation chemistry, the importance, relevance and valuable nature of the research is indisputable. The topic of metallation has gripped the attention of many renowned researchers around the world with a plethora of journal articles,<sup>[1-8]</sup> review papers<sup>[9-16]</sup> and book chapters<sup>[17-20]</sup> devoted to the subject. The reason for this huge volume of interest is that metallation involves converting a commonly encountered but somewhat chemically redundant C-H bond into a reactive and hence more exploitable  $C^{\delta-}$ -metal $^{\delta+}$  bond. The labile nature of this newly formed bond in turn allows for the construction of new C-C or C-X bonds, through subsequent bond-forming approaches, leading to a multitude of synthetic pathways available to pursue. As a consequence, this seemingly simple chemical transformation has become an indispensable reaction in many areas of the industrial sector, ranging from the synthesis of fine chemicals<sup>[5]</sup> through to the production of everyday items such as perfumes<sup>[21]</sup> and perhaps more notably, pharmaceuticals.<sup>[22-24]</sup>

Whilst the goals that metallation chemistry has allowed us to achieve (and hopefully surpass in the future) are widely recognised by both those in academia and industry, it does not come without its shortfalls. Continuous development and optimisation is in the nature of science and with conventional metallation procedures there is such room for improvement. For example, typical approaches often require sub-ambient temperatures, which necessitate the use of expensive cryogenic cooling systems. For progression's sake, the focus has been shifting slightly in recent years to a "second generation" of metallating agents. These bimetallic reagents are gaining widespread interest owing to milder reaction conditions and increased functional group tolerance in comparison to their traditionally used monometallic counterparts.

This chapter aims to briefly describe some of the most important metallating reagents, both first and second generation, that are currently in circulation in both research and industrial laboratories around the world. Initially, conventional monometallic reagents will be discussed, with emphasis on organo-lithium and -zinc reagents. The remainder of the chapter will then deal with the up-and-coming area of bimetallic systems and the advantages they can offer over the first generation compounds.

## 1.2 Conventional Metallating Agents

At present there are a number of well-known organometallic reagents employed within chemical reactions to accomplish the desired metallation of a molecule. As one may expect however different classes of reagents can offer varying reactivities and regio-/stereo-selectivities and hence depending on the substrate and desired product of the reaction careful consideration must be given when choosing from the vast selection on offer. This section of the chapter deals with some of the common monometallic reagents available, and highlights both the advantages and disadvantages of using such systems.

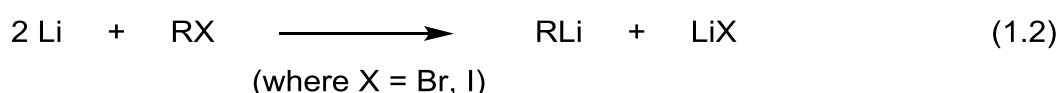
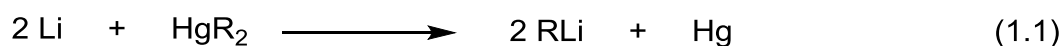
### 1.2.1 Organolithium Reagents

Hailed by many as the frontrunners of organometallic reagents, organolithium compounds have been around for almost a century.<sup>[25]</sup> These staple reagents are used by chemists from many backgrounds including organic, inorganic and physical chemistry as a result of their versatile structures, reactivity and applications in many areas of science, so much so it has recently been said that “hardly a molecule is made without a bottle of BuLi”.<sup>[20]</sup>

The study of such prevalent compounds began in the early 1900s with pioneering work on the alkyl species methyllithium and ethyllithium and the aryl species phenyllithium by Wilhelm Schlenk (leading to a Nobel Prize



nomination in 1920).<sup>[25]</sup> This original synthesis, employing elemental lithium to reduce the corresponding organomercury(II) compound to mercury (eq 1.1), is not one we would choose to use today however due to the toxicity of the group 12 metal.<sup>[26-27]</sup> A decade or so later Ziegler reported a more convenient route to organolithium compounds by reacting lithium metal with an alkyl or aryl halide (bromide or iodide)<sup>[28]</sup> (eq 1.2), which has become the industry standard method of preparation today [note that nowadays there is no requirement to prepare the common organolithium reagents (for example, "RLi" where R is <sup>n</sup>Bu, <sup>t</sup>Bu, Me, Ph) as they are commercially available from different sources such as Aldrich, Alfa Aesar, Acros, BOC Sciences, Rockwood, TCI and FMC, reflecting their widespread industrial as well as academic importance].



Schlenk's pioneering research was especially challenging however due to the acute air- and moisture-sensitivity of, as it turns out, all known organolithium compounds, which necessitated the design of specialised experimental apparatus that enabled the handling of these compounds under an inert atmosphere to avoid decomposition. Simple but ingenious, Schlenk tubes are still used today (including routinely in the work reported herein) for the laboratory-scale preparation and manipulation of organolithium and other air-sensitive organometallic compounds.<sup>[29]</sup> As well as the need for specialist glassware this somewhat problematic characteristic meant it was not until many years after the initial work by Schlenk that the first organolithium compound was characterised by X-ray crystallography. The task was completed by Dietrich in 1963,<sup>[30-31]</sup> a significant milestone within organolithium chemistry, and the compound he skilfully managed to characterise was that of

ethylolithium. The molecular structure was found to contain tetrameric units of EtLi (Figure 1.1) revealing that these organolithium compounds are not simply R-Li monomers as their empirical formula may suggest (to the untrained eye), but rather have a tendency to aggregate both in solution and the solid state. The degree of aggregation is determined by several factors, namely the organic group attached to Li, the presence or absence of a donor ligand and the solvent choice, hence aggregation states can vary between different organolithium compounds. In general, an increase in the bulk of the organic group attached to the metal results in a decrease in the aggregation state.<sup>[20]</sup> Introducing coordinating solvents and/or ligands [e.g. commonly tetrahydrofuran (THF), *N,N,N',N'*-tetramethylethylenediamine (TMEDA)] to the system also generally results in a decrease in the aggregation state of the organolithium compound. In both cases the presence of a donor ligand capable of solvating the metal centres breaks down the unsolvated oligomers into smaller solvated aggregates, stabilised by the extra electron density from the ligand.

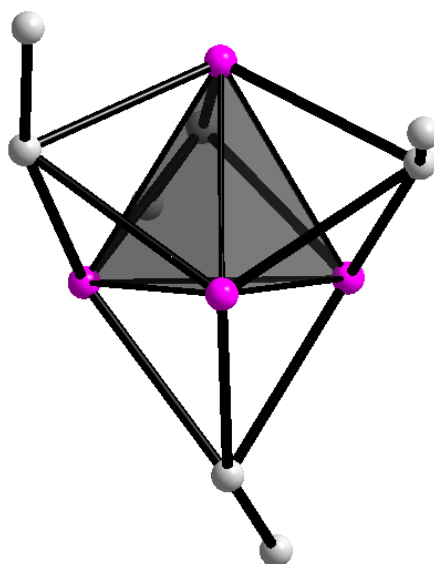
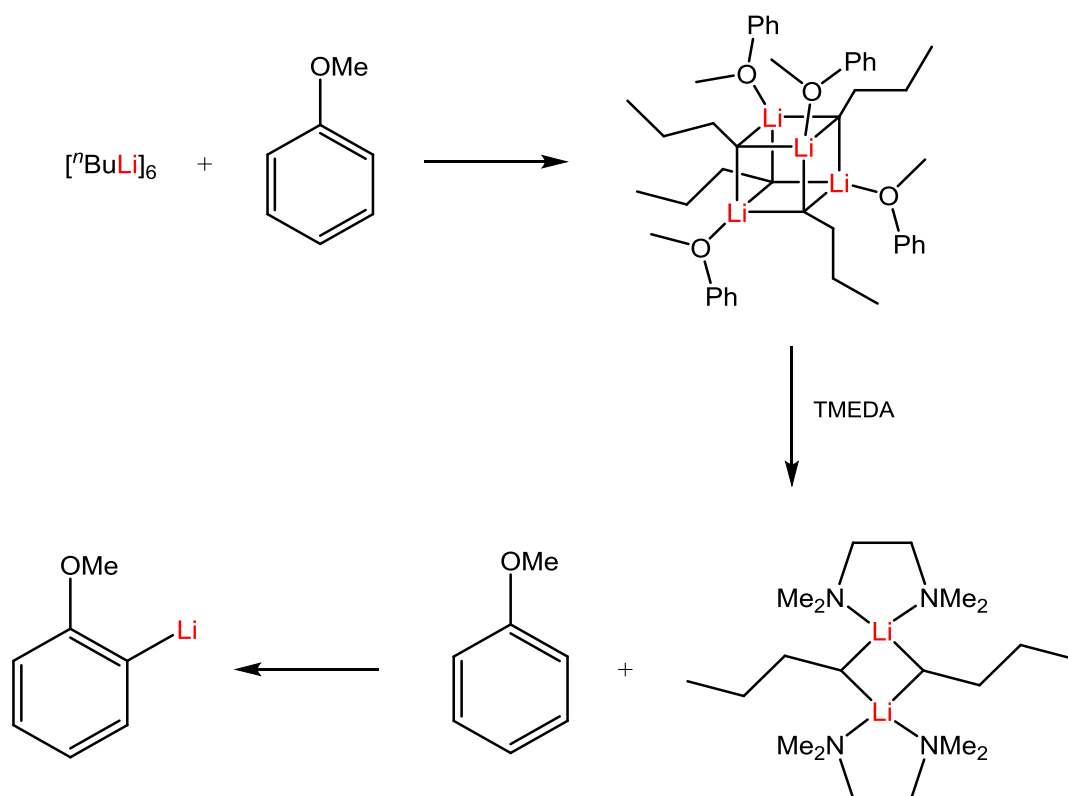


Figure 1.1. Molecular structure of  $[\text{EtLi}]_4$  highlighting the tetrameric “ $\text{Li}_4$ ” core with an ethyl group capping each face.

A nice example, where both TMEDA and the substrate work together to lower the aggregation state of the organolithium compound is the metallation reaction of anisole by  $n\text{BuLi}$  (Scheme 1.1). It involves a two-step process whereby the anisole first coordinates to the  $n\text{BuLi}$  hexamer breaking it into a tetrameric complex containing four anisole molecules coordinating to the lithium centres. The TMEDA subsequently displaces the anisole molecules allowing the newly formed and more reactive  $\text{BuLi}\cdot\text{TMEDA}$  dimer to successfully metallate the now free anisole.<sup>[32-33]</sup>



Scheme 1.1. Metallation of anisole using an  $n\text{BuLi}$ /TMEDA mixture (note the stoichiometry is not taken into account in this depiction).

Researchers who study organolithium chemistry cannot fail to be impressed by the aesthetic attractiveness and bewildering number of organolithium structures that have led to their adornment in the pages of several textbooks and reviews.<sup>[34-38]</sup> Although Dietrich reported the first crystal structure of an

organolithium compound (*vide supra*), textbooks generally give more emphasis to the related structure of the simplest organolithium, methyllithium, reported by Weiss initially in 1964<sup>[39]</sup>, then updated in 1970.<sup>[40]</sup> Methyllithium is also tetrameric in the form of a distorted cube, made up of interpenetrating  $\text{Li}_4$  and  $\text{C}_4$  tetrahedra, but the diminutive size of this smallest of alkyllithium compounds enables the methyl C atoms at each alternate corner of the cube to engage intermolecularly with lithium atoms from neighbouring cubes to generate a three-dimensional “polymer of tetramers” (Figure 1.2).

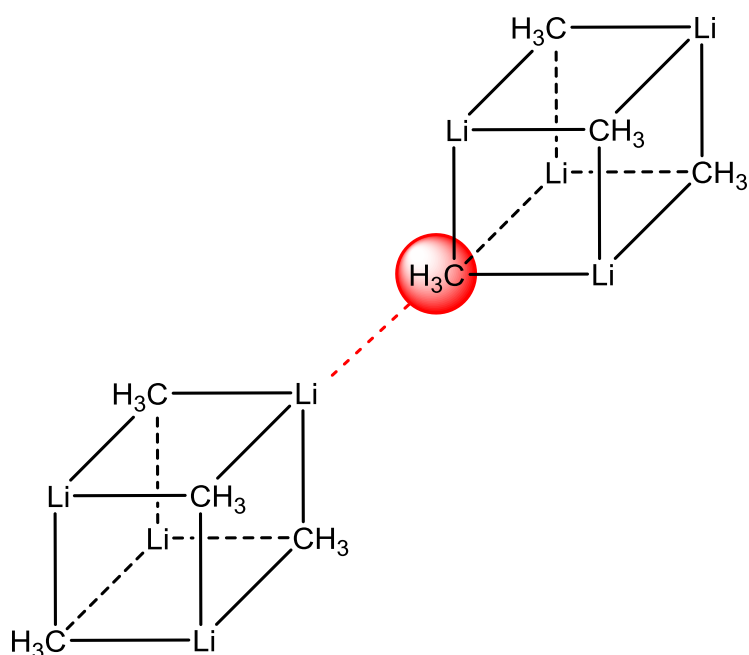


Figure 1.2. Highlighting the intermolecular bridging between two tetrameric units in methyllithium allowing for an infinite three-dimensional arrangement.

Methyllithium also provides a good teaching example of an electron deficient compound as its tetrameric arrangement of 12 Li-C bonds is held together by only 8 valence electrons, which equates to a bond order of 1/3. In general all aggregated organocarbon-lithium compounds (that is, dimers and higher oligomers) are electron deficient with only monomers conforming to localised

two-centre, two-electron bonding rules. Ironically the structure of methyllithium is atypical of the features that make organolithium compounds so appealing for synthetic exploitation. Its infinite three-dimensional arrangement renders it insoluble in hydrocarbon and arene solvents; whereas bona fide molecular organolithium compounds such as hexameric *n*-butyllithium or tetrameric *t*-butyllithium with bulkier, more space-consuming organic moieties that preclude interaggregate interactions are soluble. Phenyllithium is the other common organolithium reagent that is insoluble in hydrocarbon and arene solvents due to its polymeric constitution, but as with methyllithium, it can be easily dissolved by the introduction of a donor additive (e.g., commonly THF, ether or TMEDA) of which usually a stoichiometric equivalent is sufficient.

Phenyllithium, the simplest lithium aryl compound, exemplifies the structural diversity of crystallographically characterized organolithium structures (Figure 1.3). Determined by a Synchrotron study, the parent compound exists as an infinite ladder arrangement of four-atom (LiC) rings in which the carbon atom is the deprotonated ipso carbon if one was starting from benzene.<sup>[41]</sup> Three-coordination being insufficient for a sterically exposed lithium atom (a four-coordinate, tetrahedral geometry is the most common), the  $\pi$ -face of the aromatic ring engages in an electrostatic interaction with it. Addition of monodentate ether donor molecules breaks up the infinite ladder arrangement to give a pseudo-cubane tetrameric structure which can be considered as a stack of two of the (LiC)<sub>2</sub> rings of the parent structure with the lithium corners being filled by the donating O atoms.<sup>[42]</sup> Because of its bidentate potential TMEDA can deaggregate phenyllithium further to a discrete (LiC)<sub>2</sub> dimer which, as in the ether solvate, has four-coordinate, distorted (2xC; 2xN) tetrahedral lithium atoms.<sup>[43]</sup> Following this pattern, potentially tridentate *N,N,N',N'',N'''*-pentamethyldiethylenetriamine (PMDETA) chelates to the lithium atoms with all three of its nitrogen donor atoms to leave a single Li-C(Ph) bond in an electron-precise monomeric complex.<sup>[44]</sup> Chiral (-)-sparteine illustrates that organolithium compounds can exist as stoichiometric variants. A 1:1 ratio of PhLi to the chiral molecule results in the crystalline dimer [PhLi·(-)-sparteine]<sub>2</sub>

with its central  $(\text{LiC})_2$  ring; whereas changing the ratio to 2:1 results in the tetranuclear variant  $[(\text{PhLi})_2 \cdot (-)\text{-sparteine}]_2$ , a ladder structure with four Li-C rungs.<sup>[45-46]</sup>

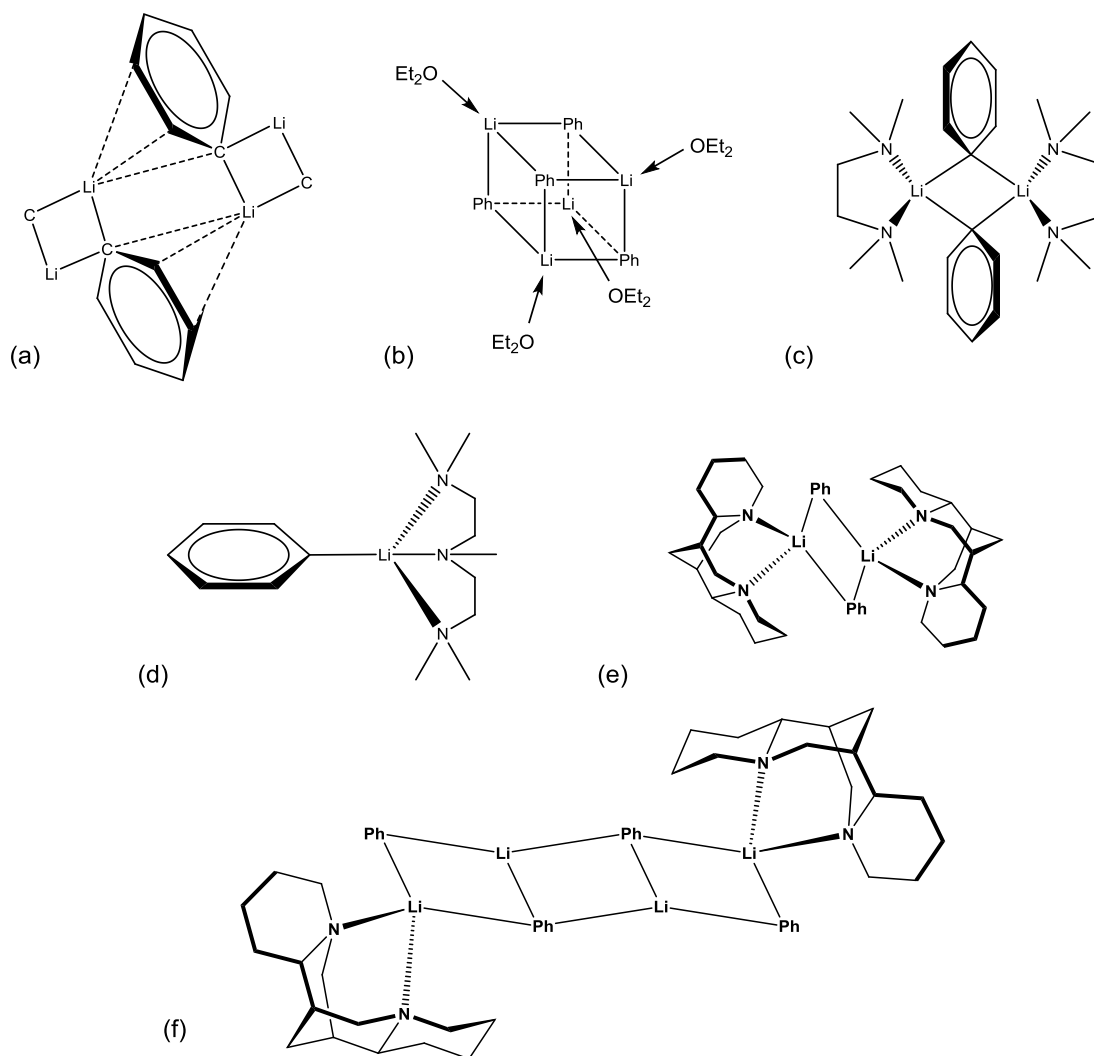


Figure 1.3. Various oligomers of phenyllithium possible when: (a) no donor ligand, (b) monodentate ether, (c) bidentate TMEDA, (d) tridentate PMDETA, (e) stoichiometric sparteine and (f) substoichiometric sparteine is present.

Describing these structures as ladders, it is appropriate at this juncture to mention “the Ring-Stacking and Ring-Laddering Principle in Organolithium Chemistry”.<sup>[47-53]</sup> Devised by Snaith with help from Wade and Mulvey, this concept can rationalise and predict the structures of a wide variety of organolithium compounds ranging from amides and imides to alkoxides, enolates and halides. Discrete rings having  $sp^3$ -hybridised N centres as in lithium amide dimers  $(LiNR_2)_2$  cannot aggregate face-to-face because of steric clashing of their  $R_2N$  groups which project above the ring plane. If space permits, these lithium amide dimers will join up laterally to form ladders that satisfy the coordination requirements of the metal-nitrogen polar building block. On the other hand, discrete lithium ketimides  $(R_2C=NLi)$  have  $sp^2$ -hybridised N centres, which sterically inhibit lateral aggregation as their R substituents block lateral space. However, if space permits aggregation can now take place face-to-face to form stack structures. In this interpretation the aforementioned  $(MeLi \cdot Ether)_4$  tetramer is considered a twofold stack of dimeric  $(MeLi)_2$  rings. The classic stack is Schleyer’s dodecameric alkyne-derived structure of  $[(tBuC \equiv CLi)_{12}(THF)_4]$ ,<sup>[54]</sup> which can be viewed as the face-to-face coming together of six  $(LiC)_2$  ring dimers. These two extreme processes of substituent stereochemistry controlled aggregation, laddering and stacking, are depicted in Figure 1.4. Though organolithium structural chemistry was once considered a structural jumble with no general patterns, this simple but ingenious ring-stacking and ring-laddering principle went a long way to unifying the subject.

It is no exaggeration to state that organolithium compounds are wholly indispensable to the synthetic chemist. While certain reagents may be better for certain synthetic applications, generally for reactions that require a Brønsted base in particular, or a carbon nucleophile to a lesser extent, organolithium reagents would be the first candidates that synthetic chemists would turn to in order to perform the desired step in their synthetic campaigns. The key to their widespread utilisation is the polarity of the lithium–carbon bond arising from the substantial electronegativity difference between the two elements (Li, 1.0; C,

2.5)<sup>[55]</sup> and their solubility in common organic solvents. As seen in Figure 1.5, organolithium compounds are intermediate in polarity between organosodium and organopotassium compounds, which are more polar, and organomagnesium and organozinc compounds which are less polar. The upper limit of this polarity scale would be free carbanions “R<sup>-</sup>”, where the metal-carbon bond is completely severed and the carbanionic moiety carries the full negative charge, which drives its reactivity.

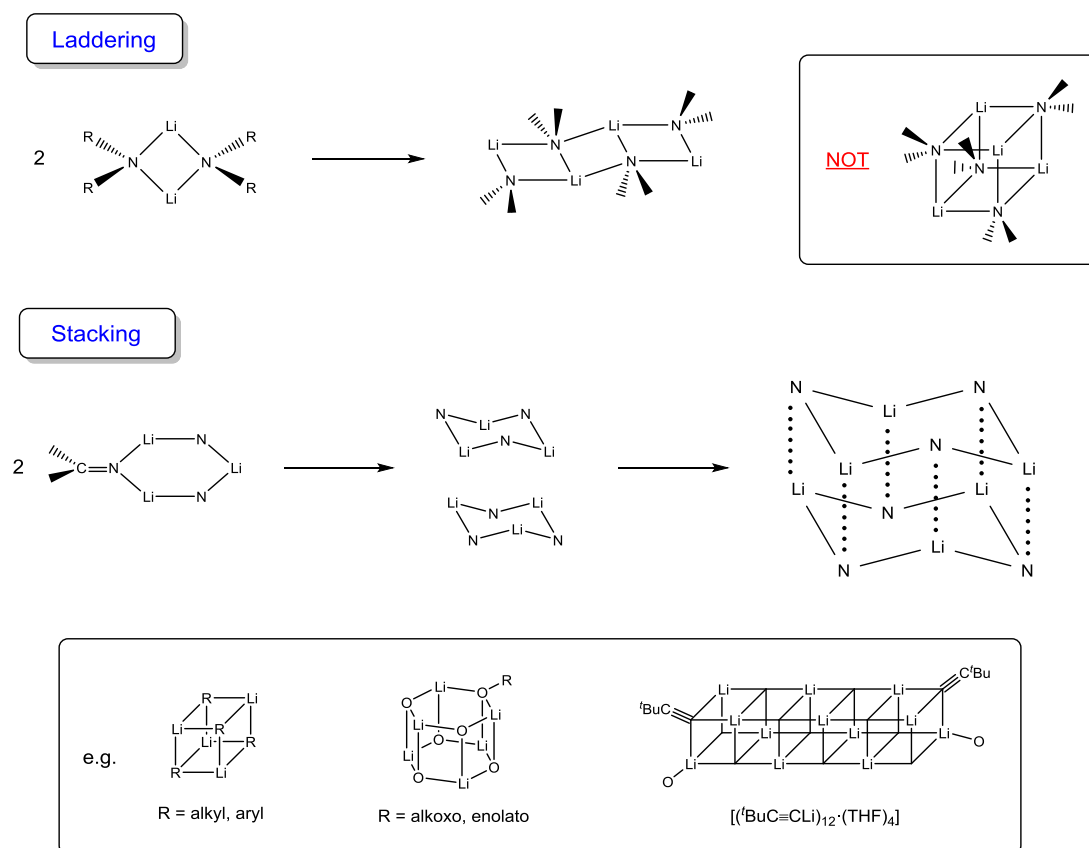


Figure 1.4. General depiction of the ring-laddering and ring-stacking principle in organolithium chemistry.

In general terms there is a close correlation between this relative polarity and reactivity with organolithium compounds being less reactive than organosodium or organopotassium compounds but more reactive than the



other two mentioned “softer” organometallic compounds. Without the stabilising support of a metal, free carbanions with full negative charges would be generally unstable unless the charge can be delocalized over several atoms. This average polar placement for organolithium compounds (note that Schlosser introduced the apt name polar organometallic compounds for these and related compounds<sup>[56]</sup>) makes them ideal tools for synthesis. Organosodium and even more so organopotassium compounds can be over-reactive, rapidly attacking functional groups or the solvent, while their pronounced ionicity can render them insoluble in the organic solvents that are necessary for synthetic transformations.

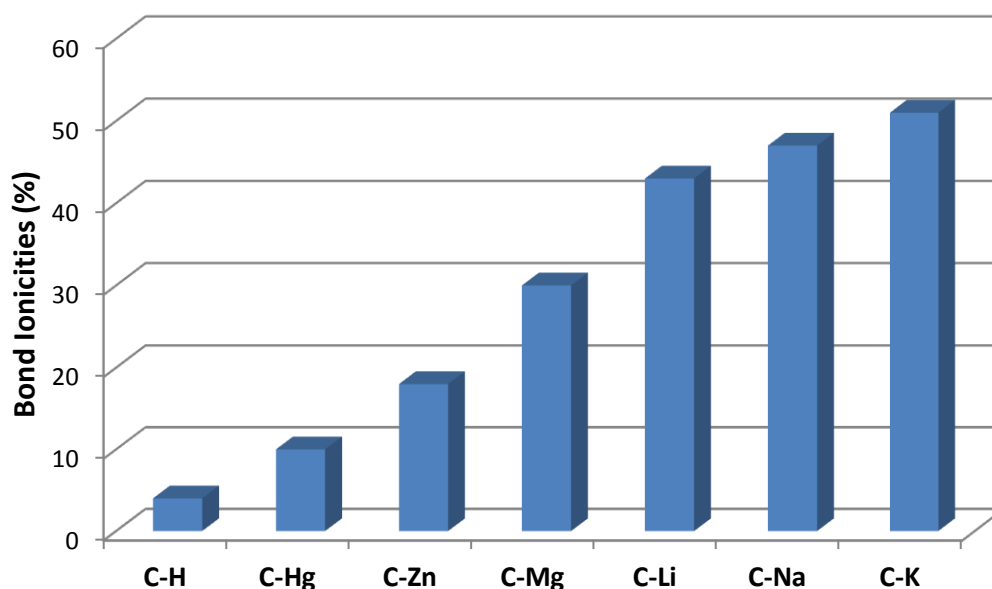
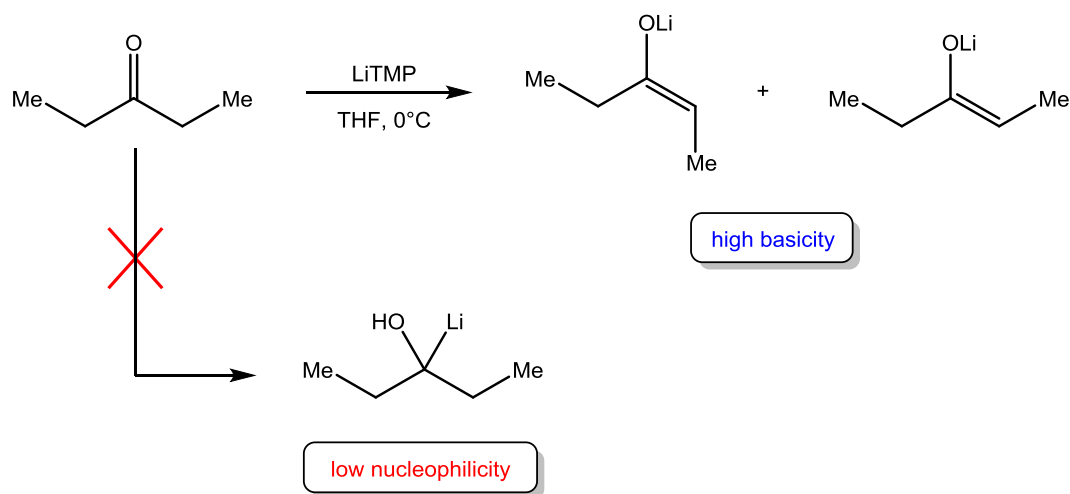


Figure 1.5. Bond ionicities of various C-Metal bonds in order of increasing ionicity.

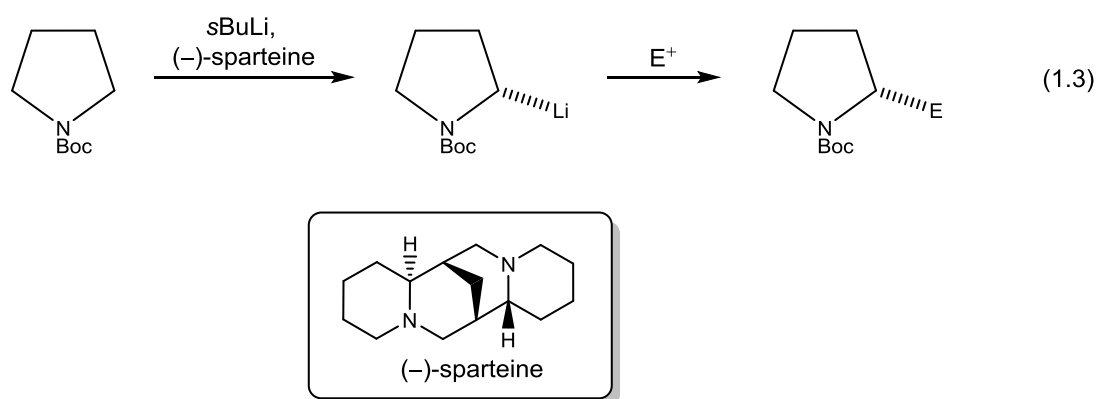
Synthetic chemists would also consider other lithium compounds where carbon-lithium bonds are absent as organolithium reagents. These would typically include lithium alkoxide compounds such as lithium *tert*-butoxide (*t*-BuOLi) and lithium methoxide (MeOLi), which are considerably less basic than the aforementioned lithium-carbon reagents. As a general rule, the  $pK_a$  of the

conjugate acid (for metal alkoxides, alcohols ROH) is a good measure of the strength of its conjugate base (MeOH, 29.0, *t*-BuOH, 32.2 c.f., *n*-BuH, 50) though such values are highly solvent dependent.<sup>[57-58]</sup> Lithium amides (R<sub>2</sub>NLi) derived from secondary amines (not from carbonyl amides) are the most synthetically important non lithium-carbon bonded reagents of this type. These lithium-nitrogen compounds are intermediate in basicity between the aforementioned lithium-oxygen and lithium-carbon (alkyl) compounds. Sterically large lithium amides, the lithium derivative of 2,2,6,6-tetramethylpiperidine (TMP) (p*K*<sub>a</sub> = 37)<sup>[59-61]</sup> LiTMP being the prime example have the added advantage of low nucleophilicity compared to that of alkyllithium reagents such as *n*-butyllithium, which makes them the Brønsted bases of choice for many reactions including for the formation of ketone and related enolates (Scheme 1.2).<sup>[62-63]</sup> Aside from this organic utilisation, lithium amides (and their heavier sodium and potassium congeners) provide a gateway to amido derivatives of many other elements in the periodic table.<sup>[64]</sup> Lithium amides will be covered in more detail in Chapter 2.



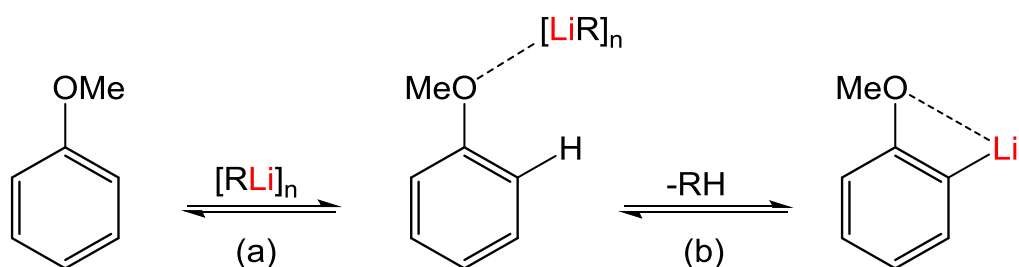
Scheme 1.2. Deprotonation of 3-pentanone by the non-nucleophilic bulky Brønsted base LiTMP.

Most of the aforementioned lithium alkyl compounds are strong bases. Combining chiral (-)-sparteine with *sec*-butyllithium can enable enantioselective deprotonation reactions such as that of *N*-Boc pyrrolidine, which selectively removes the pro-*S* hydrogen atom adjacent to the nitrogen centre to yield a configurationally stable lithium intermediate that can be intercepted by various electrophiles to produce substituted chiral products (eq 1.3).



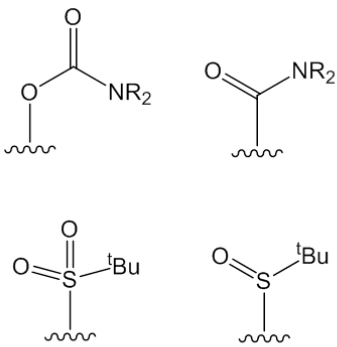
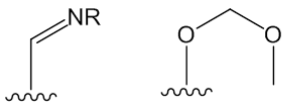
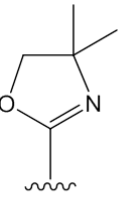
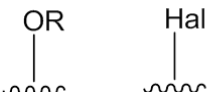
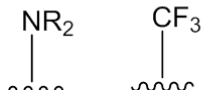
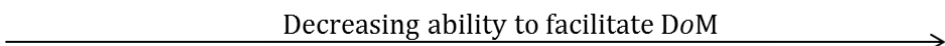
Directed-*ortho*-Metallation (DoM) is the seminal concept in C-H deprotonation chemistry, as important if not more important for the regioselective functionalisation of aromatic compounds than electrophilic aromatic substitution.<sup>[15-16]</sup> DoM is defined as a deprotonation that takes place selectively at the *ortho* position to an activating heteroatom containing functional group on an aromatic ring. The breakthrough discovery was performed independently by Gilman<sup>[8]</sup> and Wittig<sup>[65]</sup> who *ortho*-lithiated the alkyl-aryl ether anisole (Scheme 1.3), its directed metallating group (DMG) being the methoxy group. Since this pioneering reaction, the number of accessible DMGs has multiplied and been arranged in order of their directing strength (Table 1.1) as DoM chemistry has been exhaustively researched and contributed enormously to synthetic chemistry.<sup>[16, 20, 66-67]</sup> DoM is reliant on the nature of the substituent and is thought to involve two main aspects. First, any substituent heteroatoms can coordinate datively to the incoming lithium compound thus enhancing reactivity around the coordination site and directing the regioselectivity of the

subsequent lithiation to the adjacent (*ortho*) position. Second, electron-withdrawing substituents can inductively acidify the *ortho* C-H atom thus weakening it and making it more susceptible to undergo a lithium-hydrogen exchange. In an illuminating review in 2004, Snieckus and Beak introduced the notion of a “Complex-Induced Proximity Effect (CIPE)”. In cases where a CIPE operates, DoM occurs with the intermediate formation of a pre-lithiation coordination complex. These intermediates enable certain lithiation reactions to go beyond thermodynamic acidity by carrying out remote deprotonation/functionalisation on the same or even alternative aryl rings. *N,N*-dimethylbenzylamine provides a nice example. Though its aromatic hydrogen atoms are no more acidic than those of benzene, the amine is deprotonated rapidly and regioselectively at the 2-position, closest to the DMG.<sup>[68]</sup>

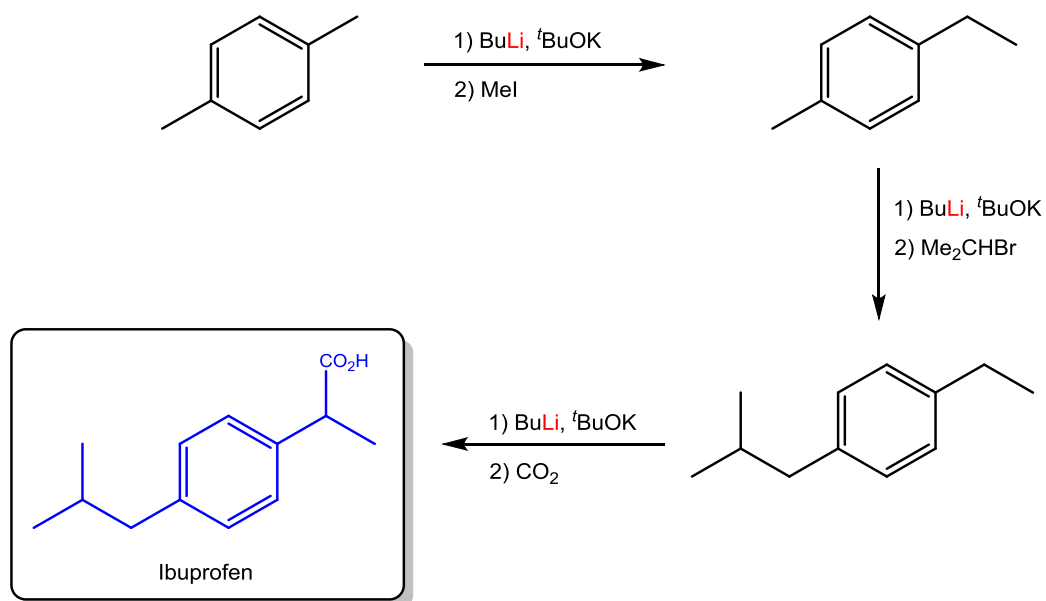


Scheme 1.3. Directed *ortho*-metallation of anisole showing: (a) coordination of the organolithium reagent to the substrate, and (b) deprotonation to generate *ortho*-lithiated anisole.

Table 1.1. Some common DMGs and their relative *ortho*-lithiating ability, indicating the general reaction temperature required when using THF as the solvent.

Strong		Moderate		Weak	
-78°C		-50°C	-20°C	0°C	>0°C
		 		 	
					

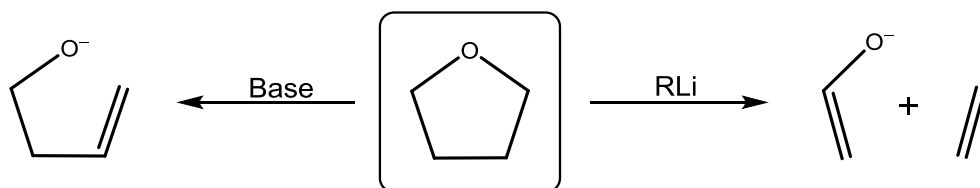
As mentioned already organolithium reagents are used in a variety of sectors. A key example of the importance of such compounds in synthesis which even the interested lay person can appreciate is the preparation of the commonly used drug Ibuprofen. Whilst the original synthesis required six steps<sup>[69]</sup> to reach the target molecule, by utilising a mixed-metal base containing an organolithium reagent (BuLi, <sup>t</sup>BuOK) the number of steps required can be decreased to three,<sup>[70]</sup> as shown in Scheme 1.4. The overall process contains three sequential deprotonation reactions, regioselective in each case followed by electrophilic quenching to build upon the scaffold molecule. Moving away from pharmaceutical compounds and highlighting the versatility of such reagents, organolithiums can also be utilised in the preparation of rubber and plastics due to their ability to act as initiators in polymerisation reactions,<sup>[71]</sup> as well as in the synthesis of dyes,<sup>[72]</sup> agrochemicals<sup>[73]</sup> and electronic materials<sup>[74]</sup> (particularly lithium batteries which have become one of the major applications of organolithium reagents<sup>[75]</sup>).



Scheme 1.4. The multi-use of an organolithium reagent in the synthesis of Ibuprofen.

While their superior reactivity has firmly placed organolithium compounds on the benches of most synthetic laboratories, these reagents do not come without their disadvantages. There is a general requirement for sub-ambient temperatures to be used (especially when working with the more reactive branched alkyl lithium compound <sup>t</sup>BuLi) in order to suppress the high reactivity of the reagents. As a result cryogenic cooling systems are often required, which are expensive both in terms of money and energy; maintaining reaction temperatures of below -40°C can cost upwards of £250K per batch process per year.<sup>[76]</sup> Secondly, such reagents are often incompatible with the common ethereal solvents used for reactions, an example being the degradation of THF<sup>[77]</sup> (Scheme 1.5). When attacked by alkyl lithium reagents, RLi (R = Me, <sup>t</sup>Bu, <sup>n</sup>Bu), the THF molecule is first deprotonated at the C-2 position ( $\alpha$  to oxygen) and the resulting furyl anion subsequently undergoes a reverse [3 + 2] cycloaddition, generating the lithium enolate of acetaldehyde and eliminating ethene. In special cases where RLi-HMPA (HMPA = hexamethylphosphoramide) mixtures are used, the THF ring is opened, but all five ring atoms are retained,

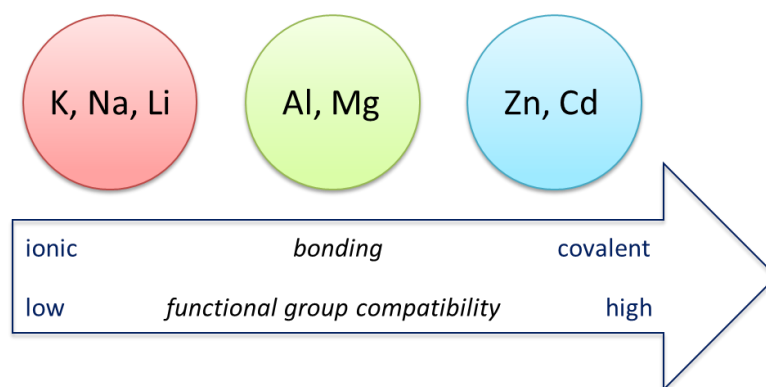
giving a lithium but-3-en-1-oxide chain.<sup>[78-79]</sup> Adding to the list, organolithium reagents also suffer from poor functional group tolerance meaning any sensitive functional groups the substrates may possess (for example carbonyl or cyano groups) are often prone to (nucleophilic) attack. Furthermore, the lithioaromatic intermediates formed from metallation suffer from low stability and indeed to ensure metallation is the outcome of the reaction, competitive reactions such as nucleophilic addition must also be avoided.<sup>[12]</sup>



Scheme 1.5. Two possible decomposition outcomes for metallated THF.

### 1.2.2 Alternative Organometallic Reagents

Switching focus now from lithium and moving across the periodic table in search of other applicable metals allows access to a wider range of organometallic compounds. Metals such as magnesium, zinc and aluminium can be easily substituted for lithium, though rather unsurprisingly switching the metal centre can have a significant impact on the reactivity of the generated organometallic species. On moving from the alkali metals towards the less electropositive metals the nature of the bonding changes from being predominately ionic in nature to a more covalent type bond (Scheme 1.6).

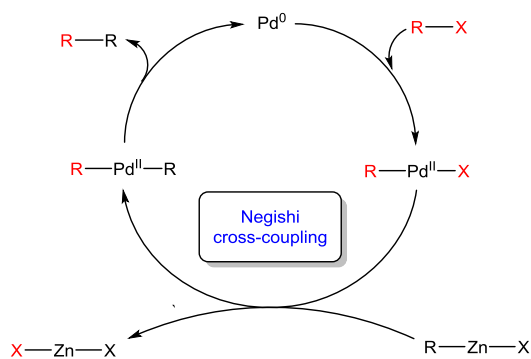
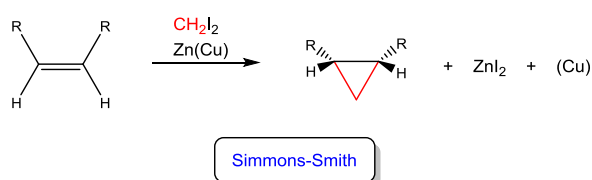
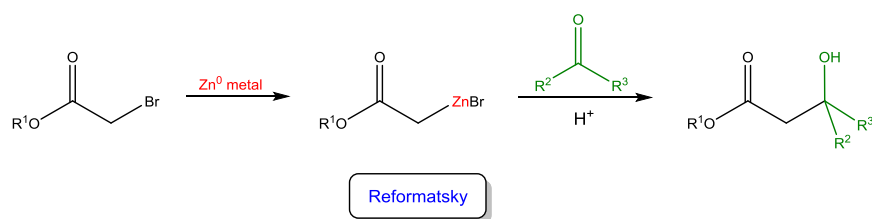


Scheme 1.6. Relative scale of bonding character and functional group tolerance of selected organometallic species.

Hand in hand with this alteration in bonding is an alteration in the reactivity and hence functional group tolerance of the organometallic species. If we move across the d-block to zinc (albeit a  $d^{10}$  element, often considered more akin to Mg than its fellow d-block metals) for example then organozinc compounds can readily be synthesised and indeed have long been a foundation of organometallic chemistry. They date back as far as 1849<sup>[80]</sup> when Frankland fortuitously discovered that heating ethyl iodide with granulated zinc produced a mixture of diethylzinc,  $ZnEt_2$  and ethylzinc iodide,  $EtZnI$ . With this finding Frankland had not only discovered the first organozinc compounds, but since zinc can be classed as a pseudo main-group metal<sup>[14]</sup> this could be considered as representing the first known example of a main-group organometallic compound.<sup>[81]</sup> Such organozinc compounds are key reagents in many fundamental organic reactions due to their “soft nucleophilicity” and hence compatibility in various reactions (e.g., addition and transmetallation), a result of the greater covalent character of a Zn-C bond than a respective Li-C bond. Most notably organozinc compounds have been used in the vital area of C-C bond formation (Scheme 1.7), having applications in the Reformatsky reaction,<sup>[82]</sup> whereby a  $\sigma$ -haloester is converted into a  $\beta$ -hydroxyester; the Simmons-Smith<sup>[83]</sup> reaction where an alkene is transformed into the corresponding cyclopropane; and perhaps most famously in cross-coupling

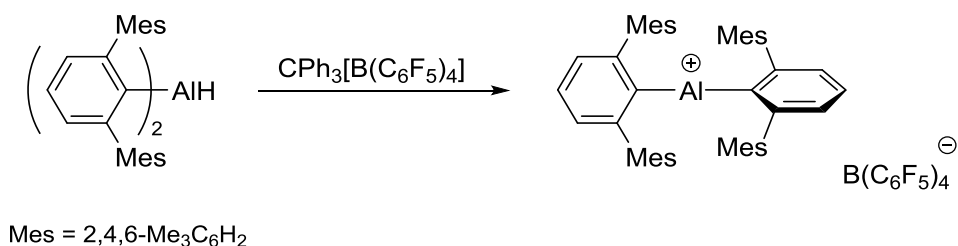


reactions<sup>[84-85]</sup> [with the Nobel Prize in Chemistry in 2010 being awarded to E. Negishi (jointly with R.F. Heck and A. Suzuki) for his pioneering research into cross-coupling reactions using organozinc reagents]. The Reformatsky reaction also highlights nicely the superior functional group tolerance of organozinc compounds with respect to organoalkali-metal reagents, as the sensitive ester functionality, which would normally be irreversibly destroyed if using the more aggressive organolithium or organomagnesium reagents, is in this case preserved. This increased tolerance for sensitive functional groups however can only arise from a decrease in the reactivity of the organometallic species and therefore despite the success of organozinc reagents in the aforementioned fields, such compounds are rarely competitive with the more polar organometallic compounds when it comes to deprotonation reactions, as they are simply not strong enough bases.



Scheme 1.7. Three named important C-C bond forming reactions utilising organozinc reagents.

Continuing across the periodic table we reach the first p-block group, namely group 13 in which lies aluminium. With a number of associated advantages including but not limited to its high natural abundance and low toxicity, aluminium is a desirable metal for use in organometallic compounds. As with the zinc systems, organoaluminium reagents offer improved reaction conditions over their group 1 competitors, and have therefore found extensive use in several branches of chemistry. For example, trialkylaluminium compounds such as  $\text{AlEt}_3$  were first synthesised by Ziegler, who also found an application for them as co-catalysts in olefin polymerisation reactions, and subsequently went on to win the Nobel Prize in 1963 (shared with Giulio Natta).<sup>[86]</sup> The citation for the Nobel Prize read “for their discoveries in the field of the chemistry and technology of high polymers”. To this day a significant proportion of the world’s polyolefins (millions of tons per year) are produced from the Ziegler-Natta process.<sup>[87]</sup> Since their discovery, organoaluminium compounds have found a large number of uses in important industrial reactions. This is mirrored in the huge production of alkylaluminium compounds, with  $\text{AlMe}_3$  holding the title as the world’s most important tonnage organometallic reagent.<sup>[88-89]</sup> Saudi Organometallics Chemicals Company have also recently opened a new aluminium alkyls production facility in Saudi Arabia, with a production capacity of 6000 tons of  $\text{AlEt}_3$  per year.<sup>[90]</sup> Rather interestingly, not all useful Al reagents are neutral or anionic, as low-coordinate aluminium cations are also known (Scheme 1.8). Such compounds, accessible by surrounding the electronically unsaturated metal centre by bulky ligands, can be used for example in the oligomerisation of alkenes.



Scheme 1.8. Generation of low-coordinate aluminium cations by employing sterically hindered ligands.

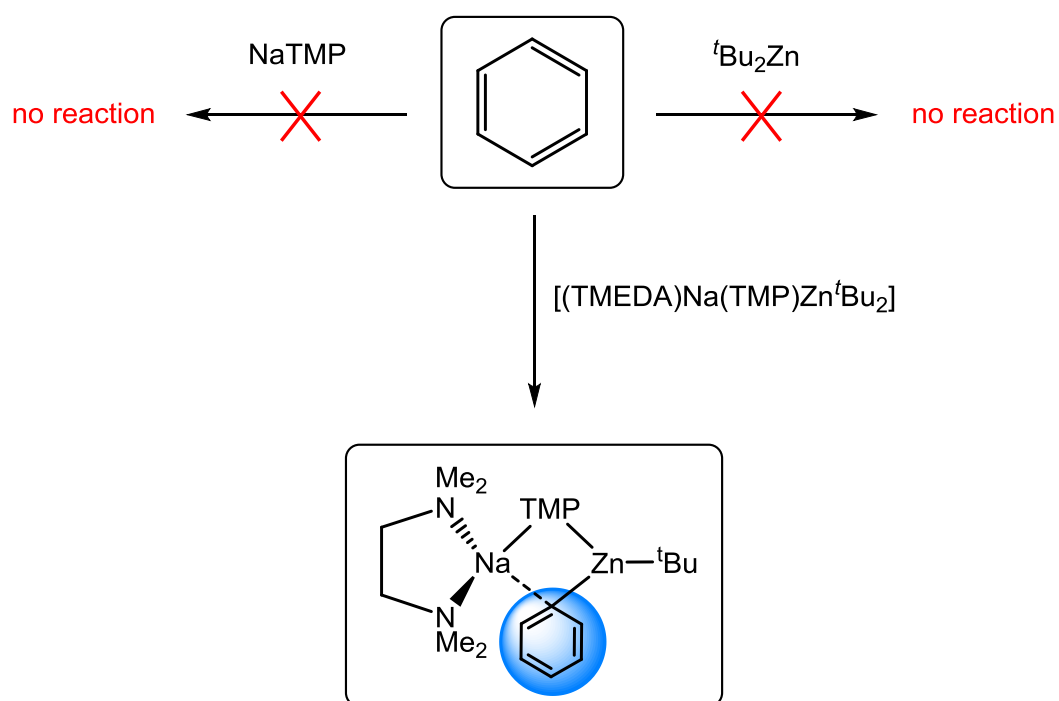
Recently the first example of an iron-catalysed, aluminium containing system, a variant on the Negishi cross-coupling was reported,<sup>[91]</sup> but in this case without the need for the costly palladium catalyst. Also, aluminium alkyls are involved in the production of “Ziegler alcohols”, which are biodegradable alcohols used for making surfactants and washing powders.<sup>[87]</sup> Interestingly, before the Ziegler alcohols were created the synthesis involved the hydration of terminal alkenes and led to secondary alcohols which can accumulate in waste water and remain in the environment due to their slow decomposition.<sup>[87]</sup> In common with the zinc systems though, there have not been significant advances in using monometallic organoaluminium compounds for metallation purposes due to the lower polarity of Al-C bonds. Chapter 3 will deal with the results obtained in this PhD study using bimetallic aluminium containing systems, and therefore further information can be found on organoaluminium reagents in Section 3.2.

Hopefully the first half of this chapter has demonstrated that while monometallic compounds are dominant in the field of organometallic chemistry and are indeed the roots of such a seminal area, no single reagent is free from its shortcomings. There is always room for growth and enhancement and hopefully the second half of this chapter can persuade that one way forward lies in the evolution of bimetallic compounds.

### 1.3 Heterobimetallic Metallating Agents

As detailed already, monometallic metallating agents play a pivotal role in the field of organometallic chemistry. Organolithium reagents for example provide excellent reactivity; whereas softer organozinc compounds are called upon when good functional group tolerance is more important. This being said, no single monometallic species possesses all the desired qualities of a metallating agent, and therefore the attention of many renowned research groups around the world [for example, in Germany (Knochel), France (Mongin), Japan (Kondo

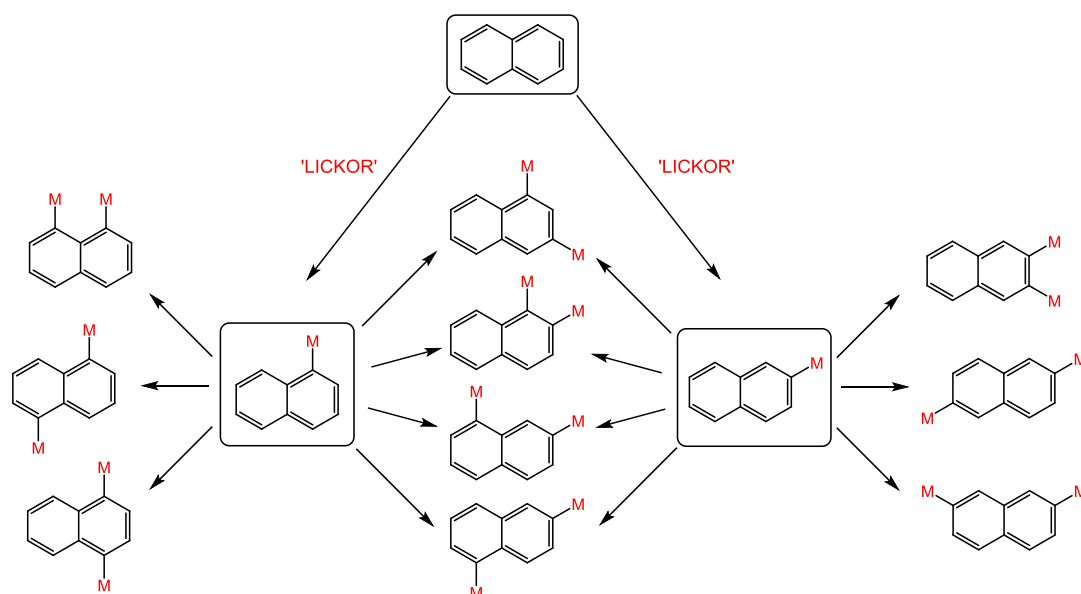
and Uchiyama) and the UK (Mulvey and Wheatley)] is now focused primarily on bimetallic or more accurately multicomponent systems. As the term suggests such bimetallic mixtures combine two different monometallic compounds into the one heterobimetallic system, often generating a new type of mixed-metal reagent. In such complexes the two metals work together in the company of appropriate ligands creating a unique synergic or synergistic effect, and in doing so allow the selling points of both classes of compounds to be exploited. As a direct result, new (improved) reactivities and selectivities, which neither of the homometallic counterparts can replicate, are therefore accessible. As an example, neither NaTMP nor  $t\text{Bu}_2\text{Zn}$  can perform the deprotonation of benzene unilaterally, but when combined into a single heterobimetallic compound one of the H atoms of the aromatic molecule is easily removed generating the phenyl  $\text{C}_6\text{H}_5$  anion (Scheme 1.9).



Scheme 1.9. Comparison between homometallic compounds and their bimetallic modification towards benzene deprotonation.

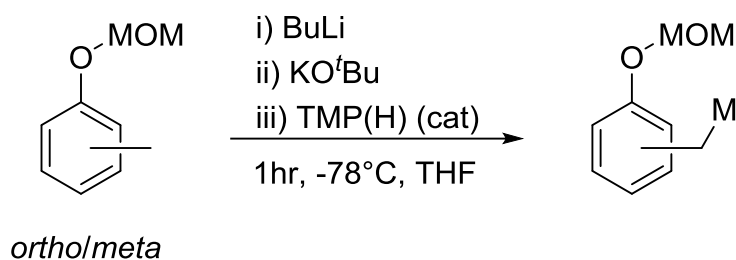
### 1.3.1 Mixed Alkali Metal Reagents

A well-known example of a bimetallic reagent is the Lochmann-Schlosser Superbase. In the late 1960s both Lochmann<sup>[92]</sup> and Schlosser<sup>[93]</sup> independently discovered that an equimolar mixture of *n*-butyllithium and potassium *tert*-butoxide formed a superbasic reagent in which the basicity of the lithium reagent was greatly enhanced compared to that of *n*-butyllithium. This new reagent displayed high metallating capabilities that neither of the two monometallic components could match, having a reactivity that lies between that of butyllithium and butylpotassium (note that although butylpotassium is more reactive, its reactivity is often too high and leads to undesired side reactions). This finding led to the generic label 'LIC-KOR'<sup>[94]</sup> being used for such reagents where 'LIC' corresponds to the alkyl lithium reagent and 'KOR' denotes the potassium alkoxide, with the most commonly utilised combination being the aforementioned *n*BuLi and KO<sup>t</sup>Bu. These superbasic reagents are capable of deprotonating molecules in the low-acidity, high pK<sub>a</sub> range (pK<sub>a</sub> 35 – 50) for example arylalkanes<sup>[92, 95]</sup> and alkenes.<sup>[92-93]</sup> Trifluoromethylbenzene for example can be readily metallated in the *ortho* position to give better yields and regioselectivities using the LIC-KOR superbase<sup>[96]</sup> than those obtained via *n*BuLi<sup>[97-98]</sup> alone. Coupled with this high reactivity though can be the sometimes unwanted outcome of poly-metallation where the substrate is metallated more than once. As an exemplar, the LIC-KOR superbase can metallate the bicyclic hydrocarbon naphthalene in hexane in either the 1- or 2- position and upon a second metallation step can lead to a mixture of up to ten distinct dimetallated products (Scheme 1.10), as well a significant amount of trimetallated product.<sup>[99]</sup>



Scheme 1.10. Mixture of metallated and dimetallated naphthalene products obtained using the LIC-KOR superbase.

A recent extension of the LIC-KOR superbase is the “LiNK” reagent developed by O’Shea.<sup>[100]</sup> This involves adding TMP(H) into the <sup>n</sup>BuLi/KO<sup>t</sup>Bu bimetallic mixture to generate a putative mixed-metal amide base. The new “LiNK” reagent was subsequently found to offer improved regioselectivity over its LIC-KOR predecessor, with in some cases TMP(H) only being required in sub-stoichiometric quantities. Scheme 1.11 shows an example of this with OMOM-substituted toluenes. With the OMOM (O-methoxymethylether) group being a strong *ortho*-directing group, the outcome of the metallation reaction when using the LIC-KOR mixture is the *ortho*-metallated product. However, adding just a small amount of TMP(H) (10%) into the mixture generates exclusively the alternative benzylic-metallated product.<sup>[100]</sup>



Scheme 1.11. Use of the “LiNK” reagent with catalytic quantities of TMP(H) to perform benzylic-metallation of OMOM-substituted toluenes.

### 1.3.2 Mixed Metal Reagents

Whilst the two mixed alkali metal reagents discussed in Section 1.3.1 have made important contributions to metallation chemistry, the reagents which are of key focus in this PhD research project are those of mixed-metal systems, where the second metal is not an alkali metal. For the sake of brevity a few such compounds will now be discussed, however the reader should be aware that the variations possible within such structures allow for a vast number of reagents to be synthesised and therefore this section of the thesis can only skim the surface of developments made to date.

On top of combining two alkali metal compounds together there is also the option to form heterobimetallic compounds by amalgamating a hard alkali metal (usually Li, Na or K) with a softer main group metal (e.g., Mg, Zn or Al) or transition metal (e.g., Mn or Fe) and a ligand set.<sup>[9-12, 14]</sup> Such multicomponent systems advantageously combine the high reactivity of polar group one organometallic reagents, under milder conditions, with the high selectivities and diverse functional group tolerance obtainable with the less polar organometallic reagents. Whilst the alkali metal is a vital component (without it the same chemistry could not be achieved), it is in fact (rather counter-intuitively) the softer, less electropositive metal that actually performs the deprotonation of the substrate. Often this is due to a special cooperative effect whereby the two metals communicate intramolecularly through ligand bridges.

By using these bases, metallations which the homometallic reagents are incapable of executing single-handedly can readily be performed. These unique metallations have been termed alkali-metal-mediated metallations (AMMM), where the italicised *M* represents the metal that performs the C-H to C-metal transformation. In a nutshell, the chemistry accessible by these mixed-metal compounds displays neither typical alkali metal nor typical Mg/Zn/Al etc. chemistry, but a new wholly distinct class of chemistry, that is best described as synergic or synergistic.

The term “ate” was coined by Wittig<sup>[101-102]</sup> in the mid-1900s to describe such compounds where an anionic metal fragment is present and is still in popular usage in journal articles and textbooks today. Wittig perceptively noticed that the triphenyl compounds LiZnPh<sub>3</sub> and LiMgPh<sub>3</sub> were capable of performing chemistry that neither of their two homometallic components could reproduce, which he attributed to the activation of Mg and Zn by the three surrounding anionic phenyl ligands. Alkali-metal ate compounds have long been known and in fact the first such compound was prepared almost a century before the name ‘ate’ was given and almost six decades before the renowned discovery of neutral organo-lithium and -sodium compounds by Schlenk.<sup>[25]</sup> The compound was the sodium trialkylzincate NaZnEt<sub>3</sub> and was prepared by Wanklyn in 1858.<sup>[103]</sup> He did so by reacting the zinc reagent diethylzinc (which interestingly his own supervisor Frankland had made a few years previously) with sodium metal. Since this seminal point in the history of organometallic chemistry synthetic chemists have proceeded to synthesise a wide range of zincate and other metallic ate compounds of various stoichiometries and structures.

Typically, 1:1 ate reagents have the general formula (AM)MR<sub>x</sub> where AM denotes the alkali metal, M denotes the softer more carbophilic metal and x is equal to 3 (for Mg and Zn compounds) or 4 (for Al compounds) (note that other stoichiometries are possible, vide infra).<sup>[14]</sup> Within such bimetallic systems the anionic charge lies on the fragment of the molecule containing the less electropositive metal due to the increase in electronegativity (Zn = 1.6 > Mg =



$1.2 > \text{Li} = 1.0$ )<sup>[104]</sup> resulting in the general  $[\text{AM}]^+[\text{MR}_x]^-$  formula. There are two possible structural combinations for these ate compounds – namely a contacted ion-pair (CIP) or a solvent-separated ion-pair (SSIP).<sup>[105]</sup> In the former both metals are connected through bridging anionic ligands; whereas in the latter the alkali metal, solvated by either a donor solvent or a stoichiometrically added Lewis base, constitutes the cationic part of the molecule and the subordinate metal, surrounded by anionic ligands, forms the counterion. One general structural design for a contacted ion-pair is shown in Figure 1.6. The three individual components that come together to form the CIP are highlighted; that is the alkali-metal amide, the neutral metal amide or alkyl compound and finally a donor molecule to solvate the alkali metal hindering polymerisation of the bimetallic compound (which would render the base insoluble). The number of anionic ligands present depends on the valency of the subordinate metal and both alkyl and amido groups can be utilised generating heteroleptic (that is, mixed ligand) systems.

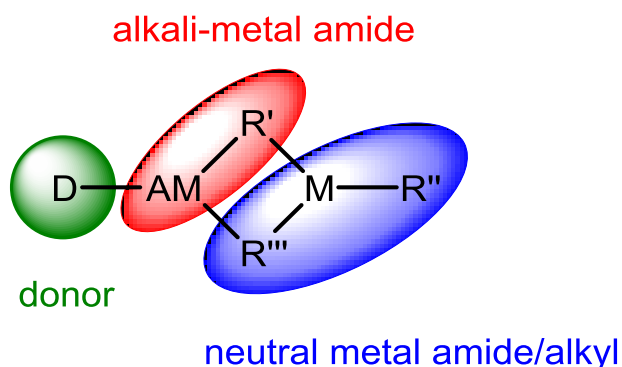


Figure 1.6. One general structure of a contacted ion-pair heterobimetallic compound.

With regards to whether a CIP or SSIP structure is adopted, the collection of solvent, donor and substituents all play a contributing role.<sup>[105]</sup> An example of the often fine balance between these structural types is provided by the triorganozincate  $\text{LiZnMe}_3$  which switches from a CIP to a SSIP structure simply by changing the donor solvent from tridentate amine PMDETA to the analogous



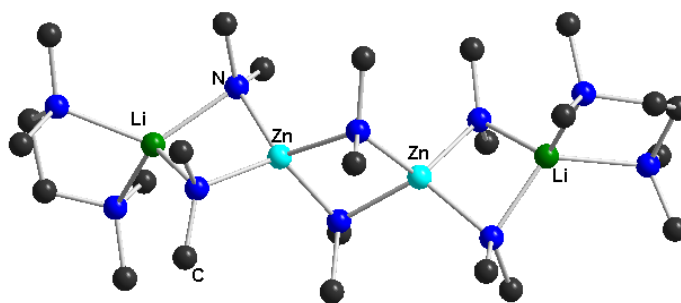


Figure 1.8. Molecular structure of the crystalline dimeric triorganoamidozincate  $[\{(TMEDA)LiZn(NMe_2)_3\}_2]$ .

Many permutations of different metals and different ligands have been investigated for use in such bimetallic compounds however those that have shown the most potential often involve zinc, aluminium or magnesium. Such systems have found great promise in the art of proton abstraction, having recently featured in world-leading journals with publications in one of the top chemistry based journals *Nature Chemistry*<sup>[79]</sup> as well as the all-encompassing highly prestigious journal *Science*.<sup>[108-109]</sup> While there are many ate bases available at our disposal, the results contained in this thesis are based around those systems which merge an alkali metal with either zinc or aluminium. Hence, for compactness this section will focus on a few of the zinc systems that have already found excellent use in the field of deprotometallation chemistry, capable of functionalising substrates at positions not accessible by either organolithium or organomagnesium species.<sup>[106]</sup> A discussion of the commonly used aluminium bases will be given in Chapter 3.

Organozincate compounds can exist usually in one of two stoichiometries; triorganozincates,  $[M^+ZnR_3^-]$  where the M:Zn ratio is 1:1 or tetraorganozincates,  $[M_2^{2+}ZnR_4^{2-}]$  where now the M:Zn ratio is 2:1, sometimes termed lower and higher order zincates respectively (Figure 1.9).<sup>[107, 110-112]</sup> In this example of a lower order zincate the zinc centre is surrounded by three anionic ligands meaning only one alkali metal is required for charge balance. However, in the

higher order ate four ligands are present around the zinc meaning now two charge-neutralising alkali metal counter-cations are needed. Which order the zincate adopts is dependent on how many (mono)anionic ligands are present around the zinc centre. Moving away from these common stoichiometries, Carmona has recently prepared a zincate with the stoichiometry  $M^+Zn_2R_5^-$  where R is  $C_5H_5$ ,<sup>[113]</sup> while Hevia has prepared both homoleptic ( $M^+Zn_2R_5^-$ ) and heteroleptic ( $M^+Zn_2R_3R'_2^-$ ) “zinc-rich” zincates where R is  $C_2H_5$  and Me respectively and R' is (NHDipp).<sup>[114-115]</sup>

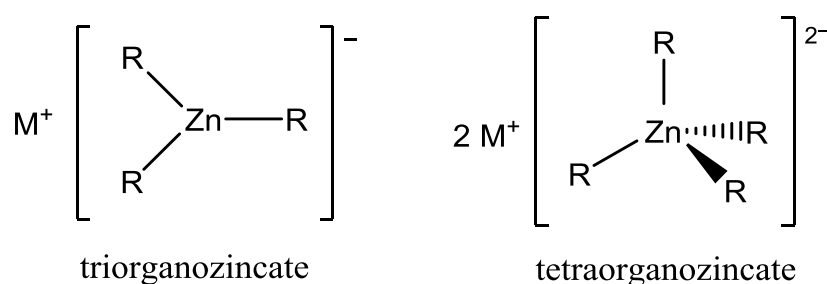
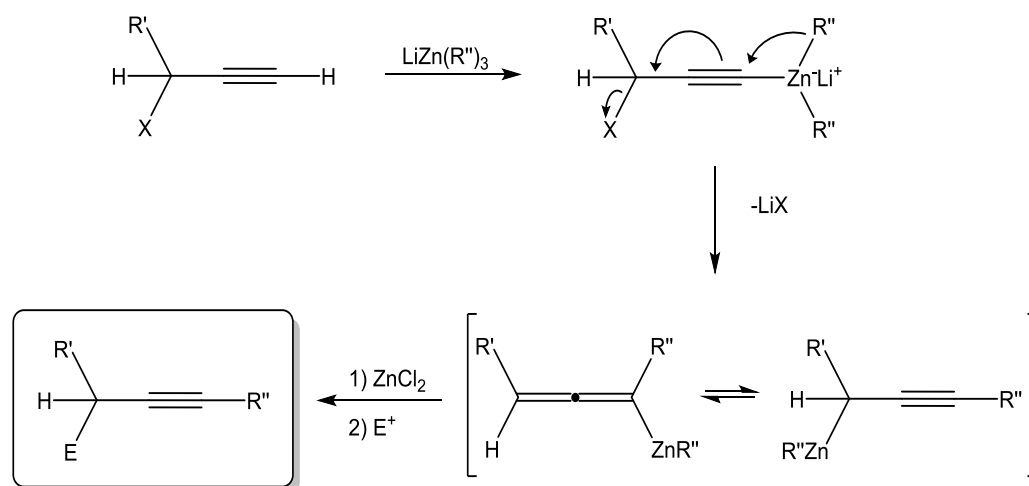


Figure 1.9. Empirical molecular formulations for general triorganozincates  $[MZnR_3]$  and tetraorganozincates  $[M_2ZnR_4]$  (R = anionic ligand, M = group 1 metal).

The first deprotonation reactions using zincates were only performed as recently as 1993<sup>[116]</sup> and employed triorganozincates (such as  $LiZnMe_3$  and  $LiZnBu_3$ ) in the metallation of alkynyl mesylates and chlorides. Deprotonation occurred on the terminal alkynyl hydrogen to generate an alkynyl zincate which then undergoes a 1,2-migration, with loss of the alkali metal, to yield the homometallic zinc intermediate product. Subsequent quenching with electrophiles allowed selective substitution at the  $\gamma$ -position (Scheme 1.13).

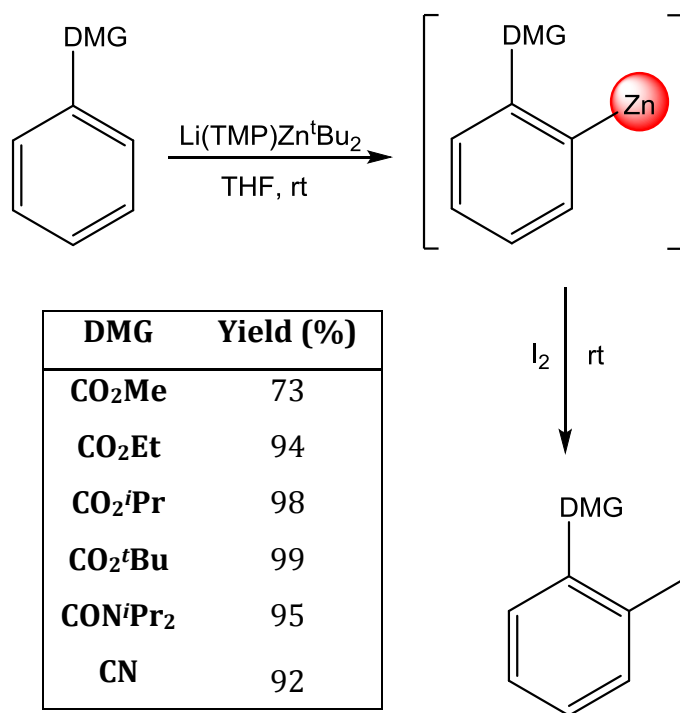


Scheme 1.13. Deprotonative zincate-induced metallation of alkynes, generating an allenyl zinc compound that is subsequently intercepted by an electrophile (e.g.,  $\text{R}' = \text{C}_8\text{H}_{17}$ ;  $\text{R}'' = \text{Bu}$ ).

While this particular reaction introduced lithium zincates into deprotonative metallation chemistry, most breakthroughs to date have been achieved not by homoleptic zincates, but heteroleptic variants (that is where the ligand set coordinating the metal has different ligands). Comprehensively studied, the homoleptic alkyl zincates  $\text{LiZnMe}_3$ ,  $\text{Li}_2\text{ZnMe}_4$  and  $\text{LiZn}^t\text{Bu}_3$ , have been shown to be valuable reagents, not for deprotonation reactions but instead for metal-halogen exchange,<sup>[111, 117-119]</sup> inter- and intra-molecular epoxide ring opening<sup>[110-111]</sup> and nucleophilic addition<sup>[120-121]</sup> applications. Prevalent in organometallic chemistry and specifically in heteroleptic zincate chemistry is the bulky TMP anion. Possessing four methyl groups which surround the nitrogen centre and containing only saturated  $\text{sp}^3$ -carbon atoms carrying electron-donating substituents, the nitrogen atom retains much of its formal negative charge. This complementary combination of steric shielding and electronic enhancement promotes the desired qualities of low nucleophilicity and high Brønsted basicity, making TMP a highly effective base. In addition, the molecule possesses no  $\beta$ -hydrogen atoms, averting the possibility of unwanted side reactions; for instance  $\beta$ -elimination can occur in other commonly used

amides most notably diisopropylamide. These advantages of TMP mean it is incorporated into most of the successful heteroleptic zincate reagents known to date.

Kondo and co-workers<sup>[122]</sup> have demonstrated that  $\text{LiZn}^t\text{Bu}_3$  showed enhanced reactivity in metal-halogen exchange reactions compared to that of  $\text{LiZnMe}_3$  and  $\text{Li}_2\text{ZnMe}_4$ ; while previously Upton and Beak<sup>[123]</sup> have shown that lithium-TMP can be used to metallate a variety of arylcarboxylic esters. A few years after his work with  $\text{LiZn}^t\text{Bu}_3$ , Kondo cleverly decided to integrate these discrete compounds by developing a heteroleptic lithium dialkyl-amidozincate, of empirical formula  $[\text{Li}(\text{TMP})\text{Zn}(^t\text{Bu})_2]$ , made from the co-complexation reaction of lithium-TMP with di-*t*-butylzinc (itself prepared by salt metathesis from  $\text{ZnCl}_2$  and  $^t\text{BuLi}$ ). With this TMP-zincate, the authors were able to efficiently *ortho*-metallate a variety of functionalised aromatics and subsequently quench the metallic intermediates with iodine yielding the iodobenzenes in impressive yields of up to 99% (Scheme 1.14).<sup>[6]</sup> Interestingly,  $\alpha$ -metallation of sensitive  $\pi$ -deficient heteroaromatic compounds was also feasible with this zincate, as pyridine, quinoline and isoquinoline were all likewise successfully metallated. The results obtained were also an improvement over previously reported work as pyridine could be selectively deprotonated at the 2-position in a yield of 76%; whereas Verbeek<sup>[124]</sup> had shown that when using the combination of  $^n\text{BuLi}$  and  $\text{KO}^t\text{Bu}$  (the LIC-KOR superbases<sup>[7, 94]</sup>) deprotonation did ensue but in an unselective way giving a complicated mixture of the 2-, 3- and 4- substituted products in an approximate ratio of 4:1:4.



Scheme 1.14. *Ortho*-metallation of functionalised aromatics using the heteroleptic TMP-zincate  $[\text{Li}(\text{TMP})\text{Zn}(\text{tBu})_2]$  and subsequent electrophilic quenching with iodine.

Whilst Kondo developed the reaction chemistry of this dialkyl-amido zincate, there had been no characterisation of it in its own right and hence no evidence for its possible structure. This situation was changed when Mulvey and co-workers synthesised and characterised a compound from the TMP-zincate reagent mixture, and using X-ray crystallography were able to report its molecular structure.<sup>[125]</sup> Kondo had proposed the empirical formula,  $\text{Li}^+\text{Zn}(\text{TMP})(\text{tBu})_2^-$ , **1.1** (Figure 1.10) however as the X-ray crystallographic data provided by Mulvey show, one molecule of THF is also included in the structure. Thus the base or at least one form of it exists as a contacted ion-pair species  $[(\text{THF})\text{Li}(\mu\text{-TMP})(\mu\text{-tBu})\text{Zn}(\text{tBu})]$ , **1.2** in which the Li and Zn metal centres connect through bridging TMP and <sup>t</sup>Bu groups (Figure 1.10).

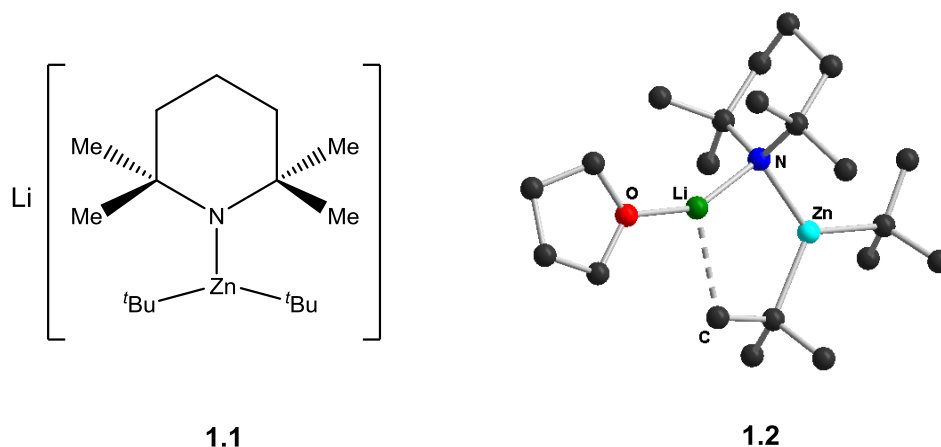


Figure 1.10. Proposed empirical formula of **1.1**, and its characterised molecular structure,  $[(\text{THF})\text{Li}(\mu\text{-TMP})(\mu\text{-}^t\text{Bu})\text{Zn}(^t\text{Bu})]$  **1.2**, in the presence of THF.

Studying the reaction of zincate **1.2** in hexane with the benchmark deprotonatable substrate anisole affords isolable crystals, which when analysed by X-ray crystallography showed a structure similar to the parent zincate (Figure 1.11).<sup>[126]</sup> While the TMP anion remains a bridge between the two metals, in contrast the bridging  $^t\text{Bu}$  group has been replaced by an *ortho*-metallated bifunctional (C, O) anisole molecule. The zinc centre interacts with the newly generated carbanion while the lithium coordinates to the methoxy substituent of the anisoyl ligand. The loss of a  $^t\text{Bu}$  anion from the system as isobutane indicates the zincate has a preference for acting as an alkyl base overall. A key advantage of such a bimetallic system is that sensitive electrophilic functional groups such as amides  $\text{CONR}_2$  or nitriles  $\text{CN}$ , which would rapidly be attacked by organolithium reagents, are left untouched even at ambient temperatures.<sup>[6]</sup>



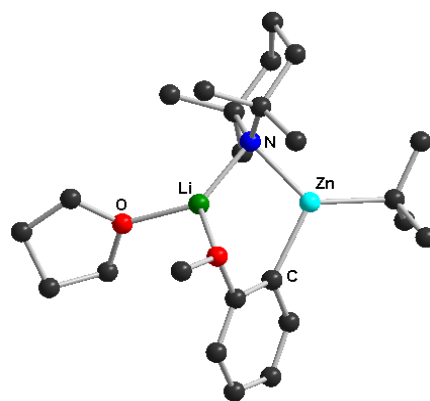


Figure 1.11. Molecular structure of heterotrileptic  $[(\text{THF})\text{Li}(\text{TMP})(o\text{-C}_6\text{H}_4\text{OMe})\text{Zn}(t\text{Bu})]$  by reacting  $[(\text{THF})\text{Li}(\mu\text{-TMP})(\mu\text{-}t\text{Bu})\text{Zn}(t\text{Bu})]$  with anisole.

An analogous zincate, to that prepared by Kondo, was synthesised in 2005 by Mulvey and co-workers – namely the sodium zincate  $[(\text{TMEDA})\text{Na}(\mu\text{-TMP})(\mu\text{-}t\text{Bu})\text{Zn}(t\text{Bu})]$ , **1.3**.<sup>[127]</sup> This compound bears a strong structural resemblance to Kondo's zincate with bridging TMP and  $t\text{Bu}$  groups; however in this case the larger sodium centre allows for chelation by the bidentate donor ligand TMEDA, which keeps the structure molecular and hence the compound soluble in a range of organic solvents. Figure 1.12 shows the crystal structure of this sodium dialkyl-amidozincate.

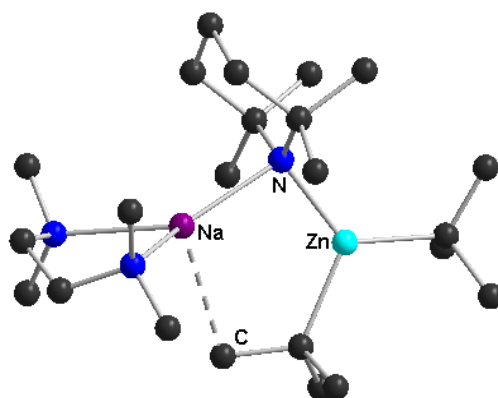


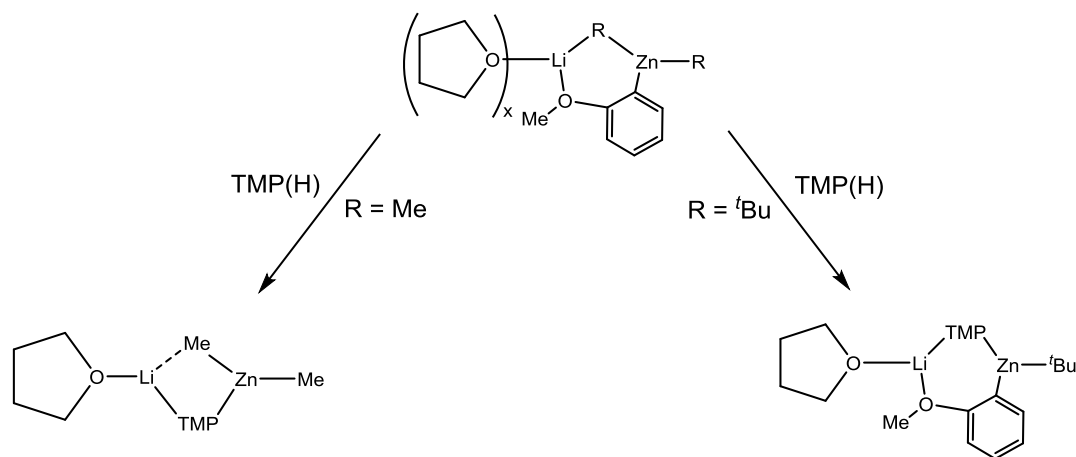
Figure 1.12. Molecular structure of the sodium zincate reagent  $[(\text{TMEDA})\text{Na}(\mu\text{-TMP})(\mu\text{-}t\text{Bu})\text{Zn}(t\text{Bu})]$  **1.3**.

Sodium zincate **1.3** exhibits a fascinating reactivity towards a whole range of organic substrates, with the alkali-metal-mediated zincation (AMMZn) of benzene,<sup>[127]</sup> toluene,<sup>[128]</sup> aniline,<sup>[129-130]</sup> naphthalene<sup>[131]</sup> as well as of benzamides,<sup>[132-133]</sup> carbamates,<sup>[133]</sup> aromatic ethers<sup>[134]</sup> and N-heterocyclic aromatic compounds<sup>[135]</sup> (Scheme 1.15). Note in particular the unusual *meta*-orientation of the metallation observed when aniline is used as the substrate; the mixture of *meta/para*-metallation when using toluene; and the dimetallation of both benzene and naphthalene; none of which are achievable with conventional organolithium or organozinc reagents. Such unique *meta*-metallation observed for aniline highlights the cooperativity at work between the sodium and zinc, as the dimethylamido functional group, being a weak *ortho*-directing group, would generate the *ortho*-metallated product when using conventional alkali-metal reagents.<sup>[136]</sup>

The reactions shown in Scheme 1.15 can be classed at least formally as deprotozincations (C-H to C-Zn) since the final products have the less electropositive metal engaging with the deprotonated substrate. Overall the sodium zincate acts as an alkyl base since the TMP ligand remains in the final structure whilst the *tert*-butyl ligand is lost as it cleaves a proton to form gaseous *isobutane*. However, mechanistically the reaction is more complicated as the zincate actually reacts in a two-step manner, as first proposed by Uchiyama in 2008.<sup>[137]</sup> His theoretical studies carried out on the simplified model [(TMEDA)Na(NMe<sub>2</sub>)ZnMe<sub>2</sub>] show that the initial deprotonation of the organic substance is more kinetically favourable (that is requires a lower activation barrier) when the amido (TMP) ligand is responsible, perhaps unsurprisingly given the greater polarity and hence lability of the Zn-N bond over its Zn-C counterpart. The mechanism for the overall reaction is therefore a two-step process where first the TMP ligand acts as a base and performs the deprotonation of the substrate. In the second step, TMP(H) re-enters the complex as the thermodynamically driven protonation of the alkyl ligand (*t*Bu) ensues, forming *isobutane* which eliminates to make the reaction irreversible.



substrate. However, with the *tert*-butyl version of the compound TMP(H) displaced one of the alkyl ligands during its transformation into the TMP anion, to give the alkylamido zincate, demonstrating the anticipated stronger basicity of the bulkier *tert*-butyl groups in comparison with methyl groups.



Scheme 1.16. Reaction of postulated lithium zincate intermediates with TMP(H).

A prestigious result, published in *Science*,<sup>[108]</sup> was recently accomplished by Mulvey and co-workers when using an analogous sodium zincate to that described above – namely,  $[(\text{TMEDA})\text{Na}(\text{TMP})\text{Zn}(\text{CH}_2\text{SiMe}_3)_2]$ . With this trimethylsilylmethyl ( $\text{Me}_3\text{SiCH}_2$ ) version of the zincate the authors were able to perform synergic sedation of sensitive anions – that is, to metallate the substrate to generate a hypersensitive anion that untypically remains fully intact. The zincate was able to metallate the cyclic ether and widely utilised solvent THF, along with its larger congener tetrahydropyran, and stabilise the emerging anions within the residue of the synergic bimetallic base. As aforementioned, when using conventional organolithium reagents deprotonation of THF commonly occurs as an unwanted side reaction. Under such unsupported lithiation (that is, without any stabilisation by a softer second metal) the developing THF anion is highly unstable due to repulsion between the negative charge formed at the  $\alpha$ -C atom and the THF O lone pairs, and hence

it spontaneously ring opens and subsequently cleaves, even at subambient temperatures. In contrast, using the sodium zincate, an  $\alpha$ -zincation (deprotonation) could be performed on the THF molecule but now the sensitive anion can be “trapped” and thus stabilised by the residue of the heterobimetallic base. As evidence of this stability, the crystal structures for both the THF and THP examples could be determined (Figure 1.13). In each case the anion can clearly be seen trapped within the bimetallic compound, with the metallated carbon exclusively bonding to the zinc, whereas the oxygen of the still cyclic ether datively coordinates to the sodium.

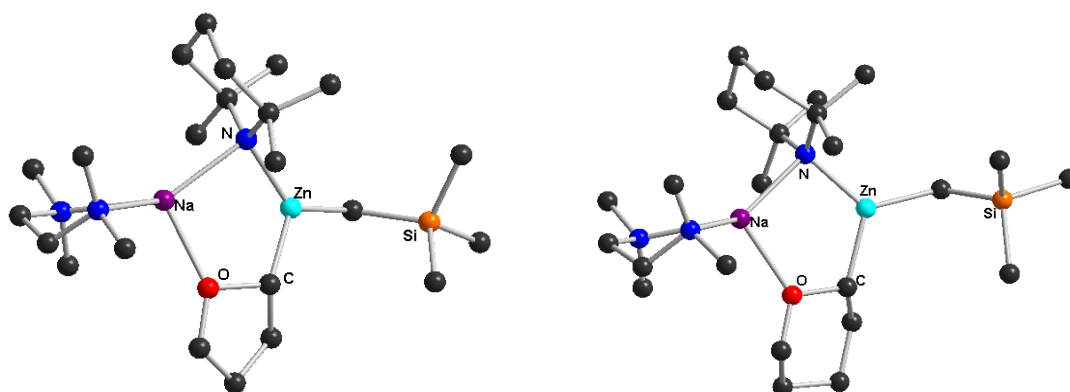


Figure 1.13. Molecular structures of  $[(\text{TMEDA})\text{Na}(\mu\text{-TMP})(\mu\text{-C}_4\text{H}_7\text{O})\text{Zn}(\text{CH}_2\text{SiMe}_3)]$  and  $[(\text{TMEDA})\text{Na}(\mu\text{-TMP})(\mu\text{-C}_5\text{H}_9\text{O})\text{Zn}(\text{CH}_2\text{SiMe}_3)]$ .

### 1.3.3 The Lithium Chloride Salt Effect

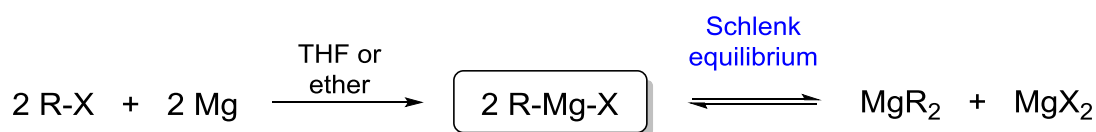
In the early 1990s the group of Seebach<sup>[139-140]</sup> published two reports on the effect of lithium-salts in peptide synthesis. They demonstrated that in peptide-coupling reactions the presence of Li-salts could greatly affect important aspects such as kinetics and racemisation. Subsequently, in more relevant studies carried out by Collum,<sup>[141]</sup> the effect that LiCl can have on the deprotonation reactions of aromatic substrates was brought to the attention of the organometallic research community. Collum and co-workers insightfully

discovered that traces of LiCl present within a reaction mixture (either introduced intentionally or unintentionally) could enhance the reaction rate considerably. Concentrations as low as 0.5 mol % (with respect to the deprotonation reagent) were found to have a noticeable effect on the rate of *ortho*-lithiation [using lithium diisopropylamide (LDA) as the base] for a variety of aromatic substrates including 1,3-dichlorobenzene and 2,6-difluoropyridine. Interestingly, it should be noted that some commercially available lithium reagents contain traces of LiCl<sup>[142]</sup> and therefore it is possible that some deprotonation reactions may have been reported without the deserved recognition for the role in which LiCl played. On the contrary however, a recent review by Mulvey and Hevia<sup>[142]</sup> has highlighted the fact that although it can have positive effects on reactions, LiCl can also play a detrimental role, hindering reactions. An example of this impedance is in the phenylations of aldehydes where the presence of LiCl can decrease a 92% enantiomeric excess (ee) to a mere 2% ee.<sup>[143]</sup> In this particular reaction the salt is present merely as a by-product from the metathesis reaction of the two starting materials (PhLi and ZnCl<sub>2</sub>) used to generate the phenylating reagent and is therefore a poignant reminder that the synthetic chemist should always consider all compounds that could be present in a reaction mixture (e.g., as a by-product or a contaminant from commercial sources) and any effect, positive or negative, they could have on the reaction pathway. This dual persona exhibited by the salt has given rise to the term “Jekyll-and-Hyde”<sup>[142]</sup> when describing its behaviour. By far, the most exploited “Jekyll” (i.e., constructive) properties have been from the group of Knochel, who have combined the salt (LiCl) with the well-known Grignard reagents, developing a new, improved class of turbo-Grignard reagents. These are described in the following section.

#### 1.3.4 Turbo-Grignard Reagents and their Hauser Base Equivalents

At the beginning of the 20<sup>th</sup> century French chemist Victor Grignard ensured himself a place in organometallic history books, by successfully inserting

magnesium metal into a carbon-halogen bond, generating an organomagnesium halide.<sup>[144]</sup> This seminal study won him a Nobel Prize in Chemistry and led to the now aptly named “Grignard reagents”, which for decades have been one of the most important and most utilised classes of organometallic reagent by both organic and inorganic chemists alike. While Grignard reagents possess the empirical formula “R-Mg-X”, studies have shown that in ethereal solutions a complex mixture of magnesium species (some in equilibrium with each other) is in fact present.<sup>[145-146]</sup> One example is the “Schlenk equilibrium”<sup>[147]</sup> which involves rearrangement of the Grignard reagent into the corresponding magnesium halide and magnesium alkyl/aryl species (Scheme 1.17). In support of this equilibrium was the finding that adding dioxane into the reaction mixture caused precipitation of the soluble  $MgX_2$  species in the form of a  $MgX_2$ -dioxane Lewis acid-Lewis base complex.<sup>[148]</sup> This particular manipulation of the Schlenk equilibrium also provides a convenient method of preparing dialkyl- or diaryl-magnesium solutions.



Scheme 1.17. General route for the preparation of Grignard reagents and the subsequent Schlenk equilibrium (disregarding aggregation effects).

Since their initial discovery Grignard reagents (as well as Hauser bases<sup>[149-150]</sup> – their amido equivalents,  $R_2N-Mg-X$ ) have been found to be valuable synthetic tools for a variety of transformations and to this day hold a prime position when it comes to carbon-carbon or carbon-heteroatom bond forming reactions.<sup>[145, 151]</sup> The group of Knochel recently extensively expanded this area of magnesium chemistry by cleverly combining LiCl (exploiting the salt-effect discussed in Section 1.3.3) with the prevalent Grignard reagents.<sup>[152]</sup> In doing so turbo-Grignard reagents were born, possessing the general formula  $RMgX \cdot LiCl$ , though

stoichiometric variants of this formula are also known. This new class of compounds acquired the “turbo” tag due to their increased reactivity, superior stereoselectivity and functional group tolerance compared to the non-salt containing original Grignard reagents.<sup>[11]</sup> Akin to these enhanced Grignard reagents, turbo versions of the Hauser bases ( $R_2NMgCl \cdot LiCl$ ) can also be prepared employing the same principle.

The first turbo-Grignard reagent, the branched alkyl derivative  $iPrMgCl \cdot LiCl$  synthesised by Knochel in 2004,<sup>[152]</sup> was used to perform Br/Mg exchange reactions. This alkyl magnesium species rapidly became a popular reagent used by many synthetic chemists, reflected in industry when it won the ‘Encyclopedia of Reagents for Organic Synthesis Best Reagent’ award in 2011,<sup>[153]</sup> and in academia with several reviews<sup>[10, 153-156]</sup> and book chapters<sup>[157-158]</sup> outlining its chemical usefulness. Another of the turbo-bases that has claimed the spotlight is the Hauser variant  $TMPMgCl \cdot LiCl$ . The demand for both these reagents is exemplified by the fact that they are commercially available from Sigma-Aldrich by the bottle.

An added advantage of the “turbo” reagents is that they possess excellent solubility in THF solutions.<sup>[11]</sup> The original Hauser bases have low solubility in THF solutions due to aggregation of the magnesium amide and as a result metallation rates of organic substrates can often be very slow. The addition of the LiCl salt though promotes solubility and this is thought to be through decreasing the aggregation state of the metal reagent. A key experimental breakthrough on the subject was obtained by Mulvey and co-workers in 2008<sup>[159]</sup> when they provided the first example of an isolated and both crystallographically and spectroscopically characterised Hauser base,  $TMPMgCl$  and its turbo-partner  $TMPMgCl \cdot LiCl$ . Following the original preparation, the Hauser base  $TMPMgCl$  was prepared in THF and using X-ray crystallography the molecular structure was determined to be  $[(THF)(TMP)Mg(\mu-Cl)_2Mg(TMP)(THF)]$  as shown in Figure 1.14, that is essentially two molecules of  $TMPMgCl$  solvated by donor THF. Interestingly though, on preparing the turbo-



Hauser reagent and studying the crystalline product obtained, it was shown that lithium was now incorporated into the tris THF solvated structure,  $[(\text{THF})_2\text{Li}(\mu\text{-Cl})_2\text{Mg}(\text{TMP})(\text{THF})]$  (Figure 1.14). This structure could equally be thought of as the combination of one molecule of  $\text{TMPMgCl}$  combined with one molecule of  $\text{LiCl}$ , with each metal coordination sphere again capped by THF. In both structures the TMP anion which is thought to be the active base component is terminal as opposed to bridging, meaning only one Mg-N bond is required to be broken to free the TMP and render it available for executing deprotonation. The authors confirmed the metallating ability of this species they had grown from the turbo-Hauser base mixture by reacting it with ethyl 3-chlorobenzoate and monitoring the metallation by NMR spectroscopy. This key result therefore established that the  $\text{LiCl}$  added to these reagents plays an integrated part in the increased reactivities observed. Presumably this could be the case in all turbo-reagents though this has not yet been established.

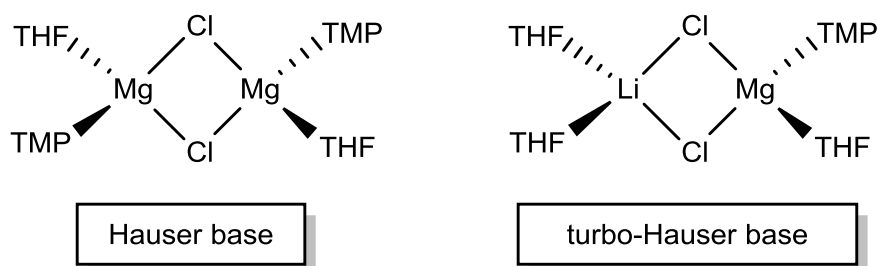


Figure 1.14. Molecular structures of the Hauser base  $[(\text{THF})(\text{TMP})\text{Mg}(\mu\text{-Cl})_2\text{Mg}(\text{TMP})(\text{THF})]$  and its turbo-Hauser relative  $[(\text{THF})_2\text{Li}(\mu\text{-Cl})_2\text{Mg}(\text{TMP})(\text{THF})]$ .

### 1.3.5 Recent Developments in Main Group Catalysis

To complete this introduction, mention must be made of the recent advances witnessed in catalysis by organic formulations of the s-block metals and the group 13 metal aluminium in processes normally considered the domain of transition metals. Activated alkenes and other unsaturated organic molecules

such as carbodiimides [RN=C=NR] and isocyanates [RN=C=O] can undergo catalytic nucleophilic addition reactions with a range of substrates that have a hydrogen atom attached to an electronegative atom, including most typically amines (primary RNH<sub>2</sub>; secondary R<sub>2</sub>NH), silanes (e.g., RSiH<sub>3</sub>) and phosphines (e.g., R<sub>2</sub>PH). Calcium compounds acting as pre-catalysts and catalysts have been especially prominent in these hydroamination,<sup>[160-162]</sup> hydrophosphination<sup>[163]</sup> and hydrosilylation<sup>[164]</sup> processes with academic group 2 specialists publishing a range of novel results. Westerhausen and co-workers<sup>[162]</sup> recently detailed the hydroamination reaction possible between diphenylbutadiyne and 2,6-diisopropylaniline when [K<sub>2</sub>Ca{N(H)Dipp}<sub>4</sub>] is employed in catalytic quantities. A few years previously the group of Hill<sup>[163]</sup> reported how the β-diketiminato complex [{HC(C(Me)<sub>2</sub>N-2,6-<sup>i</sup>Pr<sub>2</sub>C<sub>6</sub>H<sub>3</sub>)<sub>2</sub>}Ca{N(SiMe)<sub>2</sub>}(THF)] can affect the intermolecular hydrophosphination of various alkenes and alkynes, for example with the reaction of styrene and diphenylphosphine giving a 95% conversion with the addition of only 10 mol% of the Ca compound. Finally, Harder<sup>[164]</sup> published work on the hydrosilylations of alkenes using a heteroleptic half-sandwich benzylcalcium compound shown in Figure 1.15. Adding only 5 mol% of this calcium compound to a mixture of 1,1-diphenylethylene and triphenylsilane resulted in complete conversion into the hydrosilylated product after 16 hours.

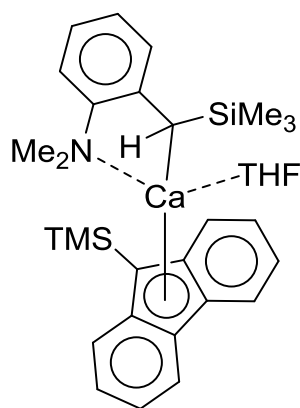
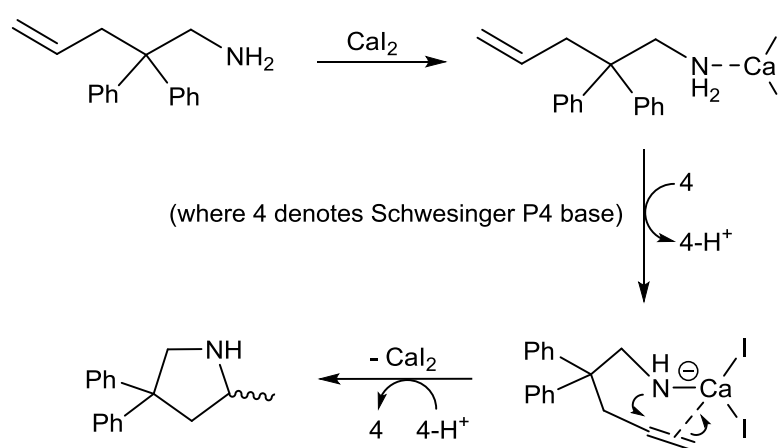


Figure 1.15. ChemDraw representation of the THF-solvated half-sandwich Ca compound used as a catalyst in hydrosilylation reactions.<sup>[164]</sup>



all under the conditions studied (5 mol%; temperature range 25 – 80 °C in benzene or THF over 3-12 days). In contrast, when calcium iodide was used as a metal additive (10 mol%) in conjunction with another metal-free base [*t*-BuN=P{N=P(NMe<sub>2</sub>)<sub>3</sub>}<sub>3</sub>], the so called Schwesinger P4 base,<sup>[166]</sup> the catalysis was facile and quantitative leading to 5-membered ring products (Scheme 1.19). Harder concluded by making the distinction that these metal-free catalytic reactions (with activated double bonds), in which the ammonium cation functions in effect as a weak metal, are examples of organocatalysis; whereas the processes (with unactivated double bonds) performed by the stronger Lewis acidic calcium are best regarded as organometallic catalysis. One important point that needs to be made in catalytic reactions of alkenes regarding the analogy of transition metal catalysts and main group s-block catalysts is that the metal interaction with the alkene is profoundly different in each case. While in the former system alkene activation occurs through a metal-alkene (d to π\*) interaction, in the latter d<sup>0</sup> system this occurs through an electrostatic interaction with the Lewis acidic cationic metal (e.g., Ca<sup>2+</sup>).



Scheme 1.19. Intramolecular hydroamination reaction of H<sub>2</sub>C=CHCH<sub>2</sub>CPh<sub>2</sub>CH<sub>2</sub>NH<sub>2</sub> with the Schwesinger P4 base and 10 mol% CaI<sub>2</sub> additive.

Aluminium is extremely attractive to chemists on account of its high abundance (in fact it is the most abundant metal in the earth's crust), being present in many common minerals including micas and feldspars.<sup>[167]</sup> Aluminium is therefore inexpensive compared to most transition metals, which makes its compounds especially appealing for stoichiometric and catalytic applications. Organoaluminium compounds have been extensively studied and utilized for about 50 years in polymerization catalysis stemming from the Nobel prizewinning research of Ziegler and Natta (*vide supra*). The original breakthrough came in the polymerization of alkenes with ethylene and propylene being transformed to polyethylene and polypropylene respectively through a  $\text{TiCl}_4/\text{Et}_3\text{Al}$  catalyst/co-catalyst,<sup>[168]</sup> but the field of Ziegler-Natta polymerization has greatly matured since and it is now well-established that the aluminium co-catalyst can function as a Lewis acid, alkylating and/or reducing agent.<sup>[169]</sup> In contrast to this extensive co-catalyst role, examples of aluminium compounds as actual catalysts in reactions such as hydroamination are exceedingly rare though some studies are beginning to emerge. For example, Bergmann<sup>[170]</sup> has synthesized a sterically demanding dianionic phenylene-diamine aluminium complex with a dimethylamino co-ligand (Figure 1.16) that can catalyse the intramolecular hydroamination of a range of aminoalkenes. Performed at the high temperature of 150 °C with 10% catalyst loading, the reactions follow a proposed catalytic cycle akin to that known for late transition metal and lanthanide catalysts. In these reactions the aluminium complex is seen as a cost effective alternative to these more precious metals.

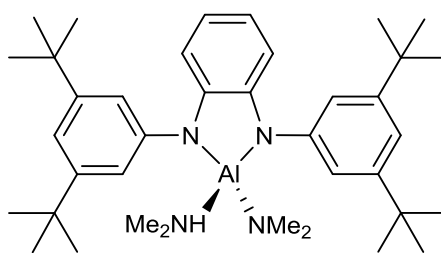


Figure 1.16. ChemDraw representation of the sterically demanding phenylene-diamine Al complex used for catalysing intermolecular hydroamination reactions.<sup>[170]</sup>

Bergmann<sup>[171]</sup> has also applied dimethylaminoaluminium complexes to the hydroamination of carbodiimides revealing that a bulky guanidinate-ligated monomeric dimethylaluminium complex (Figure 1.17) has significantly enhanced activity compared to the dimeric trisamide (Me<sub>2</sub>N)<sub>3</sub>Al. These ambient temperature reactions are complete in minutes, give yields of guanidine products ranging from 84 to 99% (Table 1.2), and follow the catalytic cycle shown in Scheme 1.20.

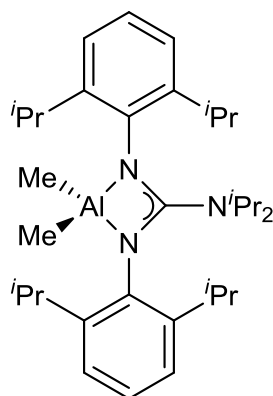
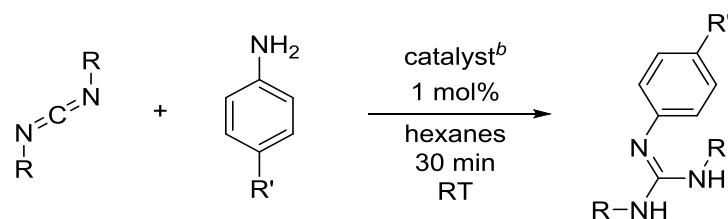
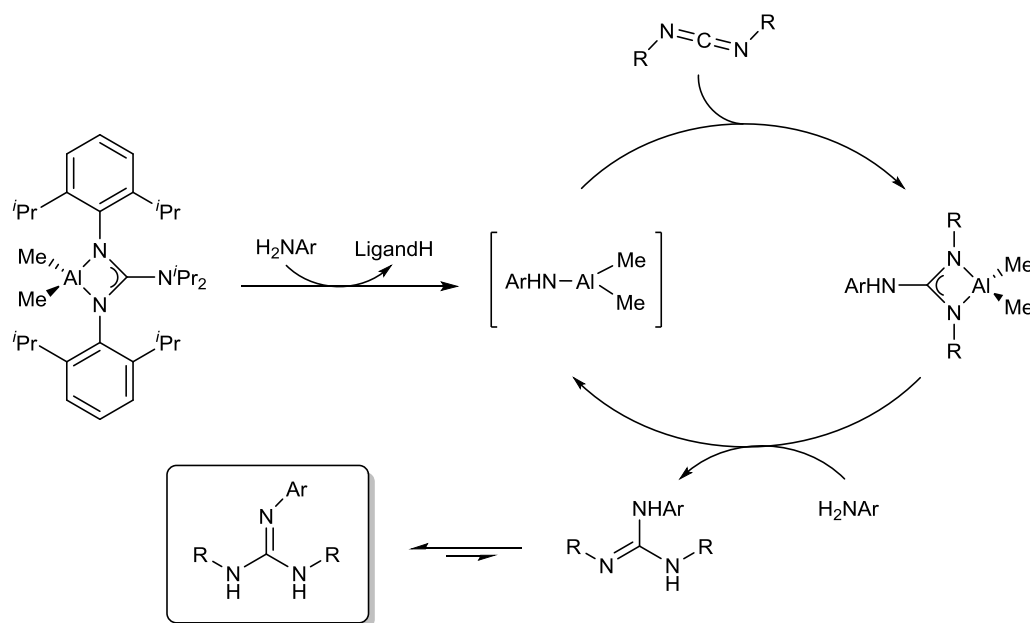


Figure 1.17. ChemDraw representation of the guanidinate-supported aluminium complex used in the hydroamination of carbodiimides.<sup>[171]</sup>

Table 1.2. Catalytic formation of guanidines using a guanidinate-ligated monomeric dimethylaluminium complex.<sup>[171]</sup>

entry	R	R'	yield (%) <sup>a</sup>
1	<i>i</i> Pr	Me	84
2	Cy	Me	97
3	<i>i</i> Pr	H	90
4	Cy	H	97
5	<i>i</i> Pr	F	92
6	Cy	F	99

<sup>a</sup> Isolated Yields, <sup>b</sup> Catalyst is the Al complex shown in Figure 1.17.

Scheme 1.20. Proposed catalytic cycle for the formation of guanidines.<sup>[171]</sup>

An especially noteworthy contribution to this area comes from Zhang, Xi and co-workers<sup>[172]</sup> who demonstrated that a wide range of NH<sub>2</sub>-substituted aromatic compounds (anilines) can add to various carbodiimides to generate substituted guanidines using simple commercially available alkylaluminium catalysts such as Me<sub>3</sub>Al, Et<sub>3</sub>Al or Et<sub>2</sub>AlCl (eq 1.4). These catalytic reactions show a high functional group tolerance (e.g., NO<sub>2</sub>, C≡C, F, Cl, Br and I can all be tolerated on the aniline ring) and can be extended to a variety of NH<sub>2</sub>-substituted heterocycles including isoxazoles, pyridines, pyrazoles and thiazoles. Adding to the importance of this study, the authors were successful in crystallographically characterizing an aluminium guanidinate complex (Figure 1.18) that they proved was a bona fide catalyst in the formation of the guanidine products.

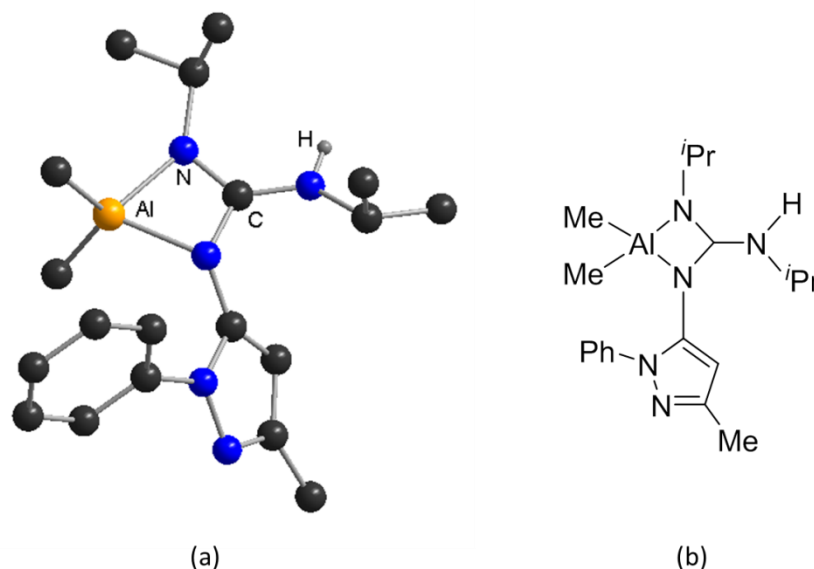
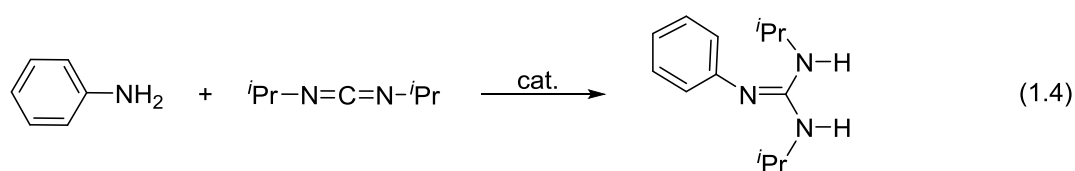


Figure 1.18. (a) Molecular structure and (b) ChemDraw representation of an aluminium guanidinate catalyst for the formation of guanidine compounds.<sup>[172]</sup>



## 1.4 Bibliography

- [1] P. J. Harford, A. J. Peel, F. Chevallier, R. Takita, F. Mongin, M. Uchiyama, A. E. H. Wheatley, *Dalton Trans.* **2014**, 43, 14181-14203.
- [2] R. E. Mulvey, *Dalton Trans.* **2013**, 42, 6676-6693.
- [3] G. Monzón, I. Tirotta, P. Knochel, *Angew. Chem. Int. Ed.* **2012**, 51, 10624-10627.
- [4] C. Unkelbach, H. S. Rosenbaum, C. Strohmann, *Chem. Commun.* **2012**, 48, 10612-10614.
- [5] J. A. Labinger, J. E. Bercaw, *Nature* **2002**, 417, 507-514.
- [6] Y. Kondo, M. Shilai, M. Uchiyama, T. Sakamoto, *J. Am. Chem. Soc.* **1999**, 121, 3539-3540.
- [7] M. Schlosser, J. Hartmann, *Angew. Chem. Int. Ed.* **1973**, 12, 508-509.
- [8] H. Gilman, R. L. Bebb, *J. Am. Chem. Soc.* **1939**, 61, 109-112.
- [9] A. Harrison-Marchand, F. Mongin, *Chem. Rev.* **2013**, 113, 7470-7562.
- [10] F. Mongin, A. Harrison-Marchand, *Chem. Rev.* **2013**, 113, 7563-7727.
- [11] B. Haag, M. Mosrin, H. Ila, V. Malakhov, P. Knochel, *Angew. Chem. Int. Ed.* **2011**, 50, 9794-9824.
- [12] R. E. Mulvey, *Acc. Chem. Res.* **2009**, 42, 743-743.
- [13] R. E. Mulvey, F. Mongin, M. Uchiyama, Y. Kondo, *Angew. Chem. Int. Ed.* **2007**, 46, 3802-3802.
- [14] R. E. Mulvey, *Organometallics* **2006**, 25, 1060-1075.
- [15] M. C. Whisler, S. MacNeil, V. Snieckus, P. Beak, *Angew. Chem. Int. Ed.* **2004**, 43, 2206-2225.
- [16] V. Snieckus, *Chem. Rev.* **1990**, 90, 879-933.
- [17] M. Schlosser, *Organometallics in Synthesis*, 3rd ed., John Wiley & Sons, New Jersey, **2013**.
- [18] L. Ackermann, B. Breit, C.-H. Jun, F. Kakiuchi, D. Kalyani, M. Miura, M. Oestreich, J.-W. Park, M. S. Sanford, T. Satoh, *Directed Metallation*, Springer Verlag, Berlin, Germany, **2007**.
- [19] Z. Rappoport, I. Marek, *The Chemistry of Organozinc Compounds*, Wiley, Chichester, **2006**.
- [20] J. Clayden, *Organolithiums: Selectivity for Synthesis*, Pergamon, Elsevier Science Ltd, Oxford, **2002**.
- [21] M. Scialdone, *WO 2005054224*, **2005**.
- [22] K. C. Nicolaou, J. S. Chen, D. J. Edmonds, A. A. Estrada, *Angew. Chem. Int. Ed.* **2009**, 48, 660-719.
- [23] R. Chinchilla, C. Najera, M. Yus, *Tetrahedron* **2005**, 61, 3139-3176.
- [24] O. Lohse, U. Beutler, P. Funfschilling, P. Furet, J. France, D. Kaufmann, G. Penn, W. Zaug, *Tetrahedron Lett.* **2001**, 42, 385-389.
- [25] W. Schlenk, J. Holtz, *Ber. Dtsch. Chem. Ges.* **1917**, 50, 262-274.
- [26] N. J. Langford, R. E. Ferner, *J. Hum. Hypertens.* **1999**, 13, 651-656.
- [27] G. Kazantzis, *Med. Lav.* **2002**, 93, 139-147.
- [28] K. Ziegler, H. Colonius, *Justus Liebigs Ann. Chem.* **1930**, 479, 135-149.
- [29] D. F. Shriver, M. A. Dreuzdon, *The Manipulation of Air-Sensitive Compounds*, 2nd ed., Wiley, New York, **1986**.

- [30] H. Dietrich, *Acta Cryst.* **1963**, *16*, 681-689.
- [31] H. Dietrich, *J. Organomet. Chem.* **1981**, *205*, 291-299.
- [32] W. Bauer, P. v. R. Schleyer, *J. Am. Chem. Soc.* **1989**, *111*, 7191-7198.
- [33] N. J. R. V. Eikema Hommes, P. v. R. Schleyer, *Tetrahedron* **1994**, *50*, 5903-5916.
- [34] H. J. Reich, *Chem. Rev.* **2013**, *113*, 7130-7178.
- [35] Z. Rappoport, I. Marek, *The Chemistry of Organolithium Compounds Part 1*, John Wiley & Sons, Chichester, **2004**.
- [36] Z. Rappoport, I. Marek, *The Chemistry of Organolithium Compounds Part 2*, John Wiley & Sons, Chichester, **2004**.
- [37] A.-M. Sapse, P. v. R. Schleyer, *Lithium Chemistry: A Theoretical and Experimental Overview*, John Wiley & Sons, New York, **1995**.
- [38] J. M. Mallan, R. L. Bebb, *Chem. Rev.* **1969**, *69*, 693-755.
- [39] E. Weiss, E. A. C. Lucken, *J. Organomet. Chem.* **1964**, *2*, 197-205.
- [40] E. Weiss, G. Hencken, *J. Organomet. Chem.* **1970**, *21*, 265-268.
- [41] R. E. Dinnebier, U. Behrens, F. Olbrich, *J. Am. Chem. Soc.* **1998**, *120*, 1430-1433.
- [42] H. Hope, P. P. Power, *J. Am. Chem. Soc.* **1983**, *105*, 5320-5324.
- [43] D. Thoennes, E. Weiss, *Chem. Ber./Recl.* **1978**, *111*, 3157-3161.
- [44] U. Schumann, J. Kopf, E. Weiss, *Angew. Chem. Int. Ed.* **1985**, *24*, 215-216.
- [45] C. Strohmann, S. Dilsky, K. Strohfeldt, *Organometallics* **2006**, *25*, 41-44.
- [46] M. Vestergren, J. Eriksson, G. Hilmersson, M. Hakansson, *J. Organomet. Chem.* **2003**, *682*, 172-179.
- [47] R. E. Mulvey, *Chem. Soc. Rev.* **1998**, *27*, 339-346.
- [48] R. E. Mulvey, *Chem. Soc. Rev.* **1991**, *20*, 167-209.
- [49] D. Barr, W. Clegg, S. M. Hodgson, G. R. Lamming, R. E. Mulvey, A. J. Scott, R. Snaith, D. S. Wright, *Angew. Chem. Int. Ed.* **1989**, *28*, 1241-1243.
- [50] D. R. Armstrong, D. Barr, W. Clegg, S. M. Hodgson, R. E. Mulvey, D. Reed, R. Snaith, D. S. Wright, *J. Am. Chem. Soc.* **1989**, *111*, 4719-4727.
- [51] D. R. Armstrong, D. Barr, R. Snaith, W. Clegg, R. E. Mulvey, K. Wade, D. Reed, *J. Chem. Soc. Dalton Trans.* **1987**, 1071-1081.
- [52] D. R. Armstrong, D. Barr, W. Clegg, R. E. Mulvey, D. Reed, R. Snaith, K. Wade, *J. Chem. Soc. Chem. Commun.* **1986**, 869-870.
- [53] D. Barr, W. Clegg, R. E. Mulvey, R. Snaith, K. Wade, *J. Chem. Soc. Chem. Commun.* **1986**, 295-297.
- [54] M. Geissler, J. Kopf, B. Schubert, E. Weiss, W. Neugebauer, P. v. R. Schleyer, *Angew. Chem. Int. Ed.* **1987**, *26*, 587-588.
- [55] L. Pauling, *The Nature of the Chemical Bond*, 3rd ed., Cornell University Press, Ithaca, **1960**.
- [56] M. Schlosser, *Organometallics in Synthesis : A Manual*, John Wiley & Sons, Chichester, **1994**.
- [57] W. N. Olmstead, Z. Margolin, F. G. Bordwell, *J. Org. Chem.* **1980**, *45*, 3295-3299.
- [58] K. Daasbjerg, *Acta Chem. Scand.* **1995**, *49*, 878-887.
- [59] R. R. Fraser, T. S. Mansour, *J. Org. Chem.* **1984**, *49*, 3442-3443.
- [60] R. E. Mulvey, S. D. Robertson, *Angew. Chem. Int. Ed.* **2013**, *52*, 11470-11487.

- [61] A. Streitwieser, A. Facchetti, L. Xie, X. Zhang, E. C. Wu, *J. Org. Chem.* **2012**, *77*, 985-990.
- [62] Z. A. Fataftah, I. E. Kopka, M. W. Rathke, *J. Am. Chem. Soc.* **1980**, *102*, 3959-3960.
- [63] P. L. Hall, J. H. Gilchrist, D. B. Collum, *J. Am. Chem. Soc.* **1991**, *113*, 9571-9574.
- [64] M. Lappert, A. Protchenko, P. Power, A. Seeber, *Metal Amide Chemistry*, John Wiley & Sons, Chichester, **2009**.
- [65] G. Wittig, G. Fuhrman, *Chem. Ber.* **1940**, *73B*, 1197-1218.
- [66] P. Beak, V. Snieckus, *Acc. Chem. Res.* **1982**, *15*, 306-312.
- [67] E. J.-G. Anctil, V. Snieckus, in *Metal-Catalyzed Cross-Coupling Reactions*, (Eds.: A. De Meijere, F. Diederich), 2nd ed., Wiley-VCH, Weinheim, **2004**, pp. 761-813.
- [68] F. N. Jones, M. F. Zinn, C. R. Hauser, *J. Org. Chem.* **1963**, *28*, 663-665.
- [69] J. S. Nicholson, S. S. Adams, *GB 971700*, **1964**.
- [70] F. Faigl, M. Schlosser, *Tetrahedron Lett.* **1991**, *32*, 3369-3370.
- [71] M. L. Hsueh, B. T. Ko, T. Athar, C. C. Lin, T. M. Wu, S. F. Hsu, *Organometallics* **2006**, *25*, 4144-4149.
- [72] C. Arbez-Gindre, B. R. Steele, G. A. Heropoulos, C. G. Screttas, J. E. Communal, W. J. Blau, I. Ledoux-Rak, *J. Organomet. Chem.* **2005**, *690*, 1620-1626.
- [73] R. Wingen, W. Schmidt, *JP 2001316323*, **2001**.
- [74] F. I. Chirskij, A. P. Boldyrev, N. N. Shapovalova, A. V. Molodyka, S. L. Sidorov, L. D. Kudryavtsev, A. A. Rylkov, G. M. Grachev, *RU 2083599*, **1997**.
- [75] P. G. Bruce, B. Scrosati, J. M. Tarascon, *Angew. Chem. Int. Ed.* **2008**, *47*, 2930-2946.
- [76] L. S. Bennie, W. J. Kerr, M. Middleditch, A. J. B. Watson, *Chem. Commun.* **2011**, *47*, 2264-2266.
- [77] R. B. Bates, D. E. Potter, L. M. Kroposki, *J. Org. Chem.* **1972**, *37*, 560-562.
- [78] J. Clayden, S. A. Yasin, *New J. Chem.* **2002**, *26*, 191-192.
- [79] R. E. Mulvey, V. L. Blair, W. Clegg, A. R. Kennedy, J. Klett, L. Russo, *Nature Chem.* **2010**, *2*, 588-591.
- [80] E. Frankland, *Justus Liebigs Ann. Chem.* **1849**, *71*, 171-213.
- [81] D. Seyferth, *Organometallics* **2001**, *20*, 2940-2955.
- [82] P. G. Cozzi, A. Mignogna, L. Zoli, *Pure Appl. Chem.* **2008**, *80*, 891-901.
- [83] H. E. Simmons, R. D. Smith, *J. Am. Chem. Soc.* **1958**, *80*, 5322-5324.
- [84] A. O. King, N. Okukado, E. I. Negishi, *J. Chem. Soc. Chem. Commun.* **1977**, 683-684.
- [85] J. A. Casares, P. Espinet, B. Fuentes, G. Salas, *J. Am. Chem. Soc.* **2007**, *129*, 3508-3509.
- [86] J. Boor, *Ziegler-Natta Catalysts and Polymerizations*, Academic Press Inc., New York, **1979**.
- [87] M. Bochmann, *Organometallics and Catalysis*, Oxford University Press, New York, **2015**.
- [88] H. Minami, T. Saito, C. Wang, M. Uchiyama, *Angew. Chem. Int. Ed.* **2015**, DOI: 10.1002/anie.201412249.

- [89] *Modern Organoaluminum Reagents, Vol. 41*, Springer, Berlin, **2013**.
- [90] Chemicals Technology (2015). *SOCC Aluminium Alkyls Facility, Al Jubail, Saudi Arabia*. [Online] Available from: <http://www.chemicals-technology.com/projects/socc-aluminium-alkyls-facility-jubail-saudi/>. [Accessed: 25/02/15]
- [91] S. Kawamura, K. Ishizuka, H. Takaya, M. Nakamura, *Chem. Commun.* **2010**, 46, 6054-6056.
- [92] L. Lochmann, J. Pospíšil, D. Lim, *Tetrahedron Lett.* **1966**, 257-262.
- [93] M. Schlosser, *J. Organomet. Chem.* **1967**, 8, 9-16.
- [94] M. Schlosser, *Pure. Appl. Chem.* **1988**, 60, 1627-1634.
- [95] M. Schlosser, J. Hartmann, *Helv. Chim. Acta* **1976**, 59, 453-466.
- [96] M. Schlosser, G. Katsoulos, S. Takagishi, *Synlett* **1990**, 747-748.
- [97] J. D. Roberts, D. Y. Curtin, *J. Am. Chem. Soc.* **1946**, 68, 1658-1660.
- [98] D. A. Shirley, J. R. Johnson, J. P. Hendrix, *J. Organomet. Chem.* **1968**, 11, 209-216.
- [99] M. Schlosser, H. C. Jung, S. Takagishi, *Tetrahedron* **1990**, 46, 5633-5648.
- [100] P. Fleming, D. F. O'Shea, *J. Am. Chem. Soc.* **2011**, 133, 1698-1701.
- [101] G. Wittig, F. J. Meyer, G. Lange, *Justus Liebigs Ann. Chem.* **1951**, 571, 167-201.
- [102] G. Wittig, *Angew. Chem.* **1958**, 70, 65-65.
- [103] J. A. Wanklyn, *Justus Liebigs Ann. Chem.* **1858**, 108, 67-79.
- [104] L. Pauling, *General Chemistry*, W.H. Freeman, San Francisco, **1947**.
- [105] C. Lambert, P. v. R. Schleyer, *Angew. Chem. Int. Ed.* **1994**, 33, 1129-1140.
- [106] S. Merkel, D. Stern, J. Henn, D. Stalke, *Angew. Chem. Int. Ed.* **2009**, 48, 6350-6353.
- [107] D. R. Armstrong, C. Dougan, D. V. Graham, E. Hevia, A. R. Kennedy, *Organometallics* **2008**, 27, 6063-6070.
- [108] A. R. Kennedy, J. Klett, R. E. Mulvey, D. S. Wright, *Science* **2009**, 326, 706-708.
- [109] A. J. Martinez-Martinez, A. R. Kennedy, R. E. Mulvey, C. T. O'Hara, *Science* **2014**, 346, 834-837.
- [110] A. E. H. Wheatley, *New J. Chem.* **2004**, 28, 435-443.
- [111] M. Uchiyama, M. Koike, M. Kameda, Y. Kondo, T. Sakamoto, *J. Am. Chem. Soc.* **1996**, 118, 8733-8734.
- [112] M. Uchiyama, M. Kameda, O. Mishima, N. Yokoyama, M. Koike, Y. Kondo, T. Sakamoto, *J. Am. Chem. Soc.* **1998**, 120, 4934-4946.
- [113] E. Alvarez, A. Grirrane, I. Resa, D. del Río, A. Rodríguez, E. Carmona, *Angew. Chem. Int. Ed.* **2007**, 46, 1296-1299.
- [114] W. Clegg, D. V. Graham, E. Herd, E. Hevia, A. R. Kennedy, M. D. McCall, L. Russo, *Inorg. Chem.* **2009**, 48, 5320-5327.
- [115] D. R. Armstrong, W. Clegg, P. García-Alvarez, M. D. McCall, L. Nuttall, A. R. Kennedy, L. Russo, E. Hevia, *Chem. Eur. J.* **2011**, 17, 4470-4479.
- [116] T. Katsuhira, T. Harada, K. Maejima, A. Osada, A. Oku, *J. Org. Chem.* **1993**, 58, 6166-6168.
- [117] T. Harada, T. Katsuhira, T. Hara, Y. Kotani, K. Maejima, R. Kaji, A. Oku, *J. Org. Chem.* **1993**, 58, 4897-4907.

- [118] T. Harada, T. Katsuhira, K. Hattori, A. Oku, *J. Org. Chem.* **1993**, *58*, 2958-2965.
- [119] Y. Kondo, N. Takazawa, C. Yamazaki, T. Sakamoto, *J. Org. Chem.* **1994**, *59*, 4717-4718.
- [120] R. A. Watson, R. A. Kjonaas, *Tetrahedron Lett.* **1986**, *27*, 1437-1440.
- [121] M. Isobe, S. Kondo, N. Nagasawa, T. Goto, *Chem. Lett.* **1977**, *6*, 679-682.
- [122] Y. Kondo, M. Fujinami, M. Uchiyama, T. Sakamoto, *J. Chem. Soc., Perkin Trans. 1* **1997**, 799-800.
- [123] C. J. Upton, P. Beak, *J. Org. Chem.* **1975**, *40*, 1094-1098.
- [124] J. Verbeek, L. Brandsma, *J. Org. Chem.* **1984**, *49*, 3857-3859.
- [125] W. Clegg, S. H. Dale, E. Hevia, G. W. Honeyman, R. E. Mulvey, *Angew. Chem. Int. Ed.* **2006**, *45*, 2370-2374.
- [126] W. Clegg, S. H. Dale, A. M. Drummond, E. Hevia, G. W. Honeyman, R. E. Mulvey, *J. Am. Chem. Soc.* **2006**, *128*, 7434-7435.
- [127] P. C. Andrikopoulos, D. R. Armstrong, H. R. L. Barley, W. Clegg, S. H. Dale, E. Hevia, G. W. Honeyman, A. R. Kennedy, R. E. Mulvey, *J. Am. Chem. Soc.* **2005**, *127*, 6184-6185.
- [128] D. R. Armstrong, J. García-Alvarez, D. V. Graham, G. W. Honeyman, E. Hevia, A. R. Kennedy, R. E. Mulvey, *Chem. Eur. J.* **2009**, *15*, 3800-3807.
- [129] D. R. Armstrong, W. Clegg, S. H. Dale, E. Hevia, L. M. Hogg, G. W. Honeyman, R. E. Mulvey, *Angew. Chem. Int. Ed.* **2006**, *45*, 3775-3778.
- [130] L. Balloch, J. A. Garden, A. R. Kennedy, R. E. Mulvey, T. Rantanen, S. D. Robertson, V. Snieckus, *Angew. Chem. Int. Ed.* **2012**, *51*, 6934-6937.
- [131] W. Clegg, S. H. Dale, E. Hevia, L. M. Hogg, G. W. Honeyman, R. E. Mulvey, C. T. O'Hara, *Angew. Chem. Int. Ed.* **2006**, *45*, 6548-6550.
- [132] W. Clegg, S. H. Dale, R. W. Harrington, E. Hevia, G. W. Honeyman, R. E. Mulvey, *Angew. Chem. Int. Ed.* **2006**, *45*, 2374-2377.
- [133] L. Balloch, A. R. Kennedy, R. E. Mulvey, T. Rantanen, S. D. Robertson, V. Snieckus, *Organometallics* **2011**, *30*, 145-152.
- [134] L. Balloch, A. R. Kennedy, J. Klett, R. E. Mulvey, C. T. O'Hara, *Chem. Commun.* **2010**, *46*, 2319-2321.
- [135] B. Conway, E. Hevia, A. R. Kennedy, R. E. Mulvey, *Chem. Commun.* **2007**, 2864-2866.
- [136] A. R. Lepley, W. A. Khan, *J. Org. Chem.* **1966**, *31*, 2047-2051.
- [137] D. Nobuto, M. Uchiyama, *J. Org. Chem.* **2008**, *73*, 1117-1120.
- [138] W. Clegg, B. Conway, E. Hevia, M. D. McCall, L. Russo, R. E. Mulvey, *J. Am. Chem. Soc.* **2009**, *131*, 2375-2384.
- [139] A. Thaler, D. Seebach, F. Cardinaux, *Helv. Chim. Acta.* **1991**, *74*, 617-627.
- [140] A. Thaler, D. Seebach, F. Cardinaux, *Helv. Chim. Acta.* **1991**, *74*, 628-643.
- [141] L. Gupta, A. C. Hoepker, K. J. Singh, D. B. Collum, *J. Org. Chem.* **2009**, *74*, 2231-2233.
- [142] E. Hevia, R. E. Mulvey, *Angew. Chem. Int. Ed.* **2011**, *50*, 6448-6450.
- [143] L. Salvi, J. G. Kim, P. J. Walsh, *J. Am. Chem. Soc.* **2009**, *131*, 12483-12493.
- [144] V. Grignard, *C. R. Hebd. Séances Acad. Sci.* **1900**, *130*, 1322-1324.
- [145] E. C. Ashby, J. Laemmle, H. M. Neumann, *Acc. Chem. Res.* **1974**, *7*, 272-280.
- [146] B. J. Wakefield, *Organomagnesium Methods in Organic Synthesis*, Academic Press Limited, London, **1995**.

- [147] W. Schlenk, W. Schlenk, *Ber. Dtsch. Chem. Ges.* **1929**, 62, 920-924.
- [148] G. S. Silverman, P. E. Rakita, *Handbook of Grignard Reagents*, Marcel Dekker Inc., New York, **1996**.
- [149] C. R. Hauser, H. G. Walker, *J. Am. Chem. Soc.* **1947**, 69, 295-297.
- [150] F. C. Frostick, C. R. Hauser, *J. Am. Chem. Soc.* **1949**, 71, 1350-1352.
- [151] P. Knochel, W. Dohle, N. Gommermann, F. F. Kneisel, F. Kopp, T. Korn, I. Sapountzis, V. A. Vu, *Angew. Chem. Int. Ed.* **2003**, 42, 4302-4320.
- [152] A. Krasovskiy, P. Knochel, *Angew. Chem. Int. Ed.* **2004**, 43, 3333-3336.
- [153] R. Li-Yuan Bao, R. Zhao, L. Shi, *Chem. Commun.* **2015**, DOI: 10.1039/C1034CC10194D
- [154] D. Tilly, F. Chevallier, F. Mongin, P. C. Gros, *Chem. Rev.* **2014**, 114, 1207-1257.
- [155] C. T. O'Hara, *Organomet. Chem.* **2011**, 37, 1-26.
- [156] Y. Y. Liu, Y. W. Fang, L. Zhang, X. P. Jin, R. F. Li, S. R. Zhu, H. Q. Gao, J. H. Fang, Q. B. Xia, *Chin. J. Org. Chem.* **2014**, 34, 1523-1541.
- [157] *Handbook of Functionalised Organometallics*, Wiley-VCH, Weinheim, **2005**.
- [158] P. Knochel, A. Gavryushin, K. Brade, in *The Chemistry of Organomagnesium Compounds*, (Eds.: Z. Rappoport, I. Marek), John Wiley & Sons Ltd, Chichester, **2008**, pp. 511-593.
- [159] P. Garcia-Alvarez, D. V. Graham, E. Hevia, A. R. Kennedy, J. Klett, R. E. Mulvey, C. T. O'Hara, S. Weatherstone, *Angew. Chem. Int. Ed.* **2008**, 47, 8079-8081.
- [160] M. R. Crimmin, I. J. Casely, M. S. Hill, *J. Am. Chem. Soc.* **2005**, 127, 2042-2043.
- [161] S. Datta, M. T. Gamer, P. W. Roesky, *Organometallics* **2008**, 27, 1207-1213.
- [162] C. Glock, F. M. Younis, S. Ziemann, H. Gorls, W. Imhof, S. Kriek, M. Westerhausen, *Organometallics* **2013**, 32, 2649-2660.
- [163] M. R. Crimmin, A. G. M. Barrett, M. S. Hill, P. B. Hitchcock, P. A. Procopiou, *Organometallics* **2007**, 26, 2953-2956.
- [164] F. Buch, H. Brettar, S. Harder, *Angew. Chem. Int. Ed.* **2006**, 45, 2741-2745.
- [165] J. Penafiel, L. Maron, S. Harder, *Angew. Chem. Int. Ed.* **2015**, 54, 201-206.
- [166] D. Margetic, in *Superbases for Organic Synthesis: Guanidines, Amidines, Phosphazenes and Related Organocatalysts*, (Ed.: T. Ishikawa), John Wiley & Sons, Ltd, Chichester, **2009**, pp. 32-33.
- [167] H. W. Roesky, *Inorg. Chem.* **2004**, 43, 7284-7293.
- [168] C. Elschenbroich, A. Salzer, *Organometallics: A Concise Introduction*, 2nd ed., VCH, Weinheim, **1992**.
- [169] S. Dagonne, C. Fliedel, in *Modern Organoaluminum Reagents*, (Eds.: S. Woodward, S. Dagonne), Springer, Heidelberg, **2013**, pp. 125-171.
- [170] J. Koller, R. G. Bergman, *Chem. Commun.* **2010**, 46, 4577-4579.
- [171] J. Koller, R. G. Bergman, *Organometallics* **2010**, 29, 5946-5952.
- [172] W.-X. Zhang, D. Li, Z. Wang, Z. Xi, *Organometallics* **2009**, 28, 882-887.

## **Chapter 2**

### **Concealed Cyclotrimeric Polymorph of Lithium 2,2,6,6-Tetramethylpiperidide Unconcealed**

## 2.1 Aims

The primary aim of the work carried out in this chapter was to study the preparation and crystallisation of the commodity chemical lithium tetramethylpiperidide (LiTMP) and ascertain whether it has different polymorphic forms, given the diverse range of oligomers that are known to exist in the solution-state.

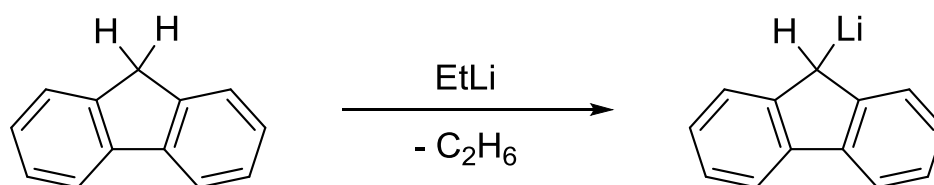
Specific objectives are outlined below:

- Explore the synthesis of LiTMP using different approaches.
- Attempt to grow crystals of LiTMP over various conditions.
- Record the NMR spectra of the isolated crystals.
- Check the unit cells of any X-ray quality crystals.
- Carry out full X-ray crystal structure determinations of any crystals with a new unit cell.



## 2.2 Introduction

Two general classes of compound dominate organolithium reagent chemistry, namely alkyllithiums and lithium amides. The former predate the latter by decades with the first examples methylolithium, ethyllithium (and the aryl relation, phenyllithium) introduced in a classic paper by Schlenk and Holtz from 1917. Early papers on convenient preparations of the two most popular alkyllithium reagents *n*-butyllithium and *t*-butyllithium appeared in 1949<sup>[1]</sup> and 1941<sup>[2]</sup> respectively. The reagent designation reflects the fact that essentially from their inception, alkyllithium compounds have proved useful if not wholly indispensable to synthetic chemists, especially in organic chemistry primarily as selective bases or nucleophiles. From the perspective of this project their basic behaviour in metallation applications is the most relevant. Alkyllithium metallation chemistry dates back to 1928 when Schlenk and Bergmann<sup>[3]</sup> deprotonated fluorene with ethyllithium to form fluorenyllithium and ethane (Scheme 2.1), immediately signalling a major advantage of alkyllithium bases that aside from effecting the desired deprotonation they can produce gaseous byproducts avoiding the need for additional separation steps in synthetic campaigns.



Scheme 2.1. First reported deprotonation of fluorene by EtLi generating fluorenyllithium and ethane.

Metallation of aromatic substrates by alkyllithium reagents soon became a popular synthetic methodology after Gilman<sup>[4]</sup> and Wittig<sup>[5]</sup> independently pioneered directed *ortho*-metallation chemistry (see Chapter 1) through

reactions with anisole. A recent excellent review by Reich<sup>[6]</sup> documents key case studies of organolithium reactions, including metallations, where mechanistic insights have been gained from significant experimental investigations.

Contrastingly, the lithium amide reagents suitable for metallation applications generally do not produce gaseous byproducts but instead form liquid amines that could interfere in syntheses. Reagent lithium amides usually mean secondary amides  $[(R_2NLi)_n]$  having substantial steric bulk. Lithium dialkylamide bases first appeared in 1932 in a paper from Ziegler.<sup>[7]</sup> Another milestone was reached in 1950 when Hammel and Levine<sup>[8]</sup> reported the use of LDA for the  $\alpha$ -deprotonation of the ester ethyl isobutyrate where they highlighted the fast kinetics of the reaction. Surprisingly, LDA was not taken up as a common reagent by the synthetic community until several years afterwards. Today, LDA, LiTMP and LiHMDS are utilised widely throughout synthetic chemistry as to a lesser extent are their sodium and potassium congeners. A recent review lauded this trio of group one amides as the “utility amides”, complementing their inclusion in two earlier broader scoped textbooks, the first “Metal and Metalloid Amides”<sup>[9]</sup> published in 1980, the second “Metal Amide Chemistry”<sup>[10]</sup> in 2009, both authored by Lappert, Power and colleagues. As mentioned previously (in Chapter 1) lithium amides are the bases of choice when nucleophilic addition is a possible competing side reaction with a metallation reaction. Though lithium amides are generally less basic than the most powerful alkyl lithium bases (consistent with the conjugate amines being more acidic than the conjugate alkanes) meaning that based on  $pK_a$  values the range of aromatic substrates they can metallate is narrower, provided the amides possess high steric bulk they can outperform alkyl lithium bases. Possessing the most steric bulk of the three utility amido anions (see Figure 2.1), TMP has the added advantage that it does not contain any  $\beta$ -hydrogen atoms making it stable against  $\beta$ -hydride elimination, a problem that can beset LDA. Furthermore, the electron donating  $\alpha$ -methyl wingtips adjacent to nitrogen within the special cyclical architecture of TMP enhance its basic character, which is why LiTMP excels in the selective deprotonation of C-H

bonds. It is for this combination of advantages that the TMP anion has become the preferred active base component not only of LiTMP but of the plethora of multicomponent bases that have emerged over the past decade or so (see Chapter 1).

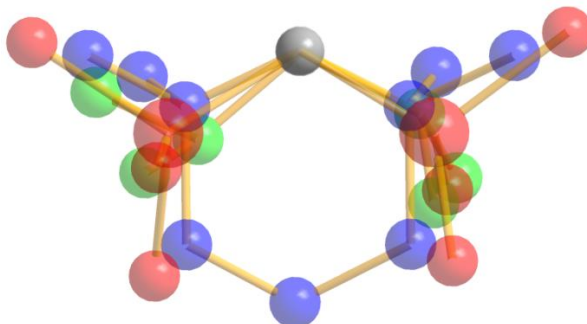
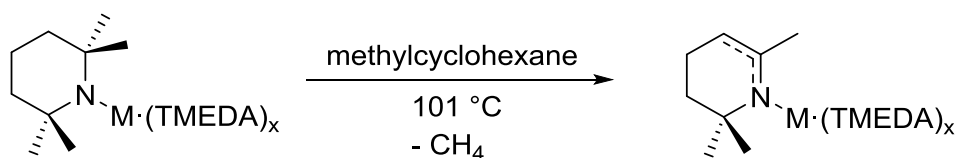


Figure 2.1. Comparison of the steric bulk of the three utility amides TMP (blue), HMDS (red) and DA (green) with the N atom (grey) occupying a common point.<sup>[11]</sup>

That notwithstanding, recent work in the Mulvey group has brought to attention the thermal limit of the TMP anion as it can lose one of its methyl wingtips in the form of methane to generate 1-aza-allyl TTHP derivatives (TTHP is 2,2,6-trimethyl-1,2,3,4-tetrahydropyridide) (Scheme 2.2).<sup>[12]</sup> Measured by Thermal Volatilisation Analysis (TVA)<sup>[13-15]</sup>, the temperature of this transformation (methane release) depends on the alkali metal to which it is attached with the trend  $\text{Li} > \text{Na} > \text{K}$  following the increasing size of the alkali metal.



where M = Li, Na, K

Scheme 2.2. Thermolysis of TMP anion to TTHP anion through loss of  $\text{CH}_4$ .<sup>[12]</sup>

### 2.2.1 Structural Considerations

Alkali metal amides have played a major role in the development of organolithium structural chemistry. It was mentioned earlier (see Chapter 1) that the study of lithium amides was a key factor in deriving the ring-laddering concept that explains the ladder-type architectures found in certain lithium amide compounds. These ladders are manifestations of the aggregation phenomena that are a central pillar of organolithium chemistry. The steric profile of the carbanion, or here, the amido anion, as discussed above for TMP, is only one factor in a lithium amide's reactivity. In general terms, too large an aggregation will inhibit the metallating ability of the base. For this reason, the utility amides have exceptionally large amido steric profiles, which significantly restricts their aggregation. Incorporating donor solvents (for example, commonly THF, TMEDA or PMDETA) within their structures reduces aggregation further and thus makes them more kinetically reactive. The study of alkali metal amide structures and indeed of organolithium structures in general is therefore of prime importance in the refining of their usage in synthetic applications.

Reported by Lappert and Atwood<sup>[16]</sup> 10 years after its first employment as a base by organic chemists,<sup>[17-18]</sup> the crystal and molecular structure of LiTMP is an aesthetic classic within organolithium chemistry.<sup>[19-23]</sup> It exists as a discrete cyclotetrameric arrangement having a (LiN)<sub>4</sub> planar ring (Figure 2.2). The TMP anions sit in the form of chairs, the steric encumbrance of which prevents any ring-laddering of the type observed in the methyl-substituent free lithium pyrrolidide structures  $[\{\text{H}_2\text{C}(\text{CH}_2)_3\text{NLi}\}_3 \cdot \text{PMDETA}]_2$  and  $[\{\text{H}_2\text{C}(\text{CH}_2)_3\text{NLi}\}_2 \cdot \text{TMEDA}]_2$  reported by Snaith and coworkers.<sup>[24]</sup> Within  $[(\text{LiTMP})_4]$  the Li atoms are 2-coordinate, while the N atoms are 4-coordinate. Interestingly, 16 years after the structure of  $[(\text{LiTMP})_4]$  was published, Lappert again, this time in collaboration with Mulvey, reported the structure of pure, unsolvated NaTMP, finding it to be a Na<sub>3</sub>N<sub>3</sub> cyclotrimer. This was a surprising discovery as intuitively one might have expected that the larger sodium amide would have adopted a larger aggregation state than its smaller lithium

congener. The results and discussion section in this chapter will shed new light on this seemingly counter-intuitive structural diversity.

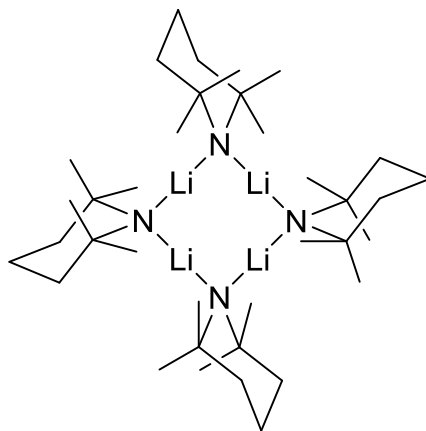


Figure 2.2. ChemDraw representation of cyclotetrameric  $[\text{LiTMP}]_4$  showing the chair conformation of each TMP group.

The solution behaviour of LiTMP is remarkably complicated and diverse in hydrocarbon media.<sup>[25-26]</sup> Meticulously performed  $^6\text{Li}/^{15}\text{N}$  NMR studies by Collum has led to the detection of high cyclic oligomers  $(\text{LiTMP})_n$  ( $n > 2$ ) in pentane. He has assigned them to tetramers and trimers reasoning that theoretically there would be as much as six such oligomers altogether due to differently arranged TMP chair conformations.<sup>[27-28]</sup> Indirect evidence from a  $^6\text{Li}-^{15}\text{N}$  HMQC (heteronuclear multiple quantum correlation) spectrum of LiPMP (PMP is 2,2,4,6,6-pentamethylpiperidide), where introducing a fifth Me substituent at the apex of the ring slows down conformational dynamics, enabled Collum to detect and assign five species, four cyclotetramers and one cyclotrimer. Since the Mulvey group subsequently performed DFT calculations that predicted these oligomeric isomers had similar relative energies<sup>[29]</sup> and knowing that polymorphs exist in related alkali metal amides (for example, NaHMDS is known in trimeric and polymeric polymorphic forms)<sup>[30-32]</sup>, it begs the question “is the solid state picture of LiTMP complete given the multiplicity

of species that co-exist in hydrocarbon solution, a medium more closely related to the solid state than to strongly solvating/deaggregating donor solution?” Significantly, Fox uncovered a monomer-dimer equilibrium for LiTMP in  $d_8$ -THF at  $-50^\circ\text{C}$ <sup>[33]</sup>. Of course, unless one deliberately searches for a LiTMP polymorph it is unlikely to be discovered fortuitously as in practical applications LiTMP is generally synthesised/dispensed *in situ* without isolation, and increasingly in THF solution as part of mixed metal reagents where it will exist at least predominately in solvated form.<sup>[34-40]</sup>

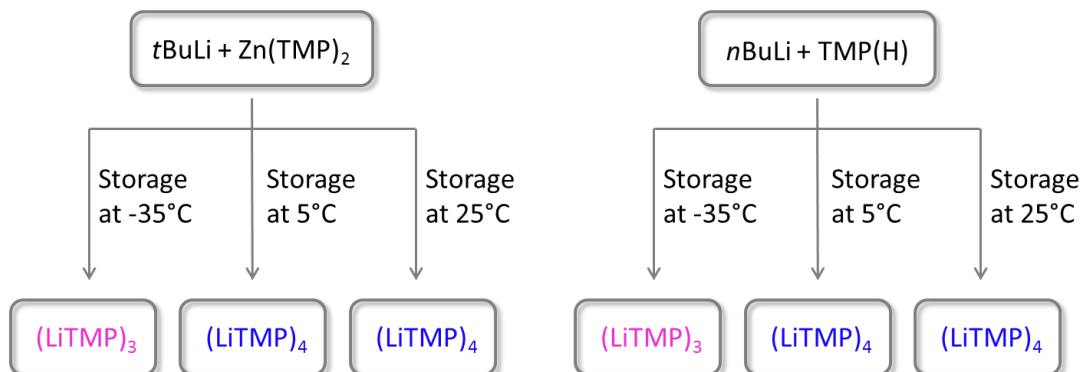
## 2.3 Results and Discussion

Here we report that changing the temperature at which LiTMP is crystallised in hexane does indeed reveal a new polymorph with a different degree of oligomerisation as elucidated by X-ray crystallography. In addition, we show that NMR spectroscopic studies, both routine ( $^1\text{H}$  and  $^{13}\text{C}$ ) and DOSY (Diffusion Ordered Spectroscopy) can easily distinguish between this long concealed polymorph and its predecessor which exist in equilibrium.

### 2.3.1 Synthesis and Crystallisation

It is standard practice to synthesise LiTMP by metallation of the parent amine TMP(H) with an alkyllithium reagent, and indeed this was the method employed by Lappert and Atwood for its crystallisation in the form of  $(\text{LiTMP})_4$ . We chose to start this speculative study by a fresh approach. Taking advantage of zinc’s superior carbophilicity,<sup>[41]</sup> we attempted a transmetallation reaction between  $\text{Zn}(\text{TMP})_2$  and *t*-butyllithium in hexane solution at ambient temperature (Scheme 2.3). Regardless of the stoichiometry used in this reaction, LiTMP was produced in crystalline form in yields of 90% or higher. An X-ray crystallographic study revealed these crystals to be predominately a cyclotrimeric polymorph,  $(\text{LiTMP})_3$ , **2.1**, of the aforementioned known cyclotetramer  $(\text{LiTMP})_4$ , **2.2** (see below). Unit cell checks of several crystals

from each of the stoichiometric variant reactions confirmed their identity as **2.1**. Significantly these crystals were grown from solutions in the freezer at  $-35^{\circ}\text{C}$ . For comparison and completeness we re-prepared LiTMP by *n*-butyllithium metallation of TMP(H) in hexane at ambient temperature (Scheme 2.3) and storing the resulting solution at different temperatures. Freezer storage at  $-35^{\circ}\text{C}$  produced mainly crystals of the cyclotrimer **2.1**, though when the storage temperature was increased to  $5^{\circ}\text{C}$  or  $25^{\circ}\text{C}$  the other polymorph **2.2** dominated. Resumption of the alternative transmetallation approach but growing crystals on the bench at  $25^{\circ}\text{C}$  or in the refrigerator at  $5^{\circ}\text{C}$  also led to the formation of **2.2**. Therefore crystallisation at low temperature favours the production of **2.1**; whereas high temperature favours **2.2**. While identities were confirmed by unit cell checks of several crystals from each reaction, as Figure 2.3 shows **2.1** and **2.2** could be distinguished qualitatively by the naked eye due to their easily differentiated habits as **2.1** forms prismatic (rod-like) crystals; whereas the crystals of **2.2** are more anhedral.



Scheme 2.3. Two contrasting syntheses of LiTMP used in this study showing the major lithium products obtained under different storage temperatures. Note these reactions do not take into account stoichiometry.

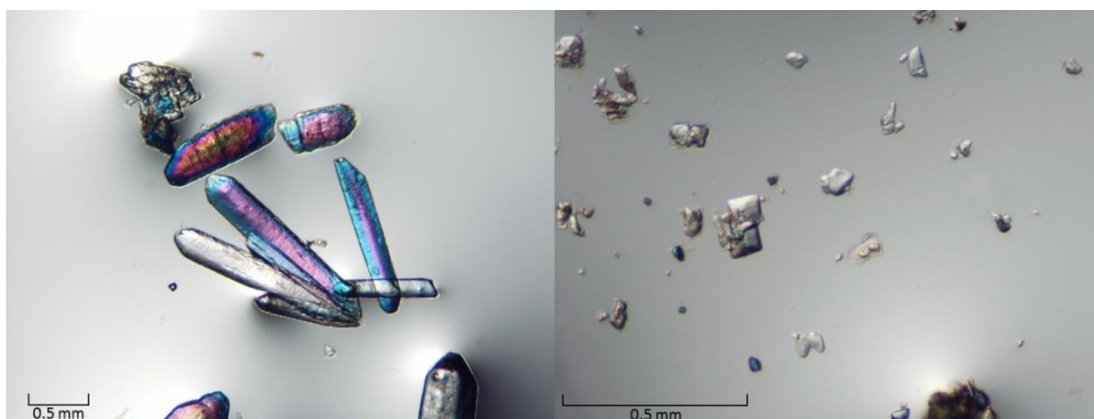


Figure 2.3. Microscope photographs of crystalline **2.1** (LHS) and **2.2** (RHS) showing the approximate scale in mm.

### 2.3.2 X-ray Crystallographic Studies

Since we determined the molecular structure of **2.1** (Figure 2.4) at low temperature [123(2) K] whereas that of **2.2** was determined originally at ambient temperature, we redetermined the structure of **2.2** (Figure 2.5) at 123(2) K both to confirm its cyclotetrameric arrangement and for a more direct comparison (refer to Table 2.2 in the experimental section for all crystallographic data). Data discussed here for **2.2** will be restricted to those of this new improved low temperature structure. Selected bond parameters for **2.1** and **2.2** are compared in Table 2.1. Trimer **2.1** crystallises in the hexagonal space group  $P6_3/m$  in contrast to the monoclinic space group  $C2/c$  of tetramer **2.2**. Strictly planar, the  $(LiN)_3$  ring of **2.1** exhibits  $C_{3h}$  symmetry, while the  $(LiN)_4$  ring of **2.2** exhibits pseudo (non-crystallographic)  $C_{4h}$  symmetry. Easily surmised from the ChemDraw depictions in Figure 2.6, these symmetries are dictated by the number and conformations of TMP ligands. In their common chair form, the TMP ligands are all strictly equivalent in **2.1** and approximately equivalent in **2.2**. Because the TMP ligand in **2.1** presents a different steric profile to the Li atoms either side of the N atom adjacent Li-N bond lengths are inequivalent, so that short [1.988(3) Å] and long [2.066(3) Å] bonds alternate around the ring with a mean length of 2.027 Å. Endocyclic bond angles at Li



[150.22(16)°] and N [89.78(16)°] show marked distortions from linear and tetrahedral geometries respectively, with the widest angle at N being 116.24(7) for C(1)-N(1)-Li(1). The reduced crystallographic symmetry in the larger ring of **2.2** means that it accommodates two distinct Li and two distinct N atoms. Mean endocyclic bond angles [at Li, 168.9°; at N, 101.01°] intimate a modest easing of ring strain in comparison to that in **2.1**. Because of its lower symmetry **2.2** displays four distinct Li-N bond lengths which as in **2.1** alternate in a short-long pattern (mean short, 1.983 Å; mean long, 2.020 Å) and have an overall mean length of 2.002 Å, slightly less than that in **2.1** (2.027 Å).

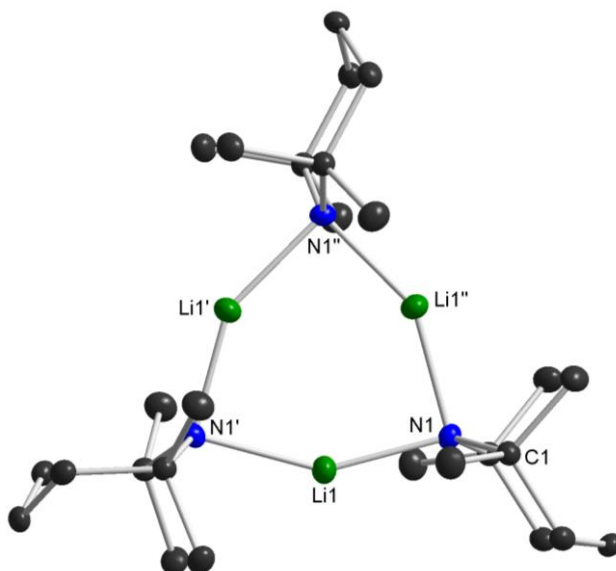


Figure 2.4. Molecular structure of **2.1**. Hydrogen atoms are omitted for clarity. The symmetry operation to generate the equivalent atoms labelled ' is  $1-y, x-y, z$  and '' is  $1-x+y, 1-x, z$ .

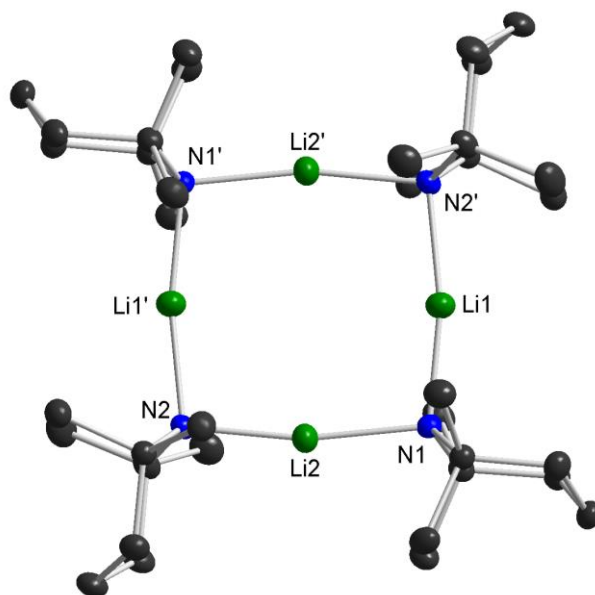


Figure 2.5. Re-determined molecular structure of **2.2**. Hydrogen atoms are omitted for clarity. The symmetry operation to generate the equivalent atoms labelled ' is  $-x+0.5, -y-0.5, -z$ .

Table 2.1. Key bond lengths (Å) and bond angles (°) within the polymorphic structures of  $(\text{LiTMP})_3$  **2.1** and  $(\text{LiTMP})_4$  **2.2**.

For <b>2.1</b>			
Li1-N1	1.988(3)	N1'-Li1-N1	150.22(16)
Li1-N1'	2.066(3)	Li1-N1-Li1'	89.78(16)
For <b>2.2</b>			
Li1-N1	1.981(3)	N1-Li1-N2'	168.51(14)
Li1-N2'	2.017(3)	N2-Li2-N1	169.29(14)
Li2-N1	2.023(3)	Li1-N1-Li2	100.97(10)
Li2-N2	1.985(3)	Li1'-N2-Li2	101.05(10)

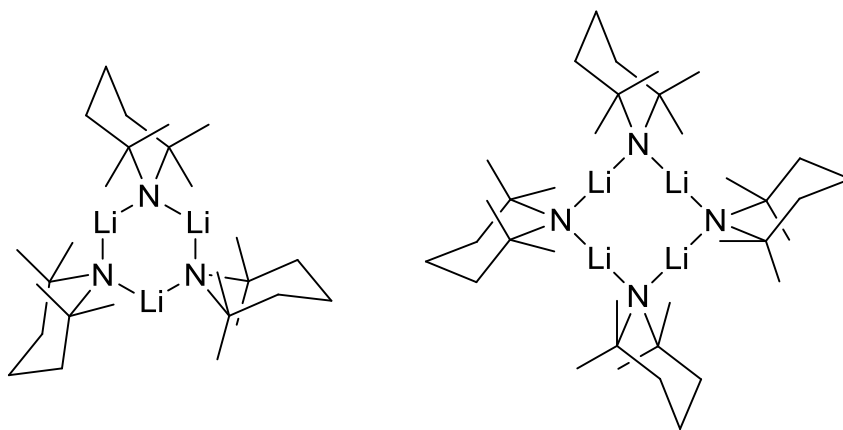


Figure 2.6. ChemDraw depictions of **2.1** (LHS) and **2.2** (RHS).

### 2.3.3 NMR Spectroscopic Studies

We were surprised to discover that cyclotrimer **2.1** and cyclotetramer **2.2** were both seen and easily distinguishable from routine  $^1\text{H}$  and  $^{13}\text{C}$  NMR spectra recorded in  $d_6$ -benzene solution. As mentioned in the introduction Collum used  $^6\text{Li}$ ,  $^{15}\text{N}$ , and  $^6\text{Li}$ - $^{15}\text{N}$  HMQC NMR spectra in pentane to observe at  $-40^\circ\text{C}$  a trimer:tetramer ratio of approximately 1:4 and at  $-120^\circ\text{C}$  a decoalescence of the tetramer resonance into several overlapping resonances indicative of several tetrameric conformers.<sup>[27-28]</sup> Significantly, though extremely informative, Collum's studies required the challenging time-consuming preparation of isotopically labelled compounds. As far as we can ascertain, the same observation of these two aggregation isomers **2.1** and **2.2** has not been noted previously in routine NMR studies using ordinary unlabelled samples. Resonances associated with the  $\alpha$ -Me groups provide excellent diagnostic markers for recognising chemically distinct TMP ligands.<sup>[42]</sup> From  $^1\text{H}$  NMR spectra recorded in  $d_6$ -benzene solution at ambient temperature we assign resonances at 1.36 and 1.30 ppm to **2.2** and **2.1** respectively (Figure 2.7 and Figure 2.8).

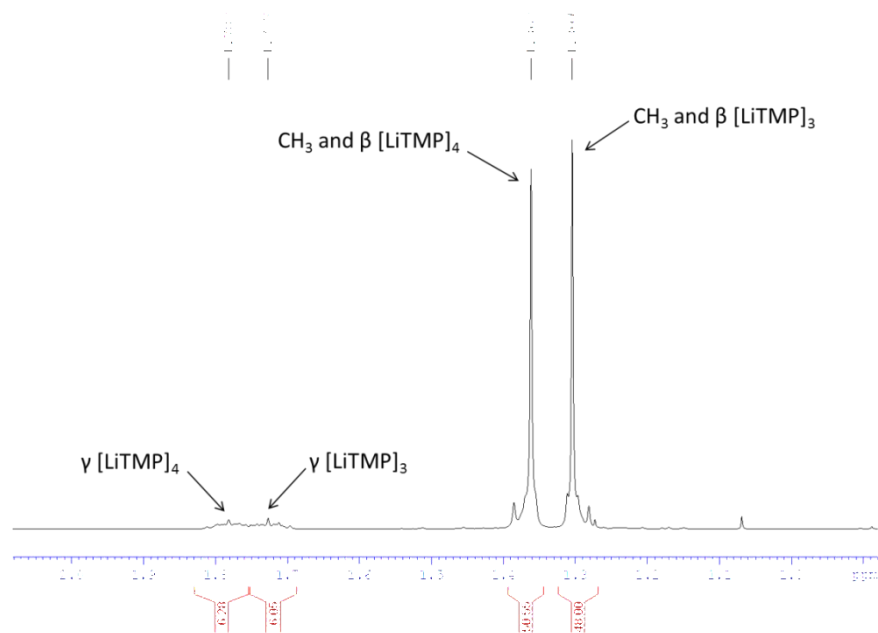


Figure 2.7.  $^1\text{H}$  NMR spectrum of  $(\text{LiTMP})_3$  **2.1** in  $\text{C}_6\text{D}_6$  solution. A small resonance is also present at 1.07 ppm which is a consequence of unavoidable hydrolysis that produces a small amount of TMP(H).

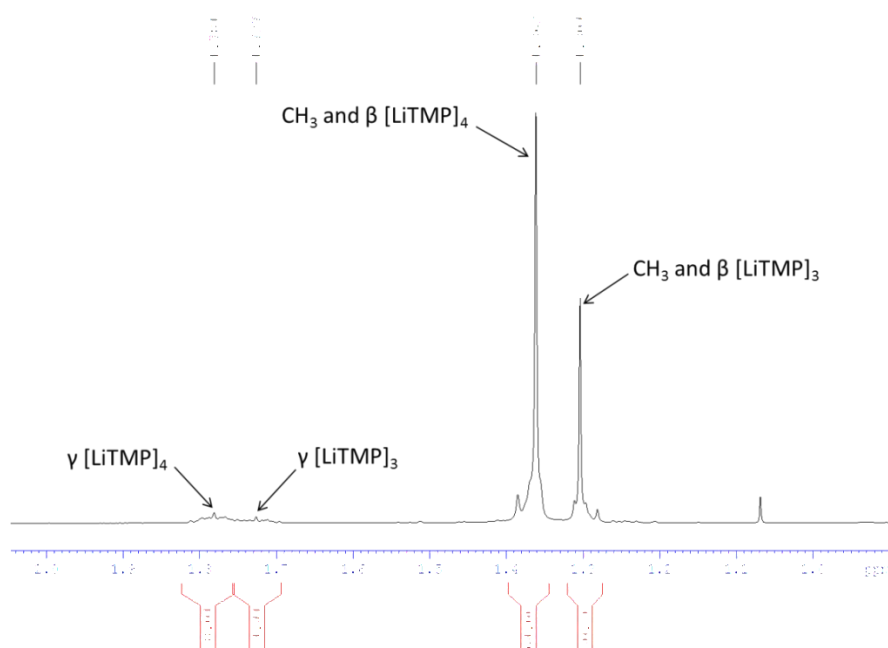


Figure 2.8.  $^1\text{H}$  NMR spectrum of  $(\text{LiTMP})_4$  **2.2** in  $\text{C}_6\text{D}_6$  solution also showing the aforementioned resonance at 1.07 ppm for TMP(H).

It transpires that **2.1** and **2.2** co-exist in solution irrespective of which crystals batches are used to make up the solution. To elaborate, when  $(\text{LiTMP})_3$  crystals (obtained at  $-35^\circ\text{C}$ ) are used to make up the solution integration values corresponding to a 1.00:0.79 molar ratio of **2.1:2.2** is obtained, that is with the cyclotrimer in a small excess (Figure 2.7). On the other hand, this ratio reverses to 1.00:1.59 with cyclotetramer **2.2** now in excess on using for the same spectrum (Figure 2.8)  $(\text{LiTMP})_4$  crystals grown either on the bench at ambient temperature or in the refrigerator at  $5^\circ\text{C}$ . Carrying out a variable temperature NMR study in  $d_8$ -toluene solution established that as the temperature falls from 300 K to 200 K the molar ratio of **2.1:2.2** increased from approximately 1.00:1.08 to 1.00:0.28 (Figure 2.9). This observation is consistent with the two cyclo-aggregates in a dynamic equilibrium with the smaller trimer favoured at lower temperature. Three solutions of  $(\text{LiTMP})_3$  crystals prepared at different concentrations of 6, 18, and 54  $\text{mg mL}^{-1}$  in  $d_{12}$ -cyclohexane solvent show a modest increase in the smaller cyclotrimer species (the **2.1:2.2** ratio changes from 1.00:0.24 to 1.00:0.16) as the concentration is decreased.

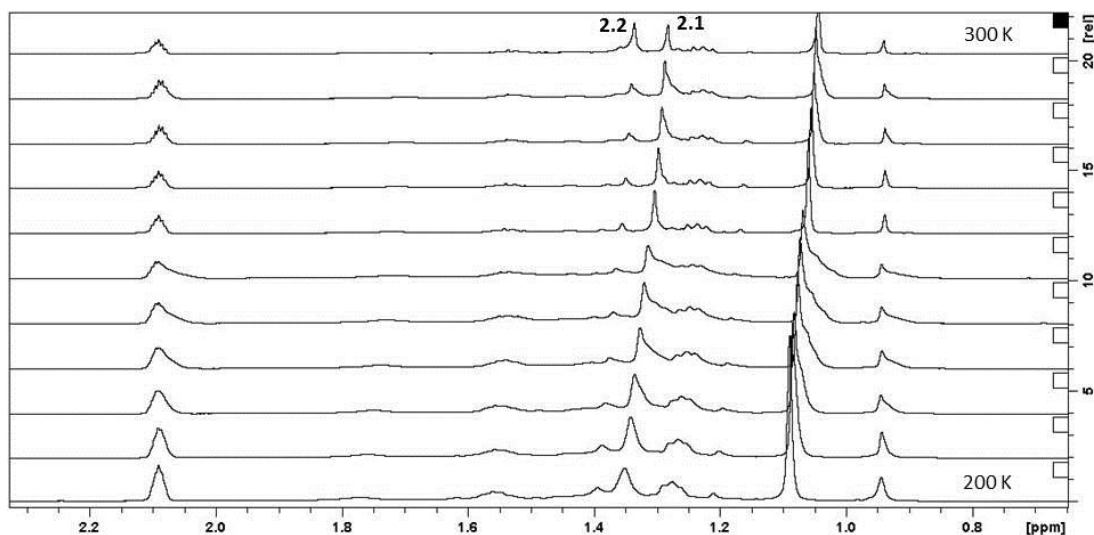


Figure 2.9.  $^1\text{H}$  NMR spectra of a variable temperature study (recorded in increments of 10 K) on  $(\text{LiTMP})_3$  **2.1** in  $d_8$ -toluene.

Measuring a  $d_6$ -benzene solution of  $(\text{LiTMP})_3$  crystals at ambient temperature over time revealed the equilibrium shifts towards the cyclotetramer as the **2.1:2.2** molar ratio drops from a starting value of 1.0:0.8 to a minimum of 1.0:1.9 (after 3 hours) after which it levels off (Figure 2.10). Moving to a  $d_{12}$ -cyclohexane ( $\text{C}_6\text{D}_{12}$ ) solution and monitoring the behaviour of **2.1** over 7 days (see the spectra in Figure 2.11) revealed that  $(\text{LiTMP})_3$  shows significantly more stability in the non-arene solvent only reaching a minimum **2.1:2.2** molar ratio of 1:1.35 after 1 week.

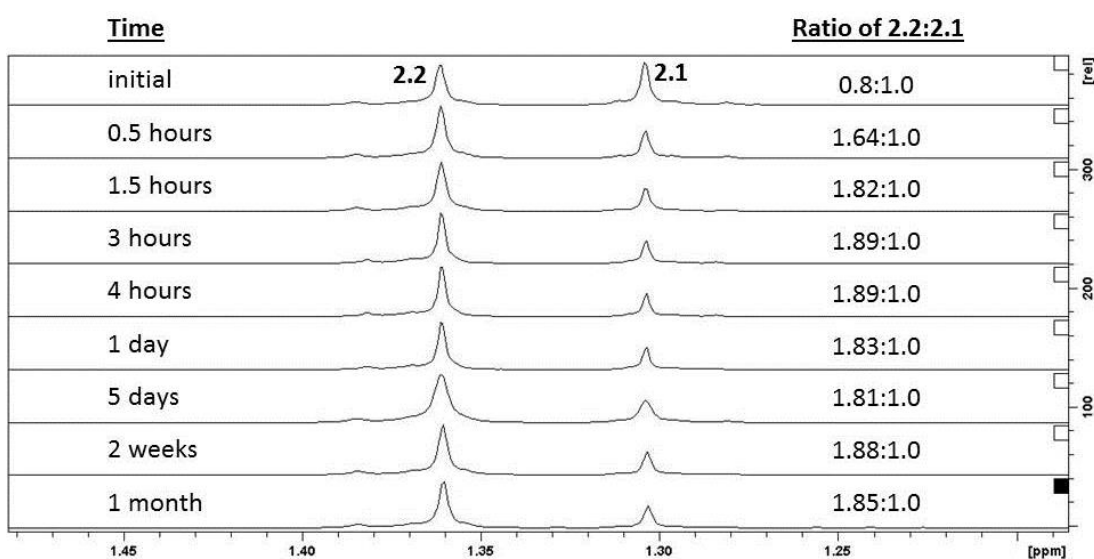


Figure 2.10.  $^1\text{H}$  NMR spectra of a variable time NMR study on  $(\text{LiTMP})_3$  **2.1** in  $\text{C}_6\text{D}_6$  solution showing the diagnostic Me resonances and approximate molar ratios of **2.2:2.1**.

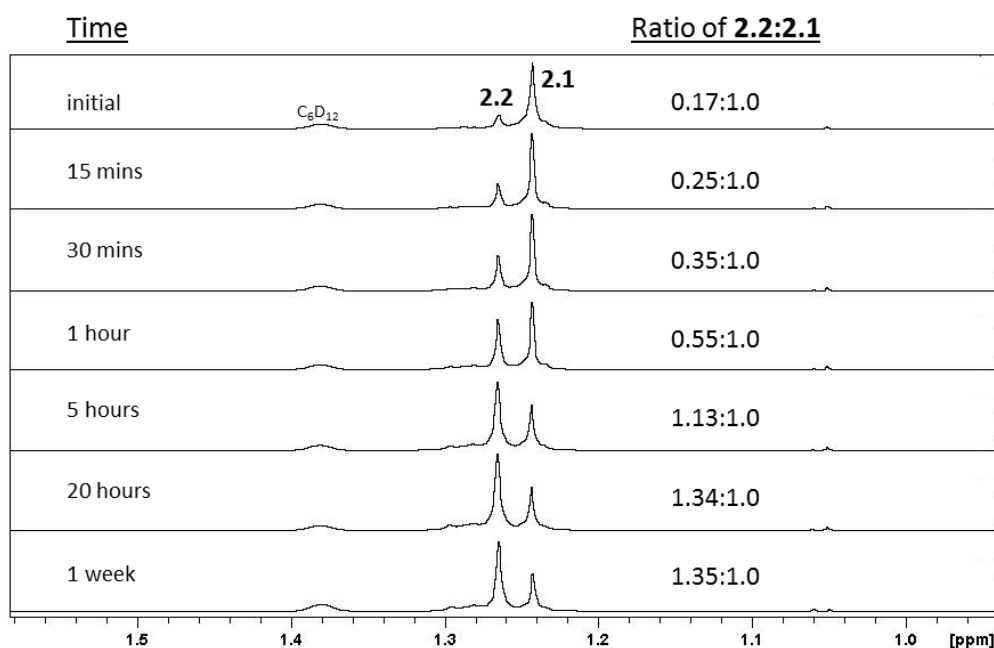


Figure 2.11.  $^1\text{H}$  NMR spectra of a variable time NMR study of  $(\text{LiTMP})_3$  **2.1** in  $\text{C}_6\text{D}_{12}$  solution showing the diagnostic Me resonances and the approximate **2.2:2.1** integration ratios.

Next we turned to DOSY  $^1\text{H}$  NMR studies. Carried out on  $(\text{LiTMP})_3$  crystals in both  $d_6$ -benzene (Figure 2.12) and  $d_{12}$ -cyclohexane solution, these spectra add good support to the above  $^1\text{H}$  assignments of **2.1** to the cyclotrimer and **2.2** to the cyclotetramer. Distinct species in solution can be separated due to their diffusion coefficients ( $d$ ), from which molecular weights ( $\text{MW}_{\text{DOSY}}$ ) can be estimated if internal inert standards of known molecular weight are employed for calibration purposes.<sup>[43-47]</sup> In this study the standards we used were tetramethylsilane, 1-phenylnaphthalene and 1,2,3,4-tetraphenylnaphthalene having molecular weights of 88, 204 and 433  $\text{g mol}^{-1}$  respectively. Estimated molecular weights in both solvents were consistent with the expected relative size order with those of cyclotrimer **2.1** smaller than those of cyclotetramer **2.2** though reflecting the limitation of the method these values fall short of those expected theoretically. In  $d_6$ -benzene solution the  $\text{MW}_{\text{DOSY}}$  is 348  $\text{g mol}^{-1}$  for **2.1** and 420  $\text{g mol}^{-1}$  for **2.2** equating to errors of -27% and -40% respectively

compared against the theoretical MWs (441 g mol<sup>-1</sup> for **2.1**; 588 g mol<sup>-1</sup> for **2.2**). Corresponding MW<sub>DOSY</sub> values in d<sub>12</sub>-cyclohexane are closer to the theoretical MWs (382 g mol<sup>-1</sup>, -15% error for **2.1**; 554 g mol<sup>-1</sup>, -6% error for **2.2**). Cyclooligomers **2.1** and **2.2** could also be distinguished in <sup>13</sup>C NMR spectra recorded in d<sub>6</sub>-benzene solution at 300 K though the chemical shift separations were diminutive (for example, CH<sub>3</sub>: 37.1 ppm for **2.1**; 37.0 ppm for **2.2**). On moving to <sup>7</sup>Li NMR studies the two species became indistinguishable with a single resonance observed in d<sub>6</sub>-benzene, d<sub>12</sub>-cyclohexane and d<sub>14</sub>-hexane solutions at 300 K with only broadening of it observed on lowering the temperature to 200 K (in d<sub>14</sub>-hexane). A <sup>1</sup>H-<sup>7</sup>Li HOESY experiment (Figure 2.13) confirmed that the single <sup>7</sup>Li resonance was associated with both **2.1** and **2.2**. The fact that <sup>7</sup>Li NMR spectroscopy on its own is a poor probe for separating **2.1** and **2.2** can be attributed to the two-coordinate equivalency of all the lithium atoms within each (LiN)<sub>n</sub> ring.

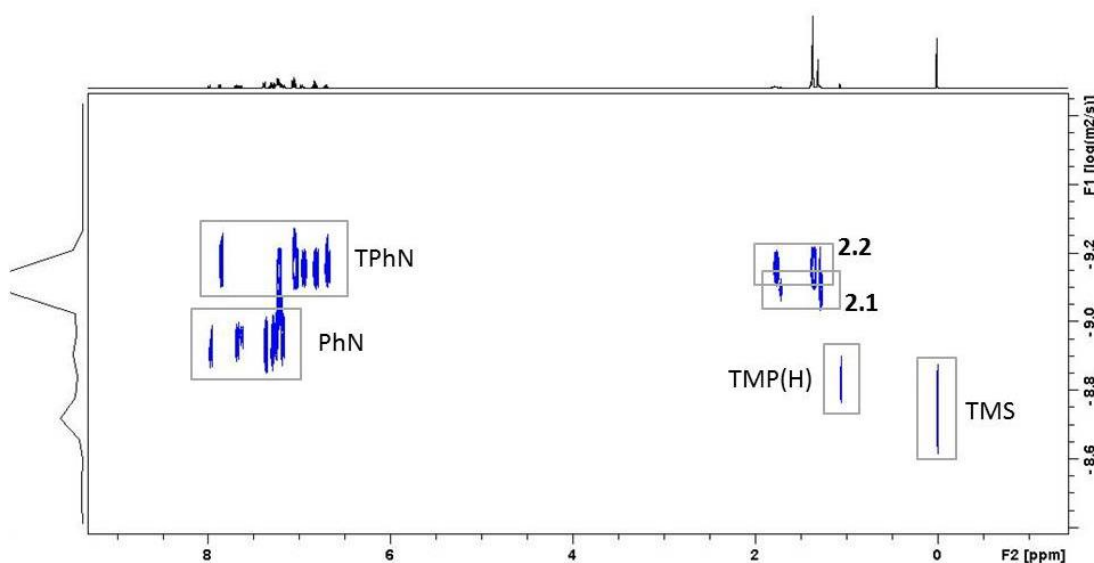


Figure 2.12. <sup>1</sup>H DOSY NMR spectrum of crystals of **2.1** in d<sub>6</sub>-benzene solution at 300 K in the presence of inert standards 1,2,3,4-tetraphenylnaphthalene (TPhN), 1-phenylnaphthalene (PhN) and tetramethylsilane (TMS). As a consequence of unavoidable hydrolysis a small amount of TMP(H) is also seen.



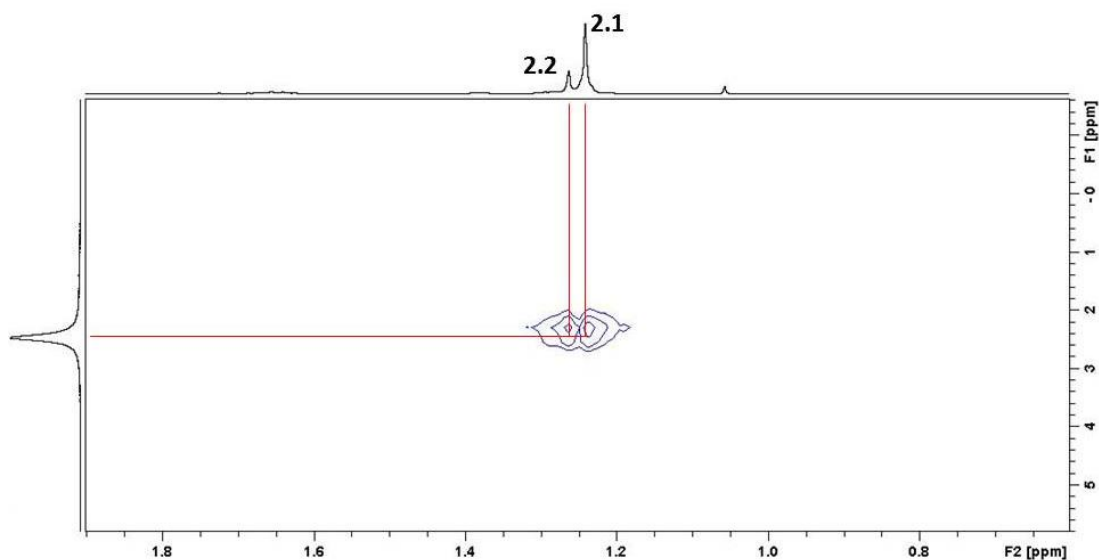


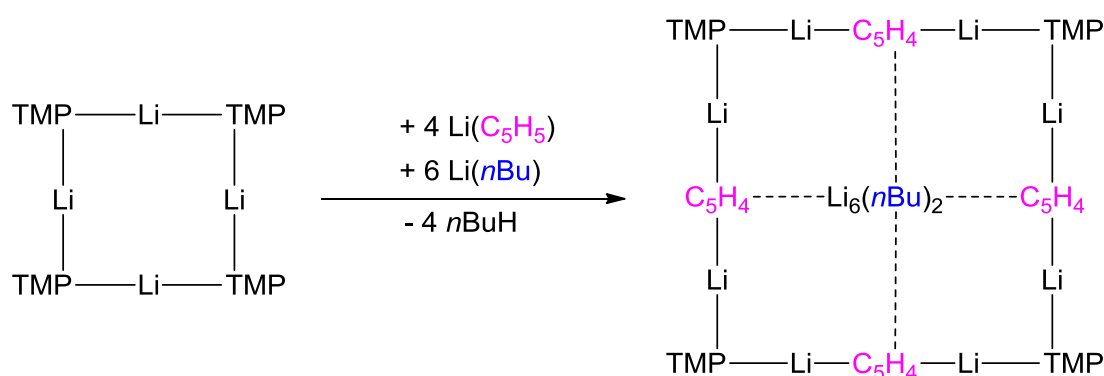
Figure 2.13.  $^1\text{H}$ ,  $^7\text{Li}$  HOESY spectrum of **2.1** in  $d_{12}$ -cyclohexane showing the  $^7\text{Li}$  resonance associated with both **2.1** and **2.2**.

### 2.3.4 Reflections on Previous Theoretical Calculations

Another factor that helped spark our interest in searching for a possible new crystalline polymorph of LiTMP came from an earlier DFT investigation at the B3LYP/6-311G\*\* level performed by the Mulvey group.<sup>[29]</sup> In the report of this work we mentioned explicitly the possibility of polymorphism on revealing that the  $\text{C}_{3\text{h}}$  cyclotrimer now verified in this new study as **2.1** was calculated to be actually  $0.04 \text{ kcal mol}^{-1}$  more stable than the  $\text{C}_{4\text{h}}$  cyclotetramer seen here in **2.2**, previously reported by Lappert and Atwood,<sup>[16]</sup> and implicated in solution by Collum.<sup>[27-28]</sup> Though these computations strictly model the gas phase only and therefore disregard crystal packing forces in solids and solvent effects in solution, the relative energy differences between this trimer and the four cyclotetramers studied in solution by Collum are so trivially small (the cyclotetramers cover a narrow range of  $0.88 \text{ kcal mol}^{-1}$ ) it is unsurprising that **2.1** and **2.2** exist side by side and easily interconvert in apolar aromatic and aliphatic solvents devoid of lone pairs of electrons.

### 2.3.5 Relevance to Reactivity and Structural Design

Synthetic organic chemistry has long recognised the importance of oligomer size in organolithium-mediated reactions with in general small oligomers, usually solvated, being more kinetically labile than large oligomers.<sup>[48-49]</sup> For this reason donor solvents such as HMPA, THF, and TMEDA often accompany organolithium reagents in their bond breaking (Brønsted basic) or bond making (nucleophilic addition) adventures.<sup>[50-59]</sup> However less interest has been shown in utilising organolithium oligomers in structural design though their propensity for aggregating and bridge bonding makes them ideal construction tools. The potential of LiTMP in structure building was recently demonstrated by Klett and the Mulvey group in the shape selective synthesis of the remarkable ring-cage hybrid compound  $[\{\text{Li}(\mu\text{-TMP})\text{Li}(\mu\text{-C}_5\text{H}_4)\}_4\text{Li}_6(n\text{Bu})_2]$  (Scheme 2.4).<sup>[60]</sup>



Scheme 2.4. Shape selective synthesis of  $[\{\text{Li}(\mu\text{-TMP})\text{Li}(\mu\text{-C}_5\text{H}_4)\}_4\text{Li}_6(n\text{Bu})_2]$ .

This truly astonishing structure was prepared by mixing (co-complexing) LiTMP with LiCp then forming a tri-co-complex with *n*BuLi. Notice however that LiTMP must exist in its cyclotetrameric architecture to facilitate the insertion of four LiCp molecules to construct the 5x5 molecular square arrangement of  $[\{\text{Li}(\mu\text{-TMP})\text{Li}(\mu\text{-Cp})\}_4]$ . If the smaller cyclotrimeric polymorph **2.1** discovered in this

work was the starting point for this LiTMP/LiCp di-crossing then the same architecture could not be realised (ignoring any equilibria processes). Significantly  $[\{\text{Li}(\mu\text{-TMP})\text{Li}(\mu\text{-C}_5\text{H}_4)\}_4\text{Li}_6(n\text{Bu})_2]$  was prepared in methylcyclohexane solution heated to 110°C for 2.5 hours, conditions which as implied here would favour the formation of the cyclotetramer **2.2** primed for executing the tri-co-complexing reaction. This prompts the intriguing thought that it may be possible to construct a series of unusual architectures/hybrid structures and by doing so create novel chemistry (note the unusual deprotonation of Cp  $[(\text{C}_5\text{H}_5)^-]$  to  $\text{C}_5\text{H}_4^{2-}$  in the formation of the ring-cage hybrid) by co-complexing different organolithium compounds (alkyls, aryls, amides, cyclopentadienyls etc.) at various temperatures in an assortment of solvents. The strategy of changing the conditions to tune the reactivity of organolithium reagents may be common in the context of synthetic organic chemistry but to the best of our knowledge they have been relatively unexplored in this area of novel structure building. Of course, in reality organolithium and lithium amide compounds exhibit complicated equilibria in solution, as this study, and most pertinently those aforementioned studies by Collum,<sup>[27-28]</sup> have established for LiTMP. Therefore any possible shape selective reactions will be strongly influenced by such equilibria. At this stage with little knowledge of the mechanisms of such reactions, the best approach to extending this idea would seemingly be through trial and error.

## 2.4 Conclusions

A new way of synthesising the increasingly popular utility amide LiTMP has been established. This is achieved by a transmetallation reaction between the zinc congener  $\text{Zn}(\text{TMP})_2$  and *t*BuLi in hexane solution. This has led to the discovery of a new crystalline polymorph in the cyclotrimer  $(\text{LiTMP})_3$  as established by X-ray crystallography. Repeating this reaction under different conditions and reinvestigating the original metallation synthesis reported in 1983 disclosed that polymorph formation was independent of the synthetic

method used but was controlled by the crystallisation temperature. Low temperature favours the smaller cyclic oligomer (LiTMP)<sub>3</sub> while high temperature favours (LiTMP)<sub>4</sub>. For an exact comparison we also performed an improved low temperature X-ray crystallographic study of previously reported (LiTMP)<sub>4</sub>. The two polymorphs were surprisingly easy to distinguish by routine <sup>1</sup>H and <sup>13</sup>C NMR studies with the results of DOSY experiments consistent with their relative sizes. Given the inordinately long wait for this new LiTMP polymorph to be unearthed – 40 years since LiTMP was first introduced to synthesis and 30 years after crystallographic characterisation of (LiTMP)<sub>4</sub> – the intriguing question to be asked in a future study is “how many other polymorphs of important organolithium compounds may have been overlooked?”

## 2.5 Future Work

In this body of work two different crystallisation temperatures were investigated and shown to generate two different polymorphs of LiTMP - a trimer and a tetramer. While one could expand this specific study by exploring a wider range of temperatures and ascertaining whether any other oligomers exist that have yet to be discovered, it may prove more worthwhile and useful investigating the crystallisation temperatures of other commonly utilised organolithium/organometallic reagents to determine whether any polymorphs of other compounds may have been overlooked in a similar to fashion to LiTMP.

The close of this chapter also touched on shape selective syntheses and highlighted the fact that different oligomers of a reagent may provoke different outcomes in certain reactions. Therefore it might be useful to probe both the trimer and the tetramer of LiTMP in various shape selective reaction pathways to see if there is any difference in the outcome of the reaction depending on which oligomer you begin with. Performing the reactions at different temperatures could make this possible though equilibria processes may

complicate matters. As LiTMP forms a cocomplex with *n*-butyllithium, a good starting point may be with the isomers *s*-butyllithium, *i*-butyllithium and *t*-butyllithium.

## 2.6 Experimental

Table 2.2. Crystallographic data and refinement details for compounds **2.1** and **2.2**.

	<b>2.1</b>	<b>2.2</b>
Formula	C <sub>27</sub> H <sub>54</sub> N <sub>3</sub> Li <sub>3</sub>	C <sub>36</sub> H <sub>72</sub> N <sub>4</sub> Li <sub>4</sub>
Formula weight	441.55	588.74
Crystal system	Hexagonal	Monoclinic
Space group	<i>P</i> 6 <sub>3</sub> / <i>m</i>	<i>C</i> 2/ <i>c</i>
Wavelength/Å	0.71073	0.71073
<i>a</i> /Å	10.3773(6)	16.6334(9)
<i>b</i> /Å	10.3773(6)	16.4942(5)
<i>c</i> /Å	14.7655(11)	15.7332(9)
$\alpha$ /°	90	90
$\beta$ /°	90	117.372(7)
$\gamma$ /°	120	90
Volume/Å <sup>3</sup>	1377.04(15)	3833.2(3)
<i>Z</i>	2	4
Refls. collected	4299	9738
2 $\theta$ <sub>max</sub>	29.2809	27.2752
R <sub>int</sub>	0.0304	0.0277
Goodness of fit	1.047	1.016
<i>R</i> [ <i>F</i> <sup>2</sup> > 2 $\sigma$ ], <i>F</i>	0.0441	0.0474
<i>R</i> <sub>w</sub> (all data), <i>F</i> <sup>2</sup>	0.1101	0.1148

### 2.6.1 Synthesis of (LiTMP)<sub>3</sub>

**Transmetallation approach** - Zn(TMP)<sub>2</sub> (0.35 g, 1 mmol) was dissolved in hexane (10 mL) and *t*BuLi (0.59 mL, 1.7 M in pentane, 1 mmol) added dropwise by syringe resulting in a pale yellow solution. After 10 min stirring the flask was placed in the freezer (-35°C) overnight to yield a crop of colourless crystals (0.132 g, 90%). The same procedure was repeated using 2 and 3 equivalents of

*t*BuLi, resulting in the same product and similar yields. **Deprotometallation approach** - *n*BuLi (0.63 mL, 1.6 M in hexanes, 1 mmol) was added dropwise by syringe to a stirring mixture of TMPH (0.17 mL, 1 mmol) and hexane (10 mL). The resulting pale yellow solution was then stored in the freezer (-35°C) overnight where a crop of colourless crystals formed (0.09 g, 20%).

**<sup>1</sup>H NMR (C<sub>6</sub>D<sub>6</sub>, 300 K):** δ=1.73 (m, 6H, TMP γ), 1.30 ppm (s, 48H, TMP CH<sub>3</sub> and β).

**<sup>13</sup>C NMR (C<sub>6</sub>D<sub>6</sub>, 300 K):** δ=52.3 (TMP α), 43.2 (TMP β), 37.1 (TMP CH<sub>3</sub>), 20.1 ppm (TMP γ) [note that these resonances are for the pure (LiTMP)<sub>3</sub> however as seen in the supporting information resonances for the other polymorph (LiTMP)<sub>4</sub> are also present].

**<sup>7</sup>Li NMR (C<sub>6</sub>D<sub>6</sub>, 300 K):** δ=2.47 ppm.

Elemental analysis of monomer calcd (%) for C<sub>9</sub>H<sub>18</sub>N<sub>1</sub>Li<sub>1</sub>: C 73.44; H 12.33; N 9.52; found: C 73.97; H 12.05; N 9.03.

## 2.6.2 Synthesis of (LiTMP)<sub>4</sub>

**Transmetallation approach** - Zn(TMP)<sub>2</sub> (0.35 g, 1 mmol) was dissolved in hexane (10 mL) and *t*BuLi (0.59 mL, 1.7 M in pentane, 1 mmol) added dropwise by syringe resulting in a pale yellow solution. A small amount of solvent was removed *in vacuo* and upon standing overnight (either on the bench or in the refrigerator) a crop of colourless crystals formed (typical yield = 0.06 g, 41%).

**Deprotometallation approach** - *n*BuLi (0.63 mL, 1.6 M in hexanes, 1 mmol) was added dropwise by syringe to a stirring mixture of TMPH (0.17 mL, 1 mmol) and hexane (10 mL) resulting in a pale yellow solution. Some solvent was removed *in vacuo* and the flask was then stored either in the refrigerator or on the bench overnight to yield a crop of colourless crystals (0.03 g, 20%).

**<sup>1</sup>H NMR (C<sub>6</sub>D<sub>6</sub>, 300 K):** δ=1.78 (m, 8H, TMP γ), 1.36 ppm (s, 64H, TMP CH<sub>3</sub> and β).

## Chapter 2: Concealed Cyclotrimeric Polymorph of Lithium TMP Unconcealed

$^{13}\text{C}$  NMR ( $\text{C}_6\text{D}_6$ , 300 K):  $\delta=52.4$  (TMP  $\alpha$ ), 42.8 (TMP  $\beta$ ), 37.0 (TMP  $\text{CH}_3$ ), 19.9 ppm (TMP  $\gamma$ ) [note that these resonances are for the pure  $(\text{LiTMP})_3$  however as seen in the supporting information resonances for the other polymorph  $(\text{LiTMP})_4$  are also present].

## 2.7 Bibliography

- [1] H. Gilman, J. A. Beel, C. G. Brannen, M. W. Bullock, G. E. Dunn, L. S. Miller, *J. Am. Chem. Soc.* **1949**, *71*, 1499-1500.
- [2] P. D. Bartlett, C. G. Swain, R. B. Woodward, *J. Am. Chem. Soc.* **1941**, *63*, 3229-3230.
- [3] W. Schlenk, E. Bergmann, *Justus Liebigs Ann. Chem.* **1928**, *463*, 98-227.
- [4] H. Gilman, R. L. Bebb, *J. Am. Chem. Soc.* **1939**, *61*, 109-112.
- [5] G. Wittig, G. Fuhrman, *Chem. Ber.* **1940**, *73B*, 1197-1218.
- [6] H. J. Reich, *Chem. Rev.* **2013**, *113*, 7130-7178.
- [7] K. Ziegler, H. Ohlinger, *Justus Liebigs Ann. Chem.* **1932**, *495*, 84-112.
- [8] M. Hamell, R. Levine, *J. Org. Chem.* **1950**, *15*, 162-168.
- [9] M. F. Lappert, P. P. Power, A. R. Sanger, R. C. Srivastava, *Metal and Metalloid Amides*, John Wiley & Sons, Chichester, **1980**.
- [10] M. Lappert, A. Protchenko, P. Power, A. Seeber, *Metal Amide Chemistry*, John Wiley & Sons, Chichester, **2009**.
- [11] R. E. Mulvey, S. D. Robertson, *Angew. Chem. Int. Ed.* **2013**, *52*, 11470-11487.
- [12] A. R. Kennedy, S. M. Leenhouts, J. J. Liggat, A. J. Martinez-Martinez, K. Miller, R. E. Mulvey, C. T. O'Hara, P. O'Keefe, A. Steven, *Chem. Commun.* **2014**, *50*, 10588-10591.
- [13] D. Allan, J. Daly, J. J. Liggat, *Polym. Degrad. Stab.* **2013**, *98*, 535-541.
- [14] M. H. Mohammed, W. M. Banks, D. Hayward, J. J. Liggat, R. A. Pethrick, B. Thomson, *Polym. Degrad. Stab.* **2013**, *98*, 1264-1270.
- [15] L. Turnbull, J. J. Liggat, W. A. MacDonald, *Polym. Degrad. Stab.* **2013**, *98*, 2244-2258.
- [16] M. F. Lappert, M. J. Slade, A. Singh, J. L. Atwood, R. D. Rogers, R. Shakir, *J. Am. Chem. Soc.* **1983**, *105*, 302-304.
- [17] C. L. Kissel, B. Rickborn, *J. Org. Chem.* **1972**, *37*, 2060-2063.
- [18] M. W. Rathke, R. Kow, *J. Am. Chem. Soc.* **1972**, *94*, 6854-6856.
- [19] P. v. R. Schleyer, W. N. Setzer, *Adv. Organomet. Chem.* **1985**, *24*, 353-451.
- [20] K. Gregory, P. v. R. Schleyer, R. Snaith, *Adv. Inorg. Chem.* **1991**, *37*, 47-142.
- [21] R. E. Mulvey, *Chem. Soc. Rev.* **1991**, *20*, 167-209.
- [22] R. E. Mulvey, *Chem. Soc. Rev.* **1998**, *27*, 339-346.
- [23] D. Stalke, T. Stey, *The Chemistry of Organolithium Compounds*, John Wiley and Sons, Chichester, **2004**.
- [24] D. R. Armstrong, D. Barr, W. Clegg, S. M. Hodgson, R. E. Mulvey, D. Reed, R. Snaith, D. S. Wright, *J. Am. Chem. Soc.* **1989**, *111*, 4719-4727.
- [25] D. R. Armstrong, P. Garcia-Alvarez, A. R. Kennedy, R. E. Mulvey, S. D. Robertson, *Chem. Eur. J.* **2011**, *17*, 6725-6730.
- [26] D. R. Armstrong, A. R. Kennedy, R. E. Mulvey, S. D. Robertson, *Chem. Eur. J.* **2011**, *17*, 8820-8831.
- [27] B. L. Lucht, D. B. Collum, *J. Am. Chem. Soc.* **1994**, *116*, 7949-7950.
- [28] J. F. Remenar, B. L. Lucht, D. Kruglyak, F. E. Romesberg, J. H. Gilchrist, D. B. Collum, *J. Org. Chem.* **1997**, *62*, 5748-5754.



- [29] D. R. Armstrong, D. V. Graham, A. R. Kennedy, R. E. Mulvey, C. T. O'Hara, *Chem. Eur. J.* **2008**, *14*, 8025-8034.
- [30] R. Grüning, J. L. Atwood, *J. Organomet. Chem.* **1977**, *137*, 101-111.
- [31] J. Knizek, I. Krossing, H. Nöth, H. Schwenk, T. Seifert, *Chem. Ber.* **1997**, *130*, 1053-1062.
- [32] M. Driess, H. Pritzkow, M. Skipinski, U. Winkler, *Organometallics* **1997**, *16*, 5108-5112.
- [33] P. Renaud, M. A. Fox, *J. Am. Chem. Soc.* **1988**, *110*, 5702-5705.
- [34] W. Clegg, S. H. Dale, A. M. Drummond, E. Hevia, G. W. Honeyman, R. E. Mulvey, *J. Am. Chem. Soc.* **2006**, *128*, 7434-7435.
- [35] M. Uchiyama, Y. Kobayashi, T. Furuyama, S. Nakamura, Y. Kajihara, T. Miyoshi, T. Sakamoto, Y. Kondo, K. Morokuma, *J. Am. Chem. Soc.* **2008**, *130*, 472-480.
- [36] W. Clegg, B. Conway, E. Hevia, M. D. McCall, L. Russo, R. E. Mulvey, *J. Am. Chem. Soc.* **2009**, *131*, 2375-2384.
- [37] B. Haag, M. Mosrin, H. Ila, V. Malakhov, P. Knochel, *Angew. Chem. Int. Ed.* **2011**, *50*, 9794-9824.
- [38] K. Snegaroff, T. T. Nguyen, N. Marquise, Y. S. Halauko, P. J. Harford, T. Roisnel, V. E. Matulis, O. A. Ivashkevich, F. Chevallier, A. E. H. Wheatley, P. C. Gros, F. Mongin, *Chem. Eur. J.* **2011**, *17*, 13284-13297.
- [39] S. Komagawa, S. Usui, J. Haywood, P. J. Harford, A. E. H. Wheatley, Y. Matsumoto, K. Hirano, R. Takita, M. Uchiyama, *Angew. Chem. Int. Ed.* **2012**, *51*, 12081-12085.
- [40] R. R. Kadiyala, D. Tilly, E. Nagaradja, T. Roisnel, V. E. Matulis, O. A. Ivashkevich, Y. S. Halauko, F. Chevallier, P. C. Gros, F. Mongin, *Chem. Eur. J.* **2013**, *19*, 7944-7960.
- [41] R. E. Mulvey, D. R. Armstrong, B. Conway, E. Crosbie, A. R. Kennedy, S. D. Robertson, *Inorg. Chem.* **2011**, *50*, 12241-12251.
- [42] E. Hevia, A. R. Kennedy, J. Klett, M. D. McCall, *Chem. Commun.* **2009**, 3240-3242.
- [43] A. Macchioni, G. Ciancaleoni, C. Zuccaccia, D. Zuccaccia, *Chem. Soc. Rev.* **2008**, *37*, 479-489.
- [44] D. Li, I. Keresztes, R. Hopson, P. G. Williard, *Acc. Chem. Res.* **2009**, *42*, 270-280.
- [45] D. R. Armstrong, P. Garcia-Alvarez, A. R. Kennedy, R. E. Mulvey, J. A. Parkinson, *Angew. Chem. Int. Ed.* **2010**, *49*, 3185-3188.
- [46] T. Tatic, K. Meindl, J. Henn, S. K. Pandey, D. Stalke, *Chem. Commun.* **2010**, 46, 4562-4564.
- [47] P. Garcia-Álvarez, R. E. Mulvey, J. A. Parkinson, *Angew. Chem. Int. Ed.* **2011**, *50*, 9668-9671.
- [48] R. E. Mulvey, F. Mongin, M. Uchiyama, Y. Kondo, *Angew. Chem. Int. Ed.* **2007**, *46*, 3802-3802.
- [49] J. Clayden, *Organolithiums: Selectivity for Synthesis*, Vol. 23, Pergamon, Oxford, **2002**.
- [50] D. W. Slocum, T. K. Reinscheld, C. B. White, M. D. Timmons, P. A. Shelton, M. G. Slocum, R. D. Sandlin, E. G. Holland, D. Kusmic, J. A. Jennings, K. C.

- Tekin, Q. Nguyen, S. J. Bush, J. M. Keller, P. E. Whitley, *Organometallics* **2013**, *32*, 1674-1686.
- [51] H. J. Reich, *J. Org. Chem.* **2012**, *77*, 5471-5491.
- [52] T. Tatic, S. Hermann, M. John, A. Loquet, A. Lange, D. Stalke, *Angew. Chem. Int. Ed.* **2011**, *50*, 6666-6669.
- [53] T. Rathman, W. F. Bailey, *Org. Process Res. Dev.* **2009**, *13*, 144-151.
- [54] M. C. Whisler, S. MacNeil, V. Snieckus, P. Beak, *Angew. Chem. Int. Ed.* **2004**, *43*, 2206-2225.
- [55] D. B. Collum, *Acc. Chem. Res.* **1992**, *25*, 448-454.
- [56] F. E. Romesberg, J. H. Gilchrist, A. T. Harrison, D. J. Fuller, D. B. Collum, *J. Am. Chem. Soc.* **1991**, *113*, 5751-5757.
- [57] W. Bauer, P. v. R. Schleyer, *J. Am. Chem. Soc.* **1989**, *111*, 7191-7198.
- [58] C. G. Screttas, I. C. Smonou, *J. Organomet. Chem.* **1988**, *342*, 143-152.
- [59] D. W. Slocum, C. A. Jennings, *J. Org. Chem.* **1976**, *41*, 3653-3664.
- [60] A. A. Fyfe, A. R. Kennedy, J. Klett, R. E. Mulvey, *Angew. Chem. Int. Ed.* **2011**, *50*, 7776-7780.

## **Chapter 3**

### **TMP-Aluminate Bases: Lithium-Mediated Almination or Lithiation – Alkylaluminium-Trapping Reagents?**

### 3.1 Aims

The overarching aim of the work carried out in this chapter was to gain a more complete characterisation and therefore understanding of the two main aluminium ate systems currently used for metallation purposes “LiTMP·Al(*i*Bu)<sub>3</sub>” and “LiTMP·Al(TMP)(*i*Bu)<sub>2</sub>” by executing an in depth study of them using new and existing information from crystallographic, spectroscopic and theoretical investigations.

Specific objectives are outlined below:

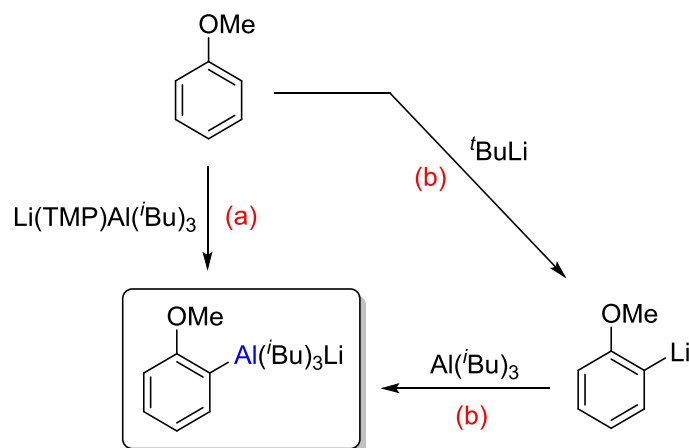
- Determine the active base/s present within Uchiyama’s mono-amido reagent LiTMP·Al(*i*Bu)<sub>3</sub>.
- Evaluate if the *in situ* version of LiTMP·Al(*i*Bu)<sub>3</sub> is consistent with its crystallised form.
- Explain any possible differences arising in reactivity between the *in situ* and crystallised form of LiTMP·Al(*i*Bu)<sub>3</sub>.
- Shed light on the composition of our bis-amido variant LiTMP·Al(TMP)(*i*Bu)<sub>2</sub>.
- Establish the active base/s present within LiTMP·Al(TMP)(*i*Bu)<sub>2</sub>.
- Elucidate the reaction mechanism associated with each of the base systems using NMR spectroscopic studies.
- Confirm such reaction mechanisms experimentally and through the use of theoretical calculations.
- Rationalise any possible differences observed between the two base mixtures based on their reaction mechanisms.

## 3.2 Introduction

Metallation, the exchange of synthetically intractable C-H bonds for synthetically tractable C-metal bonds, has been dramatically transformed over the past several years with the emergence of a plethora of new metallating agents. These second generation metallating agents (organolithium reagents would be the first generation type) contain soft metals such as magnesium, zinc, and aluminium, in particular, and copper and manganese to a lesser extent, which can now rival lithium in executing metal-hydrogen exchange on a myriad of aromatic and heteroaromatic substrates. Moreover these fundamentally important reactions of this second generation of metallating reagents can often offer general advantages (most significantly, improved functional group tolerance, milder reaction conditions, greater compatibility with tandem transition metal catalysed bond forming strategies) over those executed by long established lithium alkyl<sup>[1-2]</sup> and lithium amide<sup>[3-4]</sup> reagents. More electronegative than lithium, these other higher valent metals form less polar C-metal bonds and consequently their organometallic compounds are significantly less reactive than their organolithium predecessors. Therefore activation is necessary to modify these less reactive metals and make them basic enough for metallation applications. Two types of activation are common. That discussed in Section 1.3.3, whereby stoichiometric amounts of the salt lithium chloride can be introduced to generate mixed organometallic-salt systems such as the turbo-Hauser reagent (TMP)MgCl·LiCl.<sup>[5-7]</sup> Though organometallic-salt systems have been known for many years,<sup>[8-10]</sup> a string of papers by Knochel has established such compositions as a systematic series of versatile synthetic reagents in both metallation and metal-halide protocols.<sup>[11]</sup> The second form of activation is through mixed organometallic-organometallic systems where one metal is always an alkali metal and the second metal is one of the aforementioned nominally less reactive metals (as discussed in Section 1.3.2).<sup>[12-16]</sup> These mixed-metal systems are often supported by mixed amido-alkyl ligand sets typified by complexes such as LiTMP·Zn(*t*Bu)<sub>2</sub> <sup>[17-19]</sup> and TMEDA·Na(<sup>*n*</sup>Bu)·Mg(TMP)<sub>2</sub> <sup>[20]</sup> which can also be interpreted as ates (zincate and magnesiate respectively). The

presence of the amide ligand is essential for these complexes to function as metallating agents as those with all-alkyl ligand sets show a greater tendency for nucleophilic addition.<sup>[21-22]</sup> While in metallation reactions the efficiency and scope of these second generation metallating agents have generally been well studied, by comparison definite information on them in their own right has been rather thin on the ground prompting some to be likened to black box reagents.<sup>[23]</sup> In this particular respect they lag well behind organolithium reagents which have been extensively studied for over 50 years.

An especially attractive branch of this multicomponent ate chemistry is alkali-metal-mediated aluminations (AMMAI) due to the high abundance (as noted earlier, aluminium is the most abundant metal in the earth's crust), comparative cheapness, low toxicity and recycling opportunities of the p-block metal as well as the documented halogen tolerance of lithium aluminates.<sup>[24-25]</sup> Though mixed alkali metal aluminate compounds have been utilised for decades in synthetic chemistry with the reducing agent lithium aluminium hydride probably the most popular example,<sup>[26-29]</sup> the beginning of AMMAI came in 2004 when the group of Uchiyama published the first examples of regio- and chemo-selective aluminations of aromatic substrates using an Al ate base.<sup>[30]</sup> The aluminium base used was empirically formulated as "LiTMP·Al(*i*Bu)<sub>3</sub>" **3.1** and synthesised from a THF solution of LiTMP and Al(*i*Bu)<sub>3</sub>. The group demonstrated how an impressive assortment of aromatic compounds could be aluminated using the *in situ* base mixture, generating the organic products after a quenching step, in excellent yields. Especially noteworthy was the fact that both electron-donating and electron-withdrawing groups could be tolerated during the deprotonation reactions, allowing access to a wide range of selectively functionalised organic products. Evidence that an aluminated intermediate was formed in these deprotonation reactions came from a comparison of the <sup>13</sup>C NMR spectra of the reaction mixture [LiTMP·Al(*i*Bu)<sub>3</sub> + anisole] prior to quenching, and the co-complexation reaction between lithiated anisole and Al(*i*Bu)<sub>3</sub> (Scheme 3.1) in which the authors stated the chemical shifts obtained from both reactions were "reasonably consistent".



Scheme 3.1. *Ortho*-alumination of anisole using either (a) a direct almination pathway or (b) a stepwise lithiation and subsequent co-complexation reaction.

At the end of their initial *AMMAI* paper, the authors intimated that they planned to perform further work to determine the scope of the promising new Al ate compound, as well as to gain insights into the constitution and structure of the base. Three years later they delivered with a full paper entitled “An Aluminum Ate Base: Its Design, Structure, Function, and Reaction Mechanism”.<sup>[31]</sup> This paper elaborated on how **3.1** can be used to prepare a wide variety of organic molecules ranging from 1,2- or 1,2,3-multisubstituted aromatic compounds through to enabling the addition reactions of non-aromatic molecules. Significantly, they claimed to have uncovered the structure of the active base in **3.1** through a combination of NMR spectroscopic, X-ray crystallographic and theoretical (DFT) studies. Interrogating a THF solution of **3.1** by multinuclear  $^1\text{H}$ ,  $^{13}\text{C}$ ,  $^7\text{Li}$ ,  $^{15}\text{N}$  and  $^{27}\text{Al}$  NMR spectroscopy revealed **3.1** to be a single species which the authors suggested had the ion-pair formula  $\text{Li}^+[(\text{TMP})\text{Al}(\text{iBu})_3]^-$ . Supporting this interpretation, the authors were able to grow X-ray quality crystals from the base mixture which after analysis determined the molecular structure to actually be of a contacted ion-pair type, namely  $[\text{THF}\cdot\text{Li}(\mu\text{-TMP})(\mu\text{-iBu})\text{Al}(\text{iBu})_2]$  **3.1**·**THF** (Figure 3.1). In this structure the amido TMP group forms an asymmetrical bridge between the Li and Al centres along with one of the

three *iso*-butyl groups. Completing the structure, the remaining *iso*-butyl anions sit terminally on the Al while one neutral THF molecule caps the Li atom.

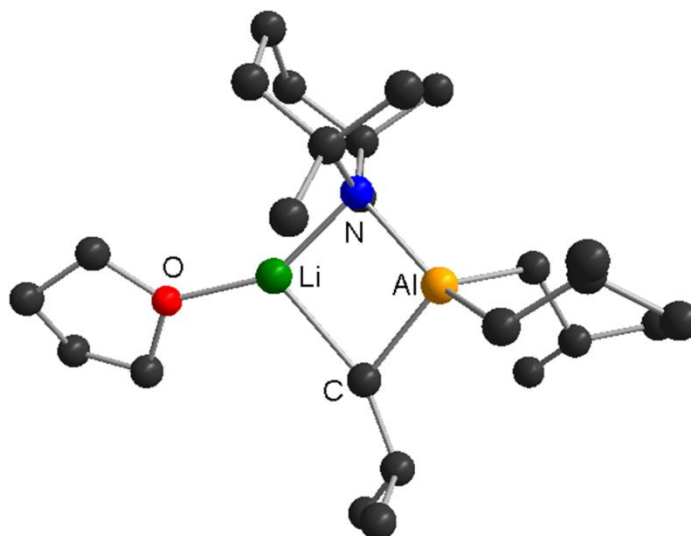
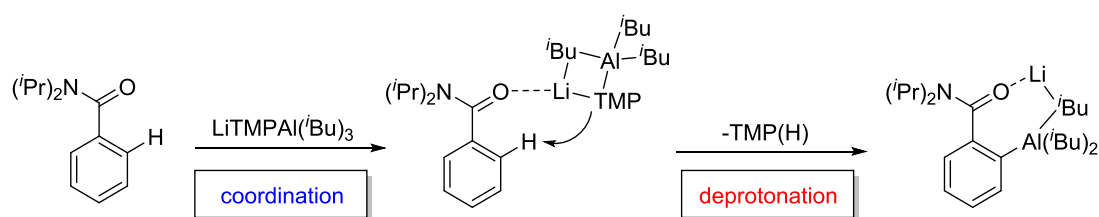


Figure 3.1. Molecular structure of [THF·Li(μ-TMP)(μ-*i*Bu)Al(*i*Bu)<sub>2</sub>] **3.1**·THF, the suspected AMMAI base.

Armed with this new knowledge, the authors then proposed a reaction mechanism for the aluminations reactions based on **3.1**·THF being the active base. This involves firstly a coordination of the base to the substrate molecule through a dative Li-X interaction which brings the anionic TMP ligand into close proximity of the *ortho* H atom and secondly, the regioselective deprotonation of the substrate (Scheme 3.2).



Scheme 3.2. Reaction mechanism for the deprotonation of *N,N*-diisopropylbenzamide by **3.1** as proposed by Uchiyama *et al.*



Following the development of this mono-amido tris-alkyl base by Uchiyama, the Mulvey group synthesised a bis-amido bis-alkyl version in  $\text{LiTMP}\cdot\text{Al}(\text{TMP})(i\text{Bu})_2$  **3.2**, where two TMP anions and two  $i\text{Bu}$  groups are incorporated into a Li-Al bimetallic mixture. The thinking behind this modified base was that the presence of the two TMP ligands could lead to a more powerful base given that TMP appeared to be the active base ligand within Uchiyama's reagent. This proved justified as **3.2** was found capable of performing the *ortho*-deprotonation on a wide variety of aromatic molecules, including those containing sensitive groups such as halides and carboxamides.<sup>[32]</sup> A particularly noteworthy result achieved with **3.2** was the  $\alpha$ -metallation of THF where, after performing deprotonation of the cyclic ether, the Li-Al base captured the remaining sensitive cycloanionic structure fully intact with no degradation whatsoever, generating the heterotrileptic complex  $[\text{THF}\cdot\text{Li}(\mu\text{-TMP})(\mu\text{-OC}_4\text{H}_7)\text{Al}(i\text{Bu})_2]$  (Figure 3.2).<sup>[33]</sup>

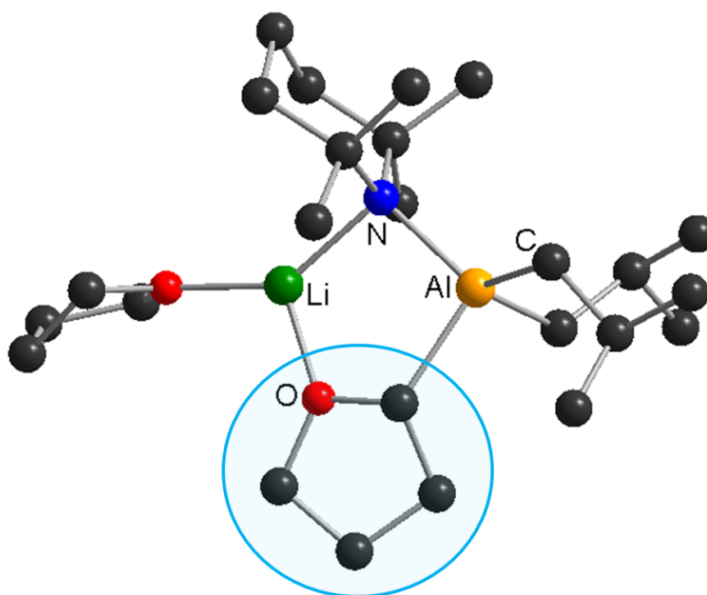
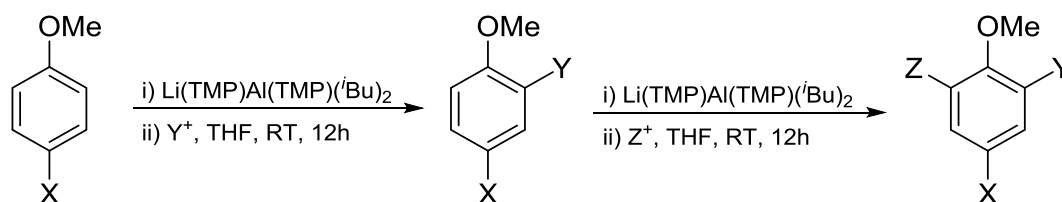


Figure 3.2. Molecular structure of  $[\text{THF}\cdot\text{Li}(\mu\text{-TMP})(\mu\text{-OC}_4\text{H}_7)\text{Al}(i\text{Bu})_2]$  highlighting the  $\alpha$ -deprotonated THF molecule.

Note the contrasting reactivity here between **3.1** and **3.2**. Mono-amido **3.1** can be stabilised as a THF solvate as shown by the crystal structure in Figure 3.1 and does not appear to deprotonate the ether. As well as this “cleave and capture” (see Chapter 4, Section 4.2) ability the bis-TMP mixture can also perform challenging intramolecular C-H deprotonations of molecules present in the system such as TMP<sup>[34]</sup> and TMEDA.<sup>[35]</sup> A recent communication also established the halogen tolerance of **3.2** with several 4-halo-anisole molecules selectively aluminated in the *ortho*-position before being quenched with electrophilic halogen species to afford a novel series of multi-heterohalogenated anisole molecules (Scheme 3.3).<sup>[25]</sup>



Scheme 3.3. Sequential aluminations and halogenations of 4-halo-anisoles leading to di- or tri-halogenated products.

With **3.1** and **3.2** being the two main reagents in aluminium ate metallation chemistry, it was appropriate that a study was undertaken to compare and contrast the two systems. This study, reported by Mulvey and co-workers<sup>[36]</sup> in 2013 probed each reagent’s reactivity in turn towards six polydentate Lewis bases (Figure 3.3). Seven of the twelve reactions carried out in apolar hexane solution produced crystalline material suitable for X-ray crystallographic determination. Interestingly when assessing the molecular structures obtained they found a key difference in the reactivity between the two bases. The reactions of **3.2** with Me<sub>2</sub>TFA, MDAE and Me<sub>4</sub>AEE provided structures which suggested that the bis-amido **3.2** had acted as a deprotonating agent, aluminating the three polydentate molecules. In contrast, the crystal structures

from the reactions of Uchiyama's **3.1** with Me<sub>2</sub>TFA, MDAE and DME, implied that the Al reagent was only coordinating datively to the heteroatom present in the substrates, failing to metallate any of these molecules. Using *N,N*-dimethyltetrahydrofurfurylamine (Me<sub>2</sub>TFA) as an example, the molecular structures shown in Figure 3.4 clearly highlight the difference in the interaction between the substrate and the two bases. With **3.1** the non-deprotonated Me<sub>2</sub>TFA substrate can be seen interacting only with the Li atom, with all the anionic ligands still present bound to the Al centre; whereas with **3.2** the Al centre is now interacting with the deprotonated C atom adjacent to the O centre on the substrate, having lost one of its *i*Bu groups.

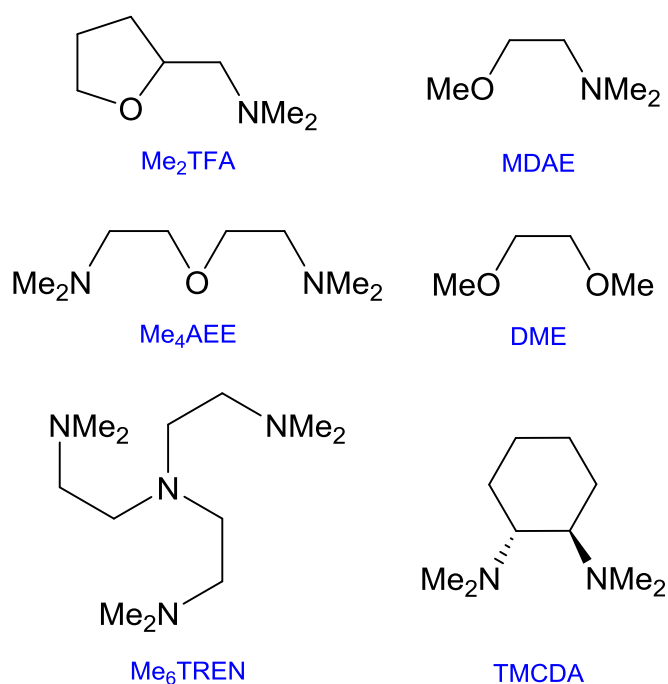


Figure 3.3. The polydentate donor molecules used as test deprotonation substrates with both **3.1** and **3.2**.<sup>[36]</sup>

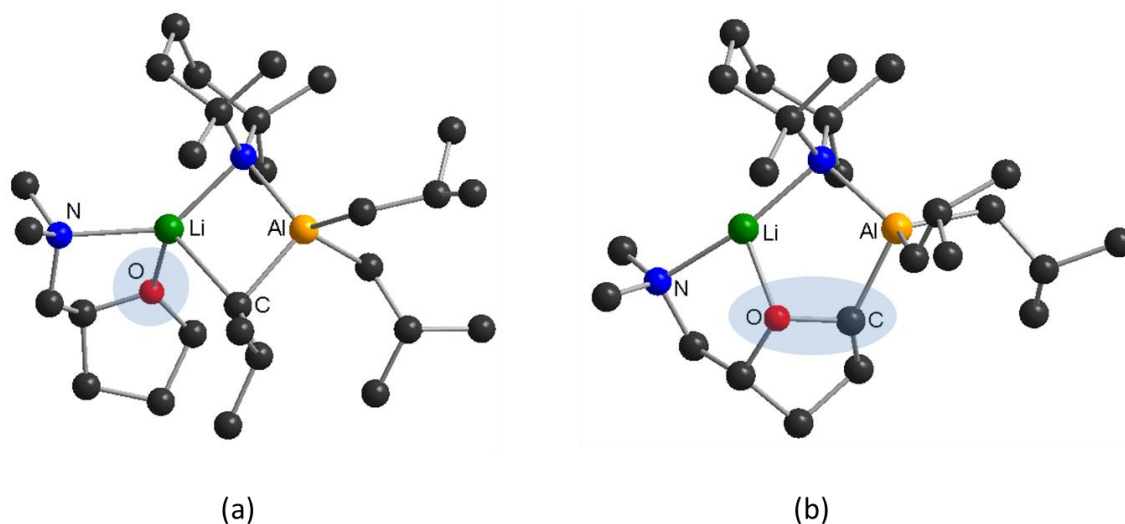


Figure 3.4. Molecular structures of the crystalline products obtained from the reactions of Me<sub>2</sub>TFA with (a) **3.1** and (b) **3.2**.<sup>[36]</sup>

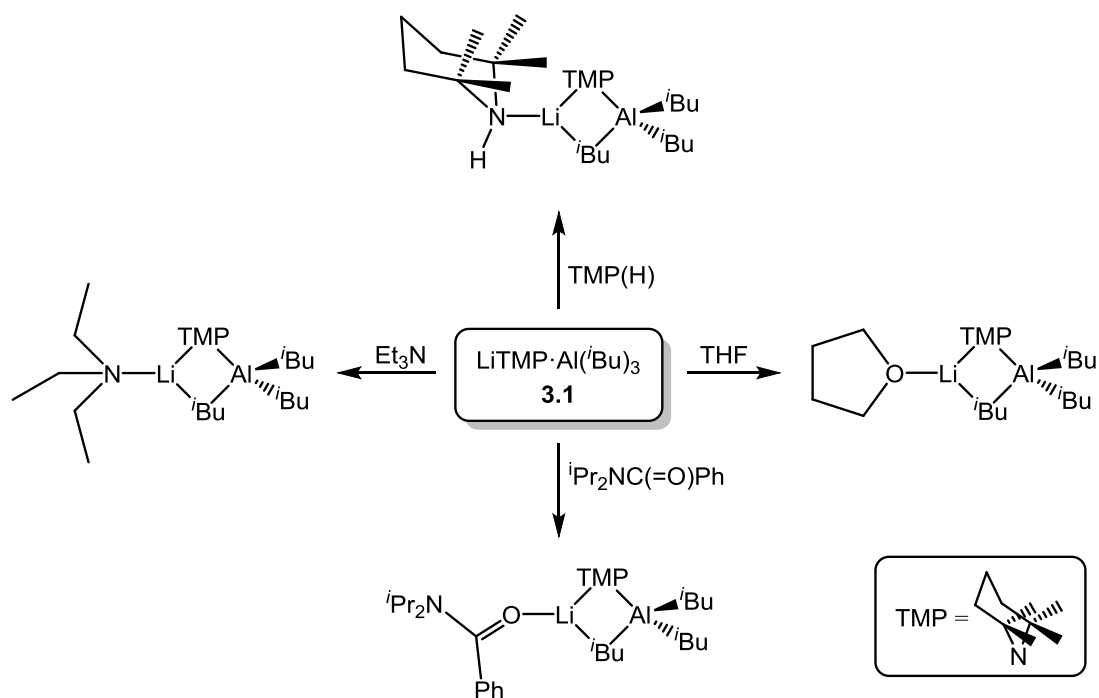
### 3.3 Results and Discussion

Following the reactivity differences alluded to in the introduction, compounded by the report of the related turbo-Hauser base “(TMP)MgCl·LiCl·AlEt<sub>3</sub>” by the Knochel group,<sup>[37]</sup> we took the decision to investigate further in their own right the two aforementioned reagents that dominate AMMAI chemistry, namely Uchiyama and Wheatley’s “LiTMP·Al(*i*Bu)<sub>3</sub>” **3.1** <sup>[30-31, 38]</sup> and our own bis-TMP version “LiTMP·Al(TMP)(*i*Bu)<sub>2</sub>” **3.2**.<sup>[32]</sup> Though each of these complexes have been studied previously many questions about them remain unanswered so this part of the PhD project was undertaken to obtain a more complete picture of these complicated multicomponent base mixtures.

#### 3.3.1 Has the Active Base of **3.1** been Crystallographically Characterised?

Uchiyama’s original 2004 synthesis of **3.1** <sup>[30]</sup> had LiTMP, prepared *in situ* by the action of *n*-butyllithium on TMP(H) at -78°C, subsequently reacted with

triisobutylaluminium then the mixture was warmed to 0°C. As in most bimetallic applications in organic synthesis, THF was used as the bulk solvent (in an approximate 25 molar excess on a 2 mmol scale reaction), though the mixture also contained hexane from the lithium and aluminium reagent solutions employed though significantly this was not referred to in the text of the paper. Evidence that LiTMP and triisobutylaluminium can interact with each other under the mediation of a Lewis base L to forge co-complexes of the type  $[L\cdot\text{Li}(\mu\text{-TMP})(\mu\text{-}i\text{Bu})\text{Al}(i\text{Bu})_2]$  came from the Mulvey group's previous crystallographic characterisation of three examples where L is *N,N*-diisopropylbenzamide, TMP(H) or triethylamine (Scheme 3.4).<sup>[30]</sup> Uchiyama in collaboration with Naka and Wheatley subsequently made what seemed the key breakthrough by crystallographically characterising an aluminate compound containing all the components of the base reaction mixture **3.1** in the mono-THF complex  $[\text{THF}\cdot\text{Li}(\mu\text{-TMP})(\mu\text{-}i\text{Bu})\text{Al}(i\text{Bu})_2]$  **3.1·THF** (Scheme 3.4).<sup>[30]</sup> These Lewis base stabilised aluminates all belong to contacted ion-pair type structures wherein ligand bridges connect Li to Al. Significantly the crystals of all of these compounds were grown in bulk hydrocarbon solutions. The most experimentally relevant set of **3.1·THF** were crystallised from a bulk hexane solution containing a stoichiometric deficiency of THF [0.625 mmol per 1 mmol of "LiTMP·Al(*i*Bu)<sub>3</sub>"].<sup>[31]</sup> However the base mixture **3.1** is prepared and utilised in a vast excess of THF in its synthetic applications so the burning question needing answered is "does **3.1·THF** represent the experimental base in the THF solution mixture of **3.1**?"



Scheme 3.4. Co-complexation reactions between LiTMP and  $\text{Al}(i\text{Bu})_3$  in bulk hexane solution mediated by different Lewis bases.

To set about trying to find an answer to this question, in this new study we prepared **3.1·THF** in crystalline form following exactly the aforementioned literature procedure and dissolved it in neat  $d_8$ -THF to replicate the environment it is utilised in during its many successful AMMAI applications. Recording the  $^1\text{H}$  NMR spectrum at ambient temperature revealed a simple pattern showing one set of  $i\text{Bu}$  and TMP resonances consistent with a single solution species (Figure 3.5). Backing up this assignment of a single species, the  $^7\text{Li}$  NMR spectrum reveals a sharp single resonance at 1.21 ppm (Figure 3.6). On re-recording the  $^1\text{H}$  NMR spectra at elevated temperatures (from 300 to 330 K) no change to this pattern was observed (Figure 3.7).

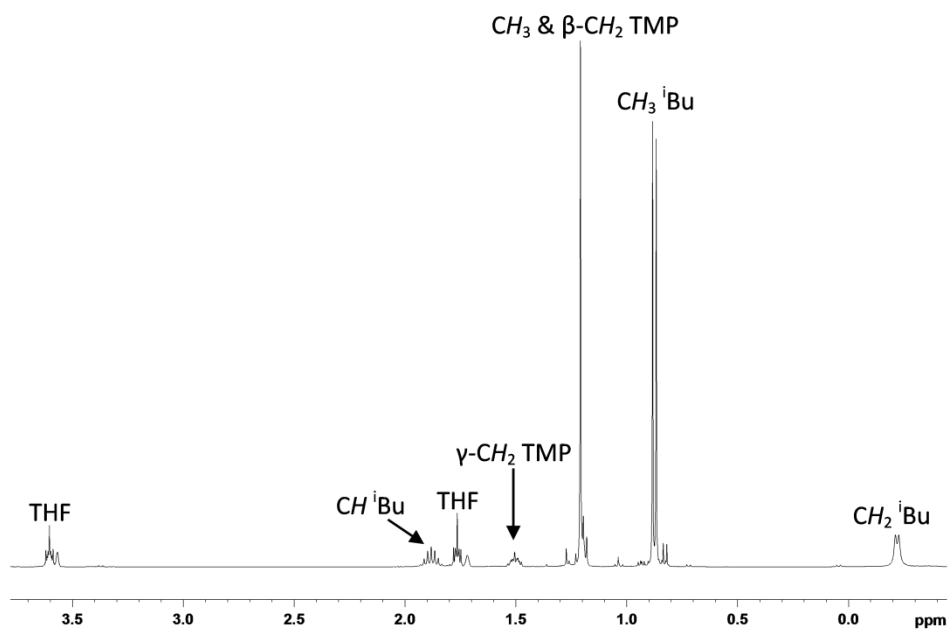


Figure 3.5.  $^1\text{H}$  NMR spectrum ( $d_8\text{-THF}$ ) of crystalline  $[\text{THF}\cdot\text{Li}(\text{TMP})\text{Al}(^i\text{Bu})_3]$   $3.1\cdot\text{THF}$ .

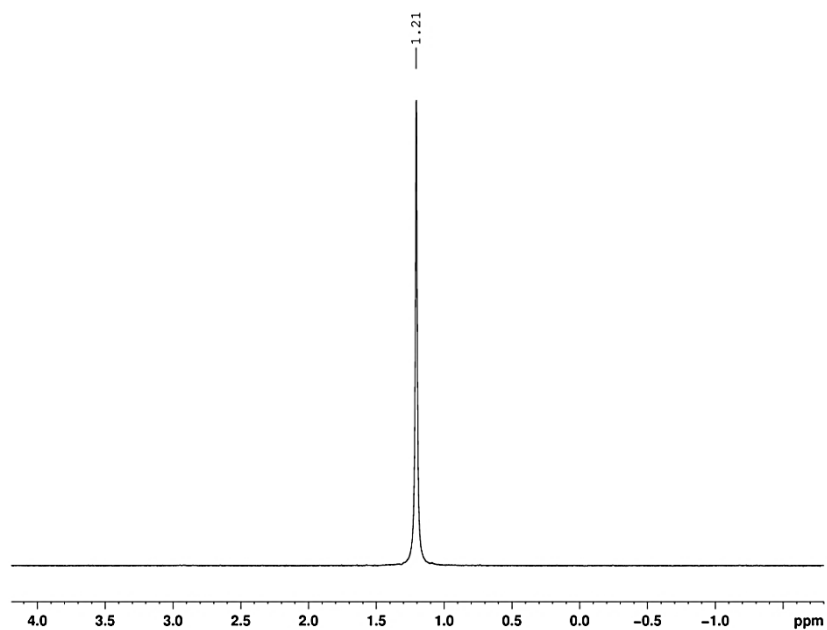


Figure 3.6.  $^7\text{Li}$  NMR spectrum ( $d_8\text{-THF}$ ) of crystalline  $[\text{THF}\cdot\text{Li}(\text{TMP})\text{Al}(^i\text{Bu})_3]$   $3.1\cdot\text{THF}$ .

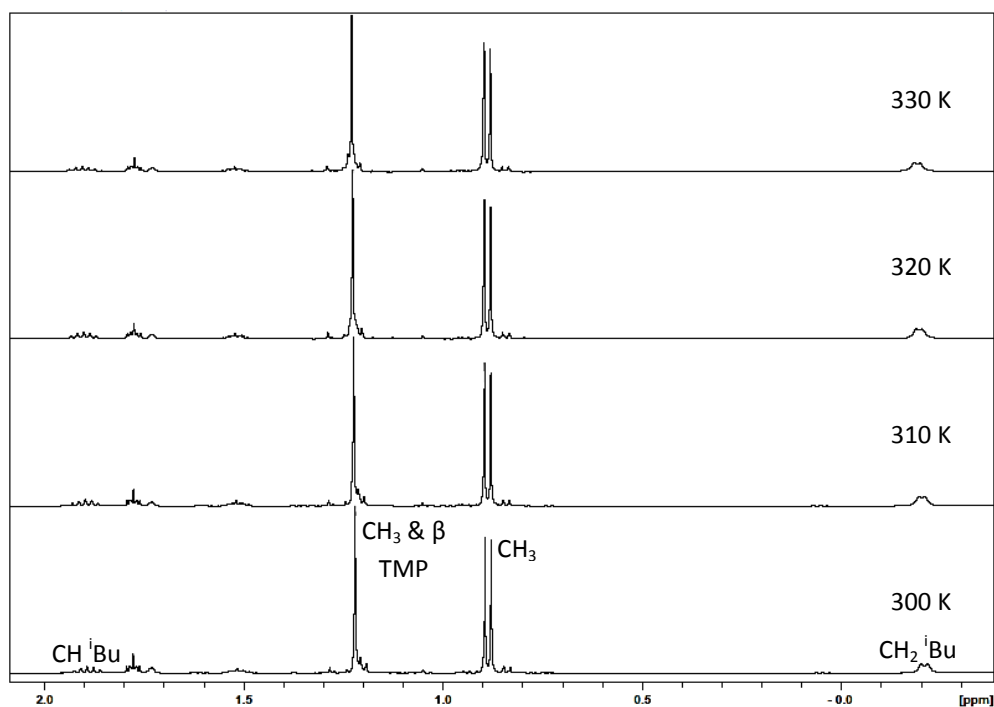


Figure 3.7. Variable temperature  $^1\text{H}$  NMR spectra (in  $\text{d}_8\text{-THF}$ ) of crystalline  $[\text{THF}\cdot\text{Li}(\text{TMP})\text{Al}(\text{iBu})_3]\cdot 3.1\cdot\text{THF}$ .

A DOSY  $^1\text{H}$  NMR <sup>[39-40]</sup> spectrum (Figure 3.8) of this  $\text{d}_8\text{-THF}$  solution of crystalline **3.1·THF** showed that all resonances associated with the aluminate moiety (namely  $\text{iBu}$ :  $\text{CH}_2$ , -0.22 ppm;  $\text{CH}_3$ , 0.88 ppm;  $\text{CH}$ , 1.88 ppm; TMP,  $\text{CH}_3$ , 1.21 ppm;  $\beta\text{-CH}_2$ , 1.20 ppm;  $\gamma\text{-CH}_2$ , 1.51 ppm) lie along the same line on the y-axis with essentially the same diffusion coefficient ( $6.95\times 10^{-10} \pm 0.09\times 10^{-10} \text{ m}^2/\text{s}$ ) implying that the two distinct ligands belong to the same compound/structure. Only the THF resonances (at 1.78 and 3.61 ppm) of the **3.1·THF** formulation lie outside of this line. The obvious explanation is that THF is labile and hence could be undergoing a metal-attached coordinative, metal-free decoordinative equilibrium in  $\text{d}_8\text{-THF}$  solution. These resonances appear lower down the y-axis as the THF has a smaller molecular weight and thus a higher diffusion coefficient ( $2.05\times 10^{-9} \pm 0.01\times 10^{-10} \text{ m}^2/\text{s}$ ) than the “ $\text{LiTMP}\cdot\text{Al}(\text{iBu})_3$ ” portion of crystalline **3.1·THF**.



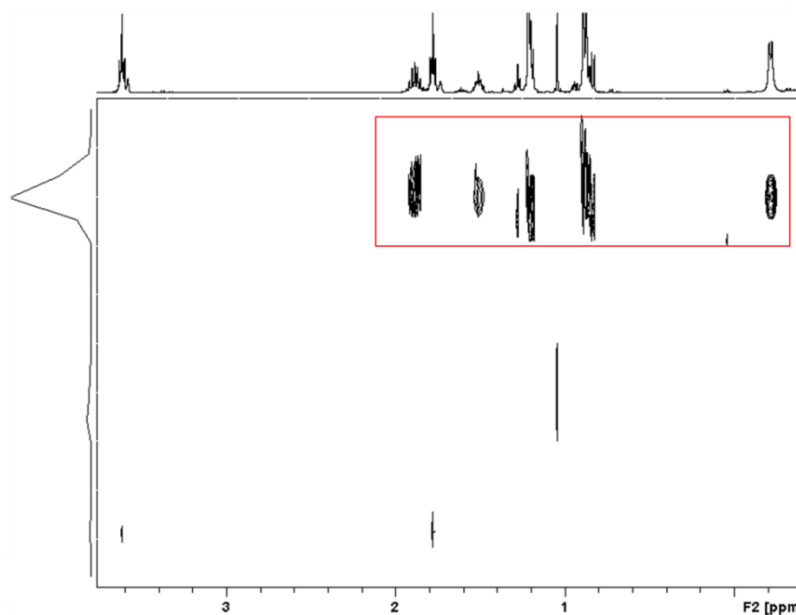


Figure 3.8. DOSY  $^1\text{H}$  NMR spectrum of crystalline  $[\text{THF}\cdot\text{Li}(\text{TMP})\text{Al}(\text{iBu})_3]\cdot 3.1\cdot\text{THF}$  in  $d_8$ -THF solution. Note that a trace amount of  $\text{TMP}(\text{H})$  is evident at 1.04 ppm.

Given that this experiment is carried out in a vast amount of THF relative to the dissolved aluminate compound, the most likely assignment for the single species present is the solvent-separated ion-pair  $[\{\text{Li}(\text{THF})_4\}^+\{\text{Al}(\text{TMP})(\text{iBu})_3\}^-]\cdot 3.1\cdot(\text{THF})_4$ . Supporting this assignment is a comparatively broad resonance at 139.8 ppm observed in the  $^{27}\text{Al}$  NMR spectrum (Figure 3.9) in  $d_8$ -THF solution consistent with an asymmetrical  $[\{\text{Al}(\text{TMP})(\text{iBu})_3\}^-]$  ion. It is well known that low local symmetry around Al centres in general,<sup>[41-43]</sup> and indeed specifically in TMP attached systems leads to broad signals [in  $(\text{TMP})_2\text{AlX}$  systems they can be hundreds or even thousands of Hz broad].<sup>[44-45]</sup> Also as mentioned above the  $^7\text{Li}$  NMR spectrum of  $3.1\cdot(\text{THF})_4$  shows a singlet resonance at 1.21 ppm (Figure 3.6) which coincides exactly with the  $^7\text{Li}$  NMR spectrum of the ate compound  $[\{\text{Li}(\text{THF})_4\}^+\{\text{Al}(\text{iBu})_4\}^-]$  implying that the separated  $\{\text{Li}(\text{THF})_4\}^+$  cation is common to both ates [note though that the chemical shift for the  $\{\text{Li}(\text{THF})_4\}^+$  cation is highly sensitive to changes in concentration – see Figure 3.10 for an example].

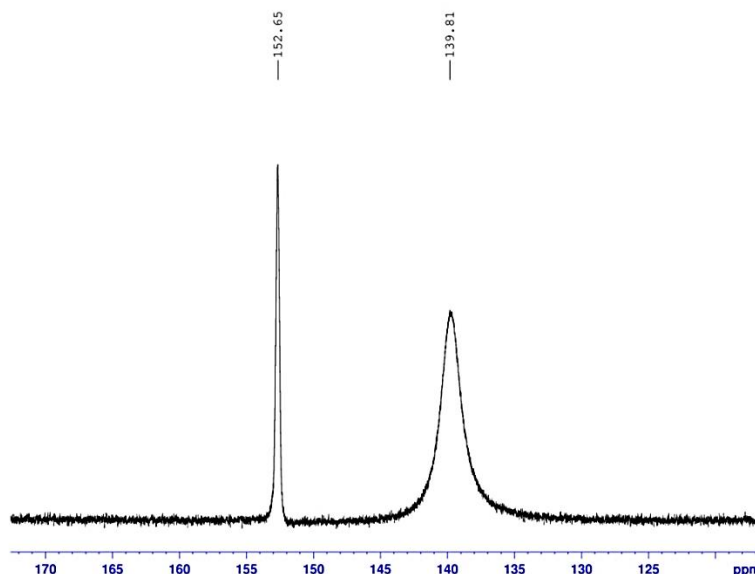


Figure 3.9.  $^{27}\text{Al}$  NMR spectrum ( $d_8$ -THF, 300 K) of crystalline  $[\{\text{Li}(\text{THF})_4\}^+\{\text{Al}(\text{TMP})(i\text{Bu})_3\}^-] \mathbf{3.1} \cdot (\text{THF})_4$  showing the  $^{27}\text{Al}$  resonance at 139.81 ppm. Note the additional presence of a small quantity of  $[\{\text{Li}(\text{THF})_4\}^+\{\text{Al}(i\text{Bu})_4\}^-] \mathbf{3.3}$  (at 152.65 ppm).

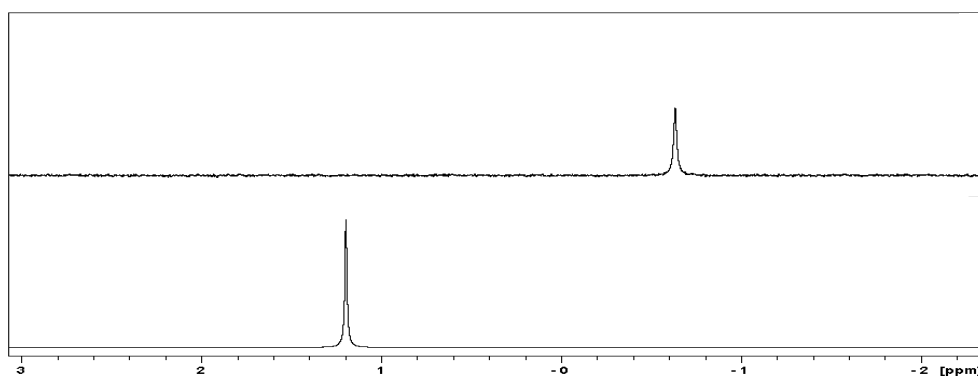
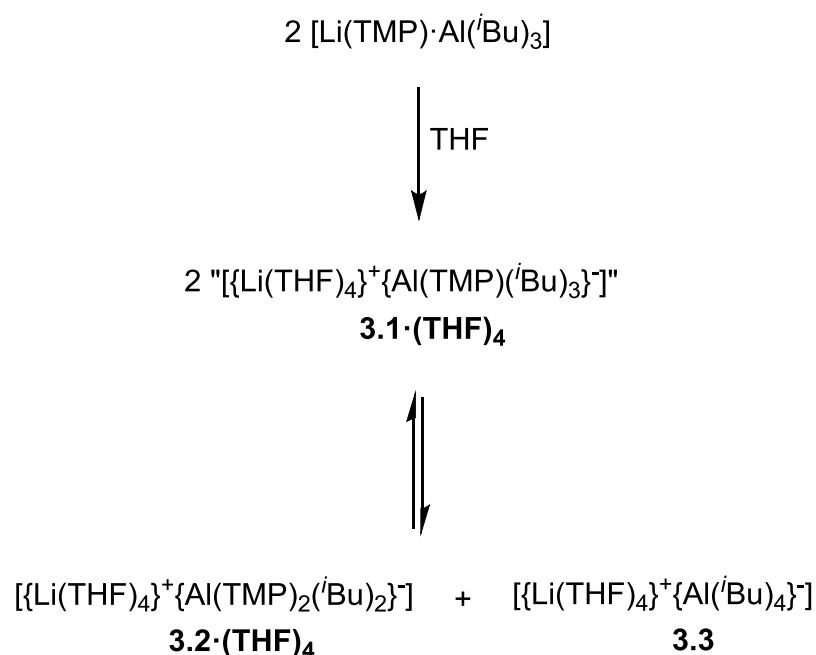


Figure 3.10.  $^7\text{Li}$  NMR spectra ( $d_8$ -THF, 300 K) of  $[\{\text{Li}(\text{THF})_4\}^+\{\text{Al}(\text{TMP})(i\text{Bu})_3\}^-] \mathbf{3.1} \cdot (\text{THF})_4$  at different concentrations (top =  $\sim 1$  mg/mL, bottom =  $\sim 30$  mg/mL) showing the changes in chemical shift of the  $[\text{Li}(\text{THF})_4]^+$  cation with concentration.

Intriguingly these NMR spectroscopic results from  $d_8$ -THF solutions of crystalline **3.1**·THF are at odds with Mulvey's earlier investigations of "LiTMP·Al(*i*Bu)<sub>3</sub>" when it was made *in situ* in bulk THF solution.<sup>[46]</sup> A combination of <sup>1</sup>H, <sup>7</sup>Li and <sup>13</sup>C NMR data pointed strongly to the existence of a dismutation process (Scheme 3.5) in contrast to the single species implicated in the  $d_8$ -THF solution of crystalline **3.1**·THF.



Scheme 3.5. Dismutation of the putative aluminate LiTMP·Al(*i*Bu)<sub>3</sub> **3.1** in bulk THF solution as previously postulated by Mulvey *et al.*<sup>[46]</sup>

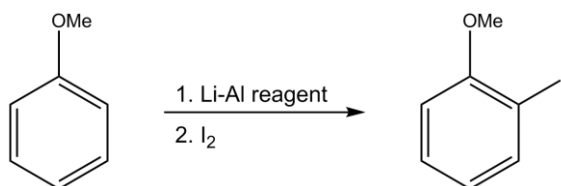
The key piece of evidence towards this dismutation was the characterisation of the tetraalkylaluminate  $[\{\text{Li}(\text{THF})_4\}^+\{\text{Al}(\textit{i}\text{Bu})_4\}^-]$ , **3.3** a solvent-separated ion-pair structure though this was the only species unequivocally identified from the mixture. Arrived at qualitatively by balancing the stoichiometry of the equilibrium reaction, the putative co-product " $[\{\text{Li}(\text{THF})_4\}^+\{\text{Al}(\text{TMP})_2(\textit{i}\text{Bu})_2\}^-]$ ", **3.2**·(THF)<sub>4</sub> inspired the Mulvey group to the idea of employing the bis-TMP species "LiTMP·Al(TMP)(*i*Bu)<sub>2</sub>", **3.2** in AMMAI reactions (see later). Knochel's

subsequent finding that a closely related equilibrium may be operating in THF solution mixtures of (TMP)MgCl·LiCl and Al(Et)<sub>3</sub> leading to the tetraalkylaluminate “MgCl·Al(Et)<sub>4</sub>” (characterised in part by a sharp resonance at 159 ppm in <sup>27</sup>Al NMR spectra) and the alkylaluminium amide (TMP)Al(Et)<sub>2</sub>·THF [37] motivated us to revisit in greater detail the comparison between the THF solutions of crystalline **3.1**·THF and its *in situ* form **3.1**. Our findings detailed in the next section were surprising.

### 3.3.2 *In Situ* **3.1** versus Crystalline **3.1**·THF: Comparative Reactivity Studies with Anisole

Anisole has long been used as a test substrate for measuring the performance of metallating agents. It has also played a key role in the development of DoM chemistry [47-48] through the classical studies of Wittig [49] and Gilman.[50] Hence there are numerous reports of the *ortho* metallation of anisole by a range of different metallating reagents. Lithium mono-TMP aluminate **3.1** is included in this number as in fact anisole was utilised as the model substrate by Uchiyama when this reagent was first introduced.[30] This opening study reported that an *in situ* THF solution of **3.1** produced a remarkable 99% yield of *o*-iodoanisole following iodine electrophilic quenching of the metallated intermediate (Table 3.1, which collates the yields of the reactions of anisole with various Li-Al and Al reagents mentioned in this thesis). This “AMMAI” was carried out at room temperature for three hours and most significantly the base:anisole stoichiometry employed to achieve this impressive quantitative yield was 2.2:1.0 molar equivalents, that is the base was in a slightly greater than twofold excess. Hence this implies that at least 50% of the base **3.1** is inactive towards anisole under the conditions carried out.

Table 3.1. Comparative reactivities of various Li-Al or Al reagents towards anisole.



Metal reagent	Solvent	Yield (%)
LiTMP·Al( <i>i</i> Bu) <sub>3</sub> ( <b>3.1</b> ) ( <i>in situ</i> 2.2 equiv)	THF	99
LiTMP·Al( <i>i</i> Bu) <sub>3</sub> ( <b>3.1</b> ) ( <i>in situ</i> 1 equiv)	THF	50
THF·Li(TMP)Al( <i>i</i> Bu) <sub>3</sub> ( <b>3.1·THF</b> ) (crystals)	THF or hexane	0
THF·Li(TMP)Al( <i>i</i> Bu) <sub>3</sub> ( <b>3.1·THF</b> ) ( <i>in situ</i> 1 equiv)	hexane	0
THF·Li(TMP)Al(TMP)( <i>i</i> Bu) <sub>2</sub> ( <b>3.2·THF</b> ) ( <i>in situ</i> 1 equiv)	hexane	77
[{Li(THF) <sub>4</sub> } <sup>+</sup> {Al( <i>i</i> Bu) <sub>4</sub> } <sup>-</sup> ] ( <b>3.3</b> )	THF	0
Al( <i>i</i> Bu) <sub>3</sub>	THF	0

For comparison, in this PhD study we repeated this original reaction but this time using a 1:1, base:anisole stoichiometry in bulk THF solution. That *in situ* **3.1** could deprotonate anisole effectively was confirmed by this repeat reaction though significantly the yield of deprotonated anisole observed in a <sup>1</sup>H NMR spectrum of a d<sub>6</sub>-benzene solution of the reaction mixture only approached 50% conversion of anisole starting material. This seemingly 50% loss of base activity is explicable if the dimerization equilibrium in Scheme 3.5 lies to the right hand side and if one of the two components, the tetrabutyl aluminate **3.3** was inactive towards anisole. In earlier work the Mulvey group had reported that **3.3** failed to react with *N,N*-diisopropylbenzamide.<sup>[46]</sup> This substrate carries a much stronger *ortho*-deprotonating directing group than the electron-donating methoxy substituent of anisole so it was anticipated that **3.3** would be inert towards anisole in bulk THF solution and a control reaction between them confirmed this view. Surprisingly we also discovered that **3.3** cannot even deprotonate the acidic *N-H* bond of TMP(H), the co-product obtained when the

TMP anion functions as a base. Further proof that tetrabutylaluminate **3.3** is a major component of *in situ* **3.1** came from the observation of a sharp resonance at 152.5 ppm in its  $^{27}\text{Al}$  NMR spectrum in  $d_8$ -THF solution that matches that of an authentic sample of **3.3**. The sharpness of this resonance is consistent with the high degree of symmetry in the tetrahedral Al centre in **3.3**. This sharp resonance (reported at 153.4 ppm)<sup>[31]</sup> appears to have been wrongly assigned as belonging to putative contacted ion-pair “LiTMP·Al(*t*Bu)<sub>3</sub>” **3.1** in an earlier Uchiyama paper.<sup>[31]</sup> A highly asymmetrical [Al(TMP)(*t*Bu)<sub>3</sub>]<sup>-</sup> centre would give rise to a broader resonance which as mentioned earlier appears in our spectrum at 139.8 ppm. It is significant as alluded to earlier that Knochel mentions a similar  $^{27}\text{Al}$  chemical shift in the related highly symmetrical tetraethylaluminate “[MgCl]<sup>+</sup>(AlEt<sub>4</sub>)<sup>-</sup>” (at 159 ppm).<sup>[37]</sup> Interestingly when we repeated the original reaction carried out by Uchiyama using a 2.2:1.0 stoichiometric ratio of *in situ* **3.1** to anisole in THF solution and recorded the NMR spectrum of the metallated intermediate in  $d_8$ -THF solvent we see lithiated anisole (confirmed by comparison to a spectrum of an authentic sample) as well as aluminated anisole through diagnostic doublet of doublet resonances for the anisoyl *meta* C-H adjacent to the *ortho* site of metallation at 7.65 and 7.48 ppm respectively in an appropriate 1:4 ratio (Figure 3.11). This provided the first strong hint that the reactions of *in situ* **3.1** are not merely, if at all, aluminium-hydrogen exchange reactions.

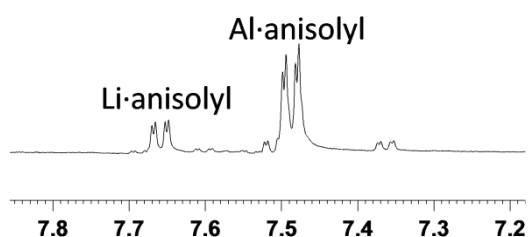


Figure 3.11. Part of the aryl region of the  $^1\text{H}$  NMR spectrum of the reaction of *in situ* LiTMP·Al(*t*Bu)<sub>3</sub> **3.1** with anisole in  $d_8$ -THF solution indicating the presence of both lithiated anisole and aluminated anisole.

Surprisingly, contrasting with the previous straightforward metallation of anisole using *in situ* prepared **3.1**, on dissolving crystalline **3.1**·THF in THF solution mixed with anisole and stirring the mixture for several hours to replicate the reaction with *in situ* **3.1** no reaction was observed to take place (Table 3.1). This was ascertained from the recovered anisole witnessed in NMR spectra (Figure 3.12).

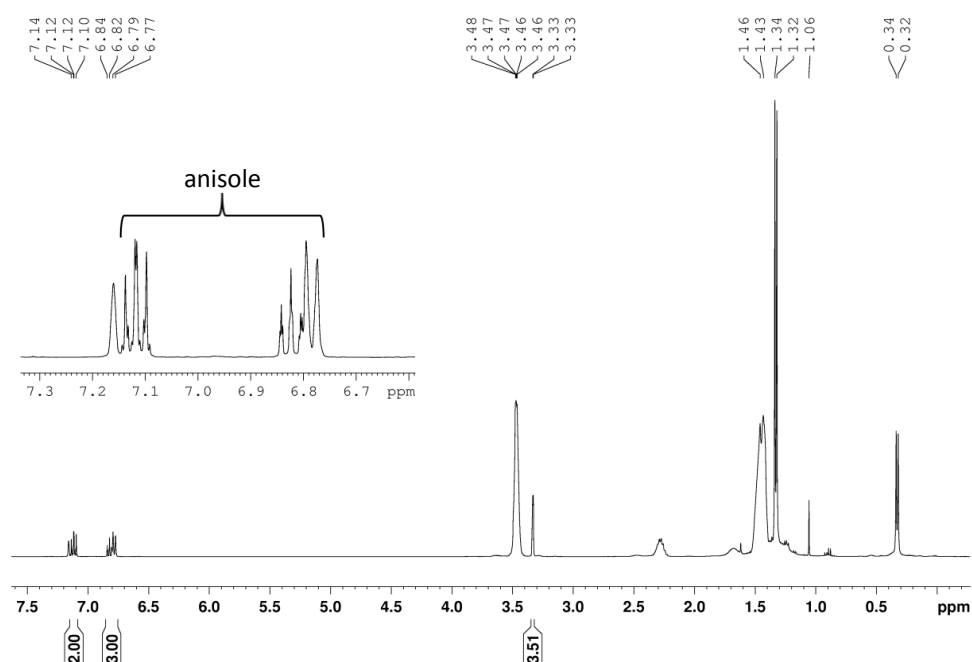


Figure 3.12. <sup>1</sup>H NMR spectrum (C<sub>6</sub>D<sub>6</sub>, 300 K) of crystalline [THF·Li(μ-TMP)(μ-*i*Bu)Al(*i*Bu)<sub>2</sub>] **3.1**·THF and anisole stirred in THF for 24 hours, showing the presence of unreacted anisole.

Intriguingly this failure to observe any reactivity implies that once the aluminate structure of **3.1**·THF, presumably as [Li(THF)<sub>4</sub>]<sup>+</sup>[Al(TMP)(*i*Bu)<sub>3</sub>]<sup>-</sup>, **3.1**·(THF)<sub>4</sub>, is formed all deprotonative reactivity of the mixture is lost. To probe this idea further **3.1**·THF was also prepared *in situ* in hexane solution by combining its three component compounds [LiTMP, Al(*i*Bu)<sub>3</sub> and THF in a 1:1:1 ratio] but even this mixture proved inert towards anisole (Figure 3.13). Under

these limited solvating conditions the aluminate will almost certainly be in its contacted ion-pair form  $[\text{THF}\cdot\text{Li}(\mu\text{-TMP})(\mu\text{-}i\text{Bu})\text{Al}(i\text{Bu})_2]$ , **3.1**·THF. Putting together these pieces of evidence allows us to draw some confident conclusions: (i) **3.1**·THF is not the active experimental base in the solution mixture **3.1**; (ii) crystalline **3.1**·THF does not undergo a dismutation equilibrium in the THF solution akin to that shown for *in situ* **3.1** in Scheme 3.5 but remains as the solvent-separated species **3.1**·(THF)<sub>4</sub>; and (iii) in contrast made to the claim in the Uchiyama/Wheatley paper<sup>[31]</sup> the active base within **3.1** has not been crystallographically characterised or more exactly  $[\text{THF}\cdot\text{Li}(\mu\text{-TMP})(\mu\text{-}i\text{Bu})\text{Al}(i\text{Bu})_2]$  **3.1**·THF is not the active base (though see qualification later in Section 3.3.4).

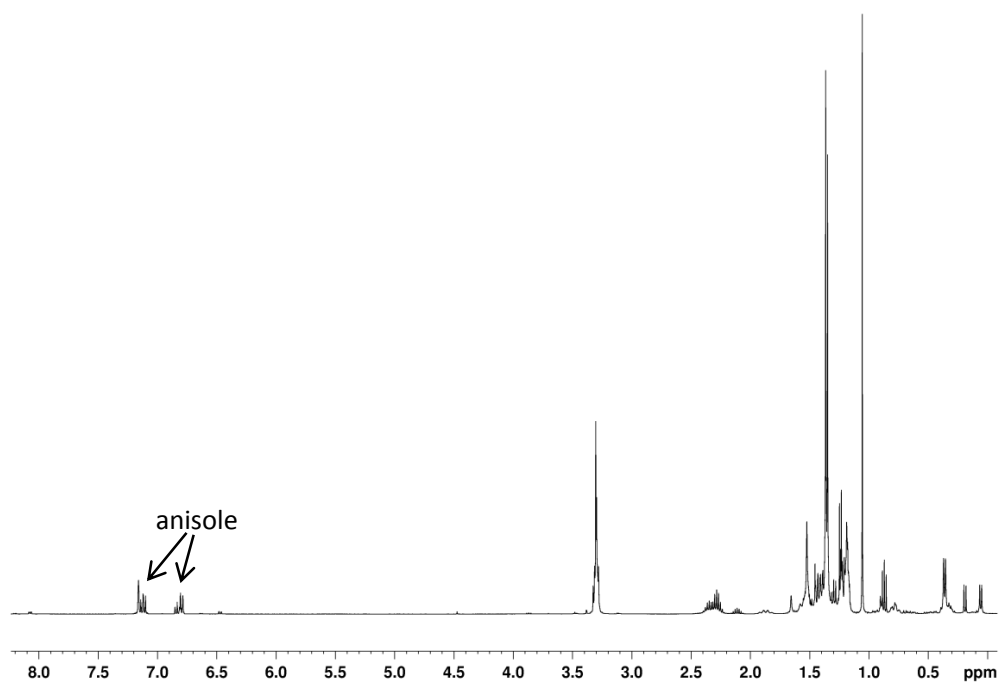


Figure 3.13. <sup>1</sup>H NMR spectrum ( $\text{C}_6\text{D}_6$ , 300 K) of *in situ*  $[\text{LiTMP}, \text{Al}(i\text{Bu})_3$  and THF] **3.1**·THF and anisole in hexane, showing unreacted anisole. Note the small amount of metallation observed due to a trace excess of LiTMP present in the mixture.



### 3.3.3 Towards Solving the Puzzle of “LiTMP·Al(TMP)(*i*Bu)<sub>2</sub>”

For reasons that will become clear later in the discussion we have been unsuccessful in our several attempts to isolate a solid form let alone a crystalline form of “LiTMP·Al(TMP)(*i*Bu)<sub>2</sub>”, **3.2**, the putative co-product of the hypothesised dismutation portrayed in Scheme 3.5. However it was the postulated presence of **3.2** in a THF solvated form **3.2**·(THF)<sub>n</sub> within this equilibrium having the attraction of seemingly possessing extra TMP power (as it is the single TMP ligand in **3.1** that is its active base component) that encouraged the Mulvey group to make a reagent of this twofold TMP stoichiometry in the first place. To begin the more comprehensive study of **3.2** documented here, we recorded the <sup>1</sup>H NMR spectra of its two individual constituent compounds LiTMP [51-52] and (TMP)Al(*i*Bu)<sub>2</sub>,<sup>[32]</sup> **3.2** itself, as well as a 1:1 mixture of **3.2** and THF in d<sub>14</sub>-hexane solution (Figure 3.14). We were surprised to learn that this comparison revealed no co-complexation into a heterobimetallic species but rather that LiTMP and (TMP)Al(*i*Bu)<sub>2</sub> remain as separate homometallic species. On adding stoichiometric THF to this mixture it appears to interact preferentially with the Al species to afford the solvated derivative [(TMP)Al(*i*Bu)<sub>2</sub>·THF], which the Mulvey group previously characterised,<sup>[32]</sup> as the chemical shifts of the *i*Bu resonances move (most diagnostically the CH<sub>2</sub> attached to the metal moves from 0.28 to 0.15 ppm) together with those for the TMP anion; whereas the LiTMP resonances remain unchanged. While these species appear to stay separated, it should be noted that there is a precedent for donor-free co-complexation in polymeric [Li(TMP)Al(Me)<sub>3</sub>]<sub>∞</sub>,<sup>[31]</sup> though significantly this crystalline compound was formed under much harsher reflux conditions in toluene than the room temperature conditions of our NMR comparison coupled with the fact that it has considerably smaller alkyl groups than those in **3.2**.

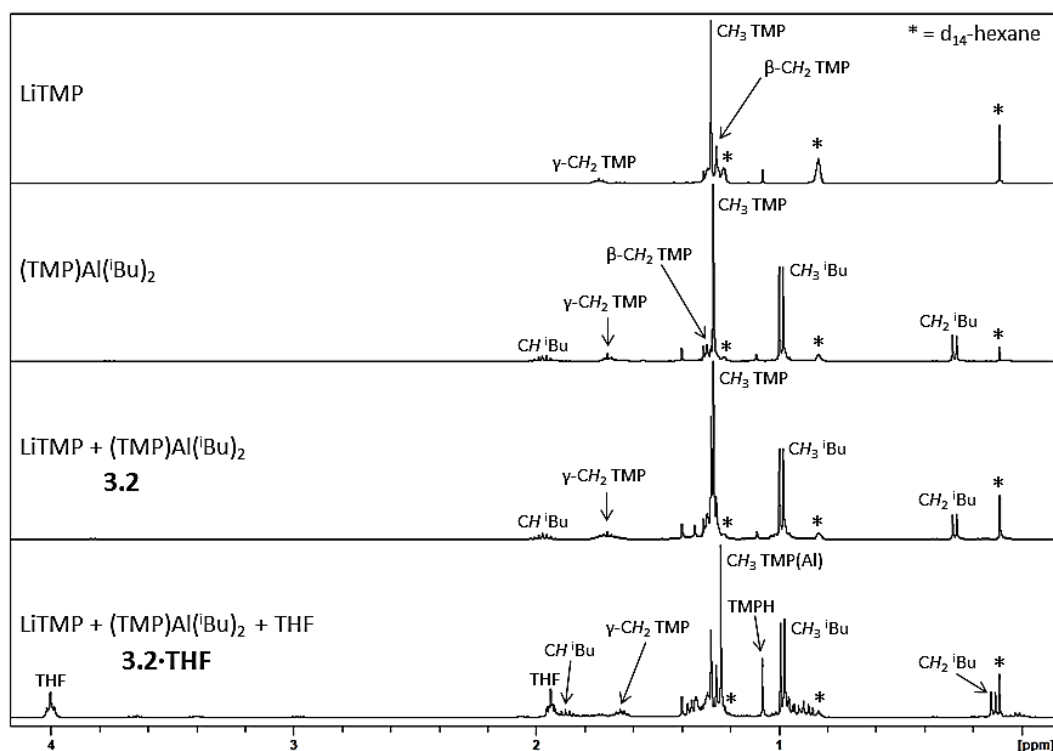
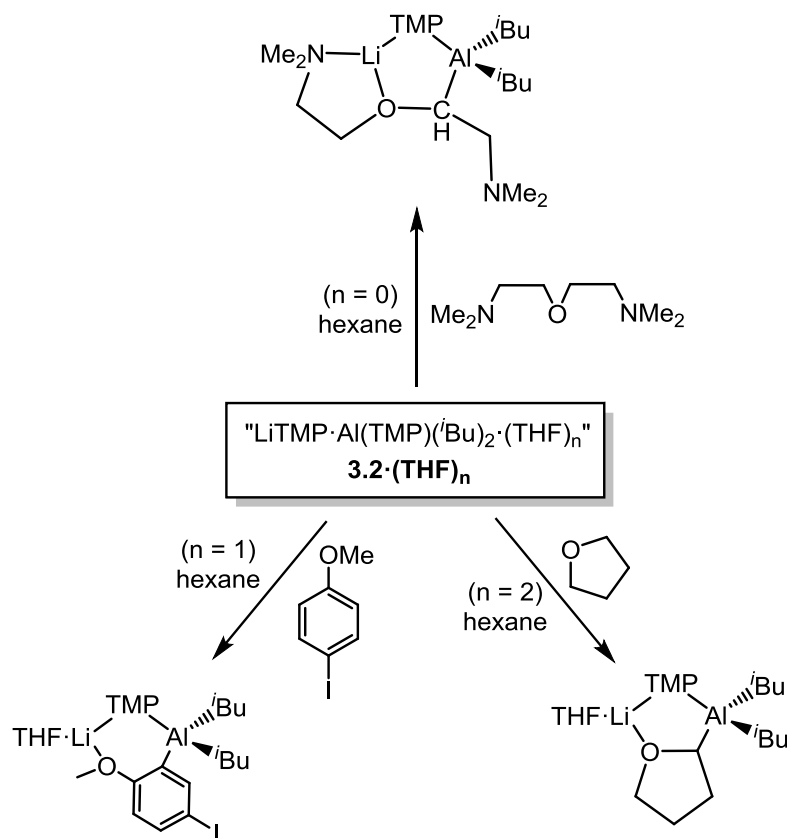


Figure 3.14. Overlay of  $^1\text{H}$  NMR spectra of  $[\text{LiTMP}$  and  $(\text{TMP})\text{Al}(\text{iBu})_2$ ] **3.2** and its component parts in  $\text{d}_{14}$ -hexane solution.

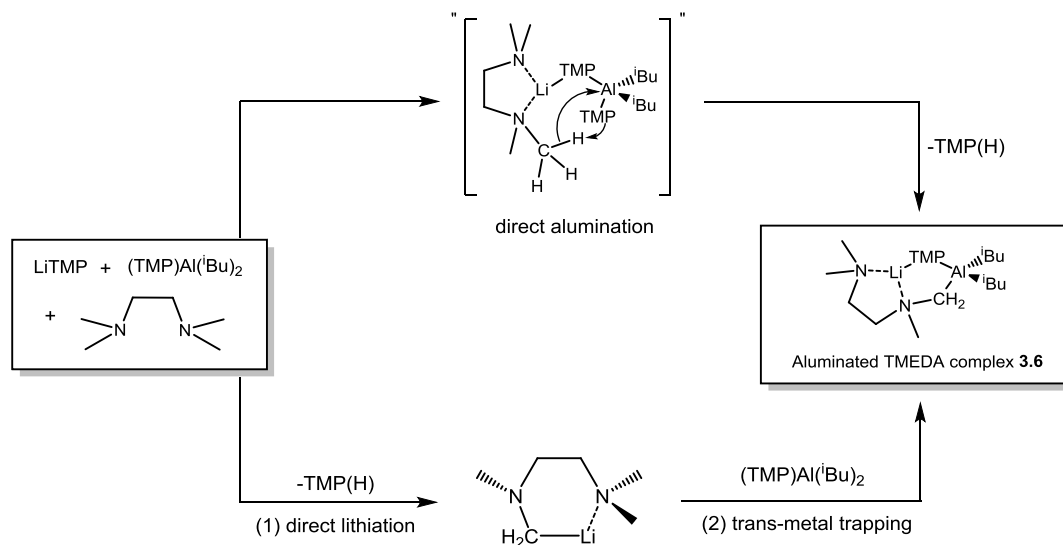
Turning to reactivity issues, an earlier investigation established the strong deprotonating power of  $\mathbf{3.2}\cdot(\text{THF})_n$  as it smoothly achieved AMMAI on a range of organic substrates (Scheme 3.6).<sup>[36]</sup> Most significantly,  $\mathbf{3.2}\cdot(\text{THF})_1$  was found to metallate THF in bulk hexane solution as evidenced by the slow appearance of resonances attributed to *ortho*-deprotonated THF ( $o\text{-OC}_4\text{H}_7^-$ ), while addition of a second THF molecule led to the formation of  $[\text{THF}\cdot\text{Li}(\mu\text{-TMP})(\mu\text{-OC}_4\text{H}_7)\text{Al}(\text{iBu})_2]$ , **3.4**, which was crystallographically authenticated (Section 3.2, Figure 3.2).<sup>[33]</sup> Crystallographic confirmation that anisole could also be *ortho*-aluminated by  $\mathbf{3.2}\cdot(\text{THF})_1$  came through  $[\text{THF}\cdot\text{Li}(\mu\text{-TMP})(o\text{-C}_6\text{H}_4\text{OMe})\text{Al}(\text{iBu})_2]$ , **3.5**, which in turn gave *o*-iodoanisole in a 77% yield when treated with iodine (Table 3.1).<sup>[32]</sup> As mentioned previously this behaviour contrasts with that of *in situ*  $\mathbf{3.1}\cdot\text{THF}$ , which fails to metallate anisole at all in hexane solution under the same conditions.



Scheme 3.6. Selected examples illustrating the deprotonating power of the bis-TMP reagent **3.2**·(THF)<sub>n</sub>.

Since the diamine TMEDA, the methyl groups of which are only weakly acidic, could also be “aluminated” at one of these terminal methyl sites by *in situ* **3.2** in hexane solution, the Mulvey group originally proposed an intramolecular mechanism through a contacted but open structure as depicted in Scheme 3.7.<sup>[35]</sup> However DFT calculations performed here in this PhD study (see below) indicate that such a twofold TMP structure would be unstable with the Al bound TMP ligand under geometry optimisation transferring to the Li centre in a non-solvated  $(\text{TMP})\text{Li}(\mu\text{-TMP})\text{Al}(i\text{Bu})_2$  structure which breaks apart to the homometallic components  $\text{THF} \cdot \text{LiTMP}$  <sup>[53]</sup> and  $(\text{TMP})\text{Al}(i\text{Bu})_2$  on addition of a single THF ligand. It is therefore envisioned that LiTMP does the metallation (lithiation) of TMEDA to give  $\text{Li}[\text{CH}_2\text{N}(\text{Me})\text{CH}_2\text{CH}_2\text{NMe}_2]$ , the reduced steric profile of which compared to that of LiTMP allows its trapping via co-

complexation (trans-metal-trapping is probably a more apt description here than the usual applied “transmetalation” for although aluminium is replacing lithium in binding to the carbanion C atom the lithium may not necessarily leave the aluminium system but could remain part of a contacted ion-pair or solvent separated ion-pair compound) with carbophilic (TMP)Al(*i*Bu)<sub>2</sub> to generate the observed heterobimetallic product Li[CH<sub>2</sub>N(Me)CH<sub>2</sub>CH<sub>2</sub>NMe<sub>2</sub>](TMP)Al(*i*Bu)<sub>2</sub> **3.6** (Scheme 3.7).



Scheme 3.7. Previously hypothesised<sup>[35]</sup> open ring structure pathway for intramolecular AMMAI reaction of TMEDA (top) and new proposed two-step mechanism for formation of “aluminated” TMEDA complex Li[CH<sub>2</sub>N(Me)CH<sub>2</sub>CH<sub>2</sub>NMe<sub>2</sub>](TMP)Al(*i*Bu)<sub>2</sub> **3.6** (bottom).

If the trans-metal-trapping by the aluminium reagent is not 100% efficient then lithiated substrates could persist, which might explain the presence of lithiated anisole as well as aluminated anisole in the aforementioned reaction with *in situ* **3.1** and anisole (this inefficient trapping was proven directly by mixing lithiated anisole and the salt [Li(THF)<sub>4</sub>]<sup>+</sup>[Al(*i*Bu)<sub>4</sub>]<sup>-</sup>, **3.3**, in d<sub>8</sub>-THF solution and recording the <sup>1</sup>H NMR spectrum which revealed no reaction had taken place (Figure 3.15) – in contrast to the neutral species (TMP)Al(*i*Bu)<sub>2</sub> which proved an

excellent trapping reagent for the lithiated anisole, as detailed below). Applying this same train of thought to the failure of **3.1**·THF to likewise metallate anisole in hexane solution can be attributed to the lack of available LiTMP in the reaction mixture as it would be locked within a closed contacted structure with a strong Li( $\mu$ -TMP)( $\mu$ -*t*Bu)Al bridge less sterically congested than an unstable Li( $\mu$ -TMP)<sub>2</sub>Al bridge. Interestingly the Mulvey group's initial empirical reasoning that installing two TMP ligands within **3.2**·THF would boost reactivity levels compared to that of the mono-TMP base **3.1**·THF appears correct but for the wrong reason: in no example yet has **3.2**·THF functioned as a di-TMP reacting species, instead it appears to be the "free" LiTMP present in the hexane solution mixture that boosts its reactivity compared to that of **3.1**·THF. Unlike other bimetallic reagents which can show unusual regioselective orientations, the regioselectivities observed here for **3.2**·THF are the same as those found for LiTMP (but in improved yields through the subsequent generation of more stable Al-C bonds rather than more polar, more unstable Li-C bonds).

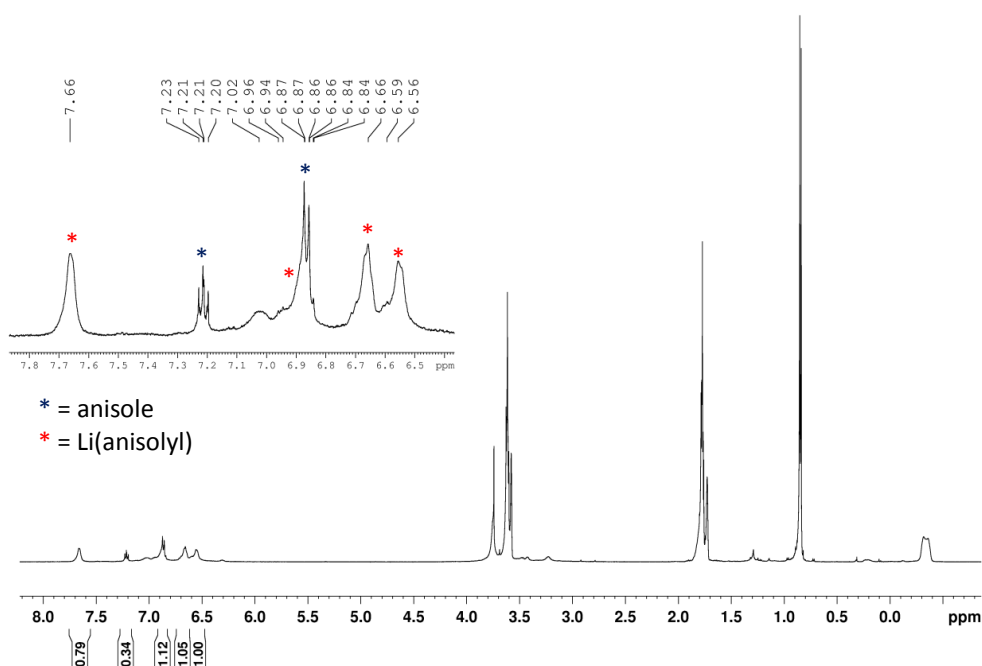


Figure 3.15. <sup>1</sup>H NMR spectrum (*d*<sub>8</sub>-THF, 300 K) of pre-prepared Li(anisoyl) and [Li(THF)<sub>4</sub>]<sup>+</sup>[Al(*t*Bu)<sub>4</sub>]<sup>-</sup> **3.3** showing the inefficient trapping by the salt.

Prior to this current investigation no comparable reactivity study of **3.2** had been carried out in bulk THF solution. Therefore we dissolved the components of **3.2** - LiTMP and (TMP)Al(*i*Bu)<sub>2</sub>, in THF solution at room temperature and added one molar equivalent of anisole then stirred the mixture for several hours. A <sup>1</sup>H NMR spectrum of the reaction mixture in d<sub>6</sub>-benzene solution (Figure 3.16) confirmed that **3.2**, as anticipated, also deprotonates anisole in this bulk polar medium.

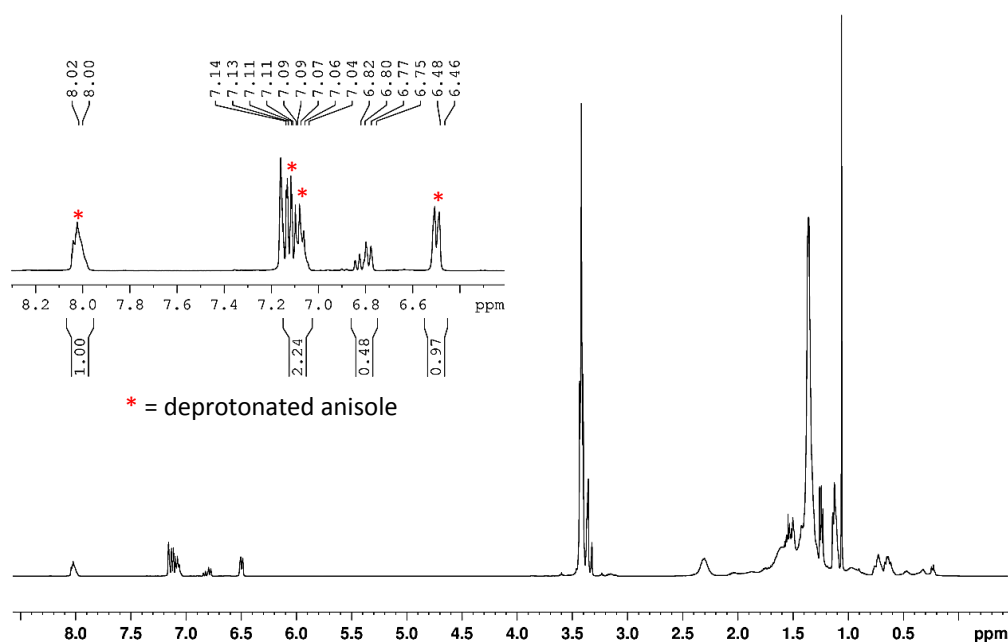


Figure 3.16. <sup>1</sup>H NMR spectrum (C<sub>6</sub>D<sub>6</sub>, 300 K) of the reaction between [LiTMP and (TMP)Al(*i*Bu)<sub>2</sub>] **3.2** and anisole in THF, showing the deprotonation of anisole producing the Al(anisoyl) complex.

The next question to ask was “what about the reactivity of **3.2** in bulk THF solution in the absence of anisole?” As aforementioned, previously the Mulvey group recognised that **3.2** can deprotonate a stoichiometric quantity of THF in bulk hexane solution to generate the crystalline, THF anion (C<sub>4</sub>H<sub>7</sub>O<sup>-</sup>) contact ion-pair complex **3.4** (with no ring opening of the heterocycle) in a striking example of “cleave and capture chemistry”.<sup>[54]</sup> Here in this work we stirred a

THF solution of **3.2** (on its own) for 24 hours at room temperature before recording a  $^1\text{H}$  NMR spectrum of an aliquot of the resulting mixture in  $\text{d}_8\text{-THF}$  solution. Resonances characteristic of the deprotonated but intact THF ring were observed (at 2.90, 3.42 and 3.74 ppm, Figure 3.17) consistent with **3.4**, but significantly these were only visible on magnifying the spectrum. A substantially larger resonance was seen for TMP(H) at 1.06 ppm, much greater in relative integration terms than could be accounted for by the  $\text{TMP}^-$  anion consumed in generating the trace amount of **3.4** witnessed in the spectrum.

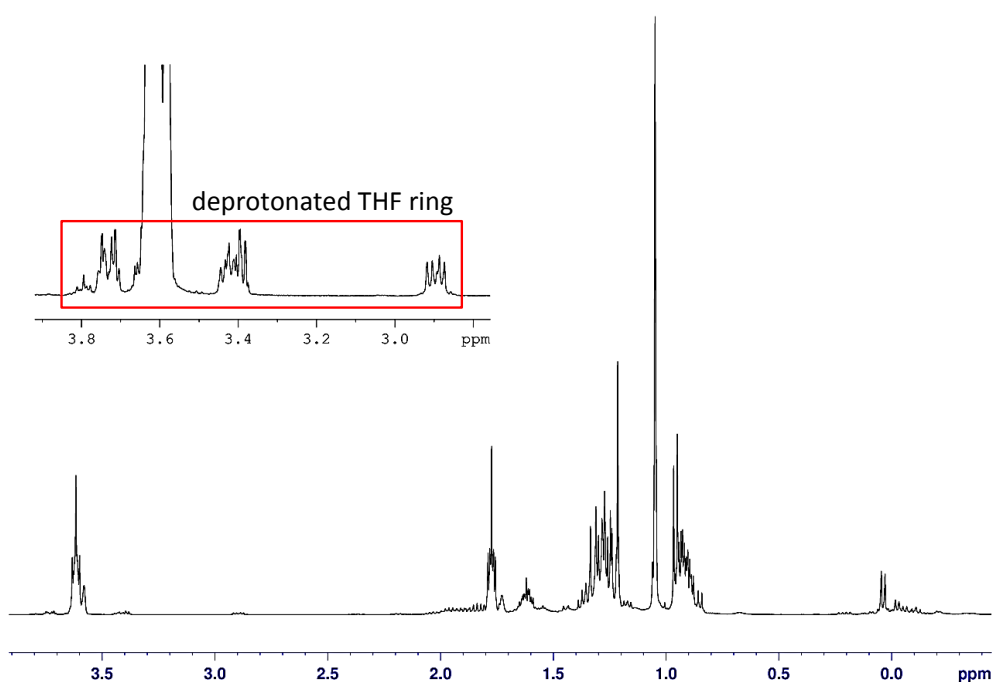


Figure 3.17.  $^1\text{H}$  NMR spectrum ( $\text{d}_8\text{-THF}$ , 300 K) of a mixture of  $[\text{LiTMP}$  and  $(\text{TMP})\text{Al}(\text{tBu})_2]$  **3.2** after 24 hours stirring in THF, showing small resonances for deprotonated THF.

While hydrolysis can never be ruled out completely as a contributing factor (though we scrupulously dried the THF solvent before employing it in the reaction), it seems more likely that the generated THF anion ( $\text{C}_4\text{H}_7\text{O}^-$ ) is

unstable in the bulk polar medium. This anion could exist initially either as part of the lithium derivative  $[(\text{THF})_x(\text{LiOC}_4\text{H}_7)_n]$  or as part of the solvent-separated aluminate  $[\{\text{Li}(\text{THF})_4\}^+\{(\text{TMP})(\text{OC}_4\text{H}_7)\text{Al}(\text{iBu})_2\}^-]$  but would then decompose (contrast this with the inherent stability of the bimetallic-stabilised contacted ion-pair form **3.4** in hexane solution)<sup>[33]</sup> presumably via a [3+2] cycloreversion to the enolate of acetaldehyde and ethene (see Section 1.2.1, Scheme 1.5).<sup>[55]</sup> To probe what effect this formation and break down of **3.4** would exert on the Brønsted basic properties of **3.2** we stirred a THF solution of **3.2** for 24 hours before introducing anisole as the metallation probe. As expected no metallation of anisole took place as a  $^1\text{H}$  NMR spectrum of the reaction mixture revealed free anisole as well as THF anions and a substantial amount of TMP(H). From these observations we conclude that if left to stir for a period of time in THF solution, **3.2** will deprotonate THF releasing TMP(H) and be consumed. To check whether all base activity is lost under such circumstances, we crystallised **3.4** from hexane solution, then isolated and dissolved it in bulk THF solution. Anisole was added subsequently and the solution was stirred for 24 hours. NMR analysis (Figure 3.18) of the resulting mixture revealed that again no metallation of anisole had occurred confirming that aluminate **3.4**, probably present in the modified solvent-separated form  $[\{\text{Li}(\text{THF})_4\}^+\{(\text{TMP})(\text{OC}_4\text{H}_7)\text{Al}(\text{iBu})_2\}^-]$  is inactive as a base even though it contains a TMP ligand.



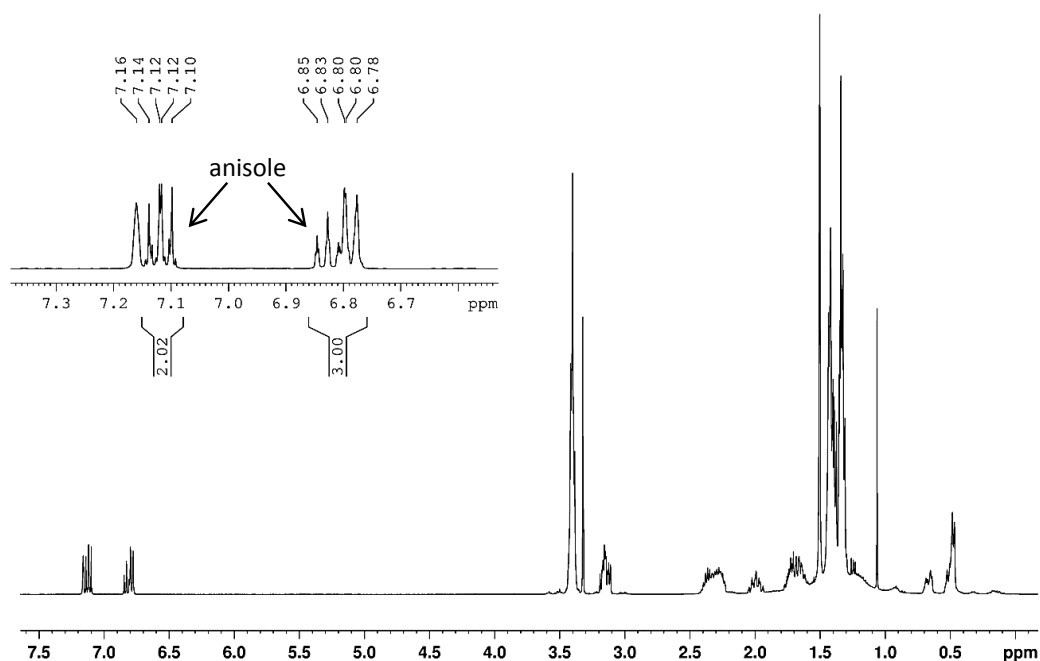


Figure 3.18.  $^1\text{H}$  NMR spectrum ( $d_8$ -THF, 300 K) of a mixture of  $[\text{THF}\cdot\text{Li}(\mu\text{-TMP})(\mu\text{-OC}_4\text{H}_7)\text{Al}(i\text{Bu})_2]$  **3.4** and anisole after stirring it in THF for 24 hours, showing unreacted anisole.

Curious about the constitution of **3.2** in THF solution we compared its  $^1\text{H}$  NMR spectrum with those of its constituent parts LiTMP and  $(\text{TMP})\text{Al}(i\text{Bu})_2$  (see composite spectra in Figure 3.19). Close examination of these spectra show that the principal resonances of LiTMP (Me of TMP at 1.07 ppm) and  $(\text{TMP})\text{Al}(i\text{Bu})_2$  (Me of TMP at 1.21 ppm;  $\text{CH}_2$  of  $i\text{Bu}$  at 0.03 ppm) match almost exactly with corresponding resonances in **3.2** (1.04, 1.21 and 0.03 ppm, respectively) though it is noticeable that the resonances associated with LiTMP are extremely sensitive to even small changes in concentration. Therefore it appears certain that under the conditions studied [longer periods of time lead to the deprotonation/decomposition of THF] LiTMP and  $(\text{TMP})\text{Al}(i\text{Bu})_2$  exist as separate species each solvated by THF. This viewpoint is supported by a DOSY spectrum (see Figure 3.31 in experimental), which shows a significant difference in the diffusion coefficients for each compound [LiTMP =  $1.22 \times 10^{-9}$   $\text{m}^2/\text{s}$ ;  $(\text{TMP})\text{Al}(i\text{Bu})_2$  =  $8.37 \times 10^{-10}$   $\text{m}^2/\text{s}$ ]. It seems clear therefore that a

formidable steric barrier prevents LiTMP and (TMP)Al(*i*Bu)<sub>2</sub> from co-complexing either in hexane or THF solution, but once LiTMP deprotonates a substrate (for example, THF or anisole) the new lithiated substrate species being of reduced steric profile and greater nucleophilicity through Li-C bond formation can join together (be trapped) with the neutral aluminium complex. Evidence that such fragments can join together comes from the previously reported crystal structures of [THF·Li(μ-TMP)(μ-OC<sub>4</sub>H<sub>7</sub>)Al(*i*Bu)<sub>2</sub>], **3.4**,<sup>[33]</sup> and [THF·Li(μ-TMP)(*o*-C<sub>6</sub>H<sub>4</sub>OMe)Al(*i*Bu)<sub>2</sub>], **3.5**,<sup>[32]</sup> respectively (see also the DFT study detailed below).

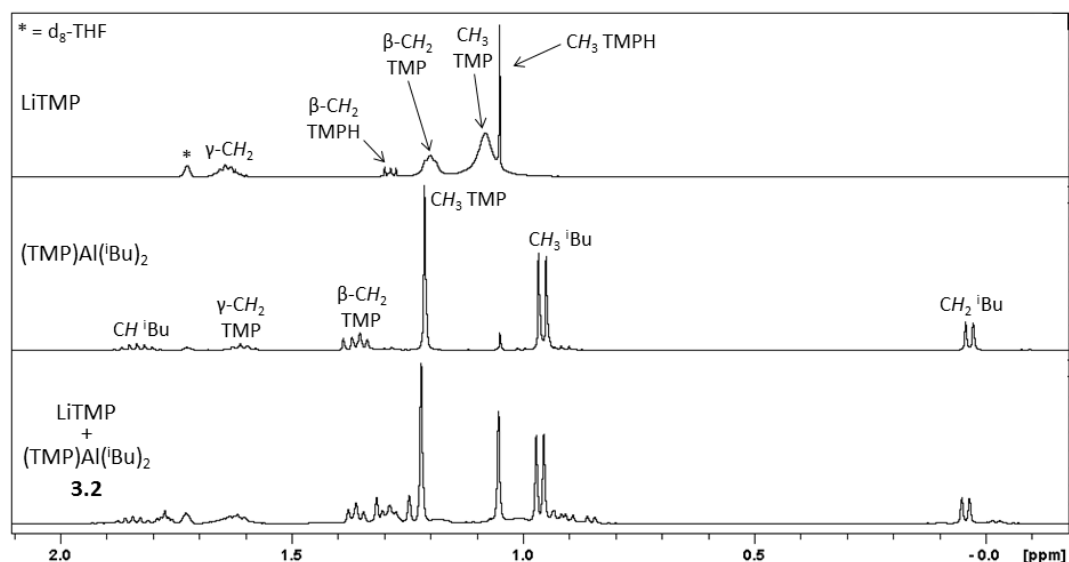


Figure 3.19. Overlay of <sup>1</sup>H NMR spectra of [LiTMP and (TMP)Al(*i*Bu)<sub>2</sub>] **3.2** and its component parts in d<sub>8</sub>-THF solution.

Adding all these new pieces of information to those previously established we can now paint a collective picture of **3.2** in bulk THF solution. Thus it seems that only LiTMP (solvated by THF) and (TMP)Al(*i*Bu)<sub>2</sub> (solvated by THF) are present. However, depending on the age and history of the solution variable amounts of the THF degradation products **3.4** (presumably in its THF-separated form

$[\{\text{Li}(\text{THF})_4\}^+\{\text{(OC}_4\text{H}_7\text{)(TMP)Al}(\text{iBu})_2\}^-]$ ,  $[(\text{THF})_x(\text{LiOC}_4\text{H}_7)_n]$ ,  $[(\text{THF})_n\text{LiO-C}=\text{CH}_2]$  <sup>[56]</sup> and ethene could also be present but usually in trace amounts. Significantly a bimetallic cocomplex “LiTMP·Al(TMP)(iBu)<sub>2</sub>” **3.2** is absent from this collective picture. This is supported indirectly by our DFT computational analysis (see below) that questions the thermodynamic feasibility of such a di-TMP contacted or solvent-separated bimetallic structure.

Having tested all of the metal species within this **3.2** mixture for their metallating ability the only possible candidate to emerge is the aforementioned LiTMP, which in bulk THF solution exists in solvated form as originally deduced by Renaud and Fox who observed both dimeric and monomeric forms through <sup>7</sup>Li NMR spectroscopic studies.<sup>[57]</sup> Wheatley *et al.* confirmed these assignments in a subsequent paper.<sup>[31]</sup>

To establish whether LiTMP was the active Brønsted base component in **3.2** we dissolved freshly prepared LiTMP in d<sub>6</sub>-benzene solution in an NMR tube to which a few drops of THF were added. A <sup>1</sup>H NMR spectrum of this mixture was recorded after 30 minutes and again after 24 hours (Figure 3.20). The presence of ethene was confirmed in both spectra through a resonance at 5.25 ppm, which grew with time, consistent with THF undergoing sequentially metallation, ring opening and cleavage. Significantly when **3.2** was left to stir in bulk THF solution for 24 hours a small amount of aluminate **3.4** was observed as mentioned previously, the implication being that LiTMP is lithiating THF to generate “C<sub>4</sub>H<sub>7</sub>O<sup>-</sup>” anions a small amount of which is trapped by (TMP)Al(iBu)<sub>2</sub> to generate  $[(\text{OC}_4\text{H}_7\text{)(TMP)Al}(\text{iBu})_2]^-$  while the remainder decompose to ethene and lithium enolate.

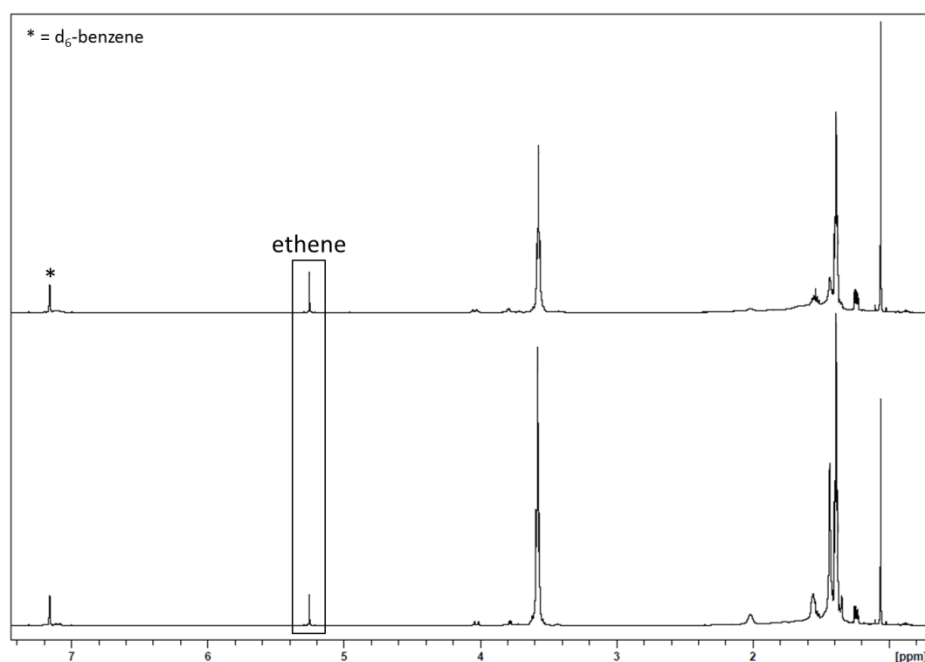
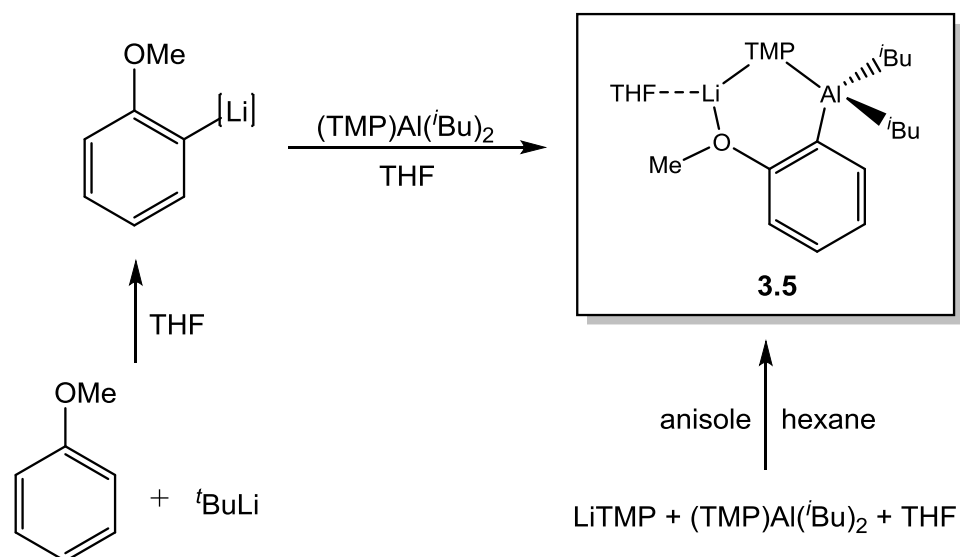


Figure 3.20. Overlay of  $^1\text{H}$  NMR spectra ( $\text{C}_6\text{D}_6$ , 300 K) of LiTMP and THF after 0.5 and 24 hours (bottom and top respectively).

We also explored the lithiation of anisole (Scheme 3.8). Uchiyama, Mongin *et al.* previously reported that subjecting anisole to one molar equivalent of LiTMP in THF solution over two hours produced after iodine quenching only 9% of *ortho*-iodoanisole.<sup>[58]</sup> To ascertain how much lithiated anisole was present prior to any quenching step we reacted LiTMP with anisole in the same stoichiometry in THF solution. However, this reaction produced only about a 5% yield of lithiated anisole (Figure 3.21).



Scheme 3.8. Capture of “aluminated” anisole by direct (RHS) and indirect (LHS) approaches.

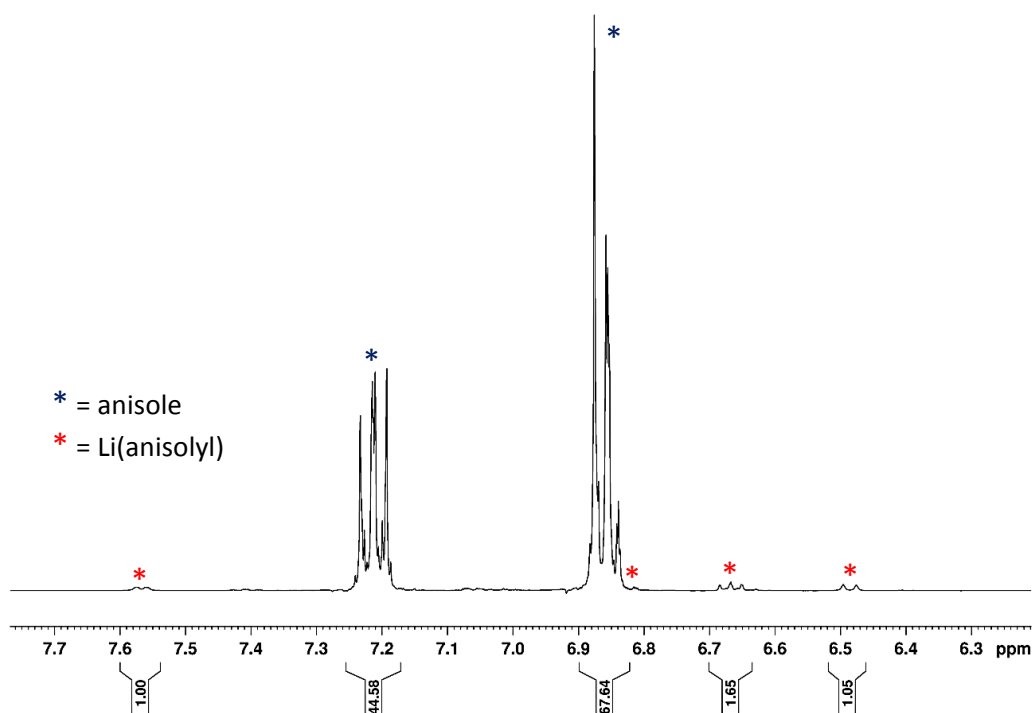


Figure 3.21. Part of the aryl region of the  $^1\text{H}$  NMR spectrum ( $d_8$ -THF, 300 K) of LiTMP and anisole in THF, showing that limited lithiation takes place.

Thus it is unequivocal that LiTMP can bring about the deprotometallation (lithiation) of anisole, albeit in small yields, in contrast to all other species identified within the mixture of **3.2** which are inert to anisole. Since **3.2** furnishes excellent yields of metallated anisole following iodine quenching the implication is that once formed any lithiated anisole will undergo an expeditious trapping by the strongly carbophilic neutral aluminium species (TMP)Al(*t*Bu)<sub>2</sub>. This was established unequivocally by taking a 1:1 mixture of lithiated anisole (prepared separately by reaction of anisole and *t*BuLi in THF at 0°C)<sup>[59]</sup> and (TMP)Al(*t*Bu)<sub>2</sub> in d<sub>8</sub>-THF solution in an NMR tube and recording its <sup>1</sup>H and <sup>13</sup>C spectra (Figure 3.22 and Figure 3.23 respectively).

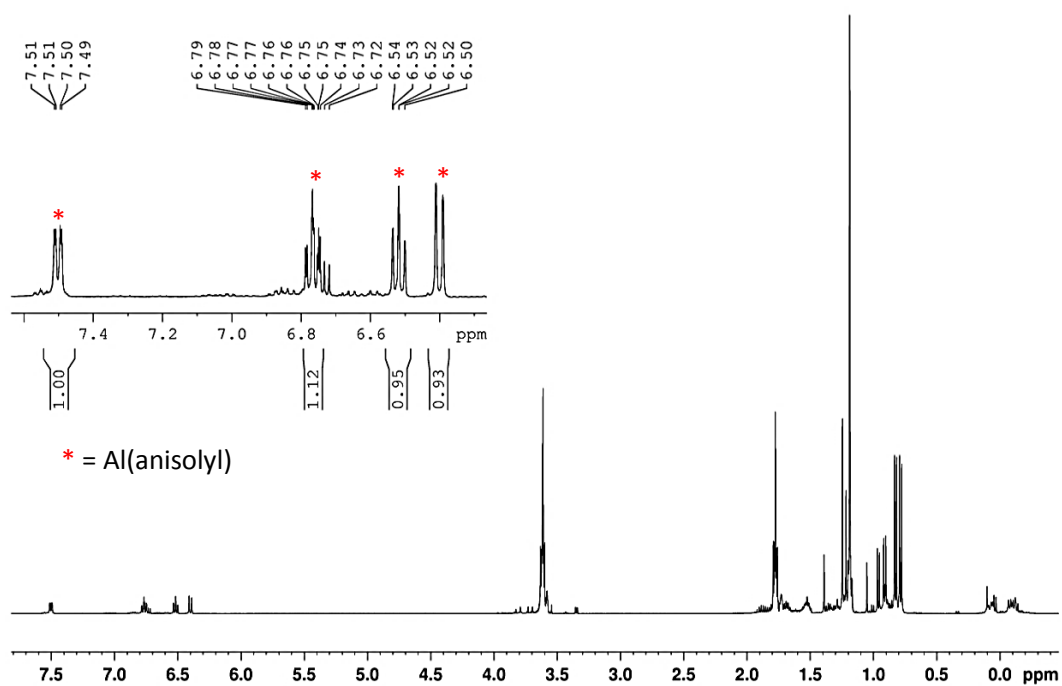


Figure 3.22. <sup>1</sup>H NMR spectrum (d<sub>8</sub>-THF, 300 K) of the reaction between prepared Li(anisoyl) and (TMP)Al(*t*Bu)<sub>2</sub> showing the near-quantitative production of the Al(anisoyl) compound.

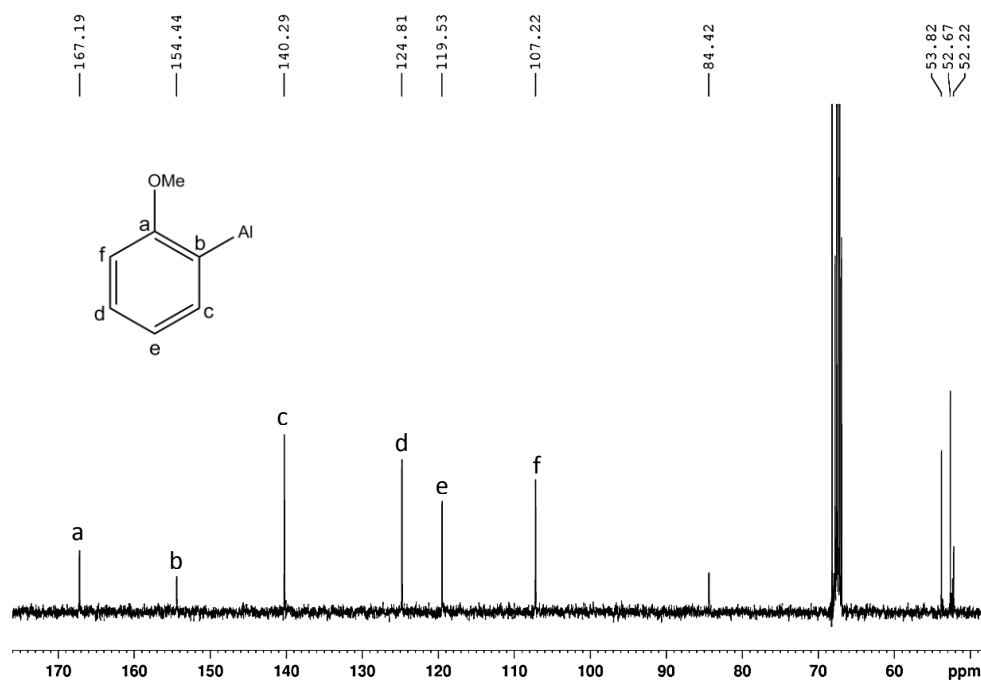
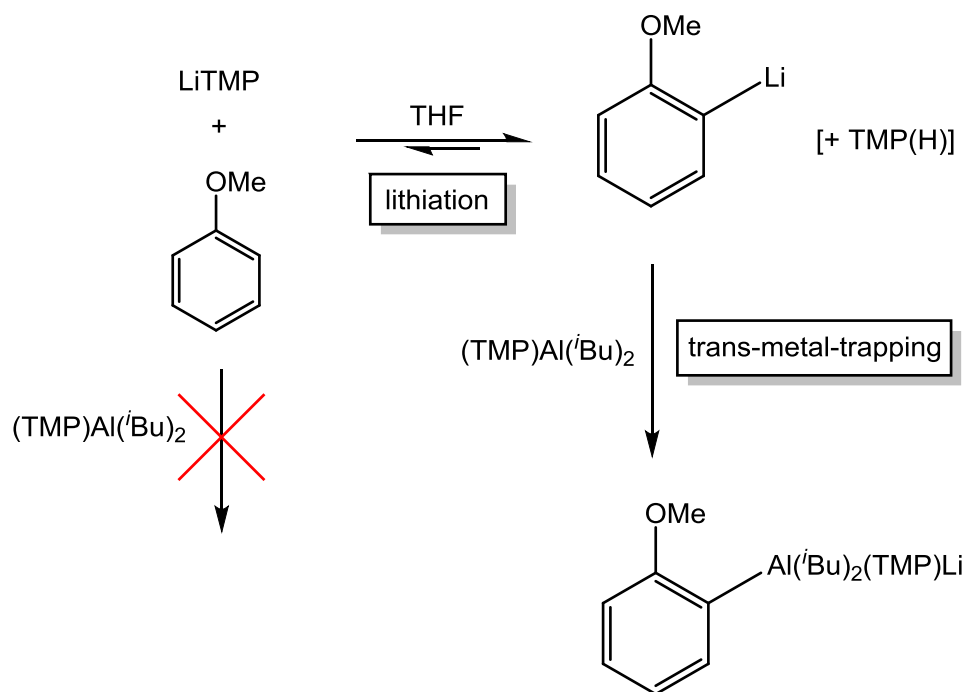


Figure 3.23. Aryl region of the  $^{13}\text{C}$  NMR spectrum ( $\text{d}_8\text{-THF}$ , 300 K) of the reaction between pre-prepared Li(anisoyl) and  $(\text{TMP})\text{Al}(^t\text{Bu})_2$  showing the Al(anisoyl) product.

The most diagnostic resonance in the  $^1\text{H}$  spectra, the *meta* C-H adjacent to the metallated C-M, shows a significant upfield shift (from 7.66 to 7.49 ppm) signifying the attached metal M has transferred from Li to Al; with a similar shift seen in the  $^{13}\text{C}$  spectra for the metallated C-M atom from 159.2 to 154.4 ppm [note that Uchiyama reported a similar but not identical upfield Li to Al shift on treating anisole with  $^t\text{BuLi}$  with the C-Al resonance appearing at 152.91 ppm, the main distinction being the trapping Al reagent used was  $\text{Al}(^t\text{Bu})_3$ ]. From integration ratios this trans-metal-trapping of the anisoyl carbanion by  $(\text{TMP})\text{Al}(^t\text{Bu})_2$  seems essentially quantitative. As depicted in Scheme 3.9, this insertion of the aluminium reagent into the polarised Li-C(anisoyl) bond should drive the equilibrium between anisole and lithiated anisole towards the lithiated species thus increasing the overall metallation yield of the reaction.



Scheme 3.9. Proposed two-step pathway for the “aluminum” of anisole.

We established that such an equilibrium exists between lithiated anisole and LiTMP by taking a freshly prepared sample of the former and mixing it with an equimolar amount of TMP(H) in  $d_6$ -benzene solution and stirring the solution for 10 minutes. A  $^1\text{H}$  NMR spectrum (Figure 3.24) confirmed the presence of LiTMP at this juncture. It should be stressed that although  $(\text{TMP})\text{Al}(i\text{Bu})_2$  is incapable of metallating aromatic substrates by itself, it actually contributes to the success of the metallation reactions of **3.2** in two important ways: firstly, it traps the carbanion generated by lithium and then stabilises it by reducing the polarity of the metal-carbon bond; secondly, by not engaging at all with LiTMP on the left hand side of the equation (Scheme 3.9) the equilibrium can shift towards the desired anisoyl aluminium product. This hypothesis of non-cocomplexed LiTMP and  $(\text{TMP})\text{Al}(i\text{Bu})_2$  homometallic species swimming separately in a pool of THF runs counter to any notion that a “LiTMP·Al(TMP)( $i\text{Bu}$ ) $_2$ ” cocomplex was responsible for these “AMMA” reactions. Therefore the weight of evidence from this work suggests these



reactions are not in fact direct aluminations (aluminium-hydrogen exchanges) at all but rather two step lithiation/trans-metal-trapping processes. It is germane to note that when LiTMP is mixed together with  $\text{Zn}(\text{TMP})_2$  [60] or  $\text{Cd}(\text{TMP})_2$  [61] they appear not to afford the cocomplexes “ $\text{LiZn}(\text{TMP})_3$ ” or “ $\text{LiCd}(\text{TMP})_3$ ” (that is, tris-TMP ates), but instead remain separated components, the metallating reactivity of which has also been ascribed to homometallic LiTMP.[23, 62]

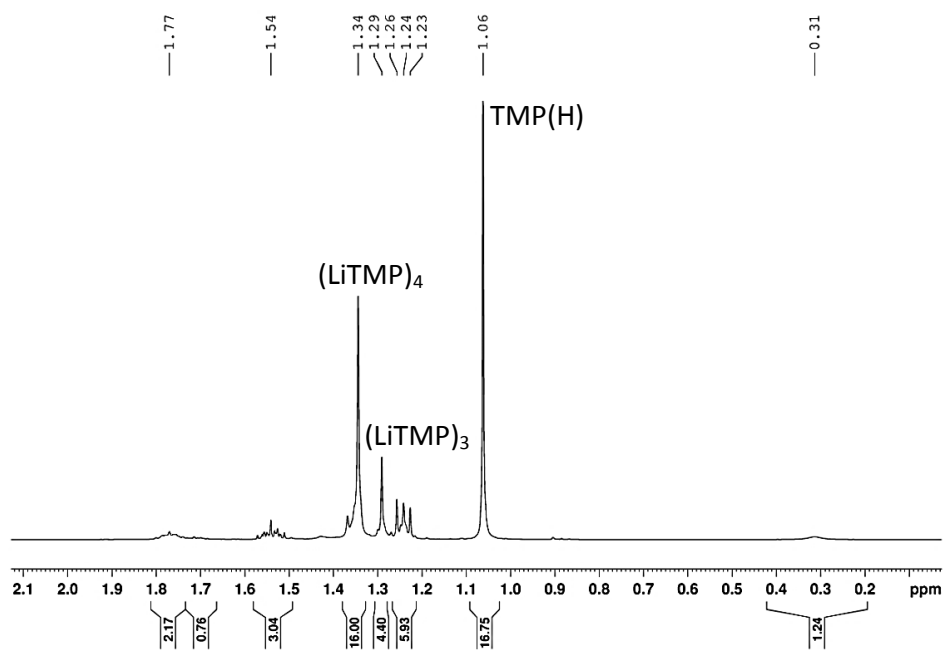


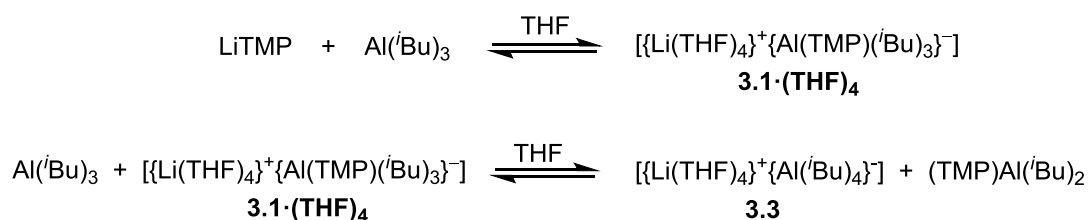
Figure 3.24.  $^1\text{H}$  NMR spectrum ( $\text{C}_6\text{D}_6$ , 300 K) of pre-prepared Li(anisoly) and TMP(H) confirming the formation of LiTMP.

To conclude this comprehensive study of the reactions of **3.2** in bulk THF solutions it is worth stressing that although these reactions are not AMMA/*s* they are still synergistic in origin. To explain, without participation of the aluminium reagent, interception of the lithiated substrates with electrophiles  $\text{E}^+$  would be unsatisfactory leading to poor yields of the desired  $\text{E}^+(\text{substrate})^-$  products. This reflects the non-selective nature of iodine quenching as it would

quench both lithiated anisole and LiTMP to prevent the equilibrium in Scheme 3.9 shifting towards lithiated anisole; whereas the aluminium reagent selectively targets lithiated anisole and ignores the bulkier LiTMP. However, unlike some other bimetallic synergistic systems mentioned within this thesis, this Li-Al type is only synergistic in efficiency not in any special regioselectivity.

### 3.3.4 Re-evaluating the Composition and Active Base Component of *In Situ* **3.1** in THF Solution

Now that the picture of **3.2** in THF solution is much more transparent following the new findings set out here, the composition of **3.1** in THF solution needed to be re-considered. Taking into account the surprising discovery that LiTMP is the active base component within **3.2** we can propose a more complete composition for **3.1** (Scheme 3.10).



Scheme 3.10. Re-evaluated composition of “single-species” [THF·Li(TMP)Al(*i*Bu)<sub>3</sub>] showing its existence as two connected equilibria involving five distinct species.

Far removed from the original idea that it existed as a single species of formula [THF·Li(TMP)(*i*Bu)Al(*i*Bu)<sub>2</sub>], in this proposal **3.1** contains no less than five species in two interconnected equilibria including most significantly the separated monometallic species LiTMP, which we have already established can perform metallation of a substrate. Convincing evidence for the second

equilibrium came from mixing authentic samples of the salt  $[\{\text{Li}(\text{THF})_4\}^+\{\text{Al}(\textit{i}\text{Bu})_4\}^-]$ , **3.3**, and  $(\text{TMP})\text{Al}(\textit{i}\text{Bu})_2$  in  $d_8$ -THF solution and recording the  $^1\text{H}$  NMR spectrum at room temperature (Figure 3.25). The low frequency region about 0 ppm is extremely informative as each species exhibits a well-defined  $\text{Al}-\text{CH}_2(\textit{i}\text{Bu})$  resonance within it. Four such resonances observed at (0.02, -0.10, -0.22 and -0.37 ppm) can be assigned to  $(\text{TMP})\text{Al}(\textit{i}\text{Bu})_2$ ,  $\text{Al}(\textit{i}\text{Bu})_3$ ,  $[\{\text{Li}(\text{THF})_4\}^+\{\text{Al}(\text{TMP})(\textit{i}\text{Bu})_3\}^-]$  and  $[\{\text{Li}(\text{THF})_4\}^+\{\text{Al}(\textit{i}\text{Bu})_4\}^-]$  respectively. Four  $\text{CH}_3(\textit{i}\text{Bu})$  resonances were also observed for the four distinct species though the doublet of doublets for  $\text{Al}(\textit{i}\text{Bu})_3$  and  $[\{\text{Li}(\text{THF})_4\}^+\{\text{Al}(\text{TMP})(\textit{i}\text{Bu})_3\}^-]$  overlap. All assignments were verified by comparison with the spectra of authentic samples of the individual components.

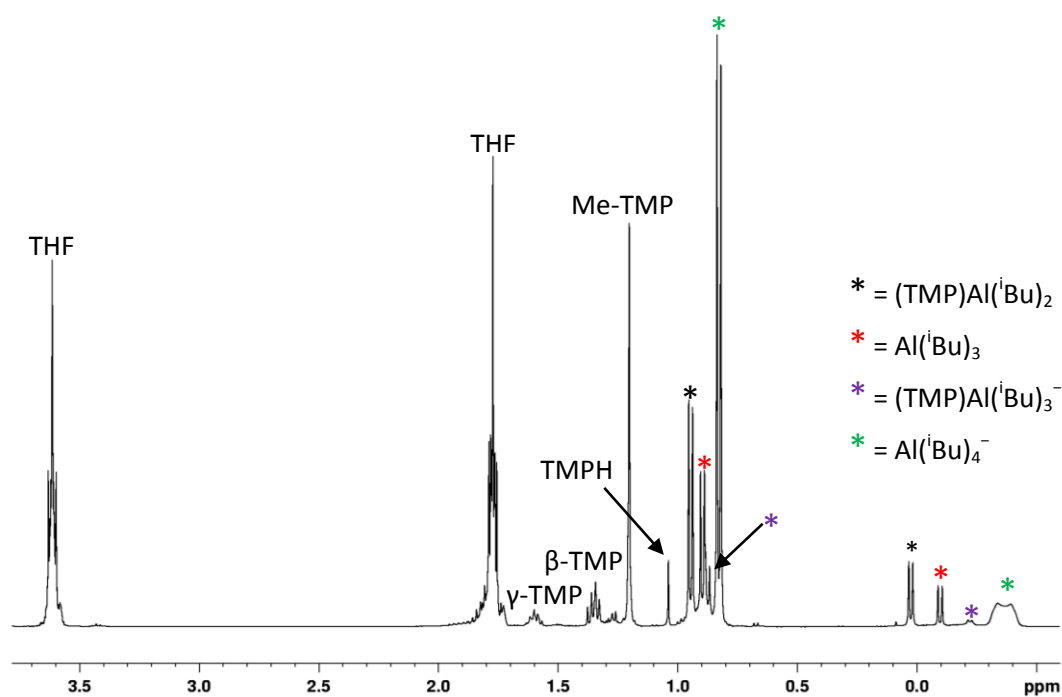


Figure 3.25.  $^1\text{H}$  NMR spectrum of a mixture of  $(\text{TMP})\text{Al}(\textit{i}\text{Bu})_2$  and  $[\{\text{Li}(\text{THF})_4\}^+\{\text{Al}(\textit{i}\text{Bu})_4\}^-]$  **3.3** in  $d_8$ -THF solution.

The trialkyl-amido aluminate  $[\text{Li}(\text{THF})_4]^+\{\text{Al}(\text{TMP})(i\text{Bu})_3\}^-$  was prepared by reacting neutral  $(\text{TMP})\text{Al}(i\text{Bu})_2$  with an equimolar amount of  $i\text{BuLi}$  in THF solution (Figure 3.26 and Figure 3.27, note the corresponding resonance for  $i\text{BuLi}$  comes more upfield at  $-0.98$  ppm) and this aluminate gave an identical spectrum to that of crystalline **3.1**·THF dissolved in  $d_8$ -THF solution, which we discovered was inactive as a base.

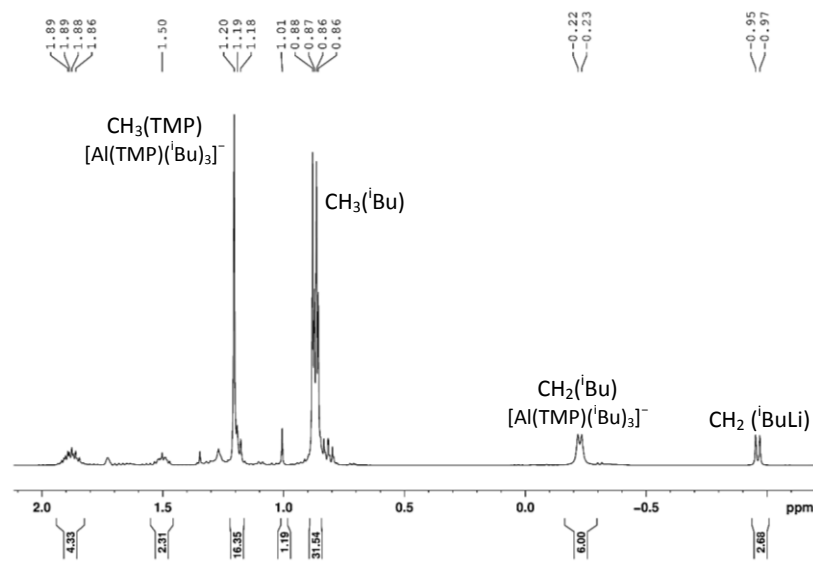


Figure 3.26.  $^1\text{H}$  NMR spectrum ( $d_8$ -THF, 300 K) of  $(\text{TMP})\text{Al}(i\text{Bu})_2$  and  $i\text{BuLi}$ .

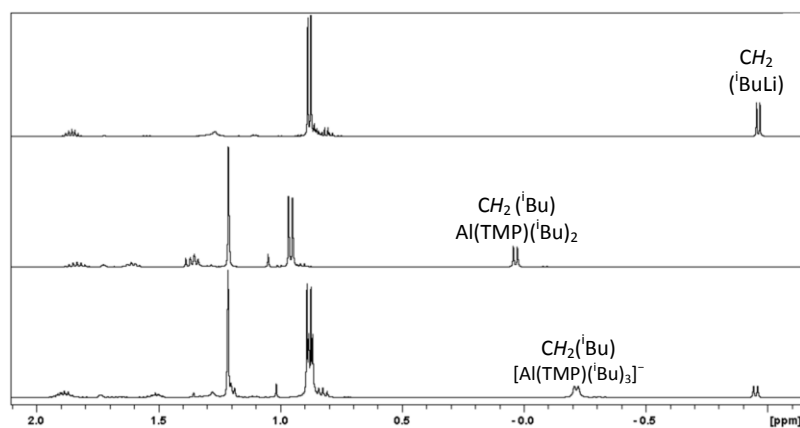


Figure 3.27. Overlay of  $^1\text{H}$  NMR spectra ( $d_8$ -THF, 300 K) of  $i\text{BuLi}$  (top),  $(\text{TMP})\text{Al}(i\text{Bu})_2$  (middle), and the mixture of both (bottom).

It is also significant that no LiTMP was found in the spectrum of the  $[\{\text{Li}(\text{THF})_4\}^+\{\text{Al}(\textit{i}\text{Bu})_4\}^-]$ , **3.3**, and  $(\text{TMP})\text{Al}(\textit{i}\text{Bu})_2$  mixture (Figure 3.25) as evidenced by the absence of a Me resonance at 1.05 ppm. When TMP is attached to Al this Me resonance moves downfield to 1.21 ppm in  $(\text{TMP})\text{Al}(\textit{i}\text{Bu})_2$  and 1.20 ppm in  $[\{\text{Li}(\text{THF})_4\}^+\{\text{Al}(\text{TMP})(\textit{i}\text{Bu})_3\}^-]$  though these signals cannot be differentiated in the combined spectrum. Since the equilibrium under these ambient temperature conditions greatly favours  $(\text{TMP})\text{Al}(\textit{i}\text{Bu})_2$ , the Me(TMP) resonance of it is much larger than that of  $[\{\text{Li}(\text{THF})_4\}^+\{\text{Al}(\text{TMP})(\textit{i}\text{Bu})_3\}^-]$ . Accurate measurement of the relative integrals of  $[\{\text{Li}(\text{THF})_4\}^+\{\text{Al}(\text{TMP})(\textit{i}\text{Bu})_3\}^-]$  and  $\text{Al}(\textit{i}\text{Bu})_3$  is problematic due to the broad nature of the Al-CH<sub>2</sub> (*i*Bu) resonance of  $\{\text{Al}(\text{TMP})(\textit{i}\text{Bu})_3\}^-$ . Note that the corresponding resonance for the homoleptic ate  $[\{\text{Li}(\text{THF})_4\}^+\{\text{Al}(\textit{i}\text{Bu})_4\}^-]$  is similarly broad.<sup>[46]</sup> In both cases the broadness can be attributed to the quadrupolar effect of the <sup>27</sup>Al centre (spin 5/2). In the symmetrical species  $[\{\text{Li}(\text{THF})_4\}^+\{\text{Al}(\textit{i}\text{Bu})_4\}^-]$  the Al-CH<sub>2</sub> (*i*Bu) resonance is a doublet due to coupling with the adjacent CH but this is further split by the Al into a doublet of sextets, though as the environment is not perfectly symmetrical some merging of the lines occurs and the resonance observed appears wide and broad. Figure 3.28 and Figure 3.29 show the results of decoupling and 2D [<sup>1</sup>H,<sup>27</sup>Al] HSQC and HSQC-TOCSY (HSQC is heteronuclear single quantum correlation and TOCSY is total correlation spectroscopy) experiments respectively which support the Al and *i*Bu assignments within **3.1·(THF)<sub>4</sub>** and **3.3**.

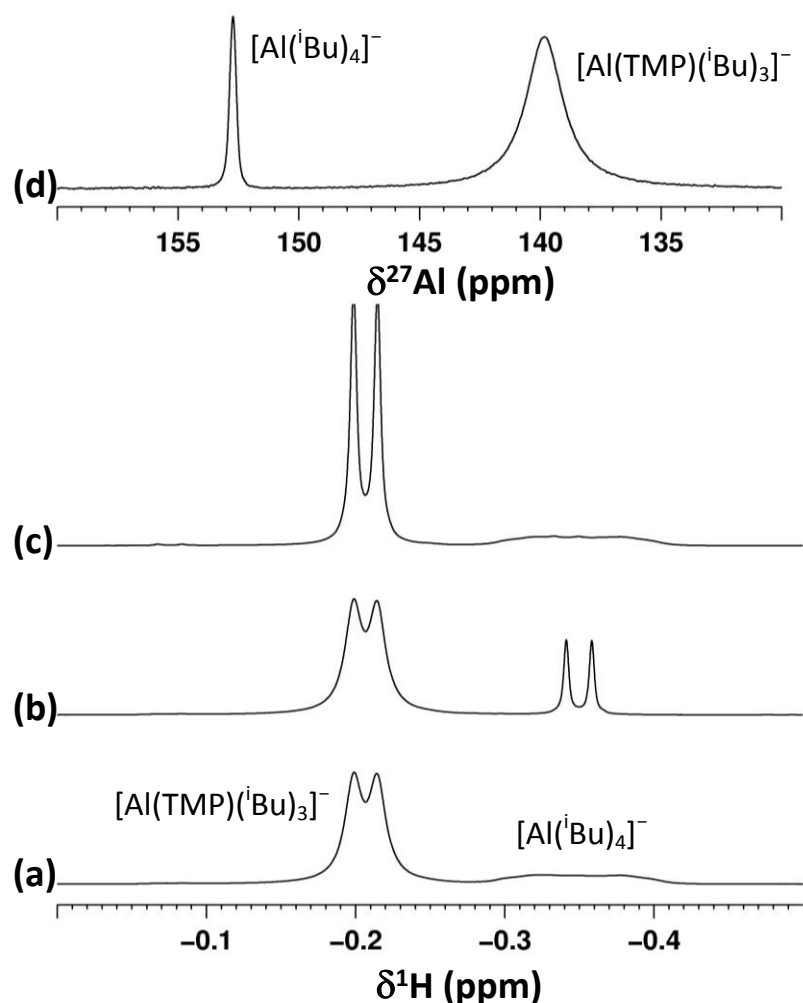


Figure 3.28. “Al-*i*Bu” methylene proton resonance region of the 1D  $^1\text{H}$ ,  $^1\text{H}\{-^{27}\text{Al}\}$  and associated  $^{27}\text{Al}$  NMR spectra of a mixture of crystalline  $[\{\text{Li}(\text{THF})_4\}^+\{\text{Al}(\text{TMP})(i\text{Bu})_3\}^-]$  **3.1**·**(THF)**<sub>4</sub> and  $[\{\text{Li}(\text{THF})_4\}^+\{\text{Al}(i\text{Bu})_4\}^-]$  (**3.3**). **(a)**  $^1\text{H}$  NMR spectrum showing broadened resonances for both species; **(b)** as for **(a)** but with continuous wave narrow-band  $^{27}\text{Al}$  decoupling by irradiation at  $\delta^{27}\text{Al} = 152.72$  ppm; **(c)** as for **(a)** but with continuous wave narrow-band  $^{27}\text{Al}$  decoupling by irradiation at  $\delta^{27}\text{Al} = 139.84$  ppm; **(d)** labelled  $^{27}\text{Al}$  spectrum from Figure 3.9.

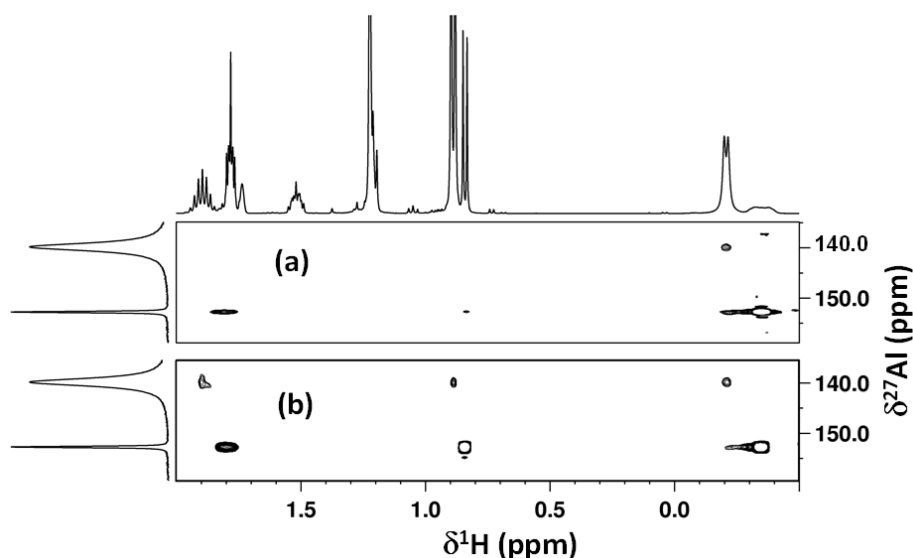


Figure 3.29. Correlation data confirming resonance relationships between  $^{27}\text{Al}$  and  $^1\text{H}$  nuclei. **(a)** Phase-sensitive gradient selected 2D [ $^1\text{H}$ ,  $^{27}\text{Al}$ ] HSQC optimized for maximum signal intensity; **(b)** Phase-sensitive gradient selected 2D [ $^1\text{H}$ ,  $^{27}\text{Al}$ ] HSQC-TOCSY revealing  $^{27}\text{Al}$ -associated *i*Bu proton spin-systems for two independent species. It is particularly notable that the presence of a signal for the *i*Bu methine proton of the more symmetrical species is detected *via* HSQC-TOCSY below the THF signal at 1.78 ppm.

The equilibria are also implicated on mixing equimolar proportions of LiTMP and  $\text{Al}(i\text{Bu})_3$  in  $d_8$ -THF solution (see the spectra comparison in Figure 3.30). On recording this  $^1\text{H}$  NMR spectrum at 0 °C, the resonances for LiTMP (most diagnostically the Me resonance at 1.05 ppm, though this overlaps with a TMPH resonance the presence of which is unavoidable due to attack of THF by LiTMP) and  $[(\text{TMP})\text{Al}(i\text{Bu})_3]^-$  (at -0.25 ppm) are the most prominent. A smaller extremely broad resonance for  $[\{\text{Li}(\text{THF})_4\}^+\{\text{Al}(i\text{Bu})_4\}^-]$  is clearly seen too. The presence of  $[\{\text{Li}(\text{THF})_4\}^+\{\text{Al}(i\text{Bu})_4\}^-]$  is also clearly distinguishable in the Me region of the *i*Bu group as a doublet at 0.84 ppm, though the analogous doublets for the other *i*Bu containing species overlap into a complex multiplet at about 0.89 ppm consistent with there being multiple species present rather than simply  $\text{Al}(i\text{Bu})_3$ .

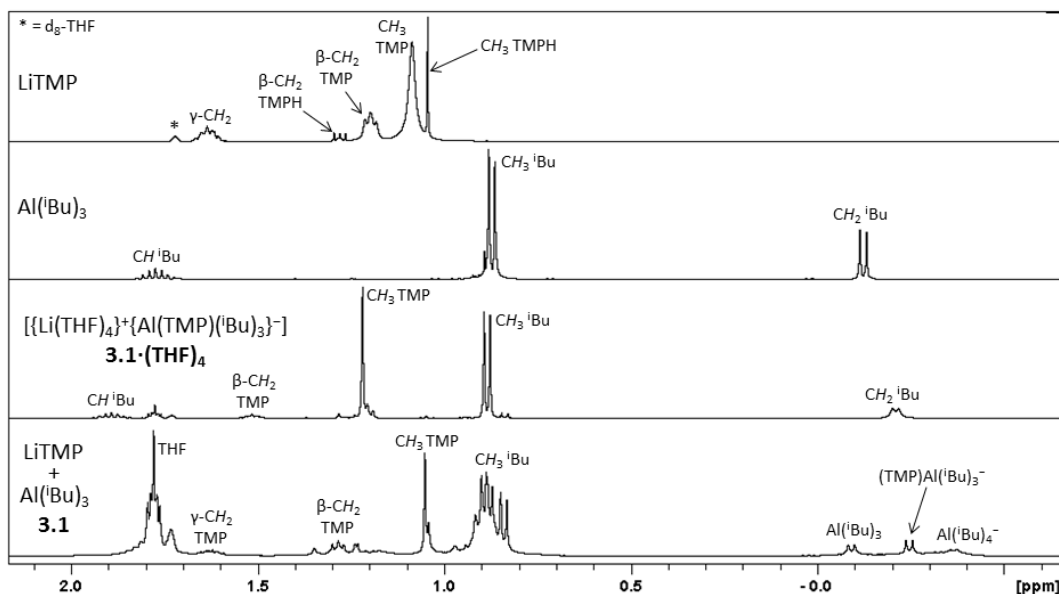


Figure 3.30. Overlay of  $^1\text{H}$  NMR spectra of LiTMP,  $\text{Al}(i\text{Bu})_3$ ,  $[\{\text{Li}(\text{THF})_4\}^+\{\text{Al}(\text{TMP})(i\text{Bu})_3\}^-]$  and  $[\text{LiTMP}$  and  $\text{Al}(i\text{Bu})_3]$  in  $d_8$ -THF solution.

Since some metallation is observed in the solution, indicated by the presence of TMP(H), then it is possible that the amount of  $(\text{TMP})\text{Al}(i\text{Bu})_2$  in solution is being decreased as this species will trap any carbanion formed upon metallation [see earlier discussion of efficient trapping of anisoyl anions by neutral  $(\text{TMP})\text{Al}(i\text{Bu})_2$ ]. Clearly the  $(i\text{Bu})\text{Me}$  region at 0.80-0.95 ppm in containing more than the four overlapping species you would expect in the equilibrium proposed supports this thinking. Other ates of formula  $(\text{TMP})\text{Al}(i\text{Bu})_2\text{Y}$  where Y is for example  $\text{C}_4\text{H}_7\text{O}^-$  or  $\text{C}_2\text{H}_3\text{O}^-$  formula could also be present. To check whether or not LiTMP was participating in an equilibrium with the salt  $[\{\text{Li}(\text{THF})_4\}^+\{\text{Al}(i\text{Bu})_4\}^-]$  we added both to a  $d_8$ -THF solution and monitored the mixture through  $^1\text{H}$  NMR spectra which revealed that the resonances associated with the two individual compounds remain unchanged. We can therefore conclude with confidence that LiTMP and  $[\{\text{Li}(\text{THF})_4\}^+\{\text{Al}(i\text{Bu})_4\}^-]$  are not in equilibrium with each other. Neither is LiTMP in equilibrium with  $(\text{TMP})\text{Al}(i\text{Bu})_2$  as we established through the aforementioned studies of **3.2·THF**.



Based on these new observations we can find no evidence at all for a species of composition “[{Li(THF)<sub>n</sub>}<sup>+</sup>{Al(TMP)<sub>2</sub>(*i*Bu)<sub>2</sub>}<sup>-</sup>]” that we had originally presumed in the dismutation process shown in Scheme 3.5. DFT calculations (see below) support the non-existence of such a heteroleptic aluminate species. It transpires that **3.1·THF** is much more complicated existing in at least five distinct species in THF solution. The complexity can be attributed to the lability of Al(*i*Bu)<sub>3</sub> which can add a TMP ligand to generate [(TMP)Al(*i*Bu)<sub>3</sub>]<sup>-</sup> and gain or lose an *i*Bu group to form [Al(*i*Bu)<sub>4</sub>]<sup>-</sup> or [Al(*i*Bu)<sub>2</sub>]<sup>+</sup> containing species; whereas by comparison the solution chemistry of **3.2·THF** is much simpler due to the relative poor lability of (TMP)Al(*i*Bu)<sub>2</sub> and specifically its inability to form a co-complex with LiTMP on steric grounds. What **3.1·THF** and **3.2·THF** do have in common is that when each is dissolved in bulk THF the active base component is LiTMP. Ironically, revisiting the original question, “has the active base of **3.1** been crystallographically characterised?”, the revised answer must be yes, as LiTMP has been crystallographically characterised in two different polymorphic forms (see Chapter 2) [51-52] as well as a THF adduct.[53] Multicomponent **3.2·THF** is the strongest base of the two mixtures because it would always have the largest proportion of LiTMP present in a solution of the same molarity; whereas some LiTMP will always be consumed in **3.1·THF** due to the complicated equilibria in operation. This last point is in agreement with the excess of **3.1·THF** (2.2 molar equivalents) used by Uchiyama *et al.* in their synthetic applications to ensure maximum yields of the metallated/quenched substrates were obtained. Furthermore **3.1·THF** is hampered as a base when utilised in hexane solution for if the LiTMP:Al(*i*Bu)<sub>3</sub> stoichiometric ratio in the starting mixture is exactly 1:1 there will be no free LiTMP available to perform a metallation. However, there are at least two qualifications. Firstly, at higher temperatures the contacted ion-pair structure of **3.1·THF** could break up and release LiTMP, making metallations of suitably thermally stable substrates a possibility though it has been established recently that LiTMP can itself also undergo bond breakage at high temperatures.[63] On the other hand free, active LiTMP should always be available in hexane solutions of **3.2·THF**. Secondly,

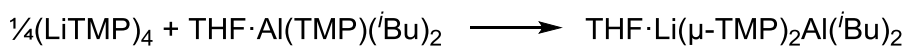
certain Lewis bases can coordinate to the Lewis acidic lithium centre to generate a contacted ion-pair aluminate with  $\text{Al}(i\text{Bu})_3$  that can subsequently metallate a C-H bond in the Lewis base in a genuine example of alkali-metal-mediated aluminations. The literature report of  $[\text{Li}\{\text{Me}_2\text{NCH}_2\text{CH}_2\text{N}(\text{Me})\text{CH}_2\}_2\text{Al}(i\text{Bu})_2]$  **3.6** made by a 1:2 stoichiometric reaction of **3.1** and TMEDA in hexane solution is a precedent for this type of reaction.<sup>[35]</sup>

### 3.3.5 Theoretical Calculations

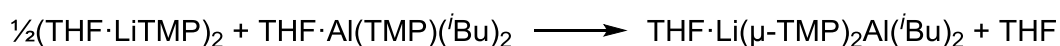
Uchiyama and Wheatley *et al.* previously investigated the structure of **3.1** “ $\text{LiTMP}\cdot\text{Al}(i\text{Bu})_3$ ” theoretically by DFT calculations using the B3LYP/6-31+G\* level of theory.<sup>[31]</sup> In this study **3.1** was modelled by  $[\text{S}\cdot\text{LiNMe}_2\cdot\text{Al}(\text{Me})_3]$  (where S = the donor solvent  $\text{Me}_2\text{O}$ ) for calculational simplicity and its metallation reaction with anisole was modelled. Possible intermediates and transition states along the reaction coordinate were determined together with a quantification of the energy differences involved. However, the starting points of this study were a contacted ion-pair structure  $[\text{S}\cdot\text{Li}(\mu\text{-Me})(\mu\text{-NMe}_2)\cdot\text{Al}(\text{Me})_2]$  and the subsequent pre-metallation complex it forms with anisole  $[\text{Ph}(\text{Me})\text{O}\cdot\text{Li}(\mu\text{-Me})(\mu\text{-NMe}_2)\cdot\text{Al}(\text{Me})_2]$ , the formation of which led to an energy saving of  $-15.8$  kcal mol<sup>-1</sup>. That notwithstanding, on the basis of the new information accrued in this project, these starting points are not relevant to the actual experimental reagent **3.1** employed in bulk THF solution. This is because all the mixed lithium-aluminium species present in bulk THF solution are solvent separated and so the Li cannot cooperate with Al by providing the anisole with a coordination point adjacent to the amido ligand attached to the Al. To put it another way, no complex induced proximity effect would be possible. We confirmed this experimentally by showing that the solvent-separated aluminate  $[\{\text{Li}(\text{THF})_4\}^+\{\text{Al}(\text{TMP})(i\text{Bu})_3\}^-]$  **3.1}\cdot(\text{THF})\_4** is incapable of metallating anisole in bulk THF solution.

In earlier work, the Mulvey group carried out DFT calculations looking at the feasibility of a structure of putative **3.2}\cdot\text{THF}** of formula  $[\text{THF}\cdot\text{Li}(\mu\text{-$

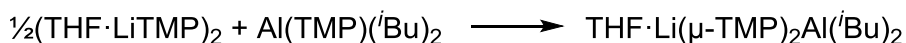
TMP)<sub>2</sub>Al(*i*Bu)<sub>2</sub>].<sup>[32]</sup> These calculations used the Gaussian 03 package with geometry optimisation using the B3LYP density functionals and the 6-311(d, p) basis set with zero point energy corrections. While this study confirmed the most energetically stable arrangement of **3.2**·THF has two bridging TMP ligands with the two terminal *i*Bu ligands on Al, significantly it also exposed the relative instability of **3.2**·THF with respect to either its homometallic components LiTMP and (TMP)Al(*i*Bu)<sub>2</sub> or THF solvates thereof. Depending on the homometallic components employed this instability ranged from +14.16 to +20.60 kcal mol<sup>-1</sup> (Scheme 3.11).



$$\Delta E = +14.16 \text{ kcal mol}^{-1}$$



$$\Delta E = +20.60 \text{ kcal mol}^{-1}$$

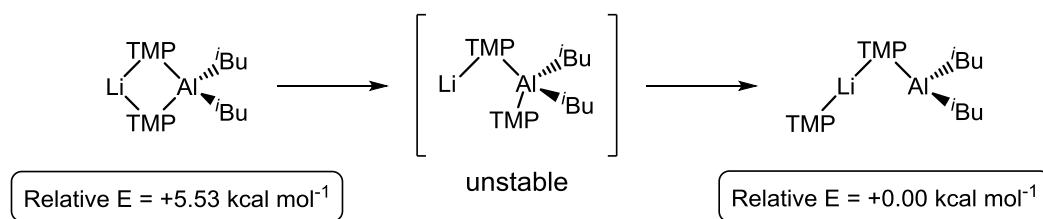


$$\Delta E = +14.19 \text{ kcal mol}^{-1}$$

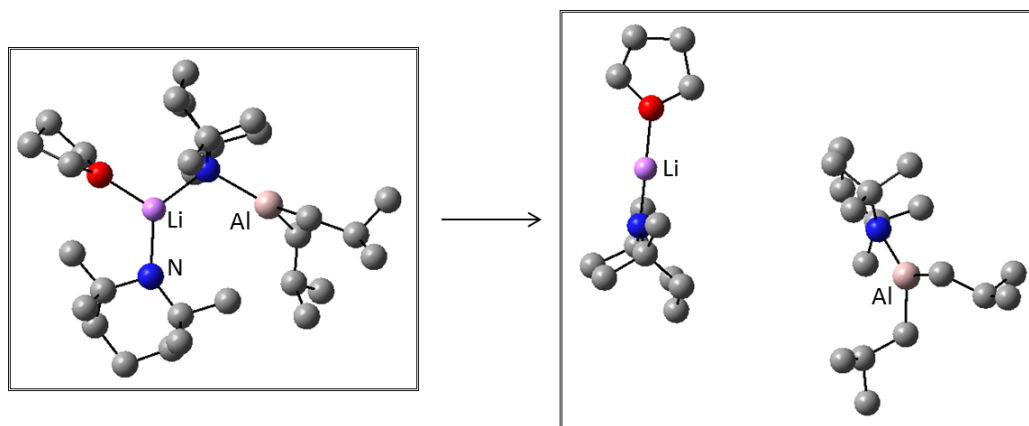
Scheme 3.11. Energies obtained from DFT calculations for the possible reactions in which putative [THF·Li(μ-TMP)<sub>2</sub>Al(*i*Bu)<sub>2</sub>] is formed.

To shed more light on **3.2** having accrued much more knowledge on the experimental system through this study we have performed extra calculations using the same parameters. We began by modelling a THF-free version of **3.2**, Li(μ-TMP)<sub>2</sub>Al(*i*Bu)<sub>2</sub>, **3.2**<sub>closed</sub>, having a closed four-atom (LiNAlN) ring, comparing it against an open version **3.2**<sub>open</sub>, to ascertain the effect that relaxing

the steric strain by opening the ring might have on the stability of **3.2** (Scheme 3.12). Our first model of **3.2<sub>open</sub>** was derived by breaking one of the Li-N(TMP) bonds in **3.2<sub>closed</sub>** to leave a single Li-N(TMP)-Al bridge with the remaining three ligands bonded solely to Al. However, under geometry optimisation this 1-coordinate Li/4-coordinate Al model rearranged through the migration of the terminal Al-attached TMP ligand to a terminal position on Li to generate a more realistic 2-coordinate Li/3-coordinate Al structure, isoelectronic with crystallographically characterized [TMEDA·Li(μ-TMP)Li(TMP)]<sup>[64]</sup> and [PMDETA·Na(μ-TMP)Li(TMP)].<sup>[65]</sup> Relieving the steric strain by opening the LiAlN ring in this way does indeed increase the stability with **3.2<sub>open</sub>** being -5.53 kcal mol<sup>-1</sup> more stable than **3.2<sub>closed</sub>**. That notwithstanding, on introducing a THF ligand to the lithium centre to mimic the experimental stoichiometry of **3.2·THF**, the structure fragmented under geometry optimisation into the homometallic components THF·LiTMP and (TMP)Al(*i*Bu)<sub>2</sub> (Scheme 3.13). The energy given by the sum of these two separated homometallic components is -1614.811704 a.u. compared to -1614.805526 a.u. for **3.2<sub>closed</sub>·THF**, equating to the former being more stable by -3.87 kcal mol<sup>-1</sup> [or by a more realistic -14.19 kcal mol<sup>-1</sup> if the dimeric aggregation of (THF·LiTMP)<sub>2</sub> is taken into account]. Collectively these results suggest that a THF solvate of the contacted ion-pair LiTMP·Al(TMP)(*i*Bu)<sub>2</sub>, whether in a closed or open ring arrangement would be too high in energy to exist, supporting the aforementioned experimental NMR investigations which failed to detect any such species.

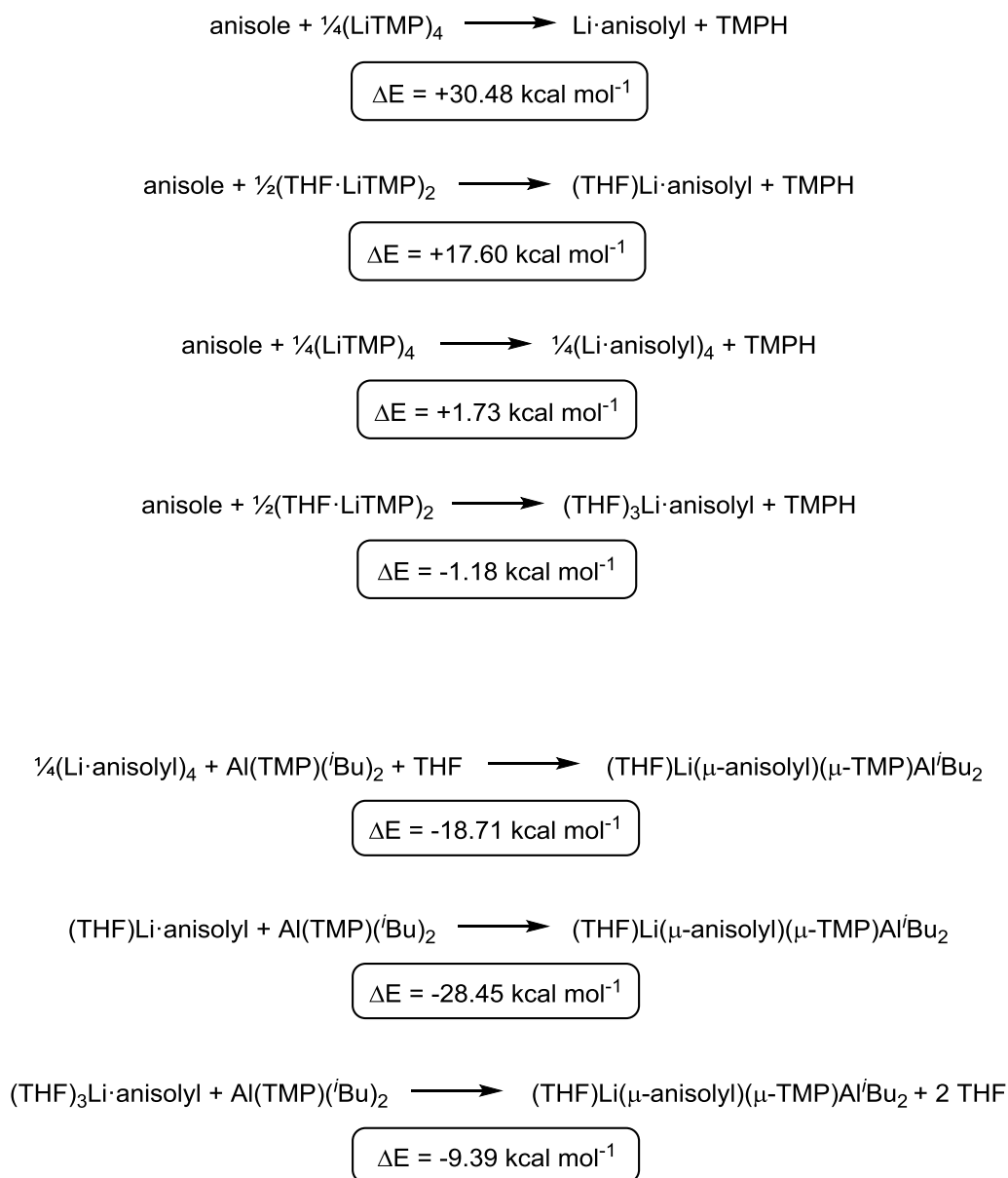


Scheme 3.12. ChemDraw representation of the rearrangement of Li(μ-TMP)<sub>2</sub>Al(*i*Bu)<sub>2</sub> **3.2<sub>closed</sub>** into (TMP)Li(μ-TMP)Al(*i*Bu)<sub>2</sub> **3.2<sub>open</sub>** as predicted by DFT calculations.



Scheme 3.13. Fragmentation of  $(\text{THF})(\text{TMP})\text{Li}(\mu\text{-TMP})\text{Al}(i\text{Bu})_2$  into its homometallic components as predicted by DFT calculations.

We have also modelled the reaction of LiTMP with anisole, which experimentally produced less than 10% of either lithiated anisole or its 2-iodo derivative following quenching with iodine. In the calculations where lithiated anisole was modelled somewhat unrealistically as an unsolvated monomer or a mono-THF-solvated monomer where the Li atoms have low coordination numbers the  $\Delta E$  values for the reactions were highly endergonic (Scheme 3.14). However even when the lithiated anisole was modelled more realistically as a tetramer<sup>[66]</sup> or tri-THF-solvated monomer starting from  $(\text{LiTMP})_4$  or  $(\text{THF}\cdot\text{LiTMP})_2$  respectively as the base, the reactions are close to thermoneutral ( $\Delta E$  is  $+1.73 \text{ kcal mol}^{-1}$  or  $-1.18 \text{ kcal mol}^{-1}$  respectively) though the latter one is marginally exergonic. The thermodynamics changed significantly when  $(\text{TMP})\text{Al}^i\text{Bu}_2$  was introduced to the lithiated anisole. Depending on what form of lithiated anisole (tetramer, mono-THF-solvated monomer or tri-THF-solvated monomer) was employed the  $\Delta E$  values ranged from  $-9.39 \text{ kcal mol}^{-1}$  to  $-28.45 \text{ kcal mol}^{-1}$ , so in all three cases the reaction proved exergonic (Scheme 3.14). Thus these calculations support and indeed strengthen our experimental observations that LiTMP can lithiate anisole to only a limited extent, but that intervention of the aluminium trapping reagent makes the C-H to C-metal transformation substantially more favourable.



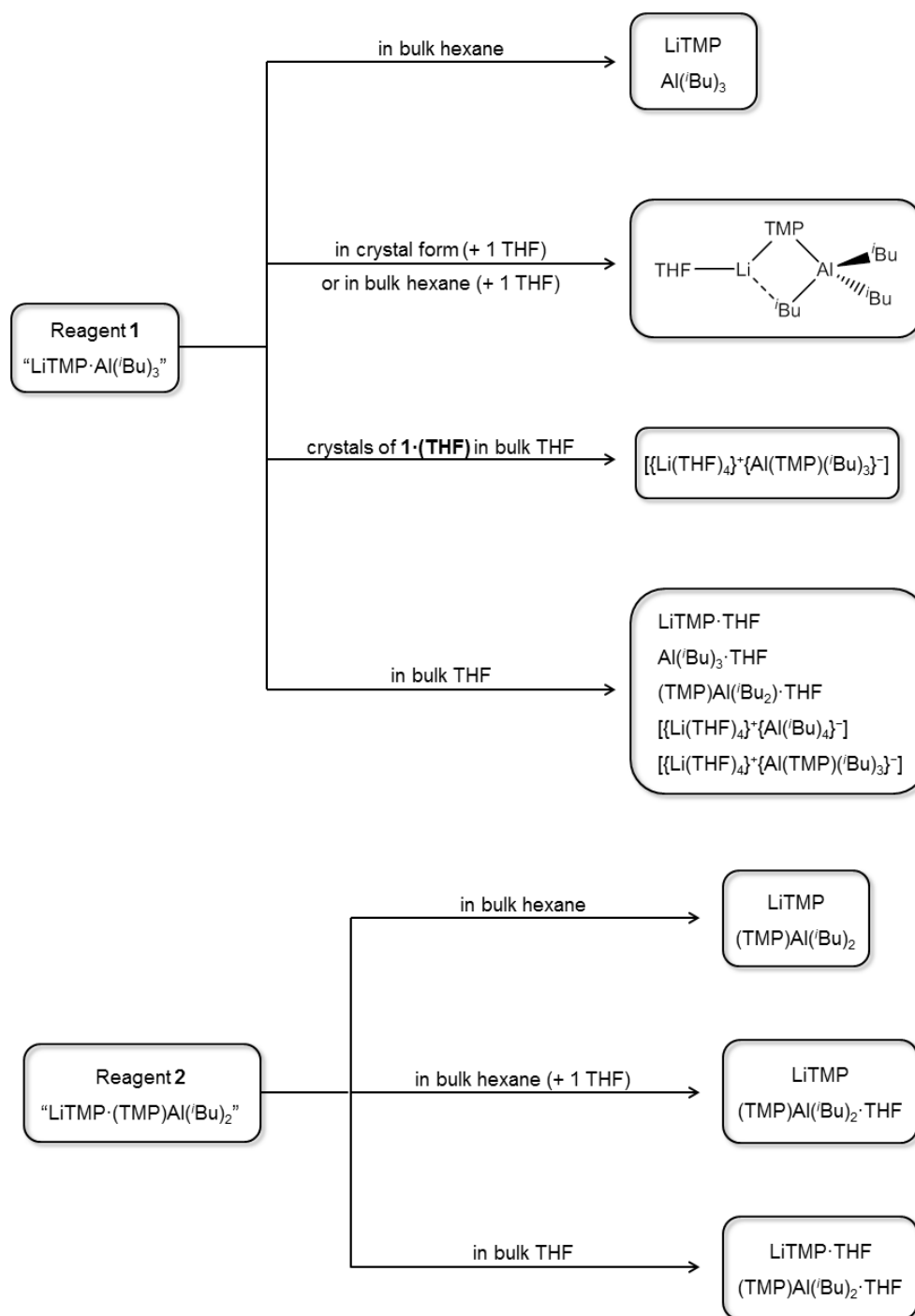
Scheme 3.14. Energies of the modelled metallations and subsequent trapping reactions of anisole.

### 3.4 Conclusions

This study examined in detail the constitutions of the two most popular alkali metal aluminating (that is, synthesising C-Al bonds from C-H bonds) reagents in “LiTMP·Al(*i*Bu)<sub>3</sub>” **3.1** and “LiTMP·Al(TMP)(*i*Bu)<sub>2</sub>” **3.2**. In stark contrast to

previous investigations that viewed **3.1** as a single species in THF solution, this study uncovered five distinct species, which appear to exist simultaneously in two connected equilibria in THF solution. For clarity, Scheme 3.15 gives a pictorial summary of the multiple species that exist in both hexane and THF solution as well as those of **3.2** in the same media. A striking observation is that the single species previously identified in crystal form  $[\text{THF}\cdot\text{Li}(\mu\text{-TMP})(\mu\text{-iBu})\text{Al}(i\text{Bu})_2]$ , **3.1**·THF, is inactive as a base in either hexane or THF solution using anisole as a test Brønsted acid. We confirmed that these crystals do indeed form a single species when dissolved in THF solution in the solvent-separated modification  $[\{\text{Li}(\text{THF})_4\}^+\{\text{Al}(\text{TMP})(i\text{Bu})_3\}^-]$  **3.1**·(THF)<sub>4</sub>. Remarkably, however, on making up **3.1** *in situ* by adding LiTMP and Al(*i*Bu)<sub>3</sub> to THF solution, four other species in addition to  $[\{\text{Li}(\text{THF})_4\}^+\{\text{Al}(\text{TMP})(i\text{Bu})_3\}^-]$  **3.1**·(THF)<sub>4</sub> are produced as identified from NMR data. Preparing authentic samples of all these species and testing them all individually with anisole, we found that only the lithium amide LiTMP was capable of metallating anisole. Though the yield of lithiated anisole was low, its expeditious trapping by an alkylaluminium species (we term this trans-metal-trapping), drives the reaction forward to a high yield of “aluminated” anisole. Reagent **3.2** is simpler remaining as its separate components LiTMP and (TMP)Al(*i*Bu)<sub>2</sub> in hexane or as THF solvates thereof when stoichiometric THF is added or in bulk THF solution. This lack of complexity reflects the extra bulk of (TMP)Al(*i*Bu)<sub>2</sub> compared to Al(*i*Bu)<sub>3</sub> which prevents its association with LiTMP so ruling out any equilibria akin to **3.1**. These findings caution against assuming that a crystalline bimetallic species grown from solution is the active reagent in AMMAI reactions; though it was only through the isolation of such a metallo intermediate that its inactivity as a base could be unequivocally exposed. An important and unexpected general message arising from this work is that unless these aluminate species are in contacted ion-pair form where the alkali metal can act as a Lewis acidic coordination point for an incoming substrate to closely approach the anionic aluminium moiety, AMMAI will not generally occur; otherwise any observed metallation may in fact be the action of the separated lithium reagent followed

by rapid trapping and stabilisation of the newly formed lithium carbanion via an alkylaluminium reagent.



Scheme 3.15. Summary of the compositions of "aluminate" reagents **3.1** and **3.2**. Note depending on the age of solutions, THF degradation products will also be present.



### 3.5 Future Work

The key result from this chapter of work is that the two most widely utilised bimetallic aluminate systems are not in fact bimetallic Li-Al systems capable of performing direct almination reactions, but instead a mixture of two monometallic reagents – LiTMP and either  $\text{Al}(i\text{Bu})_3$  or  $(\text{TMP})\text{Al}(i\text{Bu})_2$  where LiTMP performs metallation and the Al agent then traps this intermediate. Leading on from this, the next body of work to be carried out has to be to investigate if there are any other combinations of lithium and aluminium (or indeed any other metals) that could similarly perform metallation and subsequent trans-metal-trapping reactions, perhaps more efficiently than the two mixtures described in this chapter. A major point to bear in mind though is that the two reagents must not react with one another to form a bimetallic structure as, detailed in this chapter, this would likely be unreactive towards any substrates. Also, can we enhance the basicity of LiTMP beyond that of  $n\text{BuLi}$  and simultaneously prevent any nucleophilic addition side reactions?  $(\text{TMP})\text{Al}(i\text{Bu})_2$  offers many advantages over salt metathesis traps (e.g.,  $\text{AlCl}_3$  or  $\text{ZnCl}_2$ ) including increased solubility, fast reaction times, reduced ate formation (Cl often giving rise to impure mixtures), and most crucially shifting equilibria to products. Similar advantages might apply to *Organometallic Electrophilic Interception* generally. Surrounding Al with ligands of different steric bulk and electronic character should deliver complexes of divergent trapping ability. Moving on from Al, trans-metal-trapping should also be extendable to Mg and Zn. Mononuclear Mg  $\beta$ -diketiminato complexes seem ideal candidates for organoMg traps. Less bulky anionic ligands may work also where Mg is fitted with a neutral flexi-polydentate donor that can adjust its coordination on carbanion interception (e.g.  $\text{Me}_6\text{-TREN}$  can use 1, 2, 3 or 4 donor atoms in metal coordination). Using Zn is advantageous as it opens the way to further functionalization strategies such as the well-documented Negishi couplings.

## 3.6 Experimental

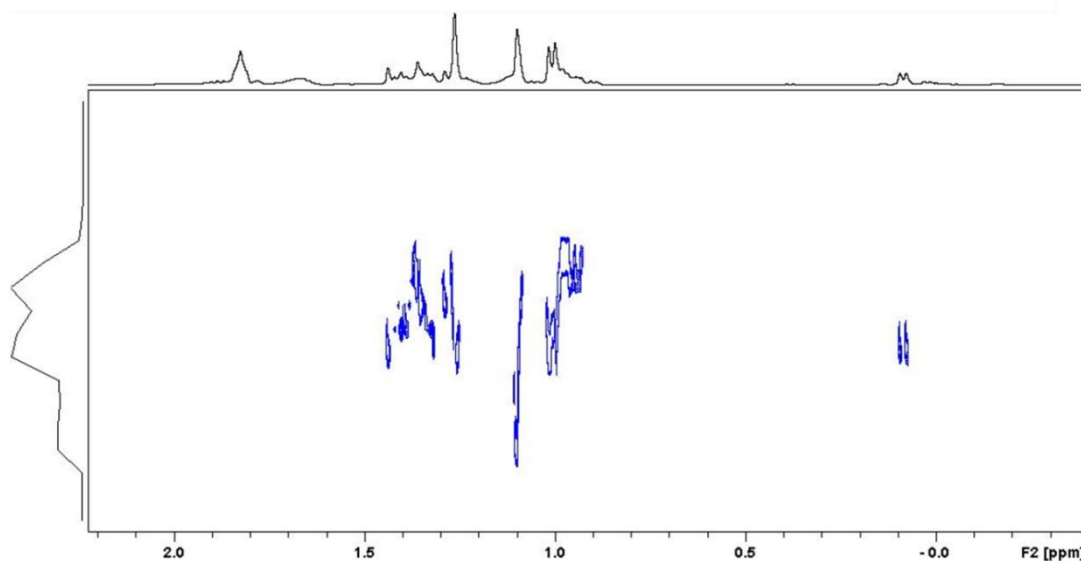


Figure 3.31.  $^1\text{H}$ -DOSY NMR spectrum of  $[\text{LiTMP and Al(TMP)(}i\text{Bu)}_2]$  **3.2** in bulk THF.

### 3.6.1 Synthesis of $(\text{TMP})\text{Al}(i\text{Bu})_2$

Hexane (50 mL) was added to an oven-dried Schlenk tube.  $n\text{BuLi}$  (1.6 M in hexanes, 12.5 mL, 20 mmol) was then added at room temperature, followed by TMP(H) (3.4 mL, 20 mmol). The reaction mixture was left to stir for 10 minutes before  $i\text{Bu}_2\text{AlCl}$  (3.8 mL, 20 mmol) was injected into the Schlenk tube, producing a white suspension almost immediately. The reaction was left to stir at room temperature for 1 hour and then filtered through Celite and glass wool to remove the solid LiCl [which was washed through with more hexane (20 mL)]. The hexane was then removed from the filtrate *in vacuo* leaving behind a pale yellow oil (5.04 g, 90%) which was stored in the glove box.

**$^1\text{H}$  NMR ( $\text{C}_6\text{D}_{12}$ , 400.13 MHz, 300 K):**  $\delta$  1.95 (sept, 2H,  $^3J(\text{H,H}) = 6.68$  Hz,  $\text{CH}_2\text{CH}(\text{CH}_3)_2$ ), 1.69 (m, 2H,  $\gamma$ -TMP), 1.27 (m, 4H,  $\beta$ -TMP), 1.25 (s, 12H,  $\text{CH}_3$  TMP), 0.97 (d, 12H,  $^3J(\text{H,H}) = 6.53$  Hz,  $\text{CH}_2\text{CH}(\text{CH}_3)_2$ ), 0.26 ppm (d, 4H,  $^3J(\text{H,H}) = 7.19$  Hz,  $\text{CH}_2\text{CH}(\text{CH}_3)_2$ ).

**$^{13}\text{C}$  { $^1\text{H}$ } NMR ( $\text{C}_6\text{D}_{12}$ , 100.62 MHz, 300 K):**  $\delta$  51.7 (TMP quaternary), 40.0 ( $\beta$ -TMP), 33.3 ( $\text{CH}_3$  TMP), 29.4 ( $\text{CH}_2\text{CH}(\text{CH}_3)_2$ ), 28.5 ( $\text{CH}_2\text{CH}(\text{CH}_3)_2$ ), 26.7 ( $\text{CH}_2\text{CH}(\text{CH}_3)_2$ ), 19.8 ppm ( $\gamma$ -TMP).

### 3.6.2 Synthesis of *in situ* “THF·Li(TMP)Al(*i*Bu)<sub>3</sub>” **3.1** in THF solution

LiTMP was prepared in hexane (10 mL) from a mixture of *n*BuLi (1.6 M in hexanes, 1.25 mL, 2 mmol) and TMP(H) (0.34 mL, 2 mmol) at room temperature. The reaction mixture was then left to stir for 30 minutes before the Schlenk flask was placed in the freezer at  $-30^\circ\text{C}$ . This produced a white solid which was isolated by filtration and stored inside the glove box. This solid LiTMP (0.29 g, 2 mmol) was then added to an oven-dried Schlenk tube and THF (10 mL) added at  $0^\circ\text{C}$ . Finally, Al(*i*Bu)<sub>3</sub> (2 mL, 1 M in hexanes, 2 mmol) was added to give the base mixture **3.1**.

### 3.6.3 Synthesis of crystalline [THF·Li(TMP)Al(*i*Bu)<sub>3</sub>] **3.1**

Hexane (50 mL) was added to an oven-dried Schlenk tube followed by *n*BuLi (1.6 M in hexanes, 12.5 mL, 20 mmol) and TMP(H) (3.4 mL, 20 mmol) at room temperature. The reaction mixture was left to stir for 10 minutes before adding Al(*i*Bu)<sub>3</sub> (20 mL, 1 M in hexanes, 20 mmol) and one molar equivalent of THF (1.6 mL, 20 mmol). The Schlenk tube was then placed in the freezer at  $-30^\circ\text{C}$  to give a crop of colourless crystals in solution. These were then isolated by filtration and stored in the glove box (1.09 g, % yield unavailable due to crystals being a mixture of **3.1** and **3.3**).

**$^1\text{H}$  NMR ( $d_8$ -THF, 400.13 MHz, 300 K):**  $\delta$  3.61 (m, 4H, OCH<sub>2</sub> THF), 1.90 (m, 3H,  $\text{CH}_2\text{CH}(\text{CH}_3)_2$ ), 1.78 (m, 4H, CH<sub>2</sub> THF), 1.51 (m, 2H,  $\gamma$ -TMP), 1.20 (m, 4H,  $\beta$ -TMP), 1.20 (s, 12H, CH<sub>3</sub> TMP), 0.88 (d, 18H,  $\text{CH}_2\text{CH}(\text{CH}_3)_2$ ), -0.21 ppm (d, 6H,  $\text{CH}_2\text{CH}(\text{CH}_3)_2$ ).

### 3.6.4 Synthesis of “THF·Li(TMP)<sub>2</sub>Al(*i*Bu)<sub>2</sub>” **3.2** in hexane solution

(TMP)Al(*i*Bu)<sub>2</sub> (0.56 g, 2 mmol) was added to an oven-dried Schlenk tube and dissolved in 20 mL of hexane. This solution was then transferred via cannula to a separate Schlenk tube containing a freshly prepared solution of LiTMP in hexane (10 mL) [prepared from a mixture of *n*BuLi (1.6 M in hexanes, 1.25 mL, 2 mmol) and TMP(H) (0.34 mL, 2 mmol)]. Finally, THF was added and the reaction mixture was left to stir for 5 minutes. **3.2** was then used as an *in situ* mixture.

**<sup>1</sup>H NMR (C<sub>6</sub>D<sub>12</sub>, 400.13 MHz, 300 K):** δ 4.04 (m, 4H, OCH<sub>2</sub> THF), 1.95 (m, 4H, CH<sub>2</sub> THF), 1.90 (sept, 2H, <sup>3</sup>J(H,H) = 6.60 Hz, CH<sub>2</sub>CH(CH<sub>3</sub>)<sub>2</sub>), 1.65 (m, 2H, γ-TMP), 1.38 (m, 4H, β-TMP), 1.26 (s, 12H, CH<sub>3</sub> TMP), 1.10 (d, 12H, <sup>3</sup>J(H,H) = 6.49 Hz, CH<sub>2</sub>CH(CH<sub>3</sub>)<sub>2</sub>), 0.12 ppm (d, 4H, <sup>3</sup>J(H,H) = 6.81 Hz, CH<sub>2</sub>CH(CH<sub>3</sub>)<sub>2</sub>).

### 3.6.5 Synthesis of “THF·Li(TMP)<sub>2</sub>Al(*i*Bu)<sub>2</sub>” **3.2** in THF solution

LiTMP was prepared in hexane (10 mL) from a mixture of *n*BuLi (1.6 M in hexanes, 1.25 mL, 2 mmol) and TMP(H) (0.34 mL, 2 mmol) at room temperature. The reaction mixture was then left to stir for 30 minutes before the Schlenk flask was placed in the freezer at -30°C. This produced a white solid which was isolated by filtration and stored inside the glove box. This solid LiTMP (0.29 g, 2 mmol) was then added to an oven-dried Schlenk tube and THF (10 mL) added at 0°C. Finally, Al(TMP)(*i*Bu)<sub>2</sub> (0.56 g, 2 mmol) was added to give the base mixture **3.2**.

### 3.6.6 Synthesis of [Li(THF)<sub>4</sub>]<sup>+</sup>[Al(*i*Bu)<sub>4</sub>]<sup>-</sup> **3.3**

*n*BuLi (3.13 mL, 1.6 M in hexanes, 5 mmol) was added to a mixture of THF (4 mL) and TMPH (0.85 mL, 5 mmol) at -78°C and the mixture was stirred for 10 min at 0°C. Al(*i*Bu)<sub>3</sub> (5 mL, 1 M in hexanes, 5 mmol) was then added at -78°C and the mixture stirred for 30 min at 0°C to give a pale yellow solution and a white solid. The reaction mixture was then heated to refluxing temperature to obtain a

clear solution and subsequent bench cooling of this solution afforded colourless crystals of **3.3** (0.55 g, 20%).

**$^1\text{H}$  NMR ( $\text{C}_6\text{D}_6$ , 400.13 MHz, 300 K):**  $\delta$  3.46 (m, 16H,  $\text{OCH}_2$  THF), 2.37 (sept, 4H,  $\text{CH}_2\text{CH}(\text{CH}_3)_2$ ), 1.38 (d, 24H,  $\text{CH}_2\text{CH}(\text{CH}_3)_2$ ), 1.32 (m, 16H,  $\text{CH}_2$  THF), 0.07 ppm (d, 8H,  $\text{CH}_2\text{CH}(\text{CH}_3)_2$ ).

**$^{13}\text{C}$   $\{^1\text{H}\}$  NMR ( $\text{C}_6\text{D}_6$ , 100.62 MHz, 300 K):**  $\delta$  67.75 ( $\text{OCH}_2$  THF), 29.55 ( $\text{CH}_2\text{CH}(\text{CH}_3)_2$ ), 28.03 ( $\text{CH}_2\text{CH}(\text{CH}_3)_2$ ), 25.48 ppm ( $\text{CH}_2$  THF) [note that the resonance for  $\{\text{CH}_2\text{CH}(\text{CH}_3)_2\}$  could not be observed in either  $\text{C}_6\text{D}_6$  or  $[\text{D}_8]\text{THF}$  solution however its existence was confirmed by a  $^1\text{H}$ - $^{13}\text{C}$  HSQC experiment];  **$^7\text{Li}$  NMR ( $\text{C}_6\text{D}_6$ , 155.50 MHz, 300 K):**  $\delta$  -1.19 ppm.

### 3.7 Bibliography

- [1] J. Clayden, *Organolithiums: Selectivity for Synthesis*, Pergamon, Elsevier Science Ltd, Oxford, **2002**.
- [2] M. Schlosser, *Organometallics in Synthesis*, 3rd ed., John Wiley & Sons, New Jersey, **2013**.
- [3] M. Lappert, A. Protchenko, P. Power, A. Seeber, *Metal Amide Chemistry*, John Wiley & Sons, Chichester, **2009**.
- [4] R. E. Mulvey, S. D. Robertson, *Angew. Chem. Int. Ed.* **2013**, *52*, 11470-11487.
- [5] A. Krasovskiy, V. Krasovskaya, P. Knochel, *Angew. Chem. Int. Ed.* **2006**, *45*, 2958-2958.
- [6] A. Krasovskiy, P. Knochel, *Angew. Chem. Int. Ed.* **2004**, *43*, 3333-3336.
- [7] P. Garcia-Alvarez, D. V. Graham, E. Hevia, A. R. Kennedy, J. Klett, R. E. Mulvey, C. T. O'Hara, S. Weatherstone, *Angew. Chem. Int. Ed.* **2008**, *47*, 8079-8081.
- [8] D. Seebach, *Angew. Chem. Int. Ed.* **1988**, *27*, 1624-1654.
- [9] B. Tchoubar, A. Loupy, in *Salt Effects in Organic and Organometallic Chemistry*, VCH, New York, **1992**, pp. 1 - 322.
- [10] P. Caubère, *Chem. Rev.* **1993**, *93*, 2317-2334.
- [11] B. Haag, M. Mosrin, H. Ila, V. Malakhov, P. Knochel, *Angew. Chem. Int. Ed.* **2011**, *50*, 9794-9824.
- [12] R. E. Mulvey, *Organometallics* **2006**, *25*, 1060-1075.
- [13] R. E. Mulvey, F. Mongin, M. Uchiyama, Y. Kondo, *Angew. Chem., Int. Ed.* **2007**, *46*, 3802-3824.
- [14] R. E. Mulvey, *Acc. Chem. Res.* **2009**, *42*, 743-743.
- [15] F. Mongin, A. Harrison-Marchand, *Chem. Rev.* **2013**, *113*, 7563-7727.
- [16] A. Harrison-Marchand, F. Mongin, *Chem. Rev.* **2013**, *113*, 7470-7562.
- [17] Y. Kondo, M. Shilai, M. Uchiyama, T. Sakamoto, *J. Am. Chem. Soc.* **1999**, *121*, 3539-3540.
- [18] W. Clegg, S. H. Dale, E. Hevia, G. W. Honeyman, R. E. Mulvey, *Angew. Chem. Int. Ed.* **2006**, *45*, 2370-2374.
- [19] M. Uchiyama, Y. Matsumoto, D. Nobuto, T. Furuyama, K. Yamaguchi, K. Morokuma, *J. Am. Chem. Soc.* **2006**, *128*, 8748-8750.
- [20] E. Hevia, D. J. Gallagher, A. R. Kennedy, R. E. Mulvey, C. T. O'Hara, C. Talmard, *Chem. Commun.* **2004**, 2422-2423.
- [21] C. T. O'Hara, *Organomet. Chem.* **2011**, *37*, 1-26.
- [22] R. E. Mulvey, S. D. Robertson, *Top. Organometal. Chem.* **2013**, *45*, 103-140.
- [23] D. R. Armstrong, A. R. Kennedy, R. E. Mulvey, J. A. Parkinson, S. D. Robertson, *Chem. Sci.* **2012**, *3*, 2700-2707.
- [24] S. H. Wunderlich, P. Knochel, *Angew. Chem. Int. Ed.* **2009**, *48*, 1501-1504.
- [25] B. Conway, E. Crosbie, A. R. Kennedy, R. E. Mulvey, S. D. Robertson, *Chem. Commun.* **2012**, *48*, 4674-4676.
- [26] G. Linti, H. Nöth, P. Rahm, *Z. Naturforsch.* **1988**, *43*, 1101-1112.

- [27] M. L. Montero, H. Wessel, H. W. Roesky, M. Teichert, I. Usón, *Angew. Chem. Int. Ed.* **1997**, *36*, 629-631.
- [28] D. J. Eisler, T. Chivers, *Can. J. Chem.* **2006**, *84*, 443-452.
- [29] R. J. Less, L. K. Allen, A. Steiner, D. S. Wright, *Dalton Trans.* **2015**, *44*, 4141-4147.
- [30] M. Uchiyama, H. Naka, Y. Matsumoto, T. Ohwada, *J. Am. Chem. Soc.* **2004**, *126*, 10526-10527.
- [31] H. Naka, M. Uchiyama, Y. Matsumoto, A. E. H. Wheatley, M. McPartlin, J. V. Morey, Y. Kondo, *J. Am. Chem. Soc.* **2007**, *129*, 1921-1930.
- [32] R. E. Mulvey, D. R. Armstrong, B. Conway, E. Crosbie, A. R. Kennedy, S. D. Robertson, *Inorg. Chem.* **2011**, *50*, 12241-12251.
- [33] E. Crosbie, P. García-Álvarez, A. R. Kennedy, J. Klett, R. E. Mulvey, S. D. Robertson, *Angew. Chem. Int. Ed.* **2010**, *49*, 9388-9391.
- [34] B. Conway, A. R. Kennedy, R. E. Mulvey, S. D. Robertson, J. Garcia-Alvarez, *Angew. Chem. Int. Ed.* **2010**, *49*, 3182-3184.
- [35] B. Conway, J. Garcia-Alvarez, E. Hevia, A. R. Kennedy, R. E. Mulvey, S. D. Robertson, *Organometallics* **2009**, *28*, 6462-6468.
- [36] R. Campbell, E. Crosbie, A. R. Kennedy, R. E. Mulvey, R. A. Naismith, S. D. Robertson, *Aust. J. Chem.* **2013**, *66*, 1189-1201.
- [37] A. Unsinn, S. H. Wunderlich, A. Jana, K. Karaghiosoff, P. Knochel, *Chem. Eur. J.* **2013**, *19*, 14687-14696.
- [38] H. Naka, J. V. Morey, J. Haywood, D. J. Eisler, M. McPartlin, F. Garcia, H. Kudo, Y. Kondo, M. Uchiyama, A. E. H. Wheatley, *J. Am. Chem. Soc.* **2008**, *130*, 16193-16200.
- [39] A. Macchioni, G. Ciancaleoni, C. Zuccaccia, D. Zuccaccia, *Chem. Soc. Rev.* **2008**, *37*, 479-489.
- [40] D. Li, I. Keresztes, R. Hopson, P. G. Williard, *Acc. Chem. Res.* **2009**, *42*, 270-280.
- [41] J. Mason, *Multinuclear NMR*, Plenum Press, New York and London, **1987**.
- [42] R. Benn, E. Janssen, H. Lehmkuhl, A. Rufinska, *J. Organomet. Chem.* **1987**, *333*, 155-168.
- [43] R. J. Less, H. R. Simmonds, D. S. Wright, *Dalton Trans.* **2014**, *43*, 5785-5792.
- [44] I. Krossing, H. Nöth, C. Tacke, M. Schmidt, H. Schwenk, *Chem. Ber./Recueil* **1997**, *130*, 1047-1052.
- [45] I. Krossing, H. Nöth, H. Schwenk-Kircher, *Eur. J. Inorg. Chem.* **1998**, 927-939.
- [46] B. Conway, E. Hevia, J. Garcia-Alvarez, D. V. Graham, A. R. Kennedy, R. E. Mulvey, *Chem. Commun.* **2007**, 5241-5243.
- [47] M. C. Whisler, S. MacNeil, V. Snieckus, P. Beak, *Angew. Chem. Int. Ed.* **2004**, *43*, 2206-2225.
- [48] V. Snieckus, *Chem. Rev.* **1990**, *90*, 879-933.
- [49] G. Wittig, G. Fuhrmann, *Ber. Dtsch. Chem. Ges.* **1940**, *73*, 1197-1218.
- [50] H. Gilman, R. L. Bebb, *J. Am. Chem. Soc.* **1939**, *61*, 109-112.
- [51] M. F. Lappert, M. J. Slade, A. Singh, J. L. Atwood, R. D. Rogers, R. Shakir, *J. Am. Chem. Soc.* **1983**, *105*, 302-304.

- [52] E. Hevia, A. R. Kennedy, R. E. Mulvey, D. L. Ramsay, S. D. Robertson, *Chem. Eur. J.* **2013**, *19*, 14069-14075.
- [53] D. R. Armstrong, P. Garcia-Alvarez, A. R. Kennedy, R. E. Mulvey, S. D. Robertson, *Chem. Eur. J.* **2011**, *17*, 6725-6730.
- [54] R. E. Mulvey, *Dalton Trans.* **2013**, *42*, 6676-6693.
- [55] R. B. Bates, L. M. Kroposki, D. E. Potter, *J. Org. Chem.* **1972**, *37*, 560-562.
- [56] J. Q. Wen, J. B. Grutzner, *J. Org. Chem.* **1986**, *51*, 4220-4224.
- [57] P. Renaud, M. A. Fox, *J. Am. Chem. Soc.* **1988**, *110*, 5702-5705.
- [58] K. Snegaroff, J.-M. L'Helgoual'ch, G. Bentabed-Ababsa, T. T. Nguyen, F. Chevallier, M. Yonehara, M. Uchiyama, A. Derdour, F. Mongin, *Chem. Eur. J.* **2009**, *15*, 10280-10290.
- [59] W. Clegg, B. Conway, E. Hevia, M. D. McCall, L. Russo, R. E. Mulvey, *J. Am. Chem. Soc.* **2009**, *131*, 2375-2384.
- [60] E. Nagaradja, F. Chevallier, T. Roisnel, V. Dorcet, Y. S. Halauko, O. A. Ivashkevich, V. E. Matulis, F. Mongin, *Org. Biomol. Chem.* **2014**, *12*, 1475-1487.
- [61] F. Chevallier, T. Blin, E. Nagaradja, F. Lassagne, T. Roisnel, Y. S. Halauko, V. E. Matulis, O. A. Ivashkevich, F. Mongin, *Org. Biomol. Chem.* **2012**, *10*, 4878-4885.
- [62] P. Garcia-Alvarez, R. E. Mulvey, J. A. Parkinson, *Angew. Chem. Int. Ed.* **2011**, *50*, 9668-9671.
- [63] A. R. Kennedy, S. M. Leenhouts, J. J. Liggat, A. J. Martinez-Martinez, K. Miller, R. E. Mulvey, C. T. O'Hara, P. O'Keefe, A. Steven, *Chem. Commun.* **2014**, *50*, 10588-10591.
- [64] P. G. Williard, Q.-Y. Liu, *J. Am. Chem. Soc.* **1993**, *115*, 3380-3381.
- [65] D. R. Armstrong, A. R. Kennedy, R. E. Mulvey, S. D. Robertson, *Chem. Eur. J.* **2011**, *17*, 8820-8831.
- [66] S. Harder, J. Boersma, L. Brandsma, G. P. M. van Mier, J. A. Kanters, *J. Organomet. Chem.* **1989**, *364*, 1-15.



## **Chapter 4**

### **Heterobimetallic Metallation Studies of *N,N*- Dimethylphenylethylamine**

## 4.1 Aims

The aim of the work described in this chapter was to investigate the cleave and capture chemistry of the bio-relevant and pharmacologically active scaffold of the tertiary amine *N,N*-dimethylphenylethylamine, DMPEA by subjecting it to a range of different mixed-metal systems.

Specific objectives are outlined below:

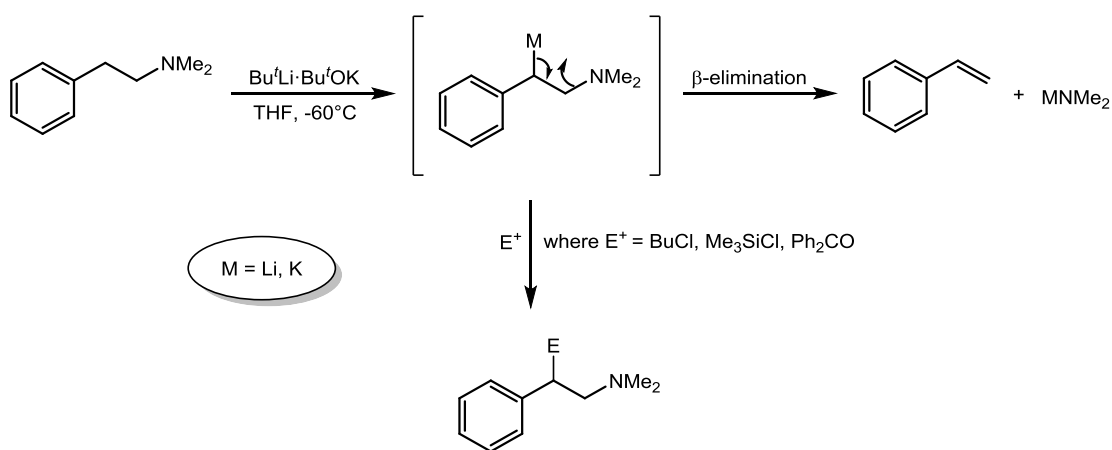
- Determine the outcome of the reaction between the sodium-zincate [TMEDA·Na(TMP)(*t*Bu)Zn(*t*Bu)] and DMPEA and characterise any metal-containing products.
- Compare and contrast the aforementioned reaction with that between the lithium-zincate [PMDETA·Li(TMP)Zn(*t*Bu)<sub>2</sub>] and DMPEA.
- Explore the reactivity of the presumed lithium-aluminium reagent “[THF·Li(TMP)<sub>2</sub>Al(*t*Bu)<sub>2</sub>]” with DMPEA.
- Observe any differences in the outcome of the reaction using the less basic zincate reagent [Li(TMP)Zn(Me)<sub>2</sub>] with DMPEA.
- Try to isolate and crystallographically characterise a metallated derivative of DMPEA with its C-C-NMe<sub>2</sub> unit still intact.

## 4.2 Introduction

As evidenced by the publication in 2014 of a book dedicated to the topic,<sup>[1]</sup> compounds (or reagents) that contain two or more metals that exhibit synergistic behaviour are increasingly attracting the curiosity of chemists. What captivates their imagination in particular are examples where the combination of different metals and/or different ligands can cooperatively realize useful chemistry that is seemingly impossible for the individual metal-ligand species. First utilised exactly 50 years ago, the Lochmann-Schlosser superbases,<sup>[2-5]</sup> empirically formulated as  $n\text{BuLi}\cdot\text{Bu}^t\text{OK}$ , could be regarded as a prototypical example of a mixed-metal, mixed-ligand synergistic metallating agent, as its reactivity generally does not follow that of its individual alkyllithium or potassium alkoxide components (see Chapter 1, Section 1.3.1). Neither does it react as the transmetallated components  $n\text{BuK}$  and  $\text{Bu}^t\text{OLi}$ .

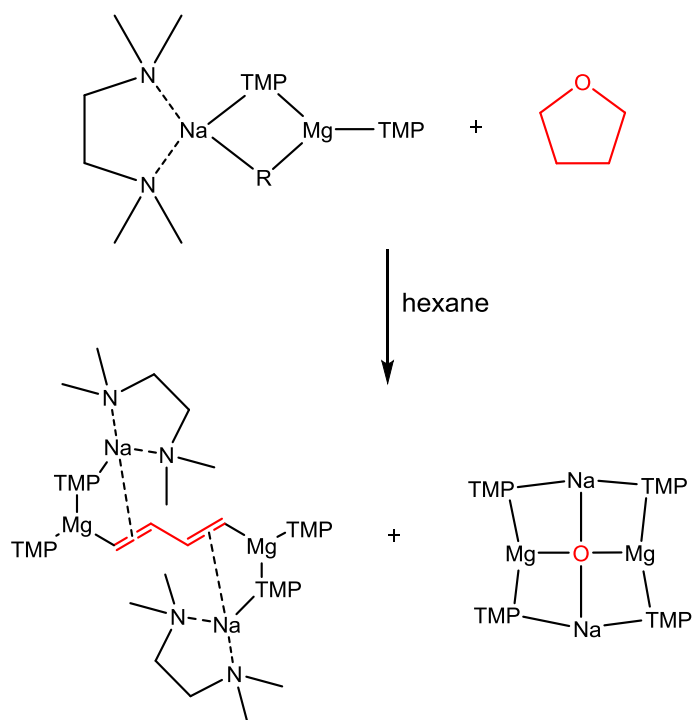
A recent example of a reaction where synergistic effects appear to dominate is that referred to by Strohmann<sup>[6]</sup> as a “sedated metallation”, with reference to the deprotonation of the tertiary amine *N,N*-dimethylphenylethylamine, DMPEA (sometimes known as 2-phenylethyldimethylamine) by the *t*-butyllithium variant of the Lochmann-Schlosser superbases  $t\text{BuLi}\cdot\text{Bu}^t\text{OK}$  (Scheme 4.1). DMPEA is well known to synthetic chemists as it is a member of the phenylethylamine family - a group of compounds that provide key structural units within many biogenic and synthetic pharmacological compounds (for example amphetamines),<sup>[7-11]</sup> as well as ingredients found in indulgence substances such as wine and chocolate.<sup>[12]</sup> Efficient, high-yielding deprotonative C-H metallation of the amine with subsequent electrophilic functionalisation by E-X is therefore an intriguing target. The drawback associated with functionalising DMPEA though, is that this class of compounds is sensitive to undergoing the unwanted side reaction of  $\beta$ -elimination making the direct benzylic metallation highly challenging (Scheme 4.1). To explain, once deprotonation of the benzylic  $\text{CH}_2$  unit attached to the phenyl ring has taken place, the electronegative Lewis basic nitrogen atom is capable of forming a

ductive bond to the metal centre, leading to the elimination of a salt, the metal dimethylamide  $[M(NMe_2)_n]$  from the C-metallated intermediate to afford the unsaturated molecule styrene. Interestingly, Strohmam reported that whereas on its own  $tBuLi$  failed to sedatively deprotonate DMPEA over a large temperature window instead producing the  $\beta$ -elimination side product styrene, the synergistic system of  $tBuLi \cdot Bu^tOK$  (at low temperatures) successfully yielded greater than 95% of the metallated intermediate. Electrophiles could then successfully intercept the metal-containing species to form the organic final products in high yields ranging from 74-92%. Theoretical studies probing the energetics and mechanism of this low-temperature metallation reaction suggested that both lithium and potassium participate in the transition structure of the heterometallated intermediate of DMPEA with the decisive factor in its stabilization [i.e., having a higher energy barrier to  $\beta$ -elimination than in the homometallated (via  $tBuLi$ ) analogue] being the greater capacity of the large potassium cation for engaging in multihapto interactions with the negative charge delocalized over the aromatic system.



Scheme 4.1. Metallation of DMPEA and subsequent possible outcomes of the reaction: unwanted  $\beta$ -elimination generating  $MNMe_2$  ( $M = Li$  or  $K$ ) or wanted electrophilic interception generating a metal-free organic product.

A recent perspective article<sup>[13]</sup> by Mulvey elaborated upon the idea of “cleave and capture chemistry” with respect to alkali-metal-mediated metallation (AMMM) reactions. He argued that these reactions have a secondary feature rather than just the primary feature of the exchange of a relatively inert non-polar C–H bond for a more reactive, more polar C–M(metal) bond by a synergistic bimetallic base combining an alkali metal with a less electropositive metal (magnesium and zinc are most common). The secondary feature is that once deprotonation has been accomplished (the cleave task), the residue of the base, in comprising a mixture of Lewis acidic and Lewis basic coordinating sites, can capture the deprotonated entity intact or at least some fragment of it. Spectacular examples of this “cleave and capture” reactivity have been displayed with the oxygen heterocycle THF. Upon the synergistic cleavage of it by AMMZn through a mixed sodium-zinc system,<sup>[14]</sup> the sensitive  $\alpha$ -OC<sub>4</sub>H<sub>7</sub> anion of THF has been captured and thereby stabilized as an intact ring, where usually it would spontaneously ring open to generate the enolate of acetaldehyde and ethene.<sup>[15]</sup> In a juxtaposition of this ring-intact stabilisation, performing AMMMg on THF does cause cleavage of THF through a synergistic sodium-magnesium system but in a remarkably different way, leading to ring opening and the formation of a trans-buta-1,3-diene dianion and an O<sup>2-</sup> dianion (Scheme 4.2).<sup>[16]</sup> Considering THF only has thirteen bonds and this reaction cleaves six of them, the authors called this a catastrophic cleavage. Remarkably, both anions are captured by mixed-metal base residues in separate crystalline complexes, that were crystallographically characterised.



Scheme 4.2. So called catastrophic cleavage of THF by AMMMg, where each THF fragment is captured within heterobimetallic residues (R = CH<sub>2</sub>SiMe<sub>3</sub>).

### 4.3 Results and Discussion

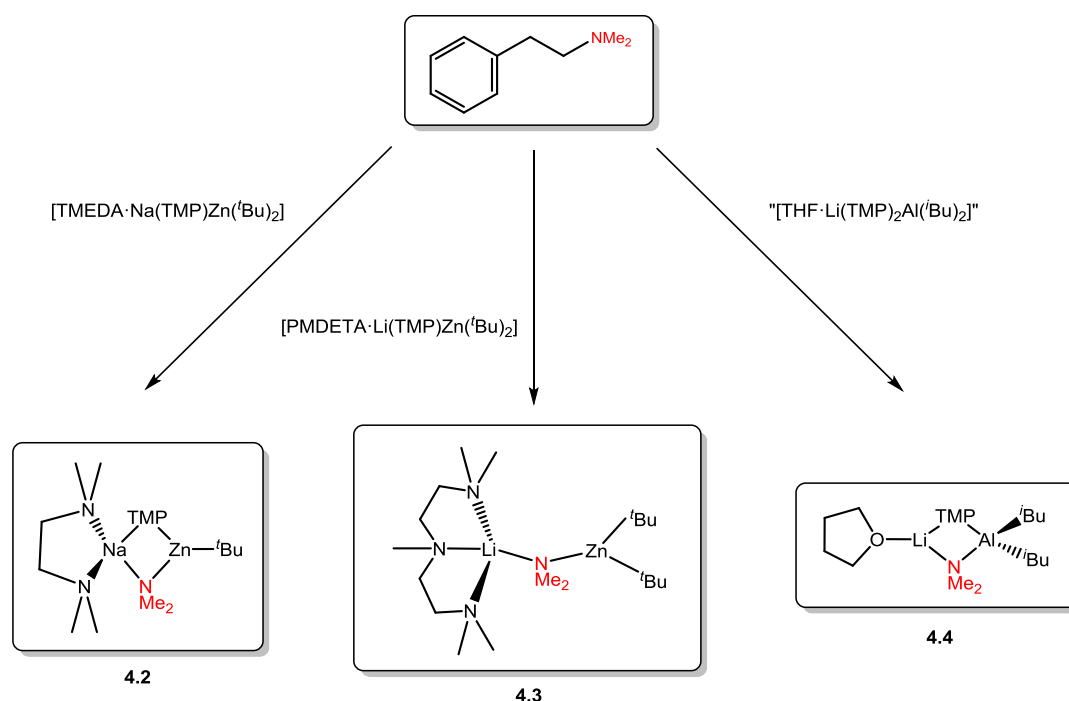
Attempting to build on the idea of cleave and capture chemistry, we subjected DMPEA to a range of different metallation possibilities. While our hope that the capturing/stabilizing capacity of mixed-metal ate systems might provide unprecedented access to a derivative of DMPEA metallated in the  $\beta$ -position that could be isolated from solution and crystallographically authenticated was not realized, the study proved informative and useful in obtaining a number of interesting findings. These include most significantly the synthesis, isolation and spectroscopic/crystallographic characterization of an organometallic compound containing intact DMPEA as a ligand. Three different AMMM reactions involving lithium-zinc, sodium-zinc or lithium-aluminium combinations, each of which captures a dimethylamino (Me<sub>2</sub>N) DMPEA fragment have been studied. Adding interest to these studies, although the molecular structures of these three

crystalline products of an  $\alpha$ - $\beta$ , Me<sub>2</sub>N-metal elimination closely resemble each other, the reactions that produced them seem to follow distinct mechanistic pathways. Most intriguingly, as the zinc systems follow a zincate mechanism, one can be misled into thinking that the related aluminium system follows an aluminate mechanism, when in fact a sequential lithiation/*in situ* alkylaluminium trapping process is in operation. The discovery of this type of lithium-aluminium *trans-metal-trapping* process has been covered in detail in Chapter 3.

#### 4.3.1 AMMM Reactions with DMPEA and Characterisation of “Captured Products”

As a consequence of the successful capturing and stabilising of the  $\alpha$ -OC<sub>4</sub>H<sub>7</sub> ring anion of THF by both the zincate and aluminate (see below) systems, we initiated this investigation by the reaction of DMPEA with (i) the sodium monoamido-bisalkylzincate [TMEDA·Na( $\mu$ -TMP)( $\mu$ -*t*Bu)Zn(*t*Bu)] **1.3** (see Chapter 1, Section 1.3.2) and (ii) the related lithium monoamido-bisalkylzincate [PMDETA·Li(TMP)Zn(*t*Bu)<sub>2</sub>] **4.1** (Scheme 4.3). Structurally defined reagent **1.3**<sup>[17]</sup> is a proven effective zincating (C-H to C-Zn transforming) agent<sup>[18-33]</sup> [most recently metallating N-heterocyclic carbenes (NHCs)<sup>[34]</sup>] though it has also been infrequently employed as a nucleophilic *t*-butyl source.<sup>[35-36]</sup> On the other hand, reagent **4.1** is a putative compound in that it has only been generated *in situ* by mixing LiTMP, *t*Bu<sub>2</sub>Zn, and PMDETA in a 1:1:1 stoichiometric ratio in hexane solution, though it bears a close resemblance to the much studied THF-solvate [THF·Li(TMP)Zn(*t*Bu)<sub>2</sub>]<sup>[37-41]</sup> pioneered by Kondo and Uchiyama. We focused our attention on trying to obtain crystalline material suitable for X-ray crystallographic determination rather than refining reactions to optimise yields. While crystallization proved challenging and required prolonged storage of the reaction solutions over several days, eventually both **1.3** and **4.1** afforded crystalline products from their reactions with DMPEA in [TMEDA·Na( $\mu$ -TMP)( $\mu$ -NMe<sub>2</sub>)Zn(*t*Bu)] **4.2** and [PMDETA·Li( $\mu$ -NMe<sub>2</sub>)Zn(*t*Bu)<sub>2</sub>]

**4.3**, respectively (refer to Table 4.2 in the experimental section for all crystallographic data). In the case of **4.3** orange crystals were grown from an orange oily mixture, though NMR spectra established the mixture contained mostly **4.3**; whereas **4.2** exists as a colourless crystalline solid. The formulae of **4.2** and **4.3** reveal that  $\alpha$ - $\beta$ ,  $\text{Me}_2\text{N}$ -metal eliminations have taken place in both reactions with the  $\text{Me}_2\text{N}$  fragment captured in their molecular structures. Reactions of this type can also be termed 1,2-eliminations and tend to be highly dependent on the stereochemistry of the components of the developing metal product as elaborated by Schlosser<sup>[42-43]</sup>.



Scheme 4.3. Reactions and isolated crystalline products of subjecting DMPEA to different bimetallic systems in hexane solutions.

Switching from zinc to aluminium, the reaction of the putative bisamido-bisalkylaluminumate “[THF·Li(TMP)<sub>2</sub>Al(*t*Bu)<sub>2</sub>]” (see later, Section 4.3.2) with DMPEA in hexane solution follows a similar pattern to the zincate reactions



producing a crystalline product with a captured Me<sub>2</sub>N fragment in [THF·Li(μ-TMP)(μ-NMe<sub>2</sub>)Al(*i*Bu)<sub>2</sub>] **4.4** (Scheme 4.3). While the yield of crystalline **4.4** was a disappointing 16%, a <sup>1</sup>H NMR spectrum of the filtrate indicated that the absolute yield was significantly higher as more of the aluminate compound remained within the solution. As all three of the reactions so far discussed in this chapter were carried out at room temperature we can assume that the β-metallated intermediates were unstable and that the energy barriers to the α-β, Me<sub>2</sub>N-metal eliminations are small and easily overcome at this temperature. On resorting to lower temperature in order to slow down the elimination, we found it was not possible to grow crystals of any product despite several attempts.

X-ray crystallographic determinations of **4.2** and **4.3** established them both to be discrete, contacted ion-pair structures (Figure 4.1 and Figure 4.2 respectively, with legends showing key dimensions). The central feature of the sodium zincate **4.2** is a four-atom (NaNZnN) ring. The three-coordinate zinc centre adopts a distorted (N<sub>2</sub>C) trigonal planar configuration comprising two different N (TMP and NMe<sub>2</sub>) bridges with a *t*Bu terminus. The larger sodium centre is four-coordinate and occupies a distorted (4xN coordinated) tetrahedral site (with a τ<sub>4</sub> value of 0.65)<sup>[44]</sup> comprising of amide bridges and one chelating (2xN coordinated) terminal TMEDA ligand. A search of the Cambridge Structural Database (CSD)<sup>[45-46]</sup> (performed in December 2014, as were all the other searches mentioned in this chapter) returned only 4 results for crystal structures containing a (NaNZnN) ring motif, namely [(TMEDA)Na(N<sup>*i*</sup>Pr<sub>2</sub>)<sub>2</sub>Zn(*t*Bu)],<sup>[47]</sup> [(TMEDA)Na(N<sup>*i*</sup>Bu<sub>2</sub>)<sub>2</sub>Zn(*t*Bu)],<sup>[48]</sup> [(THF)<sub>3</sub>Na{(*i*Pr)NCH=CHN(*i*Pr)}Zn(*t*Bu)]<sup>[49]</sup> and [(Ph<sub>2</sub>C=NH)<sub>2</sub>(Ph<sub>2</sub>C=N)<sub>4</sub>(*n*Bu)<sub>2</sub>Na<sub>2</sub>Zn<sub>2</sub>].<sup>[50]</sup> However, in all four structures the two N atoms belong to identical groups or in the case of the diazaethene the same group, indicating that **4.2** is a novel heteroamidozincate example. Underlining the uniqueness of **4.2**, no results were found by a second CSD search for a Na-NMe<sub>2</sub>-Zn fragment.

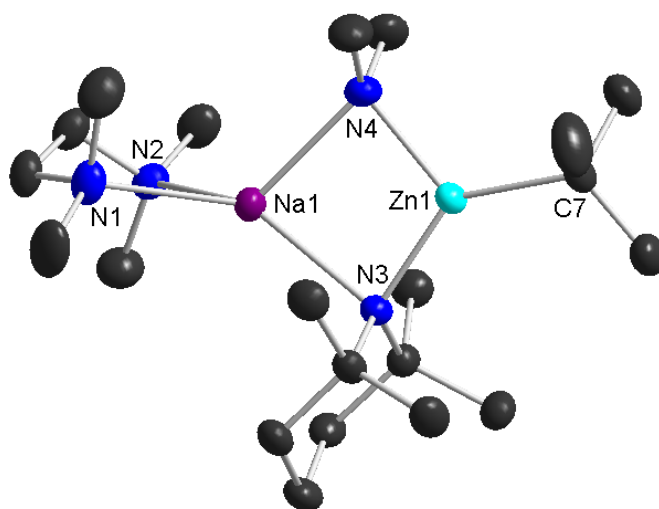


Figure 4.1. Molecular structure of [TMEDA·Na( $\mu$ -TMP)( $\mu$ -NMe<sub>2</sub>)Zn(<sup>t</sup>Bu)] **4.2**. Ellipsoids are displayed at 50% probability and hydrogen atoms have been omitted for clarity. Selected bond lengths (Å) and bond angles (°): Na(1)-N(1), 2.5000(14); Na(1)-N(2), 2.5314(14); Na(1)-N(3), 2.4480(13); Na(1)-N(4), 2.3964(14); Zn(1)-N(3), 1.9889(11); Zn(1)-N(4), 2.0322(13); Zn(1)-C(7), 2.0276(15); N(1)-Na(1)-N(2), 73.53(5); N(4)-Na(1)-N(3), 81.82(4); N(4)-Na(1)-N(1), 117.86(5); N(4)-Na(1)-N(2), 120.76(5); N(3)-Na(1)-N(1), 134.64(5); N(3)-Na(1)-N(2), 133.80(5); N(3)-Zn(1)-C(7), 135.41(6); N(3)-Zn(1)-N(4), 104.18(5); C(7)-Zn(1)-N(4), 120.32(6); Zn(1)-N(3)-Na(1), 86.77(4); Zn(1)-N(4)-Na(1), 87.22(5).

Contrasting with the closed cyclic structure of **4.2**, the contact ion-pair arrangement of **4.3** is more open with a Li-N-Zn(-C)-C chain arrangement, that branches at the Zn centre. Thus the connection between the two distinct metal atoms is exclusively through the NMe<sub>2</sub> unit captured from the break-up of DMPEA. This distinction with **4.2** is a consequence of the smaller radius of lithium versus sodium and to the larger steric capacity and denticity (tridentate compared to didentate) provided by PMDETA versus TMEDA, which prevent a second ligand gaining access into the limited space available between the two

metal centres. The four-coordinate lithium occupies a distorted (4xN) tetrahedral geometry (with a  $\tau_4$  value of 0.86)<sup>[44]</sup> comprising the bridging N(Me)<sub>2</sub> atom and the three N atoms of PMDETA. Zinc occupies a distorted (2xC; 1xN) trigonal planar site, completed by two terminal <sup>t</sup>Bu ligands.

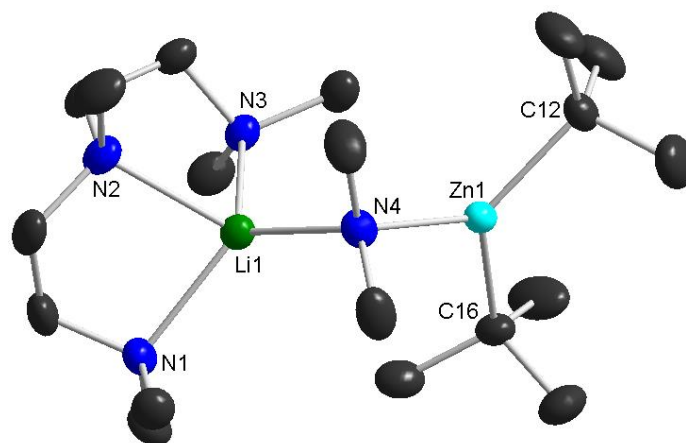


Figure 4.2. Molecular structure of [PMDETA·Li(μ-NMe<sub>2</sub>)Zn(<sup>t</sup>Bu)<sub>2</sub>] **4.3**. Ellipsoids are displayed at 50% probability and hydrogen atoms and minor disordered component of a <sup>t</sup>Bu arm have been omitted for clarity. Selected bond lengths (Å) and bond angles (°): Li(1)-N(1), 2.202(4); Li(1)-N(2), 2.223(4); Li(1)-N(3), 2.172(4); Li(1)-N(4), 2.050(4); Zn(1)-N(4), 2.0495(19); Zn(1)-C(12), 2.045(2); Zn(1)-C(16), 2.048(2); N(4)-Li(1)-N(3), 113.64(19); N(4)-Li(1)-N(1), 125.5(2); N(3)-Li(1)-N(1), 115.85(19); N(4)-Li(1)-N(2), 123.01(19); N(3)-Li(1)-N(2), 84.88(16); N(1)-Li(1)-N(2), 83.02(15); Zn(1)-N(4)-Li(1), 110.63(13); C(12)-Zn(1)-C(16), 125.12(10); C(12)-Zn(1)-N(4), 121.53(9); C(16)-Zn(1)-N(4), 112.94(9).

A CSD search revealed only two structures featuring the Li-NMe<sub>2</sub>-Zn chain (Figure 4.3) found here in **4.3**, both made by the Hevia group at Strathclyde, namely a monoalkyl-trisamido tetraorganozincate [TMEDA·<sub>2</sub>Li<sub>2</sub>ZnMe(NMe<sub>2</sub>)<sub>3</sub>] and the triorganoamidozincate [{TMEDA·LiZn(NMe<sub>2</sub>)<sub>3</sub>]<sub>2</sub>].<sup>[51]</sup> Significantly, however, in both these previously published structures the Li-NMe<sub>2</sub>-Zn chain is

not single stranded like that in **4.3**, but both metal ends join up with another atom to form a four-atom ring. Another structure having a resemblance to **4.3** is the diisopropylphenylamino derivative  $[\text{PMDETA}\cdot\text{Li}(\text{NHDipp})\text{Zn}(\text{Me})_2]^{[52]}$  (Figure 4.3), which possesses terminal  $\text{PMDETA}\cdot\text{Li}$  and  $\text{Zn}(\text{Me})_2$  groups but joined by a primary amino bridge.

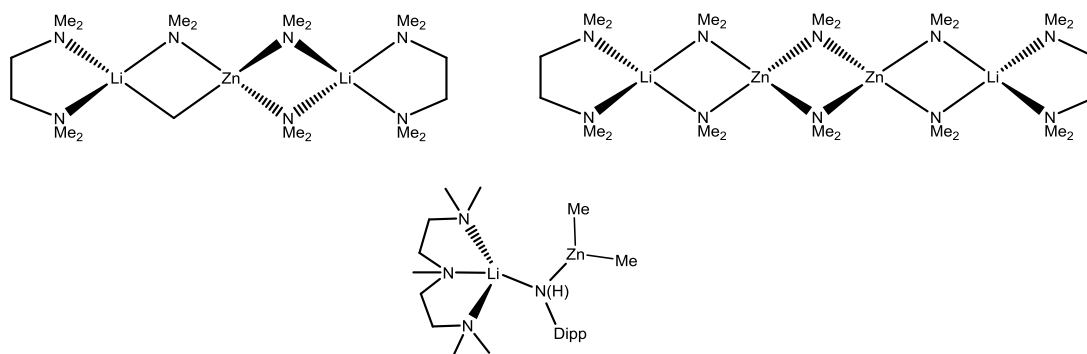


Figure 4.3. ChemDraw representations of the molecular structures of the tetraorganozincate  $[\text{TMEDA}\cdot_2\text{Li}_2\text{ZnMe}(\text{NMe}_2)_3]$  and triorganozincates  $[\{\text{TMEDA}\cdot\text{LiZn}(\text{NMe}_2)_3\}_2]$  and  $[\text{PMDETA}\cdot\text{Li}(\text{NHDipp})\text{Zn}(\text{Me})_2]$ .

The interatomic distances involving the sodium atom in **4.2** span the range 2.3964(14)-2.5314(14) Å. The shortest such bond is to the  $\text{NMe}_2$  group [2.3964(14) Å]. Zinc-ligand interatomic distances span the range 1.9889(11)-2.0322(13) Å, and in contrast to the sodium, the bond between the metal and the TMP anion is the shortest (by almost 0.04 Å). As the four endocyclic angles total 360° the (NaN<sub>2</sub>ZnN) ring is strictly planar. In comparison to the parent base  $[(\text{TMEDA})\text{Na}(\text{TMP})(^t\text{Bu})\text{Zn}(^t\text{Bu})]$ , the Na-N(TMP) bond is the same length (within experimental error), whereas the Zn-N(TMP) bond is slightly shorter in **4.2** (but only by 0.05 Å). In **4.3** the three bonds involving zinc are of equal length 2.048 Å (within experimental error); whereas the lithium-ligand bonds differ in length [from 2.050(4) to 2.223(4) Å], with the Li- $\text{NMe}_2$  bond being the shortest. The amido  $\text{NMe}_2$  ligand sits equidistant from the Li and Zn atoms with

an obtuse Li-N(4)-Zn chain angle of  $110.63(13)^\circ$  showing the arrangement of the three atoms is significantly bent, as opposed to linear, as a consequence of the pseudo-tetrahedral configuration of the N bridge and the considerable steric bulk of the different terminal groups. The metal-NMe<sub>2</sub> bond lengths in **4.3** lie within the range of values observed for the corresponding bonds in aforementioned [TMEDA·<sub>2</sub>Li<sub>2</sub>ZnMe(NMe<sub>2</sub>)<sub>3</sub>] and [{TMEDA·LiZn(NMe<sub>2</sub>)<sub>3</sub>}<sub>2</sub>].<sup>[51]</sup> Having two ligand bridges between the metal centres has a marked effect on the Li-NMe<sub>2</sub>-Zn bond angle. In single stranded **4.3** the angle is obtuse [ $110.63(13)^\circ$ ]; whereas the corresponding angles in these TMEDA-solvated structures are acute (mean angle  $80^\circ$ ) in order to place the metals close enough to a second ligand bridge to close the 4-atom rings.

Determined by an X-ray diffraction study, the molecular structure of aluminate **4.4** (Figure 4.4) is of a discrete contacted ion-pair type. Aluminate **4.4** bears some resemblance to zincate **4.2** in being heterotri-anionic and having a mixed amido (TMP and Me<sub>2</sub>N) ligand set that forms a bridge between the two metals. This dual bridge closes a four-atom, three element (LiNAlN) ring. Completed by two terminal *iso*-butyl ligands, the aluminium atom occupies a distorted (2xN; 2xC) tetrahedral site (with a  $\tau_4$  value of 0.88).<sup>[44]</sup> The two bridging amides leave only one coordination site free for a THF molecule to complete the preferred trigonal planar (2xN; 1xO) coordination of lithium under these bulky constraining ligands. Aluminate **4.4** appears novel in the sense that it is only the second known structure containing the rare LiNAlN ring in which the two N atoms belong to different amido groups, as evidenced by a CSD search. Structures with the same two amido groups accommodated within a LiNAlN ring are precedented, the closest analogy being the bis-diisopropylamide [THF·Li(μ-N(*i*Pr)<sub>2</sub>)<sub>2</sub>Al(*i*Bu)<sub>2</sub>],<sup>[53]</sup> which also has a terminal Li-O(THF) bond. The lengths of both Al-N bonds in this homoamido structure [1.935(1) and 1.936(1) Å], lie between those of the two more asymmetric Al-N bonds in heteroamido **4.4**, the shortest [1.9291(11) Å] to the smaller Me<sub>2</sub>N group and the longest to the larger TMP group [1.9930(10) Å]. The asymmetry in **4.4** has less of an effect on the length of the Li-N bonds [2.075(3) and 2.086(3) Å; mean 2.0805 Å], with

both slightly longer than the two Li-N bonds in the homoamide [1.998(2) and 2.047(2) Å; mean 2.0225 Å]. Their N-Li-N bond angles are in the same region [92.48(9)° in **4.4**: *cf.*, 91.45(10)°].

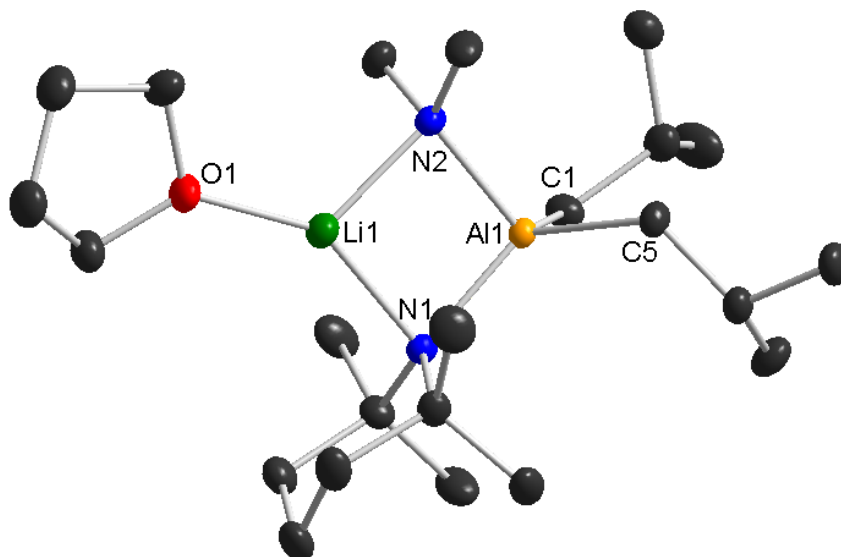


Figure 4.4. Molecular structure of [THF·Li(TMP)(NMe<sub>2</sub>)Al(*i*Bu)<sub>2</sub>] **4.4**. Ellipsoids are displayed at 50% probability and hydrogen atoms have been omitted for clarity. Selected bond lengths (Å) and bond angles (°): Li(1)-N(2), 1.998(2); Li(1)-N(1), 2.047(2); Li(1)-O(1), 1.901(2); Al(1)-N(1), 1.9930(10); Al(1)-N(2), 1.9291(11); Al(1)-C(1), 2.0316(13); Al(1)-C(5), 2.0249(13); O(1)-Li(1)-N(1), 146.49(13); O(1)-Li(1)-N(2), 120.96(12); N(2)-Li(1)-N(1), 92.48(9); Al(1)-N(2)-Li(1), 87.09(7); Al(1)-N(1)-Li(1), 84.09(7); N(2)-Al(1)-N(1), 96.32(4); N(2)-Al(1)-C(5), 106.93(5); N(1)-Al(1)-C(5), 119.87(5); N(2)-Al(1)-C(1), 109.10(5); N(1)-Al(1)-C(1), 116.51(5); C(5)-Al(1)-C(1), 106.86(6).

NMR spectroscopy was employed to characterise each new compound **4.2**, **4.3** and **4.4** in solution. Run in d<sub>12</sub>-cyclohexane solution, <sup>1</sup>H (Figure 4.5) and <sup>13</sup>C (Figure 4.6) spectra of **4.2** confirmed the formula of the molecular structure elucidated by X-ray crystallography. Single, sharp resonances can be observed for both the bridging NMe<sub>2</sub> and terminal *i*Bu groups. In contrast, the two sets of

methyl groups on the TMP anion appear as two separate singlets, indicating that they occupy non-equivalent chemical environments. This asymmetry is also apparent for the TMP  $\beta$  and  $\gamma$  hydrogen atoms.

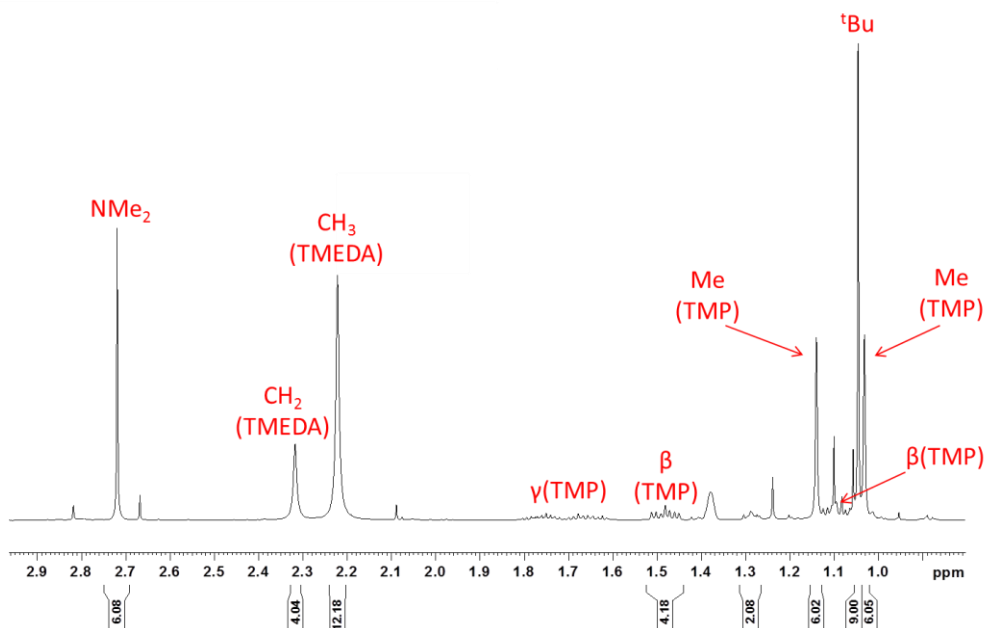


Figure 4.5.  $^1\text{H}$  NMR spectrum of the heterotrileptic complex  $[\text{TMEDA}\cdot\text{Na}(\text{TMP})(\text{NMe}_2)\text{Zn}(\text{tBu})]$  **4.2** in  $\text{C}_6\text{D}_{12}$  solution.

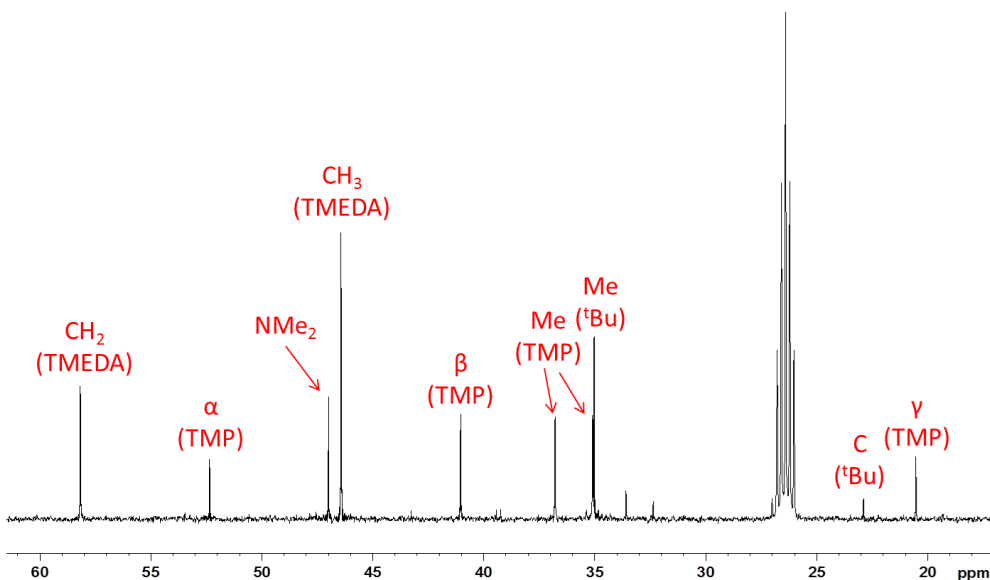


Figure 4.6.  $^{13}\text{C}$  NMR spectrum of  $[\text{TMEDA}\cdot\text{Na}(\text{TMP})(\text{NMe}_2)\text{Zn}(\text{tBu})]$  **4.2** in  $\text{C}_6\text{D}_{12}$  solution.

Inspecting the  $^1\text{H}$  NMR spectrum of the filtrate of **4.2** revealed that small resonances (located at 7.28, 7.18, 6.62, 5.63 and 5.11 ppm) corresponding to styrene were present. The presence of styrene was confirmed by comparison with a  $^1\text{H}$  NMR spectrum of an authentic commercial sample. This finding further substantiates the idea that the  $\text{NMe}_2$  fragment is produced via  $\beta$ -elimination from a benzylic metallated species of DMPEA since a metal dimethylamide and styrene would be the two expected products formed. This elimination takes on more significance, as it is the reverse of a hydroamination reaction of an alkene, here styrene. Catalytic hydroamination is currently an emerging topic of increasing importance especially with regard to trying to replace rare earth metal catalysts by novel abundant early main group catalysts.<sup>[54-59]</sup> In addition to  $^1\text{H}$  and  $^{13}\text{C}$  NMR spectroscopy (Figure 4.7 and Figure 4.8 respectively), lithium zincate **4.3** was analyzed by  $^7\text{Li}$  NMR spectroscopy (Figure 4.9) with spectra all recorded in  $\text{d}_{12}$ -cyclohexane solution. In the  $^1\text{H}$  spectrum narrow singlet resonances are observed for both the  $^t\text{Bu}$  and  $\text{NMe}_2$  groups as well as the three sets of PMDETA resonances. Attempting to dry the crystals *in vacuo* causes them to degrade to an oil and therefore it was difficult to separate the pure crystalline material from impurities within the reaction mixture. Consequently, resonances corresponding to free DMPEA and PMDETA were also present within the spectrum, together with small traces of styrene. The  $^7\text{Li}$  spectrum displayed two resonances, a major one at 0.44 ppm and a minor one at 1.31 ppm, presumably from a lithium impurity arising from the aforementioned degradation of the crystals.



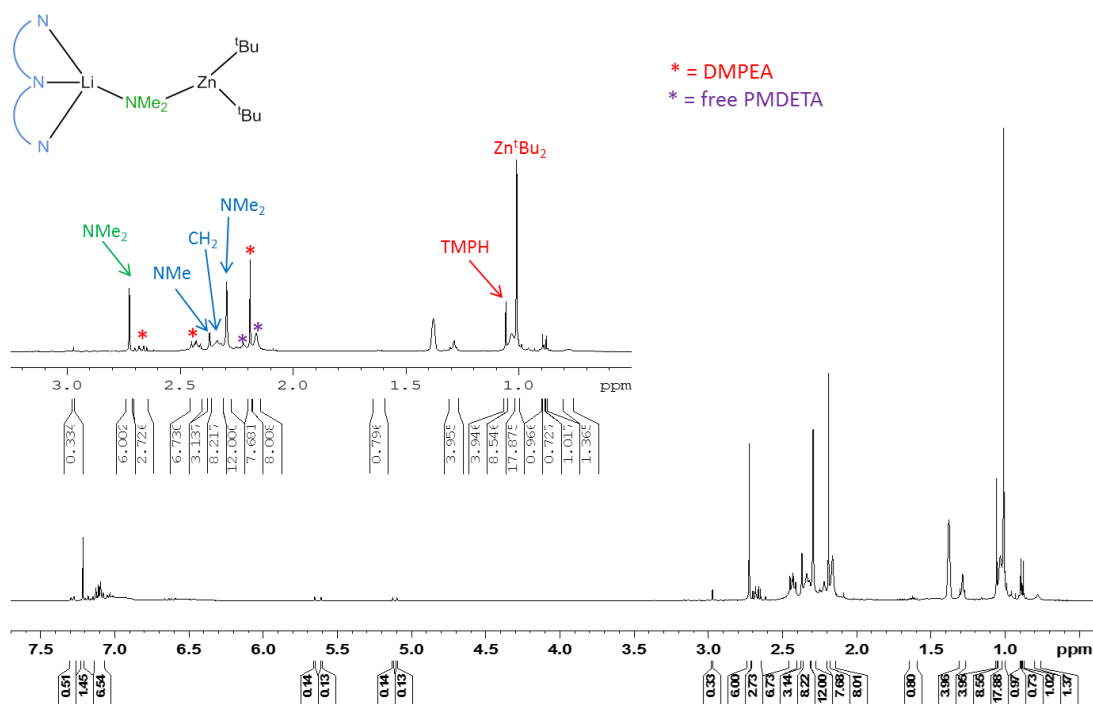


Figure 4.7.  $^1\text{H}$  NMR spectrum of  $[\text{PMDETA}\cdot\text{Li}(\text{NMe}_2)\text{Zn}(\text{tBu})_2]$  **4.3** in  $\text{C}_6\text{D}_{12}$  solution with inset showing expanded aliphatic region.

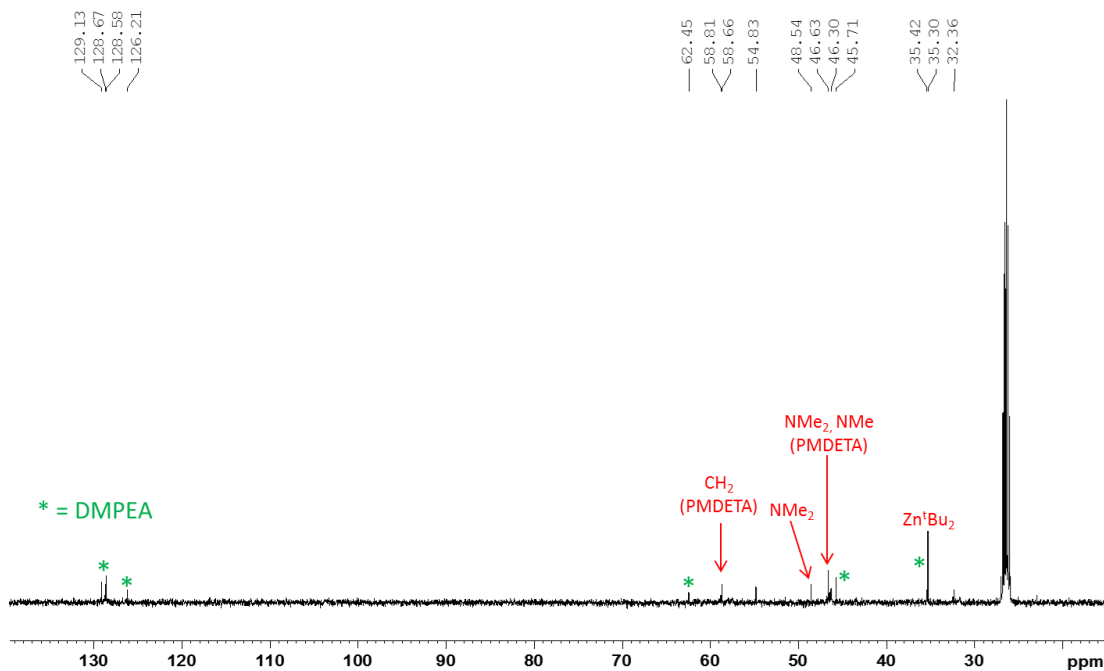


Figure 4.8.  $^{13}\text{C}$  NMR spectrum of the lithium zincate  $[\text{PMDETA}\cdot\text{Li}(\text{NMe}_2)\text{Zn}(\text{tBu})_2]$  **4.3** in  $\text{C}_6\text{D}_{12}$  solution.

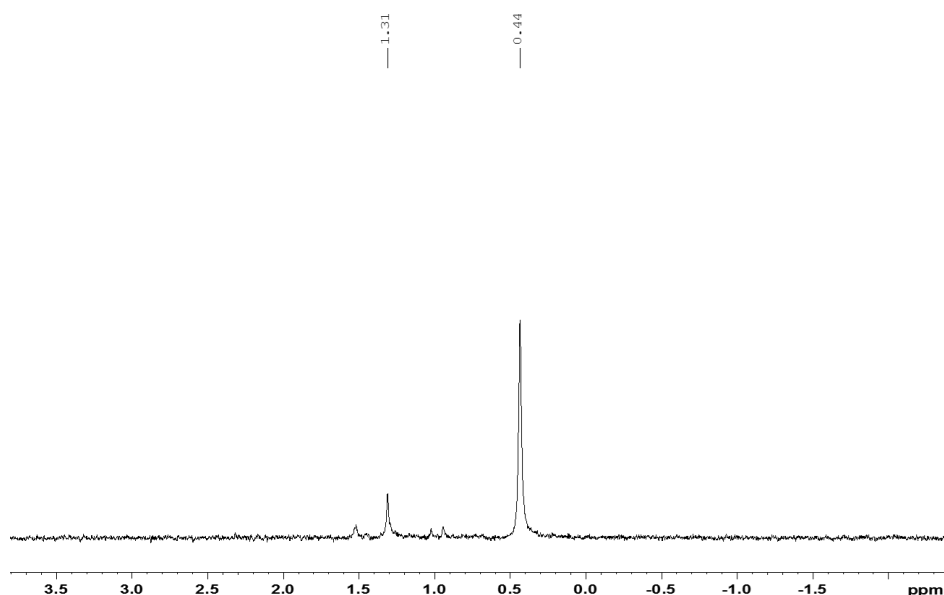


Figure 4.9.  ${}^7\text{Li}$  spectrum of  $[\text{PMDETA}\cdot\text{Li}(\text{NMe}_2)\text{Zn}(\text{tBu})_2]$  **4.3** in  $\text{C}_6\text{D}_{12}$  solution with an unidentified impurity at 1.31 ppm.

${}^1\text{H}$ ,  ${}^{13}\text{C}$  and  ${}^7\text{Li}$  NMR spectra of aluminate **4.4** (Figure 4.10, Figure 4.11 and Figure 4.12 respectively) are consistent with the molecular structure elucidated by the X-ray diffraction study. Its  ${}^1\text{H}$  spectrum shows a sharp singlet for the  $\text{NMe}_2$  group implying that the two methyl groups are equivalent on the NMR timescale at room temperature, with the same being the case for the methyl TMP signals. However, since the  $\beta$  and  $\gamma$  hydrogen atom resonances on the TMP group are split, it appears that they occupy different environments, suggesting that the TMP Me equivalency may just be a case of accidental equivalence. The  ${}^7\text{Li}$  spectrum showed a narrow singlet at 1.22 ppm in agreement with a single lithium environment. Table 4.1 compares the chemical shifts for the  $\text{NMe}_2$  group in each of the three heterobimetallic compounds, as well as the  ${}^7\text{Li}$  resonances in **4.3** and **4.4**. Both the  ${}^1\text{H}$  and  ${}^{13}\text{C}$  NMR shifts are similar for **4.2** and **4.3** in accordance that this smaller amido group coordinates to both zinc and sodium or lithium; whereas in **4.4** the resonances are further upfield in comparison reflecting its attachment to aluminium and lithium. Free DMPEA has its  $\text{NMe}_2$  chemical shift at a different position (see Table 4.1) to those of **4.2-4.4**.

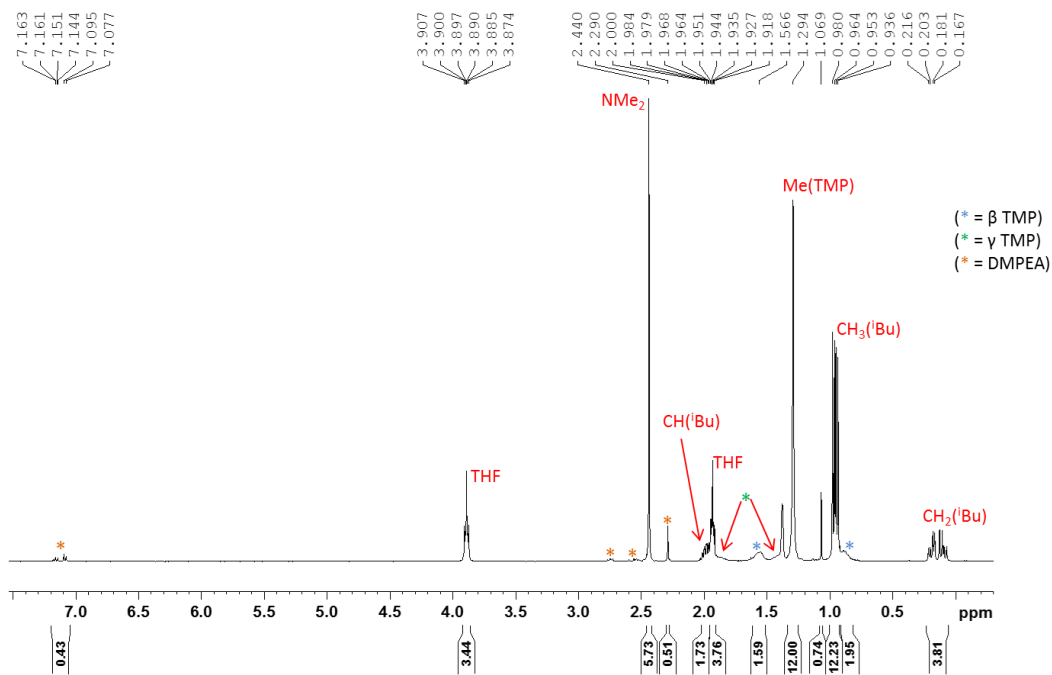


Figure 4.10.  $^1\text{H}$  NMR spectrum of the lithium aluminate  $[\text{THF}\cdot\text{Li}(\text{TMP})(\text{NMe}_2)\text{Al}(\text{iBu})_2]$  **4.4** in  $\text{C}_6\text{D}_{12}$  solution.

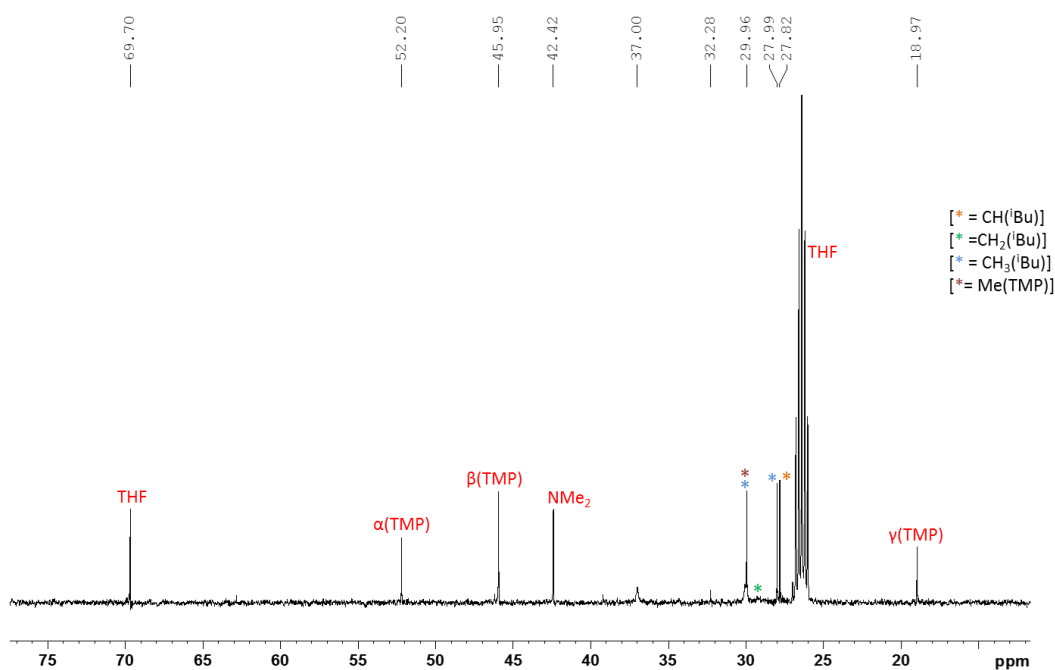


Figure 4.11.  $^{13}\text{C}$  NMR spectrum of  $[\text{THF}\cdot\text{Li}(\text{TMP})(\text{NMe}_2)\text{Al}(\text{iBu})_2]$  **4.4** in  $\text{C}_6\text{D}_{12}$  solution.

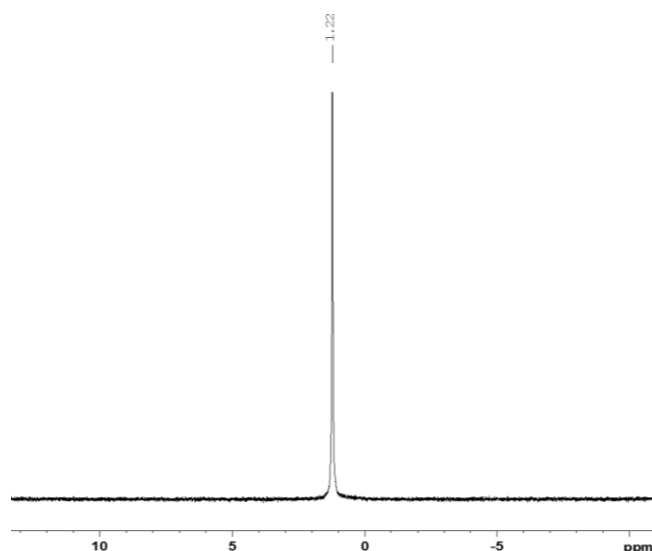


Figure 4.12.  $^7\text{Li}$  spectrum of  $[\text{THF}\cdot\text{Li}(\text{TMP})(\text{NMe}_2)\text{Al}(i\text{Bu})_2]$  **4.4** in  $\text{C}_6\text{D}_{12}$  solution.

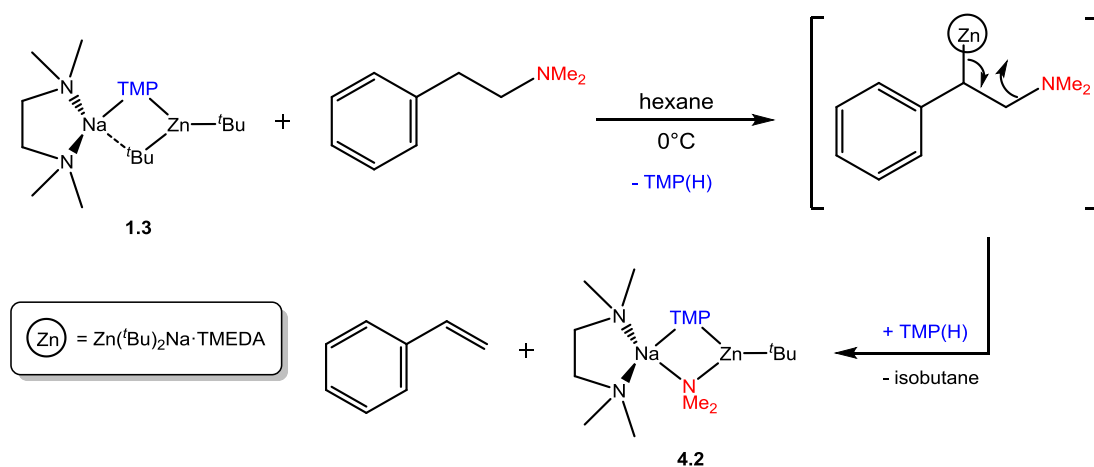
Table 4.1. Comparison of NMR chemical shifts ( $\delta$ ) of the new dimethylamido-containing ate compounds and DMPEA in  $\text{C}_6\text{D}_{12}$  solution.

Compound	$\delta$ NMe <sub>2</sub> (ppm)		$\delta$ $^7\text{Li}$ (ppm)
	$^1\text{H}$	$^{13}\text{C}$	
DMPEA	2.18	45.72	-
$[\text{TMEDA}\cdot\text{Na}(\mu\text{-TMP})(\mu\text{-NMe}_2)\text{Zn}(t\text{Bu})]$ ( <b>4.2</b> )	2.72	46.05	-
$[\text{PMDETA}\cdot\text{Li}(\mu\text{-NMe}_2)\text{Zn}(t\text{Bu})_2]$ ( <b>4.3</b> )	2.72	48.54	0.44
$[\text{THF}\cdot\text{Li}(\mu\text{-TMP})(\mu\text{-NMe}_2)\text{Al}(i\text{Bu})_2]$ ( <b>4.4</b> )	2.44	42.42	1.22

### 4.3.2 Mechanistic Implications

Combining the information accrued on the newly synthesised compounds **4.2–4.4** with previous knowledge documented in the literature, leads to interesting mechanistic insights about the reactions that produced these heterobimetallic compounds. These insights form the basis of this section.

Scheme 4.4 shows that the aforementioned sodium zincate reactant **1.3**, in forming product **4.2**, utilises one alkyl <sup>t</sup>Bu ligand in the reaction with DMPEA that is substituted by the captured Me<sub>2</sub>N elimination fragment with retention of the remainder of the structure of **1.3** in **4.2**. Though overall **1.3** has functioned as an alkyl base with concomitant production of isobutane that ensures the reaction is irreversible, it is now accepted through the evidence of a combination of theoretical<sup>[39]</sup> and experimental<sup>[60]</sup> investigations that **1.3** performs zinc-hydrogen exchange reactions in two steps. In step one, TMP functions as a kinetic base to deprotonate the organic substrate and form amine TMP(H) co-product. In the second step TMP(H) is deprotonated itself to regenerate TMP with concomitant release of isobutane (this process is illustrated for the transformation of **1.3** to **4.2** in Scheme 4.4). Accordingly, the final product **4.2** ends up as a heterotri-anionic complex. Step one can be regarded as being kinetic while step two represents the thermodynamic process.



Scheme 4.4. Proposed two-step, kinetic-thermodynamic mechanism for formation of **4.2** from **1.3**.

Inspection of the conversion of **4.1** into **4.3** reveals a different scenario as the product **4.3** ends up as a heterobianionic complex. Here TMP carries out the deprotonation of DMPEA to form TMP(H) in the first step at which point the process stops with final product **4.3** retaining the two *t*-butyl ligands of the starting material **4.1** (see earlier, Scheme 4.3). Dimethylamide ( $\text{Me}_2\text{N}^-$ ) is significantly less basic than  $\text{TMP}^-$  (experimental  $\text{p}K_{\text{a}}$  values of conjugate acids, 29.7 and 37.9, respectively)<sup>[61-62]</sup> so this would rule out a transamination reaction between **4.3** and  $\text{TMP}(\text{H})$ , but in such terms of relative basicity one would expect  $\text{TMP}(\text{H})$  to undergo deprotonation with a *t*Bu ligand to generate the hypothetical TMP-containing complex  $[\text{PMDETA}\cdot\text{Li}(\text{NMe}_2)(\text{TMP})\text{Zn}(\text{tBu})]$ . The explanation for why this does not take place must lie with steric factors. The electronic stabilization by PMDETA through its tridentate chelation fills three of the four coordination sites on the lithium cation in **4.3** with the fourth one filled by the small amide  $\text{Me}_2\text{N}$ , so clearly there is no space available for the sterically demanding secondary amine  $\text{TMP}(\text{H})$  to datively bind to Li as a prerequisite to its deprotonation by a *t*Bu ligand (Figure 4.13).

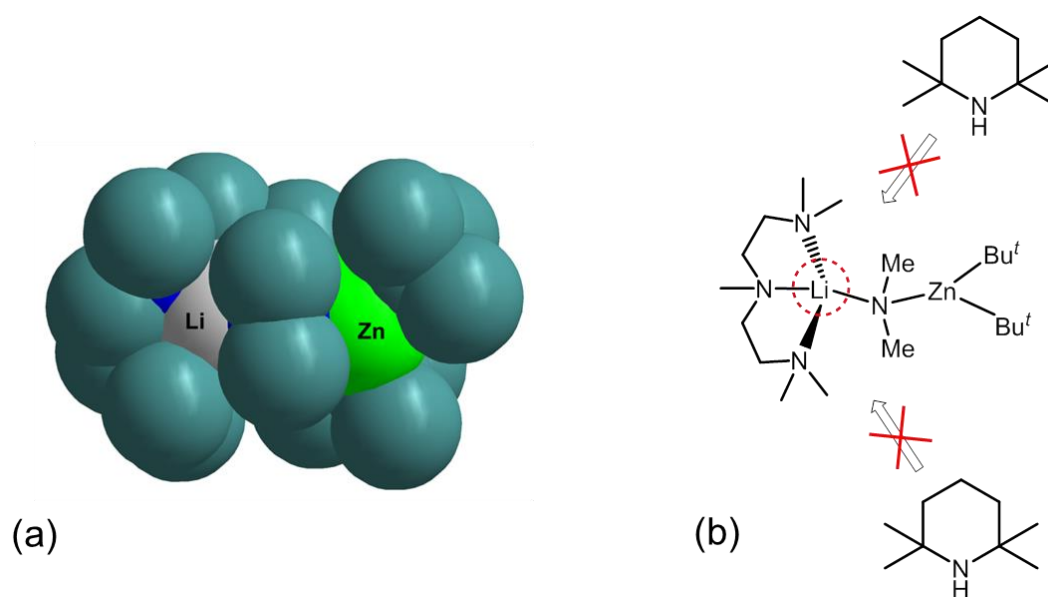
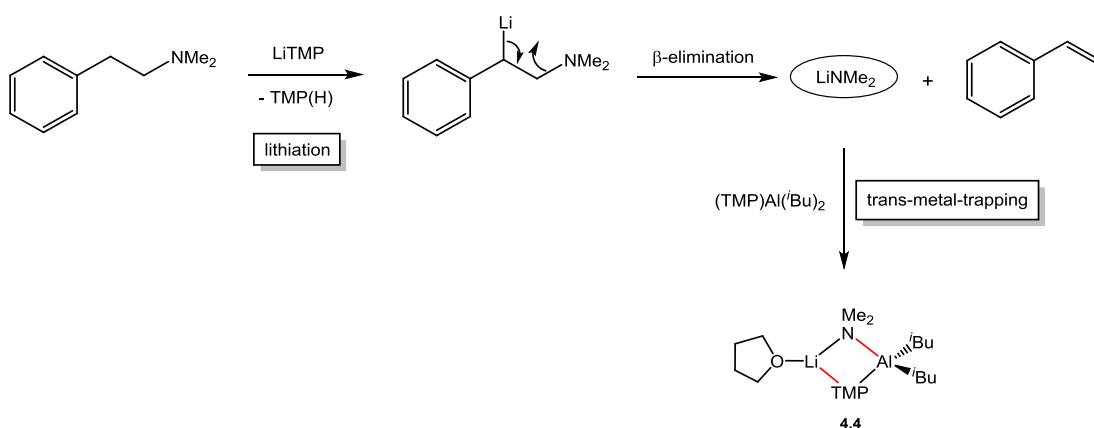


Figure 4.13. Space filling model (a) and ChemDraw representation (b) of **4.3** highlighting the restricted space available about the lithium centre preventing bulky  $\text{TMP}(\text{H})$  re-entering the system.

The fact that **4.3** is an open (chain) structure rather than a closed (ring) structure supports this steric explanation. Conversely in both **1.3** and **4.2** the larger sodium cation only carries a terminal bidentate TMEDA which leaves room for bonding to two bridging ligands to close a 4-atom ring, so it is this steric deflation which allows TMP(H) to enter the coordination sphere of Na<sup>+</sup> in **1.3** and to then exchange with a <sup>t</sup>Bu ligand via hydrogen transfer.

Drawing on the precedent of these AMMZn (zinc-hydrogen exchange) reactions, the formation of aluminate **4.4** could be considered an AMMAI (aluminium-hydrogen exchange) reaction starting from the putative contacted ion-pair complex “[THF·Li(TMP)<sub>2</sub>Al(<sup>i</sup>Bu)<sub>2</sub>]”. As covered elsewhere in this thesis (see Chapter 3), this complex has a track record of being an excellent *in situ* proton abstracting agent, cleaving an α-hydrogen atom from both THF and thiophene and capturing/stabilizing their sensitive anionic rings intact,<sup>[63]</sup> regioselectively deprotonating haloanisoles without interfering with Cl, Br or I substituents,<sup>[64]</sup> and even abstracting a hydrogen atom from the relatively non-acidic CH<sub>3</sub> group of TMEDA.<sup>[65]</sup> That notwithstanding, while undertaking the present work, a parallel study<sup>[66]</sup> (discussed in depth in Chapter 3) on “[THF·Li(TMP)<sub>2</sub>Al(<sup>i</sup>Bu)<sub>2</sub>]” established that it actually exists as the two separated components LiTMP and (TMP)Al(<sup>i</sup>Bu)<sub>2</sub>(THF). Moreover, the closely related “aluminate” base “[THF·Li(TMP)Al(<sup>i</sup>Bu)<sub>3</sub>]” introduced and widely studied by Uchiyama<sup>[67-69]</sup> was analogously found not to be a single species as originally hypothesized but a complicated mixture of neutral and ate species in THF solution. The confounding conclusion from the work carried out in Chapter 3 was that none of the aluminium species present in either of these reagent mixtures, even ate species in the latter case, could deprotonate anisole under the conditions studied and that both operate as bases through a two-step lithiation (by LiTMP) *in situ trans-metal-trapping* (by neutral aluminium species) mechanism. Furthermore it was established that in the “[THF·Li(TMP)<sub>2</sub>Al(<sup>i</sup>Bu)<sub>2</sub>]” mixture the cocomplexation of LiTMP and (TMP)Al(<sup>i</sup>Bu)<sub>2</sub> with or without THF stabilisation was not possible due to the steric bulk involved. It follows logically from this scenario that the probable mechanism for the production of **4.4**

(Scheme 4.5) must be LiTMP-executed lithiation of DMPEA followed by  $\alpha$ - $\beta$  elimination of  $\text{Me}_2\text{N-Li}$  which is subsequently trans-metal-trapped by the neutral aluminium species  $(\text{TMP})\text{Al}(\text{iBu})_2$ , though it cannot be completely ruled out that this trapping operation takes place in a more concerted fashion with the styrene molecule still coordinated at least partially to the departing lithium amide fragment as the trapping Al species enters the reaction.



Scheme 4.5. Proposed mechanism of lithiation followed by trans-metal-trapping to generate **4.4**, highlighting in red the trapping Li-N and Al-N bonds.

The key issue is that the reaction is not an *AMMAI* reaction, nor an aluminium reaction of any sort, but that the aluminium trapping agent simply cocomplexes with the eliminated  $\text{Me}_2\text{N-Li}$  to form the aluminate product. As the aluminium atom in this aluminate is coordinatively saturated (that is, being four-coordinate when bound by bulky ligands),  $\text{TMP(H)}$  cannot enter the Al coordination sphere to react with an *i*Bu ligand so the reaction is over at the first step and does not proceed to a second step like that aforementioned in the sodium zincate reactions. This applies generally as both this mixture and monoamido “[ $\text{THF}\cdot\text{Li}(\text{TMP})\text{Al}(\text{iBu})_3$ ]” react as  $\text{TMP}$  deprotonating agents, not alkyl deprotonating agents. It is also worth noting that  $(\text{Me}_2\text{NLi})_n$  on its own is



probably polymeric ( $n = \infty$ ) given lithium's propensity for high aggregation when connected to such a sterically small anion<sup>[70-71]</sup> (though its crystal structure has still not been elucidated), but in this reaction it seems never to be given an opportunity to aggregate as only a single unit is captured within **4.4** implying that the trans-metal-trapping step by the aluminium base residue takes place expeditiously.

### 4.3.3 Capture of the Whole Parent Amine, DMPEA

Approaches for performing metallation for compounds related to DMPEA do exist whereby the nitrogen centre, otherwise capable of coordinating, is made inert and protected [for example, by using a pivaloyl (CO<sup>t</sup>Bu) group]<sup>[43]</sup>, hence allowing benzylic metallation and subsequent electrophilic quenching (for example, with carbon dioxide) to be performed without any elimination competition. In the Strohmman paper which inspired this study, the synthesis and crystal structure of a potassium derivative of 2-*N*-methyl-1,2,3,4-tetrahydroisoquinoline, a relative of DMPEA where the tertiary amine residue resides in a ring, were reported. This heavier alkali metal compound was found to exist as a coordination polymer. However, despite a number of attempts in this study, we did not succeed in the challenge of going one better by synthesising and capturing a metallated derivative of DMPEA itself. That notwithstanding, as now discussed this study has produced an unprecedented result in the synthesis and structural characterisation of a bimetallic complex containing DMPEA in a fully intact state, that is, without undergoing any benzylic deprotonation or subsequent Me<sub>2</sub>N-metal elimination.

In order to try to slow down a possible benzylic deprotonation we next studied the TMP-dimethyl lithium zincate [Li(TMP)Zn(Me)<sub>2</sub>]. Through comparison experiments with anisole in the presence of THF,<sup>[60]</sup> this zincate is known to be significantly less reactive than its bulkier analogue [Li(TMP)Zn(<sup>t</sup>Bu)<sub>2</sub>]. We found that a 1:1 reaction mixture of [Li(TMP)Zn(Me)<sub>2</sub>] and DMPEA in hexane solution on stirring at room temperature for 10 minutes yielded a homogeneous yellow

solution on slight warming. Storage of this solution in the freezer at  $-28^{\circ}\text{C}$  produced a sizeable crop of small colourless needles (isolated crystalline yield, 60%). Unfortunately, the crystals were not of a good enough quality to be studied by X-ray crystallography, though NMR spectroscopic characterisation proved possible in deuterated cyclohexane ( $\text{C}_6\text{D}_{12}$ ) solution. To our surprise, the  $^1\text{H}$  NMR spectrum (Figure 4.14) disclosed a 1:1 stoichiometric mixture of DMPEA and the heterobimetallic reagent  $[\text{Li}(\text{TMP})\text{Zn}(\text{Me})_2]$  intimating that both compounds appeared to be present within the dissolved crystalline material.

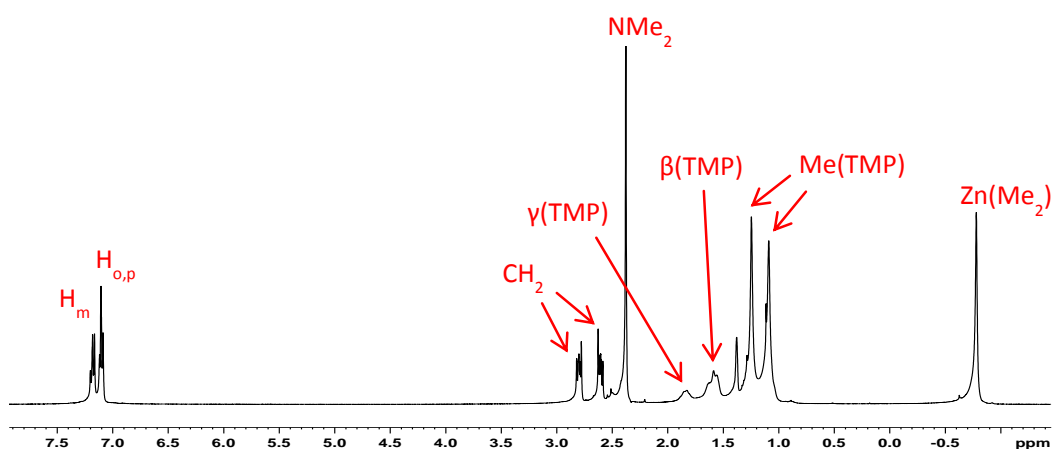
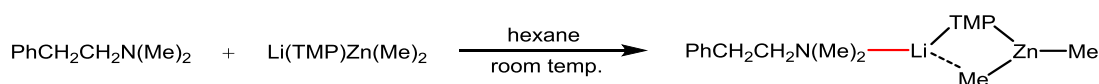


Figure 4.14.  $^1\text{H}$  NMR spectrum of isolated crystals from reaction of  $[\text{Li}(\text{TMP})\text{Zn}(\text{Me})_2]$  and DMPEA subsequently dissolved in  $\text{C}_6\text{D}_{12}$  solution.

While the spectrum revealed that the DMPEA molecule had all its component parts intact, the corresponding resonances had all shifted downfield (to 2.38, 2.61, 2.80 and 7.08-7.18 ppm) in comparison to those in free DMPEA (2.18, 2.42, 2.68 and 7.03-7.13 ppm respectively) implying that the DMPEA was no longer free. The  $^{13}\text{C}$  NMR spectrum concurred with the  $^1\text{H}$  spectrum showing resonances belonging to both TMP and  $\text{Zn}(\text{Me})_2$  as well for DMPEA [though this time an upfield shift was observed for the resonances in comparison to those in free DMPEA (from 35.4, 45.7, 62.5, 126.2, 128.6, 129.1 and 141.3 ppm to 33.4, 45.5, 62.3, 126.2, 128.1, 128.2 and 138.1 ppm)]. Completing the NMR analysis,

the  $^7\text{Li}$  NMR spectrum showed a single sharp resonance at 1.89 ppm indicating only a single lithium environment. These data are consistent with the DMPEA molecule interacting with the bimetallic reagent in some way, but without deprotonation having occurred, as both its  $\text{PhCH}_2$  hydrogen atoms are still intact. The most obvious explanation for this observation is a Lewis acid – Lewis base reaction between the two starting materials, where the DMPEA nitrogen atom forms a dative contact to the Li centre (Scheme 4.6). Implying that the amine part of DMPEA is the “business end” of the molecule, the shift experienced (from those in free DMPEA) by the  $\text{NMe}_2$  hydrogen atoms is greatest (0.2 ppm) in comparison to the shift of the remote aryl group hydrogen atoms (only 0.05 ppm), though in both cases the shift differences are rather small.



Scheme 4.6. Suspected co-complexation reaction between  $\text{Li}(\text{TMP})\text{Zn}(\text{Me})_2$  and DMPEA, highlighting in red the newly formed dative N-Li bond.

On the basis of these intriguing NMR observations we repeated this reaction several times until we finally were successful in growing X-ray quality crystals of  $[\text{DMPEA} \cdot \text{Li}(\text{TMP})\text{Zn}(\text{Me})_2]$  **4.5** from the reaction solution (isolated yield, 70%). Figure 4.15 shows the molecular structure of **4.5** from two different perspectives. A key feature of this contacted  $\text{LiTMP-ZnMe}_2$  ion-pair structure is the central four-atom, four-element (LiNZnC) ring. Rings of this type are commonly encountered in alkali metal zincate chemistry,<sup>[72-73]</sup> for example in the lithium di-*t*-butylzincate  $[\text{TMEDA} \cdot \text{Li}(\text{TMP})\text{Zn}(\text{tBu})_2]$ <sup>[74]</sup> and the aforementioned dilithium methylzincate  $[(\text{TMEDA})_2 \cdot \text{Li}_2\text{ZnMe}(\text{NMe}_2)_3]$ .<sup>[51]</sup> However in contrast to these structures which contain a conventional donor molecule (TMEDA) on the lithium centre, **4.5** is unique because it is a fully intact DMPEA molecule that acts as the Lewis base towards the Lewis acidic Li centre

within it. The connectivity within the structure reveals a three-coordinate, trigonal planar (2xN; 1xC coordinated) lithium atom consisting of two N atoms, one N atom from a bridging TMP and another from the neutral DMPEA molecule, with the C atom belonging to the bridging Me group of the Me<sub>2</sub>Zn unit. Zn also has a three-coordinate, distorted trigonal planar (1xN; 2xC) geometry, which is completed by a terminal Me ligand. The bridging Me group, the carbon atom of which (C11) is 5-coordinate, forms an electron deficient bridging bond to the Li centre and in turn this places the Li atom in close proximity to the methyl H atoms [Li1...H(11A) = 2.18(3) Å, Li1...H(11C) = 2.16(3) Å] (it should be noted that the hydrogen atoms were freely located in the X-ray diffraction analysis). The non-deprotonated DMPEA molecule coordinates to the bimetallic system through a dative nitrogen-lithium interaction, without any metallation of the amine having taken place. Figure 4.15 clearly shows that while the N(2) atom belonging to DMPEA sits approximately in the same plane as the central [LiN(1)ZnC] ring (lying only 0.04 Å out of the mean plane), the remainder of the amine molecule protrudes to one side causing the overall structure to be asymmetrical. A CSD search revealed no structures containing DMPEA in the presence of lithium, zinc, or in fact any metal, suggesting that the structure of compound **4.5** is without precedent. Bond lengths in **4.5** involving lithium cover the range 1.965(4) - 2.248(4) Å, with the Li-N(TMP) bond being the shortest and the Li-C(Me) bond being the longest. For zinc its bond lengths lie between 1.984(2) and 2.060(2) Å and in contrast, the terminal methyl group is now held closest to the metal centre (a reflection of the strong carbophilicity of Zn), while the bond to the methyl C bridge is the longest [though within experimental error of the Zn-N(TMP) bond]. The sum of the four endocyclic angles (360° within experimental error) indicates planarity of the central (LiNZnC) ring, and from Figure 4.15 it can be clearly seen that this heterobimetallic ring lies essentially perpendicular to the six-membered chair-shaped TMP ring [dihedral angle between (LiNZnC) plane and the TMP C<sub>α</sub>-N-C<sub>α'</sub> plane is 87.45°]. To make the Li1-C11 bond the Me bridge has to incline towards the lithium atom, as evidenced by the less obtuse C11-Zn1-N1 angle [105.25(7)°] in comparison to

the significantly wider C10-Zn1-N1 bond angle [124.85(9)°]. A comparison of the Li1-C11 bond length in **4.5** [2.248(4) Å] with those in the classic electron-deficient structure of methyllithium ( $2.31 \pm 0.05$  Å)<sup>[75-76]</sup> establishes they are equivalent within experimental error, consistent with the Me group in **4.5** forming an electron deficient bond to the Li centre. However, a comparison with bonds lengths in monomeric Me<sub>2</sub>Zn,<sup>[77]</sup> reveals that the C-Zn bonds are shorter by 0.133 Å than that of the Zn1-C11 bond in **4.5**, as would be expected given the C-Zn-C linearity of Me<sub>2</sub>Zn and the lower coordination number of its zinc centre (i.e., CN = 2 versus 3).

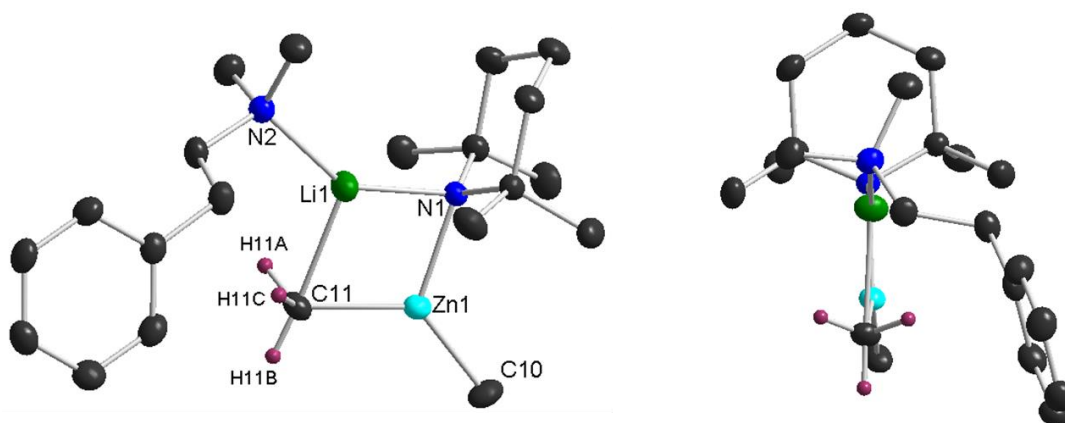


Figure 4.15. Molecular structure of [DMPEA·Li(TMP)Zn(Me)<sub>2</sub>] **4.5** from above (LHS) and along the central LiN<sub>1</sub>Zn<sub>1</sub>C<sub>11</sub> plane (RHS). Ellipsoids are displayed at 50% probability and hydrogen atoms (except those on the Me bridge C<sub>11</sub>) have been omitted for clarity. Selected bond lengths (Å) and bond angles (°): Li(1)-N(1), 1.965(4); Li(1)-N(2), 2.060(4); Li(1)-C(11), 2.248(4); Li(1)-H(11A), 2.18(3); Li(1)-H(11C), 2.16(3); Zn(1)-N(1), 2.0520(16); Zn(1)-C(10), 1.984(2); Zn(1)-C(11), 2.060(2); N(1)-Li(1)-N(2), 143.0(2); N(1)-Li(1)-C(11), 101.49(15); N(2)-Li(1)-C(11), 115.32(17); C(10)-Zn(1)-N(1), 124.85(9); C(10)-Zn(1)-C(11), 129.87(10); N(1)-Zn(1)-C(11), 105.25(7); Li(1)-N(1)-Zn(1), 79.65(12); Zn(1)-C(11)-Li(1), 73.21(10).

A CSD search for structures possessing both LiTMP and  $\text{Zn}(\text{Me})_2$  returned only one result, namely the diamine complex  $[\text{TMEDA}\cdot\text{Li}(\text{TMP})\text{Zn}(\text{Me})_2]$  **4.6** also made by the Mulvey group.<sup>[78]</sup> In this previous structure bidentate chelation by TMEDA to Li stops the Me group from forming a bridge between the two metals, resulting in a central acyclic but curved LiNZnC chain (Figure 4.16). Whilst the Zn-N(TMP) bond length in **4.6** [2.0482(19) Å] is the same within experimental error as that in **4.5** [2.0520(16) Å], the Li-N(TMP) bond is marginally longer than in **4.5** (by 0.08 Å). This is a measure of the superior Lewis basicity of TMEDA compared to monodentate DMPEA. However, the most noticeable difference caused by this change of neutral donor molecule is the substantially shorter (by 0.36 Å) Li-C distance in **4.5** [2.248(4) Å] compared to that in **4.6** [2.603(5) Å], in agreement with the Me group in **4.5** bridging the two metal centres; while in the TMEDA compound it bonds exclusively to Zn.

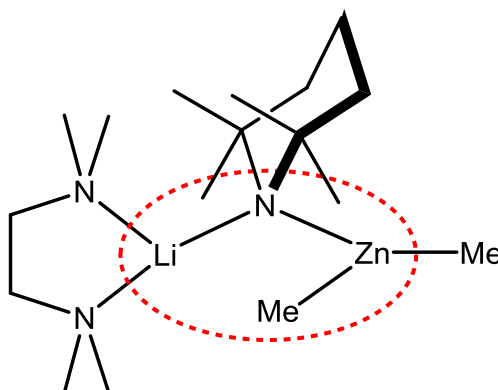


Figure 4.16. ChemDraw representation of  $\text{TMEDA}\cdot\text{Li}(\text{TMP})\text{Zn}(\text{Me})_2$  **4.6** highlighting the curved LiNZnC chain.

Further characterisation of Lewis acid – Lewis base complex **4.5** was provided by a combination of  $^1\text{H}$ ,  $^{13}\text{C}$  and  $^7\text{Li}$  NMR spectra recorded in both  $d_6$ -benzene and  $d_8$ -toluene, as well as  $d_{12}$ -cyclohexane. In its  $^1\text{H}$  NMR spectrum in  $\text{C}_6\text{D}_6$  solution (Figure 4.17), the TMP methyl groups appear as two separate resonances (at 1.08 and 1.46 ppm), confirming a difference in the surrounding

chemical environment for the two sets of methyl groups (note that the  $\beta$  and  $\gamma$  protons are each also split into separate resonances). That notwithstanding, in disagreement with the molecular structure is the single resonance (at -0.24 ppm) obtained for both methyl groups present on the zinc atom. While in the crystal the interaction between Li and the Me bridge would cause an inequivalence between the methyl groups bound to zinc, in solution at room temperature there appears to be free rotation about the Zn-N(TMP) axis resulting in both groups on average experiencing the same chemical environment.

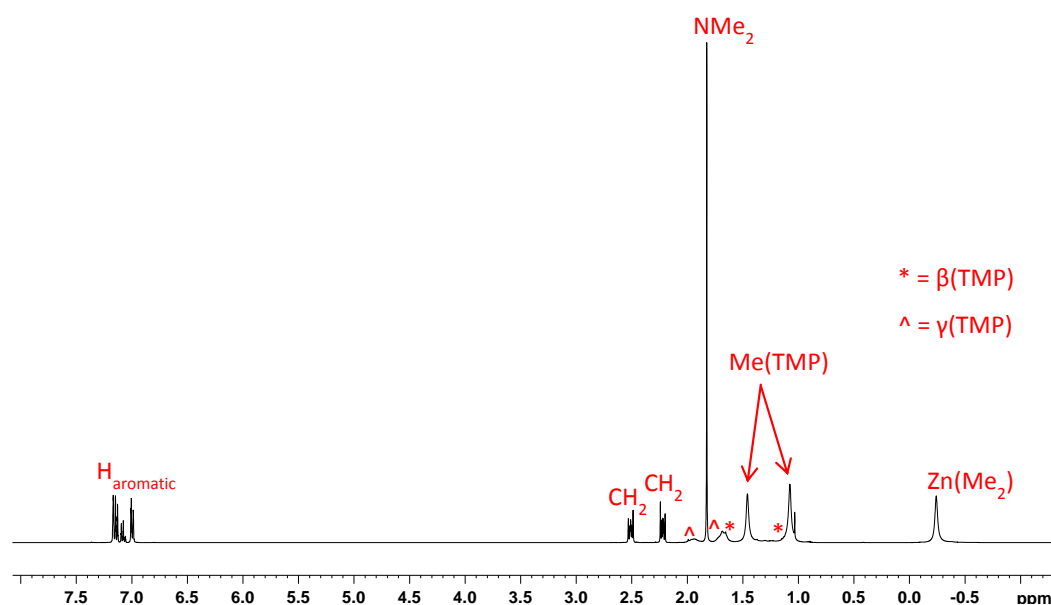


Figure 4.17. <sup>1</sup>H NMR spectrum of [DMPEA·Li(TMP)Zn(Me)<sub>2</sub>] **4.5** in C<sub>6</sub>D<sub>6</sub> solution.

This was duly confirmed by a variable-temperature NMR study. Reducing the temperature from 300 K to 210 K causes the single resonance for the Me groups to split into two separate resonances (Figure 4.18), consistent with a 'freezing out' of the structure in solution whereby the two Me groups now sit in different environments consistent with the solid state picture established by the X-ray

diffraction determination. Likewise, the room temperature  $^{13}\text{C}$  NMR spectrum reveals two distinct TMP Me resonances (located at 31.5 and 36.7 ppm) whilst only the one for those attached to zinc (located at -6.5 ppm). Though seen at different chemical shifts, the same pattern is observed for resonances of **4.5** in both deuterated cyclohexane and toluene solutions (Figure 4.19 and Figure 4.20 respectively).

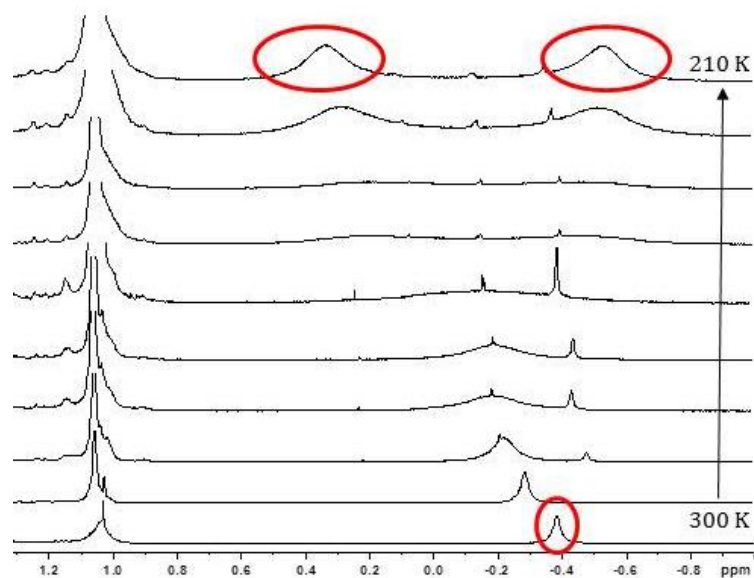


Figure 4.18. Variable temperature  $^1\text{H}$  NMR study of **4.5** in  $d_8$ -toluene solution showing decoalescence of the  $\text{Zn}(\text{Me})_2$  resonance (circled in red) as the temperature is reduced.



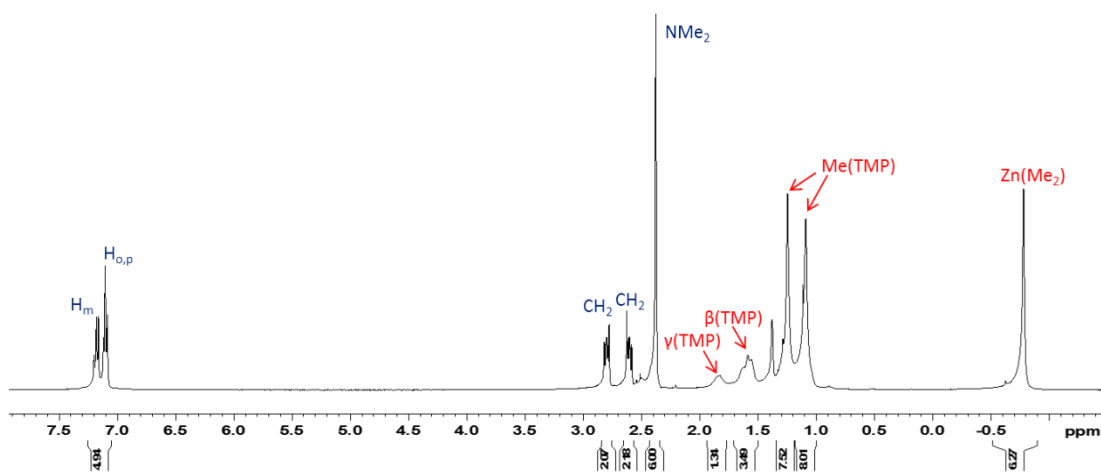


Figure 4.19. <sup>1</sup>H NMR spectrum of [DMPEA·Li(TMP)Zn(Me)<sub>2</sub>] 4.5 in C<sub>6</sub>D<sub>12</sub> solution.

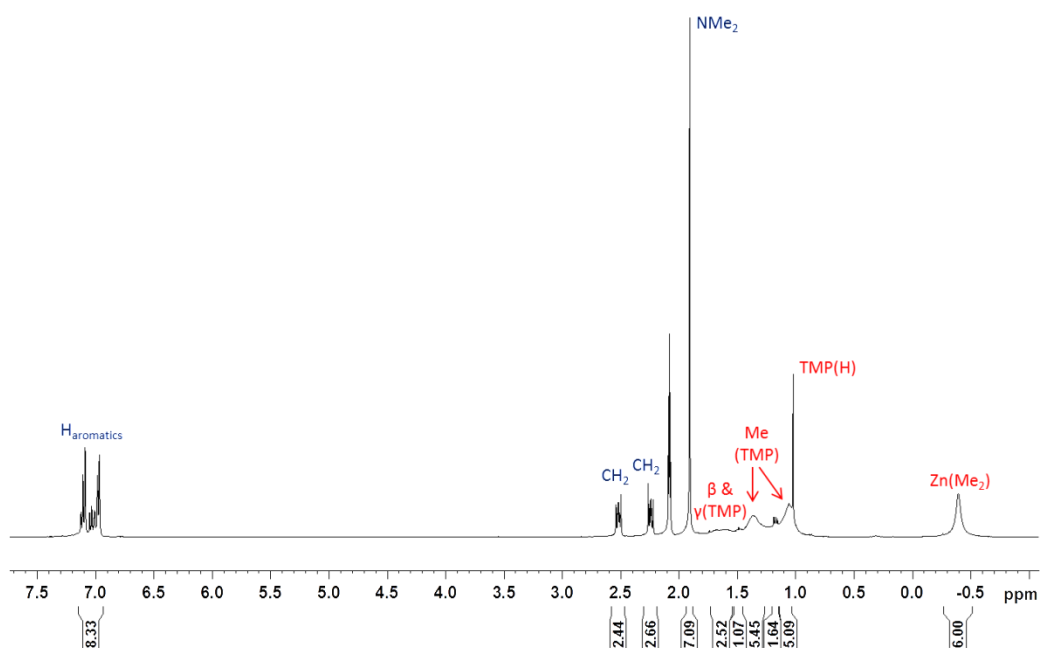


Figure 4.20. <sup>1</sup>H NMR spectrum of [DMPEA·Li(TMP)Zn(Me)<sub>2</sub>] 4.5 in d<sub>8</sub>-toluene solution.

#### 4.3.4 Is [DMPEA·Li(TMP)Zn(Me)<sub>2</sub>] a Pre-Metallation Complex?

If Lewis acid – Lewis base complex **4.5** is a genuine “pre-metallation complex”, metallation has to be achievable after the coordination of DMPEA to the bimetallic reagent. To explore whether this was possible, freshly prepared crystals of **4.5** were dissolved in hexane solution and heated to reflux for eight hours. Next an aliquot of the resulting solution was examined by <sup>1</sup>H NMR spectroscopy in C<sub>6</sub>D<sub>6</sub> solution. While this spectrum revealed the trace presence of resonances corresponding to the products formed as a result of metallation followed by elimination (that is, styrene at 5.05, 5.58 and 6.55 ppm and an NMe<sub>2</sub> fragment at 2.43 ppm) the most prominent resonances were unreacted **4.5**. Given that the metallation-elimination sequence of DMPEA with the sodium di-*t*-butylzincate **1.3** is essentially spontaneous at 0 °C, this failure to observe any significant quantity of metallation even after a sustained period of heating the reaction solution to reflux appears to negate the possibility that **4.5** is an intermediate en route to the cleaving of a benzylic hydrogen atom from DMPEA and the concomitant capture of the eliminated Me<sub>2</sub>N fragment. Two possible explanations spring to mind for this lack of activity. It could be that this dimethylzincate system is just too weakly basic to deprotonate DMPEA to any significant extent; alternatively because the DMPEA molecule is tied up in a dative contact with the lithium centre it may be inaccessible for deprotonation, that is, the stereochemistry could be wrong for the four-centred (NCCLi) transition state that would facilitate the elimination process. Further experiments point unequivocally towards the second explanation. For example, adding the diamine TMEDA seems to activate the zincate as mixing LiTMP, Me<sub>2</sub>Zn, TMEDA and DMPEA in hexane solution leads to a substantial yield of crystals of the previously alluded to dilithium heterobianionic zincate [(TMEDA)<sub>2</sub>Li<sub>2</sub>ZnMe(NMe<sub>2</sub>)<sub>3</sub>], which proves a deprotonation of DMPEA must have occurred. It can be reasoned that TMEDA being the stronger donor would preferentially bind to the lithium and thus free up the DMPEA for its intermolecular deprotonation. Moreover, taking crystals of **4.5** and dissolving them in bulk THF and monitoring the solution by <sup>1</sup>H NMR studies revealed the

disappearance of DMPEA resonances and the emergence of a Me<sub>2</sub>N resonance (at 2.99 ppm), consistent with a reaction mimicking that involving TMEDA.

## 4.4 Conclusions

This part of the PhD project has extended the cleave and capture concept within heterobimetallic ate chemistry to the important bio-relevant scaffold DMPEA. Three bimetallic mixtures were employed with products from each characterised by NMR spectroscopic and X-ray crystallographic studies. Cleavage of a benzylic CH bond in DMPEA is followed by the elimination and capture of a Me<sub>2</sub>N<sup>-</sup> fragment by the bimetallic Na-Zn, Li-Zn or Li-Al capturing agents. Interestingly, it does not appear to matter whether the initial base operates in a *synergic synchronized* style [as in {TMEDA·Na(TMP)(<sup>t</sup>Bu)Zn(<sup>t</sup>Bu)} **1.3** and {PMDETA·Li(TMP)Zn(<sup>t</sup>Bu)<sub>2</sub>} **4.1**], where the two metals work side-by-side in the same molecule, or in a *synergistic stepwise* style [as in “{THF·Li(TMP)<sub>2</sub>Al(<sup>i</sup>Bu)<sub>2</sub>}” = LiTMP and (TMP)Al(<sup>i</sup>Bu)<sub>2</sub>·THF], where the two metals work in tandem but in separate, non-cocomplexing species, as in each case once deprotonation has occurred the DMPEA Me<sub>2</sub>N fragment is captured. In an unanticipated development while trying to synthesise an isolable derivative of DMPEA metallated in the β-position, DMPEA was captured fully intact by reacting it with the weak base [Li(TMP)Zn(Me)<sub>2</sub>] to realise the novel Lewis acid – Lewis base complex [DMPEA·Li(TMP)Zn(Me)<sub>2</sub>] **4.5**, which was characterised spectroscopically and crystallographically. Complex **4.5** is also the first of its type with no other reported example of DMPEA in the presence of a metal known.

## 4.5 Future Work

Although this project nicely provided examples of the amine DMPEA both prior to and after metallation of it had occurred, it would of course be appealing to try

and trap/stabilise the metallated intermediate of these reactions, whereby the DMPEA has been metallated but has not yet undergone  $\beta$ -elimination. If this was feasible then subsequent quenching could lead to a large number of possible molecules being synthesised – with the potential of being pharmacologically active.

Whilst this project studied solely DMPEA, there are of course many other biorelevant scaffolds, also based on aromatic amines, which could be studied in the same manner as that reported here. For example, Bentley<sup>[7-8]</sup> reports a whole host of categories, such as phenylethylamines, naphthylisoquinolines and benzylisoquinolines that are all pharmacologically active compounds and potential starting building blocks.

With the concept of *cleave and capture chemistry* now firmly established, it would be timely to develop it to its full potential as a unique bimetallic tool. Fundamental to constructing compounds, cleavage of alkyl and vinyl C-H bonds is often hindered by the inherent instability of resultant anions. Metallation of cyclic ethers invariably initiates ring-opening decompositions (for example with THF). Captured molecular fragments could now be screened with a large pool of electrophiles for C-C bond forming utility. For example, the stereogenic centre generated in the  $\alpha$ -THF anion opens up the exciting prospect of enantioselective utilisation, with potentially numerous applications in natural product chemistry. Substituting TMP by a chiral amide in the base backbone or TMEDA by chiral 1R,2R-*N,N,N',N'*-tetramethyl-cyclohexane-1,2-diamine are two possible routes to achieving such enantioselectivity. “Synergic sedation”, that is where both metals interact synergically to stabilise a deprotonated anion, should be possible with a myriad of other sensitive compounds. Many cyclic and acyclic ethers, acetals, epoxides, peroxides etc., especially those carrying additional electron-withdrawing functionalities could be targeted. A key general point is that even in cases where lithiation is effective, usually subambient temperatures are needed (especially with strong *ortho* directors). *Cleave and Capture Chemistry* may circumvent this drawback by executing clean metallation at

ambient temperature and have greater metallation site flexibility (eg., at *ortho*, *meta*, or *para* sites).

## 4.6 Experimental

Table 4.2. Crystallographic data and refinement details for compounds **4.2-4.5**.

	<b>4.2</b>	<b>4.3</b>	<b>4.4</b>	<b>4.5</b>
Formula	C <sub>21</sub> H <sub>49</sub> N <sub>4</sub> NaZn	C <sub>19</sub> H <sub>47</sub> N <sub>4</sub> LiZn	C <sub>23</sub> H <sub>50</sub> N <sub>2</sub> OLiAl	C <sub>21</sub> H <sub>39</sub> N <sub>2</sub> LiZn
Formula weight	446.00	403.92	404.57	391.85
Crystal system	Orthorhombic	Orthorhombic	Monoclinic	Monoclinic
Space group	<i>P bca</i>	<i>P bcn</i>	<i>P 21/n</i>	<i>P 21/n</i>
Wavelength/Å	1.54180	0.71073	0.71073	1.54180
<i>a</i> /Å	15.4328(3)	29.1528(10)	13.5126(9)	10.3686(2)
<i>b</i> /Å	18.1148(3)	9.1827(3)	12.4361(8)	9.9831(2)
<i>c</i> /Å	18.7053(3)	18.4451(6)	15.2536(10)	21.6606(4)
$\alpha$ /°	90	90	90	90
$\beta$ /°	90	90	91.834(6)	100.177(2)
$\gamma$ /°	90	90	90	90
Volume/Å <sup>3</sup>	5229.29(16)	4937.8(3)	2562.0(3)	2206.83(7)
<i>Z</i>	8	8	4	4
Refls. collected	5215	5914	6517	10745
$2\theta_{\max}$	72.94	28.7470	29.4143	72.9589
<i>R</i> <sub>int</sub>	0.0292	0.0573	0.0303	0.0000
Goodness of fit	1.093	1.021	1.029	1.086
<i>R</i> [ <i>F</i> <sup>2</sup> > 2σ], <i>F</i>	0.0348	0.0457	0.0419	0.0498
<i>R</i> <sub>w</sub> (all data), <i>F</i> <sup>2</sup>	0.0959	0.1026	0.1132	0.1594

### 4.6.1 Synthesis of [TMEDA·Na(μ-TMP)(μ-NMe<sub>2</sub>)Zn(<sup>*t*</sup>Bu)] **4.2**

The sodium zincate starting material [TMEDA·Na(μ-TMP)(μ-<sup>*t*</sup>Bu)Zn(<sup>*t*</sup>Bu)] was prepared according to the standard literature procedure<sup>[17]</sup> and isolated in crystalline form. To an oven-dried Schlenk tube was added [TMEDA·Na(μ-TMP)(μ-<sup>*t*</sup>Bu)Zn(<sup>*t*</sup>Bu)] (0.46 g, 1 mmol) which was dissolved (with heating) in 10 mL of hexane to give a pale yellow solution. The flask was then cooled to 0°C and immediately *N,N*-dimethylphenylethylamine (0.17 mL, 1 mmol) was introduced. This resulted in the precipitation of a solid. The flask was then

placed into the refrigerator (at 5°C) and after a few days a crop of colourless crystals of **4.2** had formed in solution (0.08 g, 18% yield).

**<sup>1</sup>H NMR (C<sub>6</sub>D<sub>12</sub>, 400.03 MHz, 300K)**  $\delta$  = 2.72 (s, 6H, NMe<sub>2</sub>), 2.32 (s, 4H, CH<sub>2</sub> TMEDA), 2.22 (s, 12H, CH<sub>3</sub> TMEDA), 1.75 (m, 1H,  $\gamma$ -TMP), 1.67 (m, 1H,  $\gamma$ -TMP), 1.48 (m, 2H,  $\beta$ -TMP), 1.14 (s, 6H, CH<sub>3</sub> TMP), 1.10 (m, 2H,  $\beta$ -TMP), 1.05 (s, 9H, <sup>t</sup>Bu), 1.03 ppm (s, 6H, CH<sub>3</sub> TMP).

**<sup>13</sup>C {<sup>1</sup>H} NMR (C<sub>6</sub>D<sub>12</sub>, 100.60 MHz, 300K)**  $\delta$  = 58.2 (CH<sub>2</sub> TMEDA), 52.4 ( $\alpha$ -TMP), 47.0 (NMe<sub>2</sub>), 46.4 (CH<sub>3</sub> TMEDA), 41.0 ( $\beta$ -TMP), 36.8 (CH<sub>3</sub> TMP), 35.10 (CH<sub>3</sub> TMP), 35.0 (CH<sub>3</sub>, <sup>t</sup>Bu), 22.9 (<sup>t</sup>Bu quaternary), 20.5 ppm ( $\gamma$ -TMP).

#### 4.6.2 Synthesis of [PMDETA·Li( $\mu$ -NMe<sub>2</sub>)Zn(<sup>t</sup>Bu)<sub>2</sub>] **4.3**

The lithium di-*t*-butyl zincate compound [PMDETA·Li(TMP)Zn(<sup>t</sup>Bu)<sub>2</sub>] was first prepared *in situ* before *N,N*-dimethylphenylethylamine was added. A solution of <sup>t</sup>Bu<sub>2</sub>Zn (0.36 g, 2 mmol) in hexane (10 mL) was transferred via a cannula into a separate Schlenk tube containing a freshly prepared solution of LiTMP in hexane (10 mL) [prepared from a mixture of <sup>n</sup>BuLi (1.6 M in hexanes, 1.25 mL, 2 mmol) and TMP(H) (0.34 mL, 2 mmol)]. The resulting colourless solution was allowed to stir for 10 minutes before PMDETA (0.42 mL, 2 mmol) was injected into it, producing a yellow oil-like substance within the flask. *N,N*-Dimethylphenylethylamine (0.34 mL, 2 mmol) was then added and the flask moved to the freezer (at -28°C) for storage. After a few weeks, small star-shaped orange crystals of **4.3** had formed on an orange oily substance present in the bottom of the Schlenk tube (a yield was unattainable).

**<sup>1</sup>H NMR (C<sub>6</sub>D<sub>12</sub>, 400.03 MHz, 300K)**  $\delta$  = 2.72 (s, 6H, NMe<sub>2</sub>), 2.37 (s, 3H, NMe PMDETA), 2.34 (bs, 8H, CH<sub>2</sub> PMDETA), 2.29 (s, 12H, NMe<sub>2</sub> PMDETA), 1.01 ppm (s, 18H, <sup>t</sup>Bu<sub>2</sub>Zn).

**<sup>13</sup>C {<sup>1</sup>H} NMR (C<sub>6</sub>D<sub>12</sub>, 100.60 MHz, 300K)**  $\delta$  = 58.7 (CH<sub>2</sub> PMDETA), 48.5 (NMe<sub>2</sub>), 46.6 (NMe<sub>2</sub> PMDETA), 46.5 (NMe PMDETA), 35.3 ppm (<sup>t</sup>Bu<sub>2</sub>Zn).

$^7\text{Li}$  ( $\text{C}_6\text{D}_{12}$ , 155.50 MHz, 300K)  $\delta = 0.44$  ppm (s), with an unidentified smaller signal at 1.31 ppm.

#### 4.6.3 Synthesis of $[\text{THF}\cdot\text{Li}(\mu\text{-TMP})(\mu\text{-NMe}_2)\text{Al}(i\text{Bu})_2]$ 4.4

In an oven-dried Schlenk tube the bimetallic mixture “[ $\text{THF}\cdot\text{Li}(\text{TMP})_2\text{Al}(i\text{Bu})_2$ ]” was prepared *in situ* (in a hexane solution) according to a literature method.<sup>[63]</sup> *N,N*-Dimethylphenylethylamine (0.17 mL, 1 mmol) was then added and the reaction mixture allowed to stir for 10 minutes. The solution was then concentrated to half the volume by removing some solvent *in vacuo* and the flask transferred to the freezer (at  $-69^\circ\text{C}$ ). A crop of colourless crystals of **4.4** was deposited after a few weeks storage (0.07 g, 16% yield).

$^1\text{H}$  NMR ( $\text{C}_6\text{D}_{12}$ , 400.03 MHz, 300K)  $\delta = 3.89$  (m, 4H,  $\text{OCH}_2$  THF), 2.44 (s, 6H,  $\text{NMe}_2$ ), 2.01 (m, 2H,  $\text{CH}_2\text{CH}(\text{CH}_3)_2$ ), 1.96 (m, 4H,  $\text{CH}_2$  THF), 1.90 (bs, 1H,  $\gamma$ -TMP), 1.60 (bs, 2H,  $\beta$ -TMP), 1.45 (bs, 1H,  $\gamma$ -TMP), 1.32 (s, 12H,  $\text{CH}_3$  TMP), 0.99 (m, 12H,  $\text{CH}_2\text{CH}(\text{CH}_3)_2$ ), 0.91 (bs, 2H,  $\beta$ -TMP), 0.18 ppm (m, 4H,  $\text{CH}_2\text{CH}(\text{CH}_3)_2$ ).

$^{13}\text{C}$   $\{^1\text{H}\}$  NMR ( $\text{C}_6\text{D}_{12}$ , 100.60 MHz, 300K)  $\delta = 69.7$  ( $\text{OCH}_2$  THF), 52.2 ( $\alpha$ -TMP), 45.9 ( $\beta$ -TMP), 42.4 ( $\text{NMe}_2$ ), 30.0 (overlapping  $\text{CH}_3$  TMP and  $\text{CH}_2\text{CH}(\text{CH}_3)_2$ ), 29.3 ( $\text{CH}_2\text{CH}(\text{CH}_3)_2$ ), 28.0 ( $\text{CH}_2\text{CH}(\text{CH}_3)_2$ ), 27.8 ( $\text{CH}_2\text{CH}(\text{CH}_3)_2$ ), 26.0 [ $\text{CH}_2$  THF (under solvent peak)], 19.0 ppm ( $\gamma$ -TMP).

$^7\text{Li}$  ( $\text{C}_6\text{D}_{12}$ , 155.50 MHz, 300K)  $\delta = 1.22$  ppm (s).

#### 4.6.4 Synthesis of $[\text{DMPEA}\cdot\text{Li}(\mu\text{-TMP})\text{Zn}(\text{Me})_2]$ 4.5

$\text{Me}_2\text{Zn}$  (1.0 M in heptane, 2 mL, 2 mmol) was delivered dropwise to a freshly prepared solution of  $\text{LiTMP}$  in hexane (10 mL) [prepared from a mixture of  $n\text{BuLi}$  (1.6 M in hexanes, 1.25 mL, 2 mmol) and  $\text{TMP}(\text{H})$  (0.34 mL, 2 mmol)] resulting in the immediate precipitation of a white solid. *N,N*-Dimethylphenylethylamine (0.34 mL, 2 mmol) was then added resulting in the dissolution of the white solid to give a homogeneous yellow solution. After a

couple of minutes stirring a white solid precipitated from solution which upon gentle heating dissolved to give again a homogeneous solution. The Schlenk tube was then placed in a Dewar flask of hot water and allowed to cool to room temperature. Storage of the solution overnight in the freezer (at -28°C) provided a crop of white needles of **4.5**, which were suitable for X-ray crystallographic analysis [0.56 g, 71% yield].

**$^1\text{H}$  NMR ( $\text{C}_6\text{D}_6$ , 400.03 MHz, 300 K)**  $\delta$ =7.15 (m, 2H,  $\text{H}_{\text{meta}}$  DMPEA), 7.08 (m, 1H,  $\text{H}_{\text{para}}$  DMPEA), 7.00 (m, 2H,  $\text{H}_{\text{ortho}}$  DMPEA), 2.51 (m, 2H,  $\text{NCH}_2$  DMPEA), 2.22 (m, 2H,  $\text{PhCH}_2$  DMPEA), 1.94 (bs, 1H,  $\gamma$ -TMP), 1.82 (s, 6H,  $\text{NMe}_2$  DMPEA), 1.73 (bs, 1H,  $\gamma$ -TMP), 1.65 (bs, 2H,  $\beta$ -TMP), 1.46 (s, 6H,  $\text{CH}_3$  TMP), 1.13 (bs, 2H,  $\beta$ -TMP), 1.08 (s, 6H,  $\text{CH}_3$  TMP), -0.24 ppm (s, 6H,  $\text{Me}_2\text{Zn}$ ).

**$^{13}\text{C}$   $\{^1\text{H}\}$  NMR ( $\text{C}_6\text{D}_6$ , 100.60 MHz, 300 K)**  $\delta$ =138.9 ( $\text{C}_{\text{ipso}}$  DMPEA), 128.9 ( $\text{C}_{\text{meta}}$  DMPEA), 128.8 ( $\text{C}_{\text{ortho}}$  DMPEA), 126.8 ( $\text{C}_{\text{para}}$  DMPEA), 62.0 ( $\text{NCH}_2$  DMPEA), 53.4 ( $\alpha$ -TMP), 45.5 ( $\text{NMe}_2$  DMPEA), 41.1 ( $\beta$ -TMP), 36.7 ( $\text{CH}_3$  TMP), 33.5 ( $\text{PhCH}_2$  DMPEA), 31.5 ( $\text{CH}_3$  TMP), 20.0 ( $\gamma$ -TMP), -6.5 ppm ( $\text{Me}_2\text{Zn}$ ).

**$^7\text{Li}$  ( $\text{C}_6\text{D}_6$ , 155.50MHz, 300 K)**  $\delta$ =1.55 ppm (s).

**Elemental analysis calc (%)** C 64.35, H 10.03, N 7.15; **found:** C 64.22, H 10.16, N 7.41.



## 4.7 Bibliography

- [1] *Organo-di-Metallic Compounds (or Reagents)*, Vol. 47, Springer, Switzerland, **2014**.
- [2] L. Lochmann, J. Pospisil, J. Vodnansky, J. Trekoval, D. Lim, *Collect. Czech. Chem. Commun.* **1965**, 30, 2187-2195.
- [3] M. Schlosser, *J. Organomet. Chem.* **1967**, 8, 9-16.
- [4] M. Schlosser, S. Strunk, *Tetrahedron Lett.* **1984**, 25, 741-744.
- [5] C. Margot, H. Matsuda, M. Schlosser, *Tetrahedron* **1990**, 46, 2425-2430.
- [6] C. Unkelbach, H. S. Rosenbaum, C. Strohmman, *Chem. Commun.* **2012**, 48, 10612-10614.
- [7] K. W. Bentley, *Nat. Prod. Rep.* **1996**, 13, 127-150.
- [8] K. W. Bentley, *Nat. Prod. Rep.* **1997**, 14, 387-411.
- [9] B. E. Maryanoff, D. F. Mccomsey, H. Winston, *EP 0656002 (B1)*, **2000**.
- [10] K. Jimbow, *US 5395611*, **1995**.
- [11] K. Kojima, K. Koyama, S. Amemiya, M. Iwata, *US 5389626*, **1995**.
- [12] T. Sengupta, K. P. Mohanakumar, *Neurochem. Int.* **2010**, 57, 637-646.
- [13] R. E. Mulvey, *Dalton Trans.* **2013**, 42, 6676-6693.
- [14] A. R. Kennedy, J. Klett, R. E. Mulvey, D. S. Wright, *Science* **2009**, 326, 706-708.
- [15] R. B. Bates, D. E. Potter, L. M. Kroposki, *J. Org. Chem.* **1972**, 37, 560-562.
- [16] R. E. Mulvey, V. L. Blair, W. Clegg, A. R. Kennedy, J. Klett, L. Russo, *Nature Chem.* **2010**, 2, 588-591.
- [17] P. C. Andrikopoulos, D. R. Armstrong, H. R. L. Barley, W. Clegg, S. H. Dale, E. Hevia, G. W. Honeyman, A. R. Kennedy, R. E. Mulvey, *J. Am. Chem. Soc.* **2005**, 127, 6184-6185.
- [18] D. R. Armstrong, W. Clegg, S. H. Dale, E. Hevia, L. M. Hogg, G. W. Honeyman, R. E. Mulvey, *Angew. Chem. Int. Ed.* **2006**, 45, 3775-3778.
- [19] W. Clegg, S. H. Dale, R. W. Harrington, E. Hevia, G. W. Honeyman, R. E. Mulvey, *Angew. Chem. Int. Ed.* **2006**, 45, 2374-2377.
- [20] W. Clegg, S. H. Dale, E. Hevia, L. M. Hogg, G. W. Honeyman, R. E. Mulvey, C. T. O'Hara, *Angew. Chem. Int. Ed.* **2006**, 45, 6548-6550.
- [21] D. R. Armstrong, W. Clegg, S. H. Dale, D. V. Graham, E. Hevia, L. M. Hogg, G. W. Honeyman, A. R. Kennedy, R. E. Mulvey, *Chem. Commun.* **2007**, 598-600.
- [22] B. Conway, E. Hevia, A. R. Kennedy, R. E. Mulvey, *Chem. Commun.* **2007**, 2864-2866.
- [23] W. Clegg, S. H. Dale, E. Hevia, L. M. Hogg, G. W. Honeyman, R. E. Mulvey, C. T. O'Hara, L. Russo, *Angew. Chem. Int. Ed.* **2008**, 47, 731-734.
- [24] D. R. Armstrong, J. García-Alvarez, D. V. Graham, G. W. Honeyman, E. Hevia, A. R. Kennedy, R. E. Mulvey, *Chem. Eur. J.* **2009**, 15, 3800-3807.
- [25] D. R. Armstrong, L. Balloch, W. Clegg, S. H. Dale, P. Garcia-Alvarez, E. Hevia, L. M. Hogg, A. R. Kennedy, R. E. Mulvey, C. T. O'Hara, *Angew. Chem. Int. Ed.* **2009**, 48, 8675-8678.
- [26] L. Balloch, A. R. Kennedy, J. Klett, R. E. Mulvey, C. T. O'Hara, *Chem. Commun.* **2010**, 46, 2319-2321.

- [27] D. R. Armstrong, V. L. Blair, W. Clegg, S. H. Dale, J. Garcia-Alvarez, G. W. Honeyman, E. Hevia, R. E. Mulvey, L. Russo, *J. Am. Chem. Soc.* **2010**, *132*, 9480-9487.
- [28] L. Balloch, A. R. Kennedy, R. E. Mulvey, T. Rantanen, S. D. Robertson, V. Snieckus, *Organometallics* **2011**, *30*, 145-152.
- [29] D. R. Armstrong, L. Balloch, E. Hevia, A. R. Kennedy, R. E. Mulvey, C. T. O'Hara, S. D. Robertson, *Beilstein J. Org. Chem.* **2011**, *7*, 1234-1248.
- [30] L. Balloch, A. R. Kennedy, R. E. Mulvey, S. D. Robertson, *Acta Crystallogr C* **2011**, *67*, M252-M254.
- [31] J. A. Garden, A. R. Kennedy, R. E. Mulvey, S. D. Robertson, *Chem. Commun.* **2012**, *48*, 5265-5267.
- [32] L. Balloch, J. A. Garden, A. R. Kennedy, R. E. Mulvey, T. Rantanen, S. D. Robertson, V. Snieckus, *Angew. Chem. Int. Ed.* **2012**, *51*, 6934-6937.
- [33] E. Hevia, A. R. Kennedy, M. D. McCall, *Dalton Trans.* **2012**, *41*, 98-103.
- [34] D. R. Armstrong, S. E. Baillie, V. L. Blair, N. G. Chabloz, J. Diez, J. Garcia-Alvarez, A. R. Kennedy, S. D. Robertson, E. Hevia, *Chem. Sci.* **2013**, *4*, 4259-4266.
- [35] E. Hevia, G. W. Honeyman, A. R. Kennedy, R. E. Mulvey, *J. Am. Chem. Soc.* **2005**, *127*, 13106-13107.
- [36] D. R. Armstrong, J. A. Garden, A. R. Kennedy, R. E. Mulvey, S. D. Robertson, *Angew. Chem. Int. Ed.* **2013**, *52*, 7190-7193.
- [37] Y. Kondo, M. Shilai, M. Uchiyama, T. Sakamoto, *J. Am. Chem. Soc.* **1999**, *121*, 3539-3540.
- [38] T. Imahori, M. Uchiyama, T. Sakamoto, Y. Kondo, *Chem. Commun.* **2001**, 2450-2451.
- [39] M. Uchiyama, Y. Matsumoto, D. Nobuto, T. Furuyama, K. Yamaguchi, K. Morokuma, *J. Am. Chem. Soc.* **2006**, *128*, 8748-8750.
- [40] M. Uchiyama, Y. Matsumoto, S. Usui, Y. Hashimoto, K. Morokuma, *Angew. Chem. Int. Ed.* **2007**, *46*, 926-929.
- [41] H. J. Seo, S. K. Namgoong, *Tetrahedron Lett.* **2012**, *53*, 3594-3598.
- [42] M. Schlosser, in *Organometallics in Synthesis*, 3rd ed., John Wiley & Sons, Inc, New Jersey, **2013**, pp. 121-127.
- [43] G. Simig, M. Schlosser, *Tetrahedron Lett.* **1991**, *32*, 1963-1964.
- [44] L. Yang, D. R. Powell, R. P. Houser, *Dalton Trans.* **2007**, 955-964.
- [45] C. R. Groom, F. H. Allen, *Angew. Chem. Int. Ed.* **2014**, *53*, 662-671.
- [46] F. H. Allen, *Acta Crystallogr B* **2002**, *58*, 380-388.
- [47] D. R. Armstrong, W. Clegg, S. H. Dale, J. García-Alvarez, R. W. Harrington, E. Hevia, G. W. Honeyman, A. R. Kennedy, R. E. Mulvey, C. T. O'Hara, *Chem. Commun.* **2008**, 187-189.
- [48] R. Campbell, B. Conway, G. S. Fairweather, P. García-Álvarez, A. R. Kennedy, J. Klett, R. E. Mulvey, C. T. O'Hara, G. M. Robertson, *Dalton Trans.* **2010**, *39*, 511-519.
- [49] R. Campbell, D. Cannon, P. García-Álvarez, A. R. Kennedy, R. E. Mulvey, S. D. Robertson, J. Sassmannshausen, T. Tuttle, *J. Am. Chem. Soc.* **2011**, *133*, 13706-13717.
- [50] W. Clegg, S. H. Dale, D. V. Graham, R. W. Harrington, E. Hevia, L. M. Hogg, A. R. Kennedy, R. E. Mulvey, *Chem. Commun.* **2007**, 1641-1643.

- [51] D. R. Armstrong, C. Dougan, D. V. Graham, E. Hevia, A. R. Kennedy, *Organometallics* **2008**, *27*, 6063-6070.
- [52] W. Clegg, D. V. Graham, E. Herd, E. Hevia, A. R. Kennedy, M. D. McCall, L. Russo, *Inorg. Chem.* **2009**, *48*, 5320-5327.
- [53] R. E. Mulvey, D. R. Armstrong, B. Conway, E. Crosbie, A. R. Kennedy, S. D. Robertson, *Inorg. Chem.* **2011**, *50*, 12241-12251.
- [54] A. G. M. Barrett, M. R. Crimmin, M. S. Hill, P. A. Procopiou, *P R Soc A* **2010**, *466*, 927-963.
- [55] C. Brinkmann, A. G. M. Barrett, M. S. Hill, P. A. Procopiou, *J. Am. Chem. Soc.* **2012**, *134*, 2193-2207.
- [56] A. Hernan-Gomez, T. D. Bradley, A. R. Kennedy, Z. Livingstone, S. D. Robertson, E. Hevia, *Chem. Commun.* **2013**, *49*, 8659-8661.
- [57] C. Glock, F. M. Younis, S. Ziemann, H. Gorus, W. Imhof, S. Kriech, M. Westerhausen, *Organometallics* **2013**, *32*, 2649-2660.
- [58] M. Arrowsmith, M. S. Hill, G. Kociok-Kohn, *Organometallics* **2014**, *33*, 206-216.
- [59] J. Penafiel, L. Maron, S. Harder, *Angew. Chem. Int. Ed.* **2015**, *54*, 201-206.
- [60] W. Clegg, B. Conway, E. Hevia, M. D. McCall, L. Russo, R. E. Mulvey, *J. Am. Chem. Soc.* **2009**, *131*, 2375-2384.
- [61] A. Streitwieser, A. Facchetti, L. Xie, X. Zhang, E. C. Wu, *J. Org. Chem.* **2012**, *77*, 985-990.
- [62] H. Ahlbrecht, G. Schneider, *Tetrahedron* **1986**, *42*, 4729-4741.
- [63] E. Crosbie, P. García-Álvarez, A. R. Kennedy, J. Klett, R. E. Mulvey, S. D. Robertson, *Angew. Chem. Int. Ed.* **2010**, *49*, 9388-9391.
- [64] B. Conway, E. Crosbie, A. R. Kennedy, R. E. Mulvey, S. D. Robertson, *Chem. Commun.* **2012**, *48*, 4674-4676.
- [65] B. Conway, J. Garcia-Alvarez, E. Hevia, A. R. Kennedy, R. E. Mulvey, S. D. Robertson, *Organometallics* **2009**, *28*, 6462-6468.
- [66] D. R. Armstrong, E. Crosbie, E. Hevia, R. E. Mulvey, D. L. Ramsay, S. D. Robertson, *Chem. Sci.* **2014**, *5*, 3031-3045.
- [67] M. Uchiyama, H. Naka, Y. Matsumoto, T. Ohwada, *J. Am. Chem. Soc.* **2004**, *126*, 10526-10527.
- [68] H. Naka, M. Uchiyama, Y. Matsumoto, A. E. H. Wheatley, M. McPartlin, J. V. Morey, Y. Kondo, *J. Am. Chem. Soc.* **2007**, *129*, 1921-1930.
- [69] H. Naka, J. V. Morey, J. Haywood, D. J. Eisler, M. McPartlin, F. Garcia, H. Kudo, Y. Kondo, M. Uchiyama, A. E. H. Wheatley, *J. Am. Chem. Soc.* **2008**, *130*, 16193-16200.
- [70] R. E. Mulvey, *Chem. Soc. Rev.* **1991**, *20*, 167-209.
- [71] E. Weiss, *Angew. Chem. Int. Ed.* **1993**, *32*, 1501-1523.
- [72] A. E. H. Wheatley, *New J. Chem.* **2004**, *28*, 435-443.
- [73] T. Harada, *The Chemistry of Organozincate Compounds*, Wiley, Chichester, **2006**.
- [74] H. R. L. Barley, W. Clegg, S. H. Dale, E. Hevia, G. W. Honeyman, A. R. Kennedy, R. E. Mulvey, *Angew. Chem. Int. Ed.* **2005**, *44*, 6018-6021.
- [75] E. Weiss, G. Hencken, *J. Organomet. Chem.* **1970**, *21*, 265-268.
- [76] E. Weiss, E. A. C. Lucken, *J. Organomet. Chem.* **1964**, *2*, 197-205.

- [77] J. Bacsá, F. Hanke, S. Hindley, R. Odedra, G. R. Darling, A. C. Jones, A. Steiner, *Angew. Chem. Int. Ed.* **2011**, *50*, 11685-11687.
- [78] D. V. Graham, E. Hevia, A. R. Kennedy, R. E. Mulvey, *Organometallics* **2006**, *25*, 3297-3300.

## **Chapter 5**

### **Structurally Defined Zincated and Aluminated Complexes of Ferrocene made by Alkali-Metal- Synergistic Syntheses**

## 5.1 Aims

The aim of the work described in this chapter was to attempt to extend the alkali-metal-mediated metallation (AMMM) chemistry of ferrocene previously described for magnesium (AMMMg) to alkali-metal-mediated zincation (AMMZn) and alkali-metal-mediated alumination (AMMAI).

Specific objectives within this overarching aim were to:

- Determine the stoichiometric dependence of deprotonation reactions between the zincate base TMEDA·Na(TMP)(<sup>t</sup>Bu)Zn(<sup>t</sup>Bu) and ferrocene.
- Crystallise any zincated ferrocene products and elucidate their structures in solution by NMR spectroscopy and in the solid state by X-ray crystallography.
- Explore the trans-metal-trapping chemistry of ferrocene with the synergistic partnership of LiTMP and (TMP)Al(<sup>t</sup>Bu)<sub>2</sub>.
- Crystallise any lithiated/aluminium-trapped ferrocene products and elucidate their structures in solution by NMR spectroscopy and in the solid state by X-ray crystallography.
- Compare and contrast the zincation and alumination methodologies especially with respect to polymetallation.

## 5.2 Introduction

Alkali-Metal-Mediated Metallation (AMMM) covered in detail in Chapter 1 is a special type of metallation (C-H to C-metal exchange) reaction where the metal performing the deprotonation is a low electropositive metal, most notably magnesium, zinc or aluminium, which generally forms low polarity metal-carbon bonds of low basicity unable to perform the metallation unless an alkali metal is also present.<sup>[1-2]</sup> This mediation by the higher electropositive alkali metal frequently occurs through the formation of metallate (usually abbreviated to “ate”) complexes which have various formulas of which  $[(AM)^+(M^xR_{x+1})^-]$  (AM = alkali metal, M = secondary metal, R = anion) is one of the most common.<sup>[3-4]</sup> Although Nobel Laureate<sup>[5]</sup> Wittig spotted such cooperative metal-metal’ effects as long ago as 1951 in his study of bimetallic phenyl complexes (such as  $LiZnPh_3$  and  $LiMgPh_3$ ),<sup>[6]</sup> significant numbers of these cooperative compounds/reactions and a modicum of understanding have really only come to light in the past ten or so years through the studies of a number of research groups of which those of Knochel,<sup>[7]</sup> Mongin,<sup>[8-9]</sup> Uchiyama and Wheatley,<sup>[10-15]</sup> and Mulvey have been particularly conspicuous.<sup>[16-17]</sup> The most intriguing cases show that combining two distinct organometallic compounds,  $AM(R)$  and  $M(R')_2$  together into a single bimetallic compound (in contacted or solvent-separated form) can produce a reagent which in combining the higher reactivity of the alkali metal component with the better selectivity and functional group tolerance of the secondary metal (e.g., Mg, Zn or Al) can perform deprotometallation (that is, replacing an acidic hydrogen atom on carbon by a metal atom) reactions at room temperature (contrast the sub-ambient protocols necessary in many organolithium reactions<sup>[18]</sup>) in non-polar solvents. Neither homometallic reagent operating independently can replicate these reactions under the same conditions. However, not only can AMMM outperform existing homo-metallation protocols, it can also realise unique metallation reactions. These might include metallation at typically unreactive or remote positions; or multiple metallation of substrates generally strongly resistant to more than one metallation event (corresponding multilithiated aromatic substrates can be unstable due to having too much

charge density within the confines of the multi-carbanion). Recently discovered by the Mulvey/O'Hara group at Strathclyde the most significant examples of the former reactivity are directed *ortho-meta'* and *meta-meta'* dimetallations of a wide variety of substituted arenes (such as anisole and dimethylaniline)<sup>[19]</sup> by  $[\text{Na}_2\text{Mg}(\text{TMP})_3(^n\text{Bu})]_2$ , which the authors refer to as pre-inverse crown template bases.<sup>[20]</sup> The latter multiple metallations generally give rise to supramolecular 'inverse crown' structures, that is a polymetallic cationic ring with the single polyanionic substrate <sup>[21]</sup> or multiple monoanionic substrates encapsulated within the core of the cationic ring.<sup>[20]</sup> The term inverse crown is derived from the inverse nature of the positive and negative moieties with respect to the cation-dipole sites in a conventional alkali metal crown ether complex (see Figure 5.1).<sup>[22]</sup> A striking exemplar of this type of chemistry was the unprecedented 1,1',3,3'-tetramagnesiumiation of the iron metallocene ferrocene <sup>[23]</sup> along with that of its heavier group 8 congeners ruthenocene and osmocene,<sup>[24]</sup> with the resulting tetraanions being captured within a  $[\text{Mg}_4\text{Na}_4(\text{N}^i\text{Pr}_2)_8]^{4+}$  16-atom inverse-crown ring (Scheme 5.1). The formation of this tetramagnesiumiated ferrocene crystalline product was dependent on the identity of the secondary amido component within the ate base since substitution of diisopropylamide,  $\text{N}^i\text{Pr}_2$  by TMP resulted in an alternative trinuclear ferrocenophane product in which the three magnesium-joined ferrocene units were only 1,1'-dimetallated (Scheme 5.1).<sup>[25]</sup>

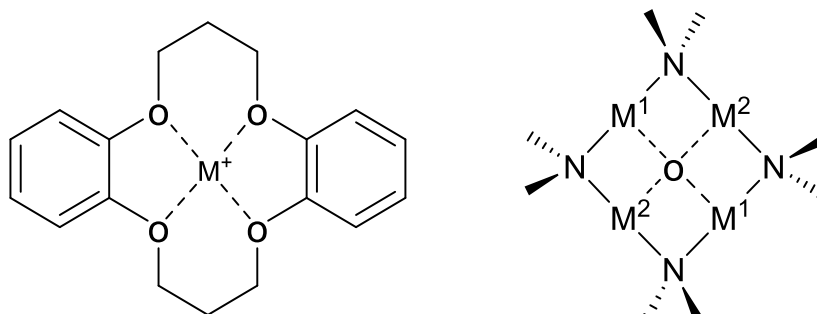
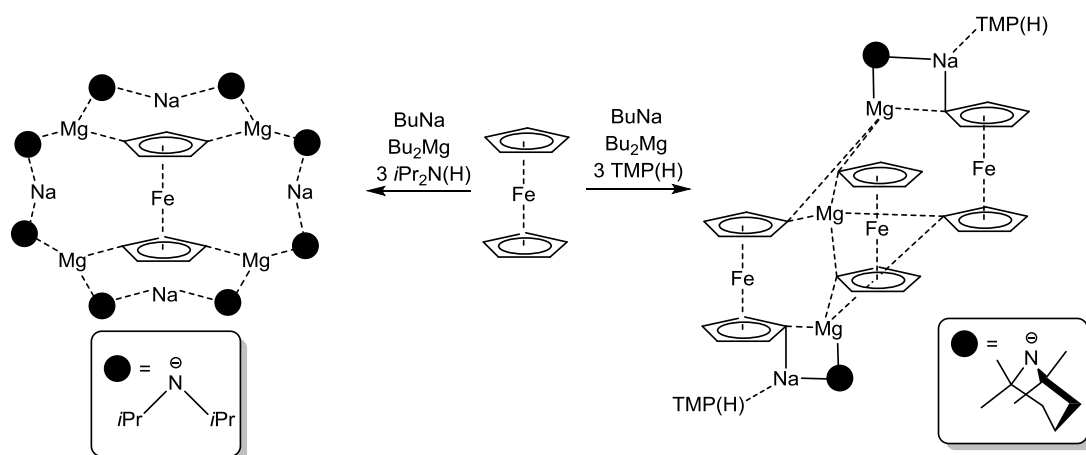


Figure 5.1. ChemDraw representations of a crown-ether complex (LHS) versus an inverse-crown complex (RHS).





Scheme 5.1. Contrasting reactivity of ferrocene with different sodium amidomagnesiate bases.

Prior to these recently described ate-based direct (that is, hydrogen-magnesium) metallations, metallo-ferrocenes containing these lower polarity bond forming metals (e.g., Mg, Zn, Al) have generally been made via salt metathesis methodologies where often the metallo component comes from metal halide starting materials. Figure 5.2 and Figure 5.3 show examples of some ferrocene complexes where their zincation or alumination respectively was achieved by a salt metathesis. Zinc species **A**, **B** and **C** are dinuclear ferrocenophanes either mono or dizincated, **E** and **F** are mononuclear monozincated ferrocenes, while **D** is a trinuclear ferrocenophane held together by a single zinc atom. Mononuclear, dinuclear and trinuclear ferrocenophane examples are also shown for the aluminium species, with **H** catching the eye with the deprotonated C atom of the mononuclear ferrocene binding to two Al centers in a four-atom, three-element AlCAI ring.

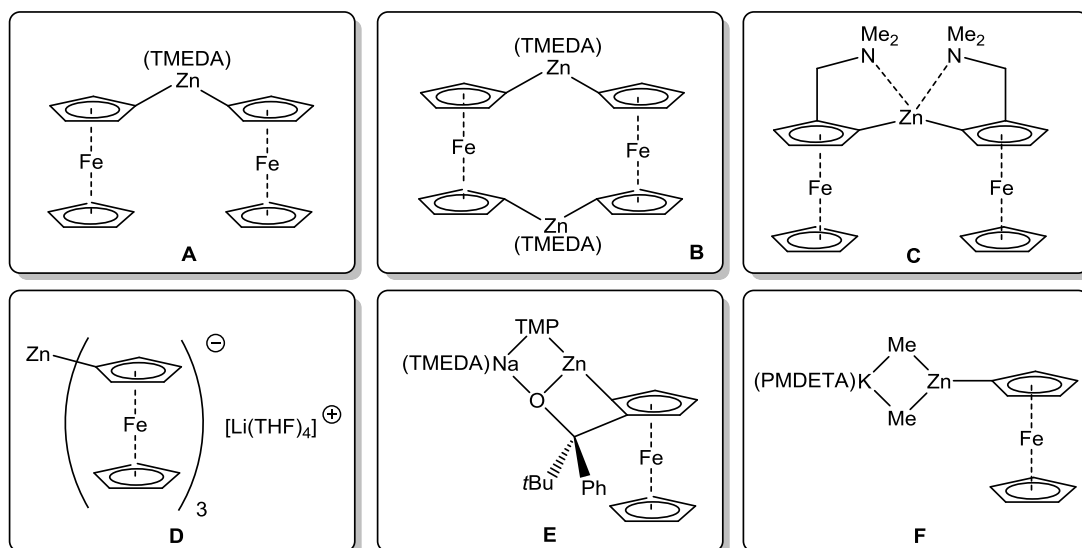


Figure 5.2. ChemDraw representations of a selection of crystallographically characterised zincated ferrocene molecules. References: **A**,<sup>[26]</sup> **B**,<sup>[27]</sup> **C**,<sup>[28]</sup> **D**,<sup>[26]</sup> **E**,<sup>[29]</sup> **F**.<sup>[30]</sup>

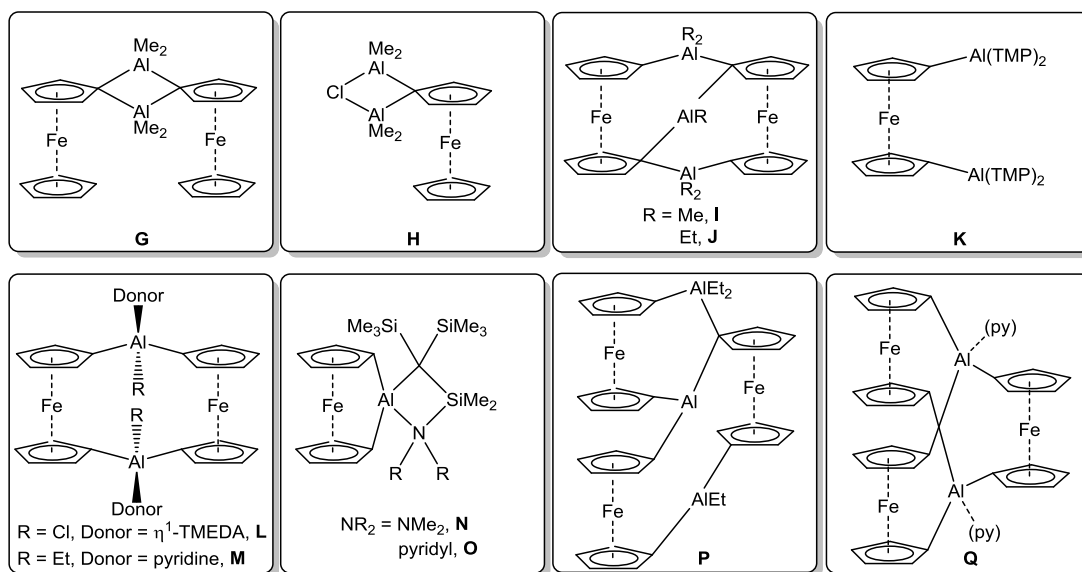


Figure 5.3. ChemDraw representations of a selection of crystallographically characterised aluminated ferrocene molecules. References: **G**,<sup>[31]</sup> **H**,<sup>[32]</sup> **I**,<sup>[33]</sup> **J**,<sup>[34]</sup> **K**,<sup>[35]</sup> **L**,<sup>[36]</sup> **M**,<sup>[37]</sup> **N**,<sup>[38]</sup> **O**,<sup>[39]</sup> **P**,<sup>[40]</sup> **Q**.<sup>[37]</sup>

From a general perspective it should be noted that salt metathesis has been one of the most widely utilized synthetic methodologies for transforming numerous polar organometallic compounds (especially those of lithium, but also to a lesser extent those of sodium and potassium) into derivatives of other metals all across the periodic table. Lappert, who died in 2014, was undoubtedly the World's leading exponent of this approach, having employed salt metathesis to synthesize a galaxy of organometallic compounds including alkyl,<sup>[41]</sup> amido,<sup>[42]</sup> azaallyl<sup>[43]</sup> and metallocenyl examples.<sup>[44-46]</sup>

Often the intermediate before the salt metathesis step is a lithiated ferrocene derivative. Accordingly lithiation of ferrocene has been widely studied. Treating ferrocene with an excess of *n*BuLi at temperatures up to 100°C has been found to generate a mixture of products ranging remarkably from mono- through to octa-lithiated species with the tetra-lithiated species being the most abundant.<sup>[47]</sup> Introducing TMEDA into this reaction shifts the selectivity towards the more anionic tetra-, penta- and hexa- metallated species consistent with the commonly encountered increased reactivity of Li reagents when donor molecules are added into the mixture (discussed in Chapter 1). However it must be stressed that these multilithiated species were not isolated nor characterised in this study. Somewhat counter-intuitively, by turning up the reactivity by moving to the stronger more aggressive bimetallic Lochmann-Schlosser superbase, the metallation of ferrocene was accomplished both in high yields (>90%) and high selectivity (mono-lithiated being the main product) after only 1 hour at -74°C.<sup>[48]</sup>

Two advantages of AMMM are worth pointing out: (i) generally reaction mixtures are homogeneous in contrast to those used in salt metathesis processes (reflecting the ionicity of the metal halide starting materials) and (ii) in the best case AMMM can provide access to compounds inaccessible via salt metathesis (for example the tetramagnesiated group 8 metallocenes alluded to earlier). Of course, functionalized ferrocene derivatives are particularly interesting due to their myriad of uses in diverse areas such as materials,<sup>[49]</sup>

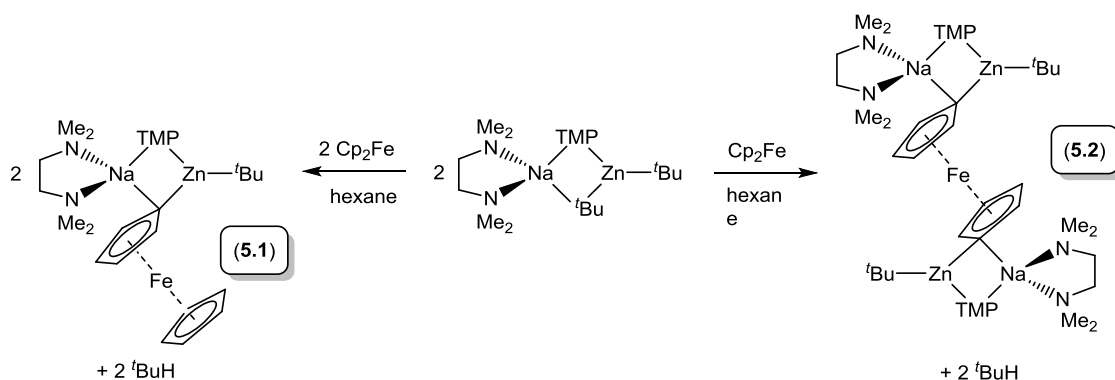
medicinal chemistry,<sup>[50]</sup> bioorganometallic chemistry <sup>[51]</sup> and as specialty ligands for asymmetric catalysis <sup>[52]</sup> amongst others. *Organometallics* even recently dedicated an entire issue to ferrocene entitled *Ferrocene – Beauty and Function*.<sup>[53]</sup> In this project we were therefore keen to examine if these discussed precedented metallation patterns, or indeed any others, could be achievable through application of other common bimetallic ate bases at our disposal and now report our findings herein.

## 5.3 Results and Discussion

It should be noted that compounds **5.1**, **5.2**, **5.4** and **5.5** detailed in the following section had previously been synthesised and crystallographically characterised by previous members of the Mulvey group. However, the characterisation of these unpublished compounds was incomplete, especially lacking NMR spectroscopic and elemental analyses. As a result the compounds were re-synthesised for this project in order to complete the study of these systems with the aim of attaining a more complete picture of the story associated with this body of work.

### 5.3.1 Studies of Sodium Zincate TMEDA·Na(μ-TMP)(μ-<sup>t</sup>Bu)Zn(<sup>t</sup>Bu)

We started our ferrocene ate base studies by investigating the sodium monoamido-bisalkylzincate reagent TMEDA·Na(μ-TMP)(μ-<sup>t</sup>Bu)Zn(<sup>t</sup>Bu) **1.3**, the chemistry of which has been detailed elsewhere in this thesis (see Chapter 1).<sup>[54]</sup> The constituent parts of this reagent, namely <sup>t</sup>Bu<sub>2</sub>Zn, NaTMP and TMEDA are simply mixed together in equimolar quantities to induce a cocomplexation reaction that affords TMEDA·Na(μ-TMP)(μ-<sup>t</sup>Bu)Zn(<sup>t</sup>Bu) *in situ* in hexane solution. A molar equivalent of ferrocene was then introduced into this solution (Scheme 5.2).



Scheme 5.2. Stoichiometric dependent reactions of ferrocene with sodium TMP-zincate.

After some gentle heating of the solution, a crystalline material was deposited upon bench cooling which was subjected to an X-ray crystallographic structure determination (one of the two independent molecules encountered in the unit cell is depicted in Figure 5.4). On the basis of this structural determination it is clear that the bimetallic base had mono-deprotonated (zincated) ferrocene to give a discrete molecular product of formula  $\text{TMEDA}\cdot\text{Na}(\mu\text{-TMP})[\mu\text{-}(\text{C}_5\text{H}_4)\text{Fe}(\text{C}_5\text{H}_5)]\text{Zn}(\text{tBu})$  (**5.1**). The spirocyclic structure consists of a central  $\text{NaNZnC}$  core with a terminal  $\text{tBu}$  group together with a mixed anionic bridge made up of a TMP anion and a monodeprotonated ferrocene anion. TMEDA bidentate chelation of sodium completes the structure. This structure could also be interpreted as a trapezium  $\text{NaNZnC}$  ring with four distinct TMEDA, TMP,  $\text{tBu}$  and ferrocenyl  $[(\text{C}_5\text{H}_4)\text{Fe}(\text{C}_5\text{H}_5)]$  corners. The zinc and sodium atoms lie in distorted trigonal planar and distorted tetrahedral environments respectively with the sum of the three bond angles at zinc being exactly  $360^\circ$  and the  $\tau_4$  value of sodium being 0.69, where a value of 1 represents a perfect tetrahedron and 0 a perfect square planar structure as outlined by Houser *et al.*<sup>[55]</sup> Such distortion from perfect tetrahedral symmetry is enforced since the sodium atom is the common atom of a spirocycle, resulting in a narrowing of these angles, with concomitantly larger non-cyclic angles greater than  $109.5^\circ$ . The central  $\text{NaNZnC}$

ring is heavily distorted due to the mismatch of longer Na-C [2.652(7) Å] and Na-N [2.487(5) Å] bonds and shorter Zn-C [2.057(7) Å] and Zn-N [2.041(5) Å] bonds.

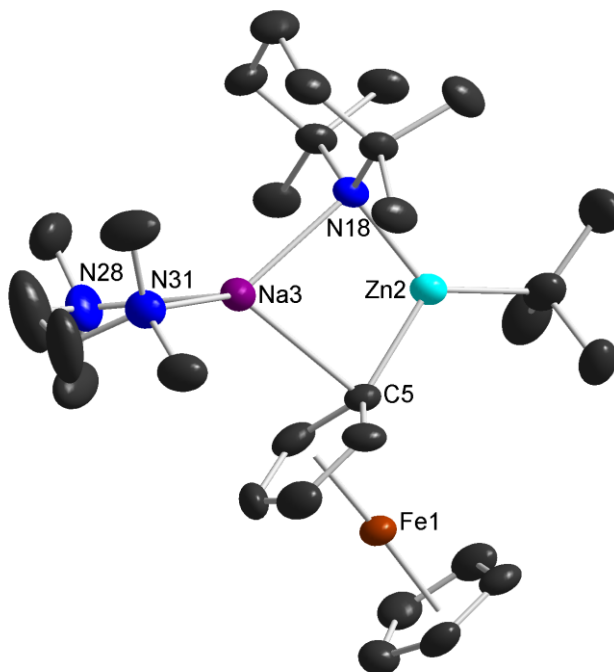


Figure 5.4. Molecular structure of one independent molecule of TMEDA·Na( $\mu$ -TMP)[ $\mu$ -(C<sub>5</sub>H<sub>4</sub>)Fe(C<sub>5</sub>H<sub>5</sub>)]Zn<sup>t</sup>Bu **5.1**. Ellipsoids are drawn at 50% probability level and all H atoms have been omitted for clarity. Selected bond lengths (Å) and bond angles (°): Na3-C5, 2.652(7); Na3-N18, 2.487(5); Na3-N28, 2.587(7); Na3-N31, 2.525(6); Zn2-C5, 2.057(7); Zn2-N18, 2.041(5); C5-Zn2-N18, 104.5(2); Zn2-N18-Na3, 91.0(2); N18-Na3-C5, 78.1(2); Na3-C5-Zn2, 86.2(2).

There is possibly a degree of coordination between the sodium cation and the  $\pi$  system of the deprotonated ferrocene with the distance of sodium to the centroid of the C<sub>5</sub> ring being 2.817 Å. This value reflects the ‘donor’ nature of the C<sub>5</sub>H<sub>4</sub> ring to the Lewis acidic sodium and is marginally longer than that seen in the ferrocene-solvated HMDS dimer [ $\{NaN(SiMe_3)_2\}_2 \cdot (Cp_2Fe)$ ] $_{\infty}$  which has a corresponding distance of 2.791 Å,<sup>[56]</sup> probably as a consequence of the

increased coordination number of **5.1** (4) with respect to that of the  $\text{NaN}(\text{SiMe}_3)_2$  complex (3). More clear-cut cation-anion interactions involving a cyclopentadienyl ring and a sodium cation are distinctly shorter, for example only 2.357 Å for solvent-free  $[\text{NaCp}]_\infty$ .<sup>[57]</sup> Unsurprisingly, solvated NaCp derivatives display longer interactions, such as in dimethoxyethane (2.55 Å),<sup>[58]</sup> 15-crown-5 (2.563 Å),<sup>[58]</sup> THF (2.455 Å),<sup>[59]</sup> ammonia (2.502 Å)<sup>[60]</sup> and TMEDA (2.667 Å) complexes,<sup>[61]</sup> although these are still understandably shorter than that in **5.1**. The Na-Cp interaction has virtually no influence on the distance of the Cp-Fe attachment.<sup>[62]</sup>

The same reaction with  $\text{TMEDA}\cdot\text{Na}(\mu\text{-TMP})(\mu\text{-}^t\text{Bu})\text{Zn}(^t\text{Bu})$  was then repeated but this time only 0.5 molar equivalents of ferrocene per mole of bimetallic base was introduced (Scheme 5.2). This second reaction produced a different crystalline product in  $[\text{TMEDA}\cdot\text{Na}(\mu\text{-TMP})\text{Zn}(^t\text{Bu})]_2(\text{C}_5\text{H}_4)_2\text{Fe}$  (**5.2**). Though having a similar structure to **5.1**, now both cyclopentadienyl rings in **5.2** have been monodeprotonated by the sodium zincate such that the dianionic ferrocene molecule functions as a metal-containing bridge between the two bimetallic units (Figure 5.5). The positions of deprotonation on each ring are staggered such that they are almost orthogonal [the dihedral angle formed between the two  $\text{Zn-C}_{5\text{centroid}}$  planes is  $84.28(2)^\circ$ ] to minimize the steric clashing of the bulky bimetallic frameworks. Formally this product can be regarded as that produced when complex **5.1** is metallated at its intact cyclopentadienyl ring by a further equivalent of the active bimetallic base (though in reality the twofold deprotonation could be sequential and not simultaneous). The distance of the  $\text{C}_5$  centroid to sodium is elongated with respect to that in **5.1** at 2.975 Å (c.f. 2.817 Å in **5.1**) although in this complex the Na- $\text{C}_5\text{H}_4$  interaction is probably better defined as  $\eta^2$  since the distance from sodium to a carbon atom adjacent to the metallated carbon [2.704(6) Å] is virtually identical to that of the Na- $\text{C}_{\text{metallated}}$  distance [2.703(6) Å; indeed on the other metallated ring the distance to the adjacent carbon atom, 2.635(6) Å, is actually shorter than the Na- $\text{C}_{\text{metallated}}$  distance, 2.762(6) Å].

Due in part to steric clashing between the top and bottom ferrocene appendages, the sodium atom of the second deprotonated ring is noticeably displaced compared to that of the first, with a longer bond to the metallated carbon atom [2.762(6) versus 2.703(6) Å for Na3-C4] and to the C<sub>5</sub> centroid [3.190 Å].

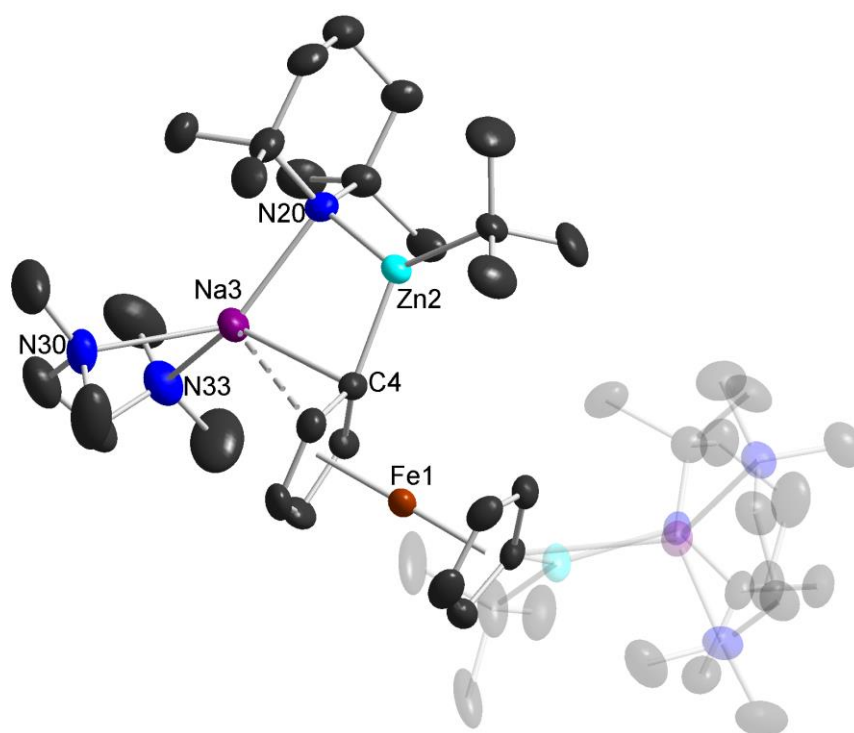


Figure 5.5. Molecular structure of [TMEDA·Na( $\mu$ -TMP)Zn( $t$ Bu)]<sub>2</sub>(C<sub>5</sub>H<sub>4</sub>)<sub>2</sub>Fe **5.2**. Ellipsoids are drawn at 50% probability level and all H atoms and minor disordered components of TMP and  $t$ Bu groups have been omitted for clarity. Selected bond lengths (Å) and bond angles (°) [values in parentheses represent equivalent parameters on the opposite (transparent) side of molecule]: Na3-C4, 2.703(6) [2.762(6)]; Na3-N20, 2.432(4) [2.434(5)]; Na3-N30, 2.602(5) [2.536(6)]; Na3-N33, 2.530(5) [2.537(5)]; Zn2-C4, 2.045(5) [2.052(5)]; Zn2-N20, 2.047(4) [2.052(4)]; C4-Zn2-N20, 105.2(2) [107.2(2)]; Zn2-N20-Na3, 91.7(2) [90.2(2)]; N20-Na3-C4, 78.4(2) [78.7(2)]; Na3-C4-Zn2, 84.3(2) [81.6(2)].



Notably, on the basis of this molecular structure it appears that no ligand redistribution to give either higher order zincate species or homometallic complexes such as seen previously when utilising the related zincate base TMEDA·Li(μ-TMP)(μ-<sup>n</sup>Bu)Zn(<sup>n</sup>Bu) has taken place.<sup>[26]</sup> Neither is there any evidence of intermolecular aggregation (via K-π-arene interactions) as observed when a related potassium zincate base metallates ferrocene.<sup>[30]</sup>

We continued the study by probing the NMR spectra of complexes **5.1** and **5.2** in C<sub>6</sub>D<sub>12</sub> solution. Comparing the <sup>1</sup>H NMR spectra of the two complexes, it was clear that each other was contaminated by traces of the other negating the obtaining of absolute yields. In this regard it is significant that other attempted metallations of ferrocene have led to complex mixtures most notably by Lerner and co-workers when metallating an activated ferrocene molecule, diaminoborylferrocene with more than one molar equivalent of homometallic Mg(TMP)<sub>2</sub>, which contains the same active amido anion as in our zinc and aluminium bases.<sup>[63]</sup> The aliphatic region of the spectra of **5.1** and **5.2** was complicated in each case due to the overlapping multiplets of the TMP resonances. However, the region around 4 ppm was indicative of the outcome of the reaction with the mono-zincated species **5.1** displaying three singlets (resonances were slightly broadened with mutual coupling not noticed) in a 2:2:5 ratio at 3.86, 4.21 and 4.02 ppm respectively, while the di-zincated complex **5.2** displayed two broad singlets in a 4:4 ratio at 3.84 and 4.29 ppm. The <sup>13</sup>C NMR spectra of these complexes were in agreement although despite several attempts involving multiple scans we could not observe a resonance for the metallated carbon atom of the cyclopentadienyl rings.

In an effort to establish whether higher zincation of ferrocene (that is, more than two) could be accessed we changed the reaction stoichiometry to four moles of base per mole of ferrocene. This reaction was carried out in the absence of donor solvent (TMEDA) since the known tetramagnesiated inverse crown complex (*vide supra*) does not contain any neutral Lewis base molecules. This reaction mixture precipitated a fine red powder (complex **5.3**), which was

collected by filtration and washed. Disappointingly, despite several efforts, this powder could not be recrystallized in a quality suitable enough for X-ray crystallographic determination. However, a  $^1\text{H}$  NMR spectrum of this sparingly soluble product was obtained in  $\text{C}_6\text{D}_6$ , which significantly disclosed two sets of three equal integration singlets in the diagnostic region of the spectrum around 4 ppm, in a ratio of 2.5:1 (Figure 5.6). Resolving three different resonances rather than two tenuously suggests that tetrametallation could have taken place as in the tetramagnesiato  $[\text{Fe}(\text{C}_5\text{H}_3)_2]^{4-}$  complex.<sup>[23-24]</sup> To the best of our knowledge no other reaction involving four zinc-hydrogen exchanges on the same substrate has been reported in the literature. The fact that there are two sets of these resonances suggests that there are two isomers present in solution. It is reasonable to assume that these could be an eclipsed and a staggered isomer. Due to the limited solubility of this compound, a useful  $^{13}\text{C}$  NMR spectrum of it (and thus a  $^1\text{H}$ - $^{13}\text{C}$  HSQC spectrum) could not be obtained, precluding definitive assignment of the many overlapping resonances in the aliphatic region.

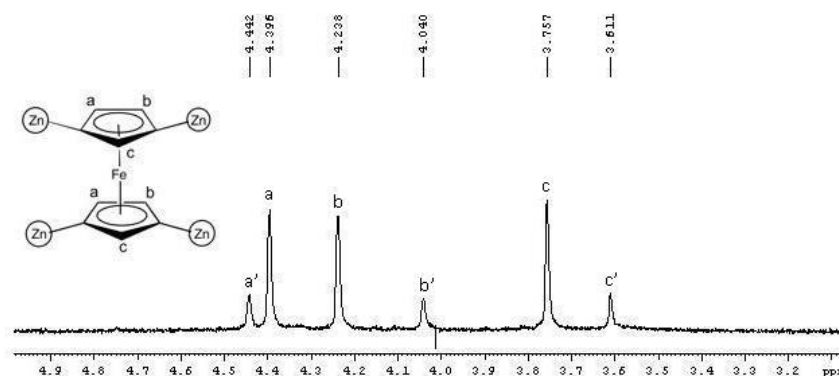
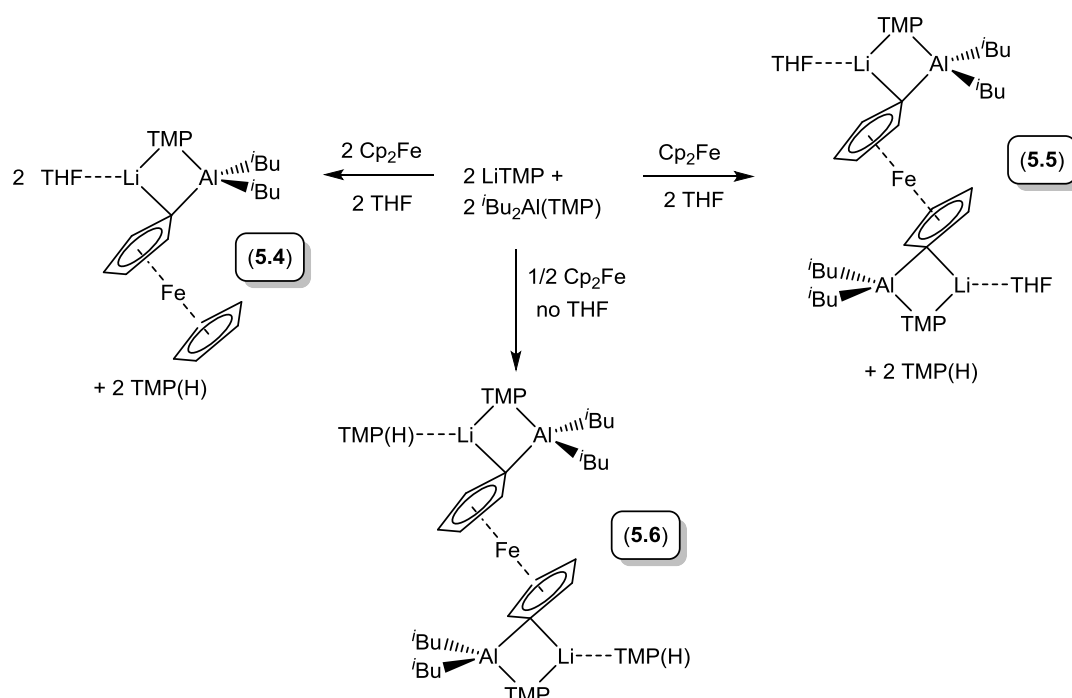


Figure 5.6. Section of  $^1\text{H}$  NMR spectrum of the suspected tetrazincated ferrocene complex **5.3** in  $\text{C}_6\text{D}_6$  solution.

5.3.2 Ferrocene Metallation by Lithium Aluminate “LiAl(TMP)<sub>2</sub><sup>*i*</sup>Bu<sub>2</sub>”

After these sodium zincate studies, we focused on a different combination that we have studied extensively, namely the putative lithium/aluminium pairing previously written as “LiAl(TMP)<sub>2</sub><sup>*i*</sup>Bu<sub>2</sub>”. Originally thought likely to be a highly reactive contacted ion-pair primed for direct aluminations,<sup>[64-70]</sup> in a parallel study<sup>[71]</sup> (summarised in Chapter 3) we recently established it actually exists as a sterically-dictated, non-interacting mixture of its component homometallic compounds, Li(TMP) and <sup>*i*</sup>Bu<sub>2</sub>Al(TMP), which in proton abstraction applications operates via a sequential two-step lithiation/aluminium trans-metal trapping protocol. The first two reactions (Scheme 5.3) of this bimetallic mixture with 1 or 0.5 molar equivalents of ferrocene, respectively, in the presence of stoichiometric THF produced crystalline mono and di-deprotonated ferrocene complexes of formula THF·Li(μ-TMP)[μ-(C<sub>5</sub>H<sub>4</sub>)Fe(C<sub>5</sub>H<sub>5</sub>)]Al(<sup>*i*</sup>Bu)<sub>2</sub> (**5.4**, Figure 5.7) and [THF·Li(μ-TMP)Al(<sup>*i*</sup>Bu)<sub>2</sub>]<sub>2</sub>(C<sub>5</sub>H<sub>4</sub>)<sub>2</sub>Fe (**5.5**, Figure 5.8) respectively.



Scheme 5.3. Stoichiometric dependent lithiation/trans-metal-trapping reactions of ferrocene with the “LiAl(TMP)<sub>2</sub><sup>*i*</sup>Bu<sub>2</sub>” mixture.

As is the case with complexes **5.1** and **5.2**, the secondary metal of lower electropositivity than lithium has replaced the abstracted hydrogen atom with the alkali-metal lying outside the plane of the C<sub>5</sub>H<sub>4</sub> ring, although as the smaller alkali-metal in these cases is less  $\pi$ -philic, it is best described as an  $\eta^1$  interaction. In both cases, the lithium atoms occupy a three-coordinate (1xN; 1xN; 1xO) environment with a bridging N from TMP and an O from neutral THF completing their coordination spheres.

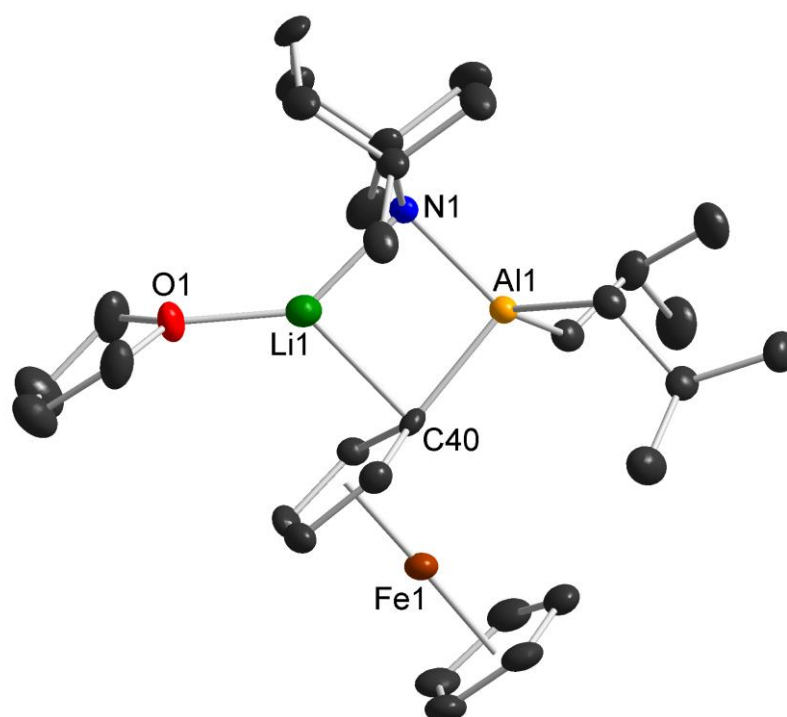


Figure 5.7. Molecular structure of the monoaluminated ferrocene THF·Li( $\mu$ -TMP)[ $\mu$ -(C<sub>5</sub>H<sub>4</sub>)Fe(C<sub>5</sub>H<sub>5</sub>)]Al(*i*Bu)<sub>2</sub> **5.4**. Ellipsoids are drawn at 50% probability level and all H atoms have been omitted for clarity. Selected bond lengths (Å) and bond angles (°): Li1-C40, 2.188(6); Li1-N1, 2.005(5); Li1-O1, 1.866(6); Al1-C40, 2.039(3); Al1-N1, 1.994(2); C40-Al1-N1, 96.1(1); Al1-N1-Li1, 89.3(2); N1-Li1-C40, 91.2(2); Li1-C40-Al1, 83.3(2).

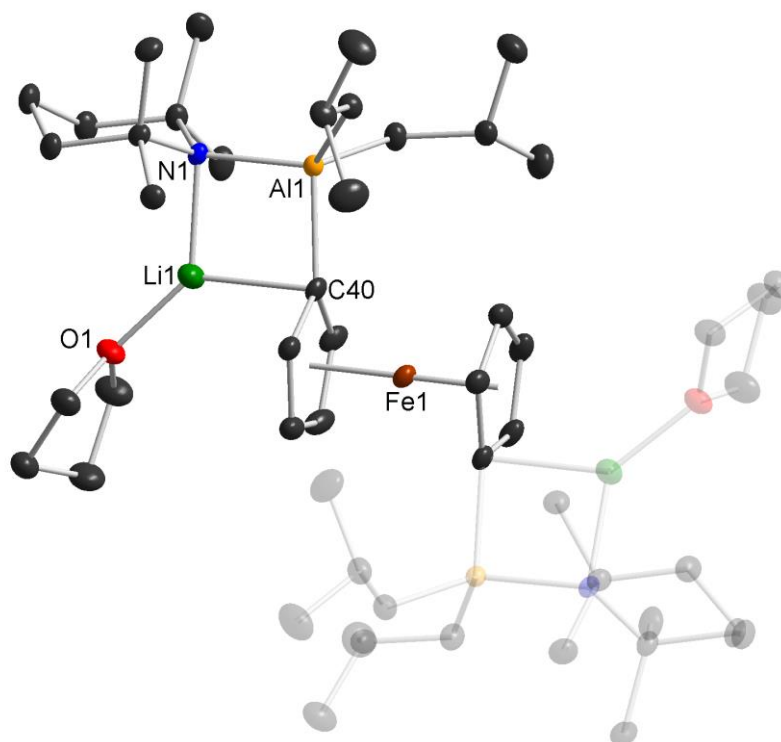
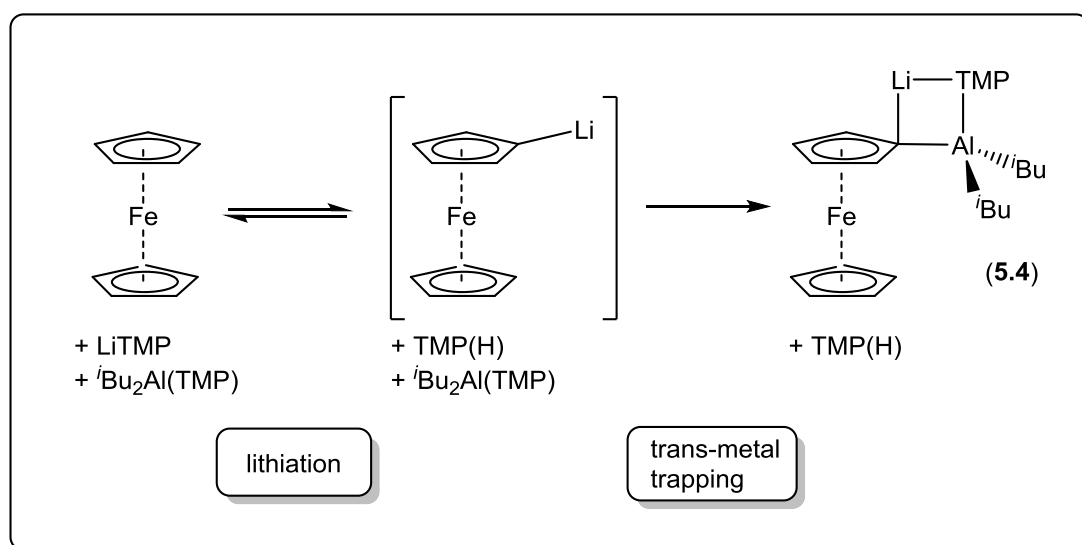


Figure 5.8. Molecular structure of the dialuminated ferrocene  $[\text{THF}\cdot\text{Li}(\mu\text{-TMP})\text{Al}(i\text{Bu})_2]_2(\text{C}_5\text{H}_4)_2\text{Fe}$  **5.5**. Ellipsoids are shown at 50% probability level and all H atoms have been removed for clarity. Symmetry operation to generate second half of structure (shown in transparency form):  $2.5-x, y, 2-z$ . Selected bond lengths ( $\text{\AA}$ ) and angles ( $^\circ$ ): Li1-C40, 2.194(3); Li1-N1, 2.032(2); Li1-O1, 1.884(2); Al1-C40, 2.053(1); Al1-N1, 1.996(1); C40-Al1-N1, 97.3(4); Al1-N1-Li1, 88.2(1); N1-Li1-C40, 91.9(1); Li1-C40-Al1, 82.5(1).

Unsurprisingly the micro environments surrounding the deprotonated ferrocene molecules are similar in complexes **5.4** and **5.5**. Specifically, there is essentially little difference in the dimensions of the four-atom, four-element Li-N-Al-C rings of each as evidenced by comparison of their Al-C [2.039(1) and 2.053(1)  $\text{\AA}$  respectively], Al-N [1.994(2)/1.996(1)  $\text{\AA}$ ], Li-N [2.005(5)/2.032(2)  $\text{\AA}$ ] and Li-C [2.188(6)/2.194(3)  $\text{\AA}$ ] bond distances. In complex **5.5**, the sites of

deprotonation of the cyclopentadienyl rings (that is the emerging Al-C bonds) are perfectly staggered as a reflection of its centrosymmetric nature.

Considering as an example complex **5.4** (although the same principle applies to the second Cp ring to yield **5.5**) the mechanism is, as aforementioned, likely to involve a two-step process of lithiation, which occurs in only a poor yield using Li(TMP) as a metallating agent, followed by trans-metal trapping with the soluble monomer (TMP)Al<sup>i</sup>Bu<sub>2</sub> (Scheme 5.4).



Scheme 5.4. Proposed two-step (i) lithiation, (ii) trans-metal-trapping mechanism for the monoalumination of ferrocene.

Although not directly involved in the first step as it cannot cocomplex with LiTMP nor deprotonate ferrocene, the presence of the aluminium reagent is necessary for the reaction to proceed by mopping up the product on the right hand side of the equilibrium and thus this can be considered a synergistic reaction (some chemists may express this behaviour in terms of frustrated Lewis pair, FLP, chemistry<sup>[72-75]</sup>). Indeed this process is likely to be involved in other metallations of functionalized ferrocene with bimetallic combinations<sup>[76]</sup>

which are sterically prevented (through the use of bulky amides such as TMP) from combining into a contacted molecular bimetallic ate type base.<sup>[77]</sup> This contrasts with the *modus operandi* of TMEDA·Na(μ-TMP)(μ-<sup>t</sup>Bu)Zn(<sup>t</sup>Bu) **1.3**, which has been established as a contacted ion-pair zincate that generally deprotonates aromatic substrates intramolecularly with sodium acting as a Lewis acidic coordination point, though it occasionally acts as a <sup>t</sup>Bu group transfer agent.<sup>[78]</sup>

In the subsequent part of this work we attempted to prepare a tetra-aluminated ferrocene complex by adding 0.25 molar equivalents of ferrocene to the synergistic lithium/aluminium mixture (Scheme 5.3). Following the preparation of **5.3**, no donor solvent was included as this could potentially cap the Lewis acidic metal and inhibit any inverse crown ring formation. Disappointingly, the crystalline product [TMP(H)·Li(μ-TMP)Al(<sup>t</sup>Bu)<sub>2</sub>]<sub>2</sub>(C<sub>5</sub>H<sub>4</sub>)<sub>2</sub>Fe **5.6** (Figure 5.9) resulting from this reaction turned out to be only a di-aluminated derivative (similar to **5.5**). Interestingly, in the absence of THF the non-volatile, bulky amine TMP(H), liberated as a co-product from the deprotonation reaction due to amine basicity, acts as a Lewis donor, capping the lithium and preventing the bimetallic units from linking up further into a ring as observed in the sodium magnesiate inverse crown depicted in Scheme 5.1. Dative TMP(H)···Li contacts are relatively rare in the literature with the bond length in complex **5.6** [mean, 2.229 Å] being longer than those previously reported in TMP(H)·LiN(<sup>t</sup>Bu)B(Ph)(TMP) [2.155(5) Å],<sup>[79]</sup> TMP(H)·Li(μ-<sup>t</sup>Bu)(μ-TMP)Al(<sup>t</sup>Bu)<sub>2</sub> [2.165(5) Å]<sup>[80]</sup> or [TMP(H)·Li]<sub>4</sub> [mean, 2.104 Å].<sup>[69]</sup>

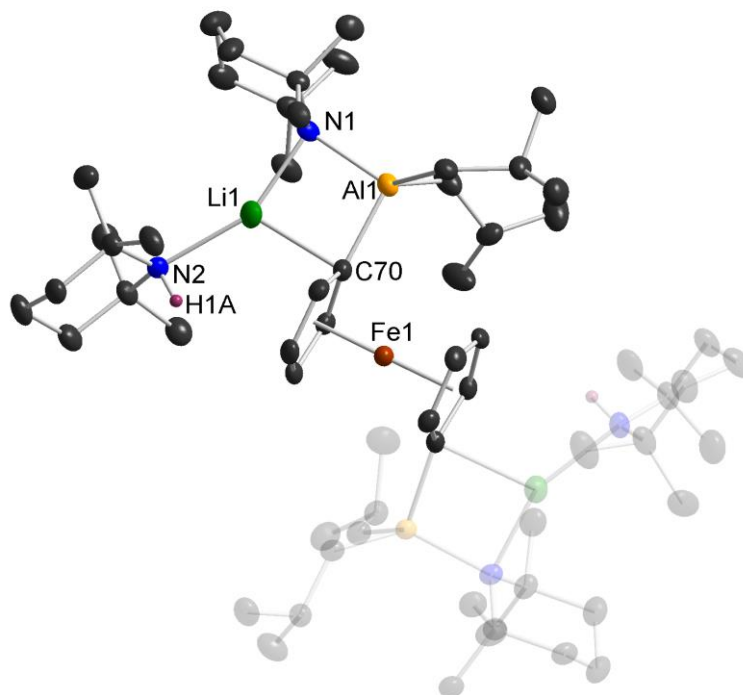


Figure 5.9. Molecular structure of the dialuminated ferrocene  $[\text{TMP}(\text{H})\cdot\text{Li}(\mu\text{-TMP})\text{Al}(\text{i-Bu})_2(\text{C}_5\text{H}_4)_2\text{Fe}]$  **5.6**. Ellipsoids are drawn at 50% probability level and all H atoms [except on the N in  $\text{TMP}(\text{H})$ ] have been omitted for clarity. Selected bond lengths ( $\text{\AA}$ ) and angles ( $^\circ$ ) [values in parentheses represent equivalent parameters on the opposite (transparent) side of molecule]: Li1-C70, 2.248(6) [2.297(5)]; Li1-N1, 2.106(5) [2.095(6)]; Li1-N2, 2.223(5) [2.236(6)]; Al1-C70, 2.043(3) [2.030(3)]; Al1-N1, 1.996(2) [1.993(2)]; C70-Al1-N1, 97.5(1) [97.8(1)]; Al1-N1-Li1, 89.2(2) [90.7(2)]; N1-Li1-C70, 88.4(2) [87.2(2)]; Li1-C70-Al1, 84.3(2) [84.3(2)].

Continuing the theme running throughout this chapter, the mono-deprotonated version of compound **5.6** can also be prepared by increasing the ferrocene quantity from 0.25 to 1 molar equivalent with respect to the base mixture. The resulting complex  $\text{TMP}(\text{H})\cdot\text{Li}(\mu\text{-TMP})[\mu\text{-}(\text{C}_5\text{H}_4)\text{Fe}(\text{C}_5\text{H}_5)]\text{Al}(\text{i-Bu})_2$  **5.7** bears a close resemblance to that of **5.4** in containing a mono-deprotonated ferrocene molecule capped by an extremely bulky  $\text{Li}\cdots\text{Al}$  moiety (Figure 5.11). In fact the



only significant difference is that the monodentate solvating ligand THF in **5.4** has been replaced by the much bulkier monodentate amine molecule TMP(H), as the remainder of the structure is identical in composition and disposition in both aluminated ferrocene molecules. With regard to their syntheses, there is another important distinction in that in **5.4** the THF molecule was deliberately added as a donor ligand; whereas in **5.7** TMP(H) formed as a co-product of the amidoaluminum of ferrocene and since it is non-volatile (contrast with alkyl basicity which would give rise to the elimination of a gaseous alkane co-product) it remains in solution and datively binds to the lithium centre to saturate its coordination sphere. In **5.7** this Li-N(TMP(H)) bond has a length of 2.218(4) Å compared to that of 1.866(6) Å for the Li-O(THF) bond in **5.4** (note that the TMP(H) hydrogen atom on the N was independently refined in the crystallographic study). Other key dimensions in **5.7** are given in the legend to Figure 5.11 but because of their similarity to those in **5.4** no further discussion is necessary. It should be noted, as mentioned already, that TMP(H) has been encountered in other crystal structures acting as a lone pair donor molecule to Li (though only in four cases). Two examples, both of which were made at Strathclyde, are the Li-Al and Li-Zn structures [TMP(H)·Li(μ-TMP)(μ-*i*Bu)Al(*i*Bu)<sub>2</sub>] <sup>[80]</sup> and [ {TMP(H)}<sub>2</sub>·Li<sub>2</sub>Zn{OC(=CH<sub>2</sub>)Mes}<sub>4</sub>] <sup>[81]</sup> depicted in Figure 5.10. Note the latter falls into the category of a higher order zincate having a 2:1, Li:Zn stoichiometry.

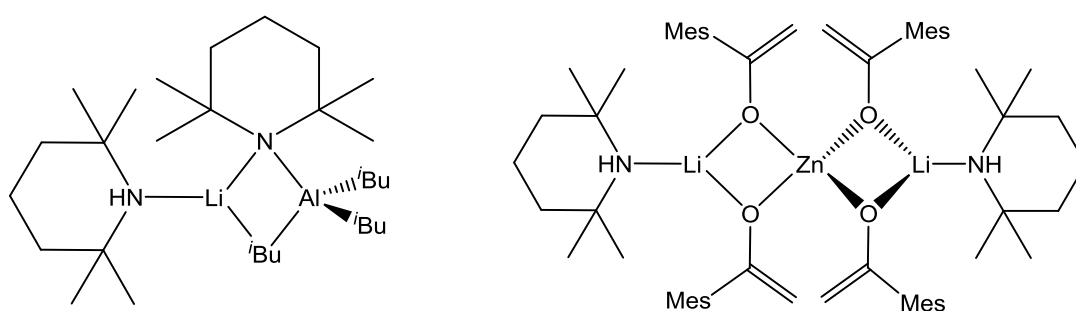


Figure 5.10. ChemDraw representations of known structures where TMP(H) is acting as a donor molecule towards lithium.

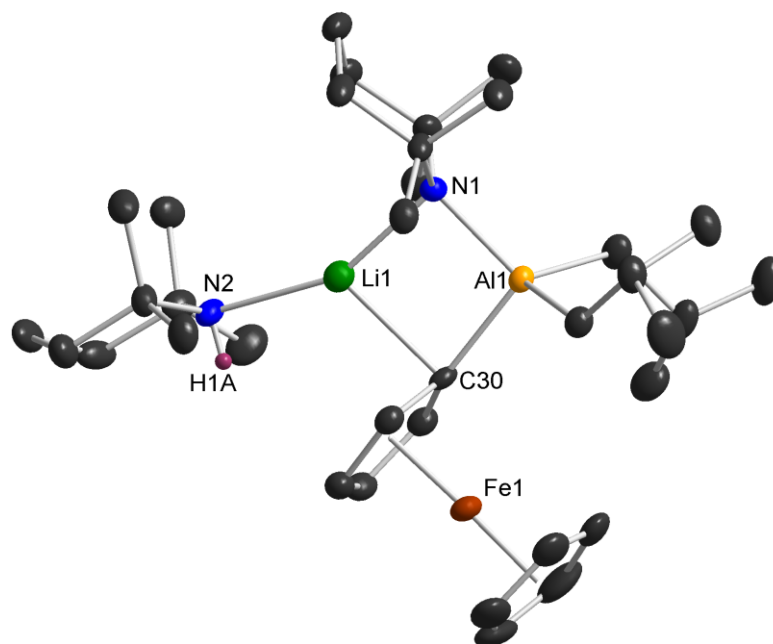
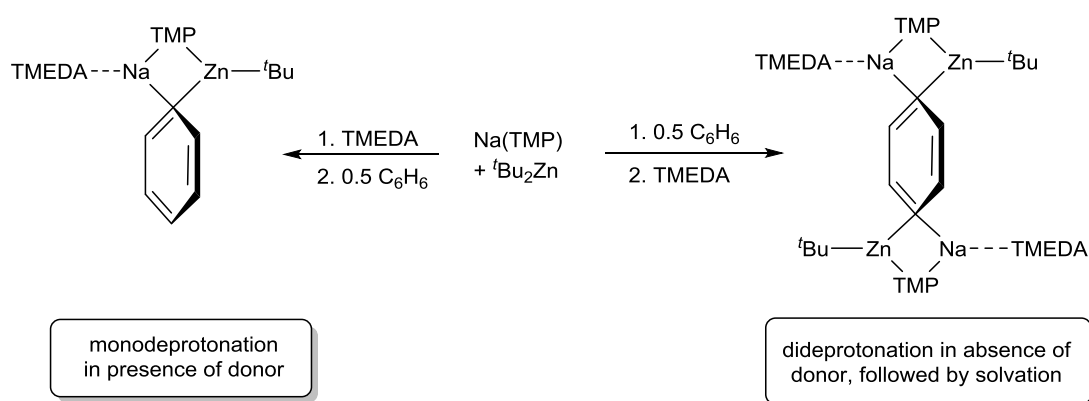


Figure 5.11. Molecular structure of the monoaluminated ferrocene  $\text{TMP(H)} \cdot \text{Li}(\mu\text{-TMP})[\mu\text{-(C}_5\text{H}_4\text{)Fe(C}_5\text{H}_5\text{)]Al}(\text{iBu})_2$  **5.7**. Ellipsoids are drawn at 50% probability level and all H atoms [except on the N in  $\text{TMP(H)}$ ] have been omitted for clarity. Selected bond lengths ( $\text{\AA}$ ) and bond angles ( $^\circ$ ): Li1-C30, 2.293(4); Li1-N1, 2.105(4); Li1-N2, 2.218(4); Al1-C30, 2.041(2); Al1-N1, 1.9820(18); C30-Al1-N1, 98.09(8); Al1-N1-Li1, 90.53(12); N1-Li1-C30, 87.29(15); Li1-C30-Al1, 83.96(12).

The failure of this non-contacted but still synergistic mixture of  $\text{Li(TMP)}$  and  $\text{iBu}_2\text{Al(TMP)}$  to effect a dual deprotonation of each ring due to the presence of (in this case *in situ* generated) donor is reminiscent of the alkali-metal mediated metallation of other simple arenes such as benzene or toluene. While the donor-free base  $\text{NaMg}^n\text{Bu(TMP)}_2$  can easily twofold deprotonate these aromatic rings (with the remarkable extra novelty in the toluene case that the most acidic methyl substituent is left untouched),<sup>[82]</sup> solvation of the base with TMEDA prior to introducing the substrate results in only monodeprotonation (this effect may have a steric origin).<sup>[83-84]</sup> Likewise, and more directly related to this work, the

NaTMP/*t*Bu<sub>2</sub>Zn combination will twofold deprotonate benzene prior to TMEDA addition but only monodeprotonate in the presence of TMEDA at the onset of the reaction (Scheme 5.5).<sup>[85]</sup> It is worth emphasising that to doubly deprotonate a non-metallocenic cyclopentadiene ring is extremely challenging with to the best of our knowledge the only example being the <sup>n</sup>BuLi induced deprotonation of Cp<sup>-</sup> (C<sub>5</sub>H<sub>5</sub> to C<sub>5</sub>H<sub>4</sub>) in the molecular square complex [Li(μ-TMP)Li(μ-Cp)]<sub>4</sub> to generate [Li(μ-TMP)Li(μ-Cp\*)]<sub>4</sub>Li<sub>6</sub>(<sup>n</sup>Bu)<sub>2</sub> as reported by the Mulvey group and Klett.<sup>[86]</sup>



Scheme 5.5. Contrasting reactivity of a sodium zincate reagent with and without TMEDA, towards benzene.

In contrast to the architecture in complex **5.5**, the deprotonated rings in **5.6** are not perfectly staggered, with the Al-C bonds lying at an angle of 145.65(2)° to each other. The greater steric bulk of the TMP(H) donor ligand compared to that of THF may be a factor in the elongation of the Li-N and Li-C bonds within the four-atom ring to 2.106(5) and 2.248(6) Å respectively (c.f. Li-N [2.005(5)/2.032(2) Å] and Li-C [2.188(6)/2.194(3) Å] in THF solvated complexes **5.4** and **5.5** respectively).

Complexes **5.4** (in C<sub>6</sub>D<sub>12</sub> solution) and **5.6** (in C<sub>6</sub>D<sub>6</sub> solution, as the resonances in C<sub>6</sub>D<sub>12</sub> were very broad) proved to be of higher purity than the aforementioned

zinc complexes with only resonances corresponding to their molecular structures being seen in their solution  $^1\text{H}$  NMR spectra. This was corroborated further by the appearance of the  $^7\text{Li}$  NMR spectra, which showed only one sharp resonance. In the case of **5.5**, a small amount of complex **5.4** was evidently present in  $\text{C}_6\text{D}_{12}$  solution as observed in both the  $^1\text{H}$  and  $^7\text{Li}$  spectra. Although the aliphatic region of the  $^1\text{H}$  spectra is cluttered with overlapping resonances, the middle region around 4 ppm was especially informative as a consequence of the excellent resolution of the cyclopentadienyl resonances of ferrocene. Monodeprotonated complex **5.4** displayed three characteristic singlets in a 2:2:5 ratio at 4.00, 4.25 and 4.09 ppm while the dideprotonated complexes gave a pair of equal intensity singlets at 3.97/4.47 ppm (**5.5**) and 4.15/4.29 ppm (**5.6**). Interestingly, the lower field resonance in complex **5.6** is considerably broadened. As in compounds **5.1** and **5.2**, a resonance for the metallated carbon atom could not be located in the  $^{13}\text{C}$  spectra despite several attempts at recording the spectra.

In the final part of this work, speculating whether it would be possible to prepare a multi-metallic compound containing up to five distinct metals (Al, Fe, Li, Na, Zn), ferrocene was subjected to both a Na-Zn [(TMEDA)Na(TMP)Zn( $^t\text{Bu}$ ) $_2$ ] **1.3** and a Li-Al [THF·LiTMP·Al(TMP)( $^t\text{Bu}$ ) $_2$ ] **3.2** base mixture within the one pot. The reaction was successful in that it produced a crystalline product but this product  $[\{\text{Fe}(\text{C}_5\text{H}_4)_2\}_2\{\text{Na}_2\text{Zn}_2(^t\text{Bu})_2\cdot(\text{THF})_6\}]$  **5.8**, shown in Figure 5.12, differs from the structures discussed so far in this chapter in that two independent, symmetrically-equivalent ferrocene-derived molecules reside in the compound leading to a ferrocenophane type structure, centrosymmetric in nature.

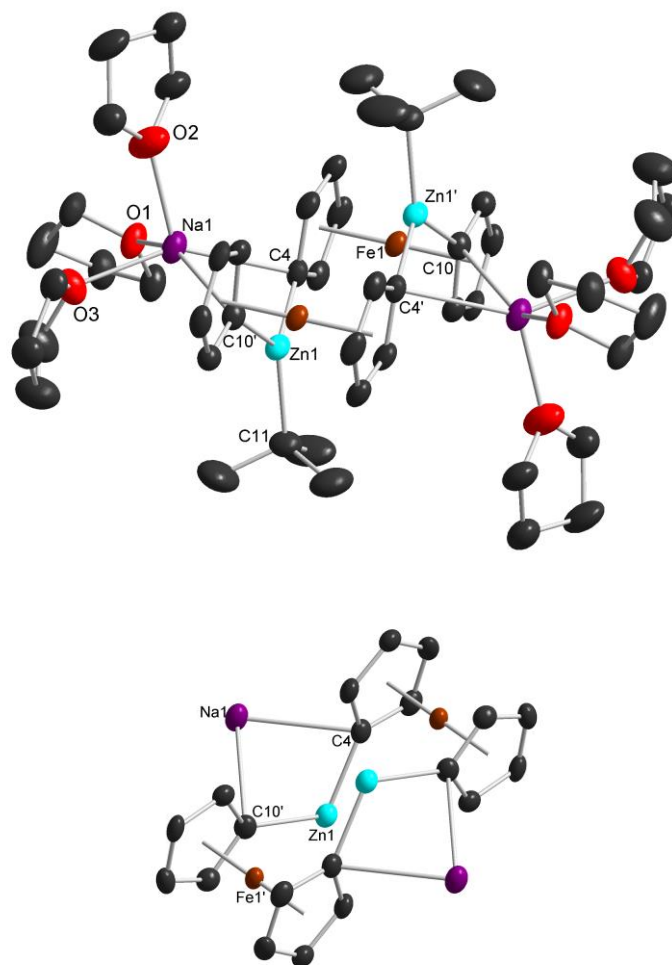


Figure 5.12. Molecular structure of the full dizincated ferrocene complex  $[\{\text{Fe}(\text{C}_5\text{H}_4)_2\}_2\{\text{Na}_2\text{Zn}_2(\text{tBu})_2\cdot(\text{THF})_6\}]$  **5.8** (top) and partial structure with the  $\text{tBu}$  and THF ligands removed for clarity (bottom). Ellipsoids are shown at 50% probability level and all H atoms have been removed for clarity. Symmetry operation to generate the equivalent atoms labelled ' is  $2-x, 1-y, 1-z$ . Selected bond lengths ( $\text{\AA}$ ) and bond angles ( $^\circ$ ): Na1-C4, 2.745(3); Na1-C10', 2.708(3); Na1-O1, 2.292(3); Na1-O2, 2.257(3); Na1-O3, 2.335(3); Zn1-C4, 2.027(3); Zn1-C10', 2.035(3); Zn1-C11, 2.038(3); C10'-Na1-C4, 76.82(10); C10'-Zn1-C4, 76.82(10); Na1-C4-Zn1, 74.05(10); Na1-C10'-Zn1, 74.79(10).

Each ferrocene molecule is 1,1'-di-deprotonated (once on each Cp ring) with both a Zn and a Na centre attached to the carbanions on each ring. Both the

sodium and zinc atoms hold the structure together by forming bridges between the two separate ferrocene molecules. As seen in many other sodium-mediated zincated aromatic structures, zinc lies more towards the plane of the C<sub>5</sub> ring to maximise sigma bonding; while the sodium tends to be more in contact with its π-face in a η<sup>1</sup>-arrangement. Significantly, most of the motif is made up from only one of the starting base mixtures, with both metals and the <sup>t</sup>Bu ligands coming from the Na-Zn system with the Li-Al mixture seemingly providing only the THF solvating molecules. Interestingly, the TMEDA molecule that was present on the sodium atom in the starting base has been replaced by three molecules of THF. Turning to the bond lengths, the smaller three-coordinate Zn atom is held closer to the ferrocene with bond lengths of 2.027(3) and 2.035(3) Å compared to 2.745(3) and 2.708(3) Å for the Na-C bonds. The five-coordinate Na lies instead much closer to the three THF donor molecules with Na-O bond lengths in the range 2.257(3)-2.335(3) Å.

A structure similar to **5.8** was prepared some years ago at Strathclyde, that of the magnesiate [ $\{\text{Fe}(\text{C}_5\text{H}_4)_2\}_3\{\text{Na}_2\text{Mg}_3(\text{TMP})_2\cdot(\text{TMPH})_2\}$ ]. Comparable to **5.8** it is a bimetallic (discounting iron) compound whereby the Mg atoms bridge di-deprotonated ferrocene molecules, though in this case each Mg atom is connected to three separate ferrocene molecules unlike in **5.8** where each metal centre bridges only two. Inspecting its dimensions, the Mg-C bonds lie between the Na-C and Zn-C bond lengths in **5.8**, ranging from 2.157(7) to 2.448(8) Å.

## 5.4 Conclusions

Previously successful with a wide variety of arene substrates, the sodium zincate reagent TMEDA·Na(μ-TMP)(μ-<sup>t</sup>Bu)Zn(<sup>t</sup>Bu) has proved to be effective at removing one or two hydrogen atoms from ferrocene to afford the zincated derivatives TMEDA·Na(μ-TMP)[μ-(C<sub>5</sub>H<sub>4</sub>)Fe(C<sub>5</sub>H<sub>5</sub>)]Zn(<sup>t</sup>Bu) **5.1** or [TMEDA·Na(μ-TMP)Zn(<sup>t</sup>Bu)]<sub>2</sub>(C<sub>5</sub>H<sub>4</sub>)<sub>2</sub>Fe **5.2**, respectively. Although the number of C-H deprotonations/C-Zn metallations essentially matches the stoichiometry of the

zincate reagent employed in the reaction (1 or 2 equivalents respectively), the reactions are not perfectly clean in that there are always trace amounts of **5.2** found in solid samples of **5.1** and *vice versa*. This may be a reflection of the fact that the experimental protocol employed may not exactly have the correct 1:1 or 2:1 base:substrate stoichiometry. The crystal structures of the zinc ferrocene derivatives obtained are generally akin to those previously witnessed using other (non-zincating) metal bases. Where a sodium zincate could be unique is in generating the suspected tetradeprotonated ferrocene **5.3**. Zinc ate reagents are not generally known for multiple (more than two) zinc-hydrogen exchanges within the same molecule nor generating inverse crown architectures like those known for their magnesium counterparts (the best example being the aforementioned tetra-magnesiated ferrocene) so the full formulation and structural characterisation of such a polyzincated species would be a particularly intriguing finding though this has proved elusive in this study. It seems that the aluminium reactions produce cleaner stoichiometric products in monodeprotonated ferrocene THF·Li(μ-TMP)[μ-(C<sub>5</sub>H<sub>4</sub>)Fe(C<sub>5</sub>H<sub>5</sub>)]Al(*i*Bu)<sub>2</sub> **5.4**, and the dideprotonated ferrocene [THF·Li(μ-TMP)Al(*i*Bu)<sub>2</sub>]<sub>2</sub>(C<sub>5</sub>H<sub>4</sub>)<sub>2</sub>Fe **5.5**. Interestingly, however, unlike the aforementioned zincate reactions which are direct zinc-hydrogen exchange processes these reactions are two-step lithiation, trans-metal(aluminium)-trapping (that is, indirect aluminations) akin to but superior to salt metathesis processes as it has the significant advantage that the trapping agent, the neutral alkylaluminium amide *i*Bu<sub>2</sub>Al(TMP), is hydrocarbon soluble. In contrast to the findings of the zincation (or magnesiating) reactions, a tetra-aluminated ferrocene has not been observed or implied, even in the total absence of neutral Lewis donating solvent, with only a di-aluminated product solvated by the *in situ* generated secondary amine, [TMP(H)·Li(μ-TMP)Al(*i*Bu)<sub>2</sub>]<sub>2</sub>(C<sub>5</sub>H<sub>4</sub>)<sub>2</sub>Fe **5.6**, being identified and characterised. As TMP(H) is co-produced in these reactions, they can never be considered truly donor solvent free as also emphasized from the presence of TMP(H) in the monoaluminated product TMP(H)·Li(TMP)[(C<sub>5</sub>H<sub>4</sub>)Fe(C<sub>5</sub>H<sub>5</sub>)]Al(*i*Bu)<sub>2</sub> **5.7**. This leads us to tentatively suggest (tentatively as only a very small number of

reactions have been considered for this effect), that multiple C-H deprotonations of a substrate, often ending up as the guest of a host-guest inverse-crown type structure, is not possible when a non-volatile secondary amine Lewis base is co-produced as a part of the original deprotonation reaction and that overall alkyl basicity (that is, in the sense that the alkyl group deprotonates TMP(H) to enable TMP to re-enter the coordination sphere of the deprotonated substrate as discussed in several papers [87-90]) with its concomitant generation of non-donating, volatile alkanes is more suited for such polymetallation reactions. Further work will be necessary to establish if there is any merit in this tentative suggestion. Notably zincation appears to be preferred over alumination as can be surmised from the preparation and isolation of  $[\{\text{Fe}(\text{C}_5\text{H}_4)_2\}_2\{\text{Na}_2\text{Zn}_2(\text{tBu})_2\cdot(\text{THF})_6\}]$  **5.8** from a solution containing both zinc and aluminium bases, though more work would have to be carried out to quantify the extent of this preference.

## 5.5 Future Work

One of the most interesting results from this chapter is the possible formation of a tetrametallated ferrocene species (**5.3**). The clear goal would be to try and prepare a crystalline version of compound **5.3** for confirmation of polymetallation but also to ascertain a molecular structure and identify which anionic groups performed the C-H deprotonations. This work could be extended to the whole of group 8 to compare and contrast with ruthenocene and osmocene. The tetrametallated species could then be screened with a suite of different electrophiles to establish whether fourfold quenches can be achieved regioselectively.

Briefly touched on in this chapter was the fact that TMP(H) acting as the basic component of the mixture seemingly hinders polymetallation due to the amine remaining in solution and using its donor ability to cap the alkali metal. Additional work should therefore be carried out to determine whether



polymetallations can arise only from alkyl basicity where the by-product (for example butane) is volatile and is expelled from the system. DFT calculations could also be used to model such systems.

The possibility of synthesising some compounds containing multiple metal centres was also briefly studied towards the end of this chapter. A short study of varying parameters and the starting base mixtures could easily be employed to establish whether this is possible. Having combinations of different metals would be of fundamental interest as this may lead to novel electronic and/or magnetic effects if open shell transition metal centres are included in the study.

## 5.6 Experimental

Table 5.1. Crystallographic data and refinement details for compounds **5.1-5.8**.

	<b>5.1</b>	<b>5.2</b>	<b>5.4</b>	<b>5.5</b>
Formula	C <sub>29</sub> H <sub>52</sub> N <sub>3</sub> NaZnFe	C <sub>48</sub> H <sub>94</sub> N <sub>6</sub> Na <sub>2</sub> Zn <sub>2</sub> Fe	C <sub>31</sub> H <sub>53</sub> NOLiAlFe	C <sub>52</sub> H <sub>96</sub> N <sub>2</sub> O <sub>2</sub> Li <sub>2</sub> Al <sub>2</sub> Fe
Formula weight	586.95	987.86	545.51	905.00
Crystal system	Triclinic	Monoclinic	Triclinic	Monoclinic
Space group	<i>P</i> -1	<i>P</i> 21/ <i>n</i>	<i>P</i> -1	<i>I</i> 2/ <i>a</i>
Wavelength/Å	0.71073	0.71073	0.71073	0.71073
<i>a</i> /Å	10.535(6)	13.4467(13)	10.6687(7)	16.3217(8)
<i>b</i> /Å	11.698(11)	30.620(3)	11.1600(6)	14.7125(4)
<i>c</i> /Å	26.32(3)	13.450(3)	13.8524(7)	22.5707(12)
$\alpha$ /°	90.11(13)	90.00	94.846(4)	90.00
$\beta$ /°	91.55(7)	94.393(17)	95.578(5)	98.785(10)
$\gamma$ /°	103.46(11)	90.00	108.439(5)	90.00
Volume/Å <sup>3</sup>	3153(5)	5521.4(15)	1545.58(15)	5356.4(4)
<i>Z</i>	4	4	2	4
Refls. collected	11026	9617	6073	6218
2 $\theta$ <sub>max</sub>	27.5	27.5	31.0246	28.9957
R <sub>int</sub>	0.1691	0.1005	0.0852	0.0191
Goodness of fit	1.022	1.183	0.797	1.103
<i>R</i> [ <i>F</i> <sup>2</sup> > 2 $\sigma$ ], <i>F</i>	0.0715	0.0792	0.0482	0.0299
<i>R</i> <sub>w</sub> (all data), <i>F</i> <sup>2</sup>	0.1450	0.1332	0.0731	0.0864

Table 5.1 cont.

	5.6	5.7	5.8
Formula	C <sub>62</sub> H <sub>118</sub> N <sub>4</sub> Li <sub>2</sub> Al <sub>2</sub> Fe	C <sub>36</sub> H <sub>64</sub> N <sub>2</sub> LiAlFe	C <sub>52</sub> H <sub>82</sub> O <sub>6</sub> Na <sub>2</sub> Zn <sub>2</sub> Fe <sub>2</sub>
Formula weight	1043.29	614.66	1091.60
Crystal system	Monoclinic	Triclinic	Triclinic
Space group	<i>P</i> 21/ <i>c</i>	<i>P</i> -1	<i>P</i> -1
Wavelength/Å	0.71073	0.71073	0.71073
<i>a</i> /Å	22.5681(17)	10.5982(5)	10.2720(6)
<i>b</i> /Å	17.2275(12)	12.1634(7)	12.0956(7)
<i>c</i> /Å	16.3790(14)	15.7584(7)	12.2913(7)
$\alpha$ /°	90.00	105.669(4)	79.543(5)
$\beta$ /°	94.583(7)	99.177(4)	67.053(5)
$\gamma$ /°	90.00	108.807(5)	68.630(5)
Volume/Å <sup>3</sup>	6347.7(8)	1782.47(15)	1308.22(13)
<i>Z</i>	4	2	1
Refls. collected	12152	7502	6074
2 $\theta$ <sub>max</sub>	27.7257	28.345	28.016
R <sub>int</sub>	0.0687	0.0228	0.0428
Goodness of fit	0.985	1.016	1.057
$R[F^2 > 2\sigma], F$	0.0592	0.0464	0.0518
$R_w$ (all data), $F^2$	0.1089	0.1063	0.1275

### 5.6.1 Synthesis of TMEDA·Na( $\mu$ -TMP)[ $\mu$ -(C<sub>5</sub>H<sub>4</sub>)Fe(C<sub>5</sub>H<sub>5</sub>)]Zn<sup>*t*</sup>Bu 5.1

A Schlenk flask was charged with <sup>*t*</sup>Bu<sub>2</sub>Zn (0.358 g, 2 mmol) which was dissolved in hexane (10 mL). In a separate Schlenk flask BuNa (0.160 g, 2 mmol) was suspended in hexane (10 mL) and TMP(H) (0.34 mL, 2 mmol) was added via syringe to give a creamy white suspension which was allowed to stir for an hour. After this time the <sup>*t*</sup>Bu<sub>2</sub>Zn solution was introduced to the mixture via syringe to give a yellow suspension. TMEDA (0.30 mL, 2 mmol) was added via syringe and the reaction mixture was heated gently to form a yellow solution.

Once this mixture had returned to ambient temperature ferrocene (0.372 g, 2 mmol) was added via solid addition tube and this was heated gently to give a transparent solution. Upon cooling the solution at  $-35^{\circ}\text{C}$  a crop of orange crystals of **5.1** formed (0.22 g, not an absolute yield due to traces of **5.2** also being present).

**$^1\text{H}$  NMR ( $\text{C}_6\text{D}_{12}$ , 400.03 MHz, 300K)**  $\delta$  = 4.21 [2H, s,  $\text{C}_5\text{H}_4\text{Fe}$ ], 4.02 [5H, s,  $\text{C}_5\text{H}_5\text{Fe}$ ], 3.86 [2H, s,  $\text{C}_5\text{H}_4\text{Fe}$ ], 2.16 [4H, s, TMEDA  $\text{CH}_2$ ], 2.06 [12H, s, TMEDA Me], 1.71 [2H, m, TMP  $\gamma$ - $\text{CH}_2$ ], 1.54 [2H, m, TMP  $\beta$ - $\text{CH}_2$ ], 1.23 [2H, m, TMP  $\beta$ - $\text{CH}_2$ ], 1.21 [9H, s,  $t\text{Bu}$ ], 1.20 [6H, s, TMP Me], 1.06 ppm [6H, s, TMP Me].

**$^{13}\text{C}$  { $^1\text{H}$ } NMR ( $\text{C}_6\text{D}_{12}$ , 100.60 MHz, 300K)**  $\delta$  = 76.1 [ $\text{C}_5\text{H}_4\text{Fe}$ ], 70.4 [ $\text{C}_5\text{H}_4\text{Fe}$ ], 68.5 [ $\text{C}_5\text{H}_5\text{Fe}$ ], 58.0 [TMEDA  $\text{CH}_2$ ], 53.2 [TMP  $\alpha$ ], 46.6 [TMEDA Me], 40.5 [TMP  $\beta$ ], 35.7 [TMP Me], 35.5 [ $\text{CMe}_3$ ], 35.4 [TMP Me], 20.5 [TMP  $\gamma$ ], 19.4 ppm [ $\text{CMe}_3$ ].

### 5.6.2 Synthesis of $[\text{TMEDA}\cdot\text{Na}(\mu\text{-TMP})\text{Zn}(t\text{Bu})]_2(\text{C}_5\text{H}_4)_2\text{Fe}$ **5.2**

A Schlenk flask was charged with  $t\text{Bu}_2\text{Zn}$  (0.358 g, 2 mmol) which was dissolved in hexane (10 mL). In a separate Schlenk flask BuNa (0.160 g, 2 mmol) was suspended in hexane (10 mL) and TMP(H) (0.34 mL, 2 mmol) was introduced via syringe. The resulting creamy white suspension was then stirred for an hour. After this time the  $t\text{Bu}_2\text{Zn}$  solution was added via syringe to give a yellow suspension to which TMEDA (0.30 mL, 2 mmol) was also added. This mixture was then heated gently to form a yellow solution. Once this solution had cooled to ambient temperature ferrocene (0.186 g, 1 mmol) was added via solid addition tube and this was heated gently to give a transparent solution. Upon cooling this solution at  $-35^{\circ}\text{C}$  a crop of orange crystals formed of **5.2** (0.98 g, not an absolute yield due to traces of **5.1** also being present) were obtained.

**$^1\text{H}$  NMR ( $\text{C}_6\text{D}_{12}$ , 400.03 MHz, 300K)**  $\delta$  = 4.29 [4H, s,  $\text{C}_5\text{H}_4\text{Fe}$ ], 3.84 [4H, s,  $\text{C}_5\text{H}_4\text{Fe}$ ], 2.22 [4H, s, TMEDA  $\text{CH}_2$ ], 2.13 [12H, s, TMEDA Me], 1.71 [2H, m, TMP  $\gamma$ - $\text{CH}_2$ ], 1.55 [2H, m, TMP  $\beta$ - $\text{CH}_2$ ], 1.24 [2H, m, TMP  $\beta$ - $\text{CH}_2$ ], 1.22 [9H, s, *t*Bu], 1.18 [6H, s, TMP Me], 1.02 ppm [6H, s, TMP Me].

**$^{13}\text{C}$   $\{^1\text{H}\}$  NMR ( $\text{C}_6\text{D}_{12}$ , 100.60 MHz, 300K)**  $\delta$  = 75.9 [ $\text{C}_5\text{H}_4\text{Fe}$ ], 71.4 [ $\text{C}_5\text{H}_4\text{Fe}$ ], 58.1 [TMEDA  $\text{CH}_2$ ], 53.2 [TMP  $\alpha$ ], 46.7 [TMEDA Me], 40.4 [TMP  $\beta$ ], 35.8 [ $\text{CMe}_3$ ], 35.7 [TMP Me], 35.2 [TMP Me], 20.5 [TMP  $\gamma$ ], 17.6 ppm [ $\text{CMe}_3$ ].

### 5.6.3 Synthesis of $\text{Na}_4(\text{TMP})_4\text{Zn}_4(\text{tBu})_4[(\text{C}_5\text{H}_3)_2\text{Fe}]$ **5.3**

A Schlenk flask was charged with  $\text{tBu}_2\text{Zn}$  (0.358 g, 2 mmol) which was dissolved in hexane (10 mL). In a separate Schlenk flask BuNa (0.160 g, 2 mmol) was suspended in hexane (10 mL) and TMP(H) (0.34 mL, 2 mmol) was added via syringe, the resulting creamy white suspension being allowed to stir for an hour. Next the  $\text{tBu}_2\text{Zn}$  solution was added via syringe followed by ferrocene (0.09 g, 0.5 mmol) via a solid addition tube. This mixture was stirred for 2 hours during which time the suspension changed from yellow to orange to red. The resulting red powder of **5.3** was collected via filtration, washed with hexane and dried *in vacuo* (0.08 g, 10%, based on the above formula being correct).

### 5.6.4 Synthesis of $\text{THF}\cdot\text{Li}(\mu\text{-TMP})[\mu\text{-}(\text{C}_5\text{H}_4)\text{Fe}(\text{C}_5\text{H}_5)]\text{Al}(\text{iBu})_2$ **5.4**

In a Schlenk flask,  $n\text{BuLi}$  (1.25 mL, 1.6M in hexanes, 2 mmol) was suspended in hexane (10 mL) and TMP(H) (0.34 mL, 2 mmol) was added via syringe, before  $\text{iBu}_2\text{AlCl}$  (0.38 mL, 2 mmol) was introduced via syringe producing a white suspension almost immediately. This suspension was stirred for one hour and then filtered through Celite and glass wool to remove solid LiCl. In a separate Schlenk flask LiTMP was prepared in hexane (10 mL) from a mixture of  $n\text{BuLi}$  (1.25 mL, 2 mmol) and TMP(H) (0.34 mL, 2 mmol). The  $\text{iBu}_2\text{AlTMP}$  solution was added to the LiTMP solution via cannula to give a colourless solution. THF (0.16 mL, 2 mmol) and ferrocene (0.372 g, 2 mmol) were added producing an orange

solution which was stirred overnight at room temperature and then allowed to stand until a crop of orange needles of **5.4** formed (0.52 g, 48%).

**$^1\text{H}$  NMR ( $\text{C}_6\text{D}_{12}$ , 400.03 MHz, 300K)**  $\delta$  = 4.25 [2H, s,  $\text{C}_5\text{H}_4\text{Fe}$ ], 4.09 [5H, s,  $\text{C}_5\text{H}_5\text{Fe}$ ], 4.00 [2H, s,  $\text{C}_5\text{H}_4\text{Fe}$ ], 3.50 [4H, m, 2 x  $\alpha\text{CH}_2$  of THF], 2.14 [2H, sept,  $^3J(\text{H,H}) = 6.42$  Hz, 2 x CH of *i*Bu], 1.84 [1H, m, 1 x  $\gamma\text{CH}_2$  of TMP], 1.73 [4H, s, 2 x  $\beta\text{CH}_2$  of THF], 1.48 [2H, d,  $^3J(\text{H,H}) = 12.43$  Hz, 2 x  $\beta\text{CH}_2$  of TMP], 1.33 [6H, s, 2 x TMP Me], 1.27 [7H, s, 2 x TMP Me + 1 x  $\gamma\text{CH}_2$  of TMP (confirmed by HSQC)], 1.09 [12H, 2 x overlapping d,  $^3J(\text{H,H}) = 6.49$  Hz, 4 x  $\text{CH}_3$  of *i*Bu], 0.75 [2H, t,  $^3J(\text{H,H}) = 12.44$  Hz, 2 x  $\beta\text{CH}_2$  of TMP], 0.37 ppm [4H, d,  $^3J(\text{H,H}) = 5.03$  Hz, 2 x  $\text{CH}_2$  of *i*Bu].

**$^{13}\text{C}$  { $^1\text{H}$ } NMR ( $\text{C}_6\text{D}_{12}$ , 100.60 MHz, 300K)**  $\delta$  = 77.1 [ $\text{C}_5\text{H}_4\text{Fe}$ ], 71.7 [ $\text{C}_5\text{H}_4\text{Fe}$ ], 69.5 [ $\text{C}_5\text{H}_5\text{Fe}$ ], 69.1 [THF  $\alpha\text{CH}_2$ ], 53.1 [TMP  $\alpha$ ], 45.2 [TMP  $\beta$ ], 36.8 [TMP Me], 31.0 [ $\text{CH}_2\text{CHMe}_2$ ], 29.8 [TMP Me], 29.2 [ $\text{CH}_2\text{CHMe}_2$ ], 28.0 [ $\text{CH}_2\text{CHMe}_2$ ], 25.3 [THF  $\beta\text{CH}_2$ ], 18.7 ppm [TMP  $\gamma$ ].

**$^7\text{Li}$  NMR ( $\text{C}_6\text{D}_{12}$ , 155.46 MHz, 300K)**  $\delta$  = -0.56 ppm.

**Elemental Analysis:** Calculated (%) for  $\text{Al}_1\text{C}_{31}\text{Fe}_1\text{H}_{53}\text{Li}_1\text{N}_1\text{O}_1$ : C, 68.25; H, 9.79; N, 2.57; found: C, 67.99; H, 10.06; N, 3.11.

### 5.6.5 Synthesis of $[\text{THF}\cdot\text{Li}(\mu\text{-TMP})\text{Al}(\textit{i}\text{Bu})_2]_2(\text{C}_5\text{H}_4)_2\text{Fe}$ **5.5**

In a Schlenk flask, *n*BuLi (1.25 mL, 1.6M in hexanes, 2 mmol) was suspended in hexane (10 mL) and TMP(H) (0.34 mL, 2 mmol) was added via syringe, before *i*Bu<sub>2</sub>AlCl (0.38 mL, 2 mmol) was introduced via syringe producing a white suspension almost immediately. This was stirred for one hour and then filtered through Celite and glass wool to remove LiCl. In a separate Schlenk flask LiTMP was prepared in hexane (10 mL) from a mixture of *n*BuLi (1.25 mL, 2 mmol) and TMP(H) (0.34 mL, 2 mmol). The *i*Bu<sub>2</sub>AlTMP solution was added to the LiTMP solution via cannula to give a colourless solution. THF (0.16 mL, 2 mmol) and ferrocene (0.186 g, 1 mmol) were added producing an orange solution which

was stirred for 2 hours at reflux and then stored at -30°C until a crop of orange crystals formed (0.50 g, not an absolute yield due to traces of **5.4** also being present).

**<sup>1</sup>H NMR (C<sub>6</sub>D<sub>12</sub>, 400.03 MHz, 300K)** δ = 4.47 [4H, s, C<sub>5</sub>H<sub>4</sub>Fe], 3.97 [4H, s, C<sub>5</sub>H<sub>4</sub>Fe], 3.53 [8H, s, 4 x αCH<sub>2</sub> of THF], 2.15 [4H, sept, <sup>3</sup>J(H,H) = 6.37 Hz, 4 x CH of <sup>i</sup>Bu], 1.84 [2H, m, 2 x γCH of TMP], 1.78 [8H, s, 4 x βCH<sub>2</sub> of THF], 1.47 [4H, d, <sup>3</sup>J(H,H) = 12.38 Hz, 2 x βCH<sub>2</sub> of TMP], 1.32 [12H, s, 4 x TMP Me], 1.29 [2H, m, 2 x γCH of TMP], 1.25 [12H, s, 4 x TMP Me], 1.10 [24H, t, <sup>3</sup>J(H,H) = 7.55 Hz, 8 x CH<sub>3</sub> of <sup>i</sup>Bu], 0.75 [4H, t, <sup>3</sup>J(H,H) = 12.29 Hz, 2 x βCH<sub>2</sub> of TMP], 0.38 ppm [8H, m, 4 x CH<sub>2</sub> of <sup>i</sup>Bu].

**<sup>13</sup>C {<sup>1</sup>H} NMR (C<sub>6</sub>D<sub>12</sub>, 100.60 MHz, 300K)** δ = 77.4 [C<sub>5</sub>H<sub>4</sub>Fe], 74.7 [C<sub>5</sub>H<sub>4</sub>Fe], 69.2 [THF αCH<sub>2</sub>], 53.0 [TMP α], 45.1 [TMP β], 36.8 [TMP Me], 30.8 [CH<sub>2</sub>CHMe<sub>2</sub>], 29.7 [TMP Me], 29.4 [CH<sub>2</sub>CHMe<sub>2</sub>], 28.1 [CH<sub>2</sub>CHMe<sub>2</sub>], 25.9 [THF βCH<sub>2</sub>], 18.7 ppm [TMP γ].

**<sup>7</sup>Li NMR (C<sub>6</sub>D<sub>12</sub>, 155.46 MHz, 300K)** δ = -0.69 ppm.

**Elemental Analysis:** Calculated (%) for Al<sub>2</sub>C<sub>52</sub>Fe<sub>1</sub>H<sub>96</sub>Li<sub>2</sub>N<sub>2</sub>O<sub>2</sub>: C, 69.01; H, 10.69; N, 3.10; found: C, 68.54; H, 10.60; N, 3.39.

### 5.6.6 Synthesis of [TMP(H)·Li(μ-TMP)Al(<sup>i</sup>Bu)<sub>2</sub>]<sub>2</sub>(C<sub>5</sub>H<sub>4</sub>)<sub>2</sub>Fe **5.6**

In a Schlenk flask, <sup>n</sup>BuLi (2.50 mL, 1.6 M in hexanes, 4 mmol) was suspended in more hexane (10 mL) and TMP(H) (0.68 mL, 4 mmol) was added via syringe, before <sup>i</sup>Bu<sub>2</sub>AlCl (0.76 mL, 4 mmol) was introduced via syringe producing a white suspension almost immediately. This suspension was stirred for one hour and then filtered through Celite and glass wool to remove solid LiCl. In a separate Schlenk flask LiTMP was prepared in hexane (10 mL) from a mixture of <sup>n</sup>BuLi (2.50 mL, 4 mmol) and TMP(H) (0.68 mL, 4 mmol). Next, ferrocene (0.186 g, 1 mmol) was added to the LiTMP solution followed immediately by the <sup>i</sup>Bu<sub>2</sub>AlTMP

solution via cannula. This mixture was gently heated to give an orange solution and then stored at room temperature until a crop of orange crystals of **5.6** formed (0.50 g, 48%).

**$^1\text{H}$  NMR ( $\text{C}_6\text{D}_6$ , 400.03 MHz, 300K)**  $\delta$  = 4.29 [4H, br s,  $\text{C}_5\text{H}_4\text{Fe}$ ], 4.15 [4H, s,  $\text{C}_5\text{H}_4\text{Fe}$ ], 2.30 [4H, m, 4 x CH of *i*Bu], 1.77 [4H, br m, 2 x  $\gamma\text{CH}$  of TMP(H)], 1.50 [4H, br m, 2 x  $\beta\text{CH}_2$  of TMP], 1.49 [4H, m, 2 x  $\gamma\text{CH}$  of TMP], 1.43 [24H, s, 8 x TMP Me], 1.34 [24H, m, 8 x  $\text{CH}_3$  of *i*Bu], 1.20 [8H, t,  $^3J(\text{H,H}) = 6.46$  Hz, 4 x  $\beta\text{CH}_2$  of TMP(H)], 1.04 [24H, s, 8 x TMP(H) Me], 0.66 [4H, br m, 2 x  $\beta\text{CH}_2$  of TMP], 0.58 ppm [8H, m, 4 x  $\text{CH}_2$  of *i*Bu].

**$^{13}\text{C}$   $\{^1\text{H}\}$  NMR ( $\text{C}_6\text{D}_6$ , 100.60 MHz, 300K)**  $\delta$  = 77.5 [ $\text{C}_5\text{H}_4\text{Fe}$ ], 72.6 [ $\text{C}_5\text{H}_4\text{Fe}$ ], 52.5 [TMP  $\alpha$ ], 49.9 [TMP(H)  $\alpha$ ], 45.5 [TMP  $\beta$ ], 38.6 [TMP(H)  $\beta$ ], 37.1 [TMP Me], 32.0 [TMP(H) Me], 30.6 [ $\text{CH}_2\text{CHMe}_2$ ], 30.0 [ $\text{CH}_2\text{CHMe}_2$ ], 29.6 [TMP Me], 28.3 [ $\text{CH}_2\text{CHMe}_2$ ], 27.7 [ $\text{CH}_2\text{CHMe}_2$ ], 18.6 [TMP(H)  $\gamma$ ], 18.2 ppm [TMP  $\gamma$ ].

**$^7\text{Li}$  NMR ( $\text{C}_6\text{D}_6$ , 155.46 MHz, 300K)**  $\delta$  = 2.27 ppm.

### 5.6.7 Synthesis of $\text{TMP(H)}\cdot\text{Li}(\mu\text{-TMP})[\mu\text{-}(\text{C}_5\text{H}_4)\text{Fe}(\text{C}_5\text{H}_5)]\text{Al}(\textit{i}\text{Bu})_2$ **5.7**

In a Schlenk flask, *n*BuLi (1.25 mL, 1.6 M in hexanes, 2 mmol) was suspended in hexane (10 mL) and TMP(H) (0.34 mL, 2 mmol) was added via syringe generating a pale yellow solution of LiTMP which was allowed to stir for 10 minutes. Ferrocene (0.372 g, 2 mmol) was then introduced to give an orange solution and left to stir for 5 minutes. In a separate Schlenk flask *i*Bu<sub>2</sub>AlTMP (0.56 g, 2 mmol) was dissolved in 2 mL of hexane and then added to the LiTMP/ferrocene mixture to produce a slightly cloudy orange mixture. The mixture was then left to stir for 1 hour and gentle heating afforded a transparent solution. Standing the solution overnight led to the deposition of a crop of small orange crystals of **5.7** (0.4 g, 33%).



**$^1\text{H}$  NMR ( $\text{C}_6\text{D}_6$ , 400.03 MHz, 300K)**  $\delta$  = 4.24 [2H, s,  $\text{C}_5\text{H}_4\text{Fe}$ ], 4.09 [2H, s,  $\text{C}_5\text{H}_4\text{Fe}$ ], 3.97 [5H, s,  $\text{C}_5\text{H}_5\text{Fe}$ ], 2.35 [2H, sept,  $^3J(\text{H,H}) = 6.50$  Hz, 2 x CH of *i*Bu], 1.79 [1H, m, 1 x  $\gamma\text{CH}_2$  TMP(H)], 1.49 [6, m,  $\beta\text{CH}_2$  &  $\gamma\text{CH}_2$  TMP], 1.43 [12H, s, Me TMP], 1.21 [4H, t,  $\beta\text{CH}_2$  TMP(H)], 1.37 [6H, d,  $^3J(\text{H,H}) = 6.38$  Hz, 2 x  $\text{CH}_3$  of *i*Bu], 1.33 [6H, d,  $^3J(\text{H,H}) = 6.38$  Hz, 2 x  $\text{CH}_3$  of *i*Bu], 1.29 [1H, m, 1 x  $\gamma\text{CH}_2$  TMP(H)], 1.04 [12H, s, Me TMP(H)], 0.63 ppm [4H, d,  $^3J(\text{H,H}) = 6.00$  Hz, 2 x  $\text{CH}_2$  of *i*Bu].

**$^{13}\text{C}$  { $^1\text{H}$ } NMR ( $\text{C}_6\text{D}_6$ , 100.60 MHz, 300K)**  $\delta$  = 78.4 [ $\text{C}_5\text{H}_4\text{Fe}$ ], 72.9 [ $\text{C}_5\text{H}_4\text{Fe}$ ], 68.1 [ $\text{C}_5\text{H}_5\text{Fe}$ ], 52.3 & 49.7 [TMP & TMP(H)  $\alpha$ ], 45.3 [TMP  $\beta$ ], 38.5 [TMP(H)  $\beta$ ], 36.7 [TMP Me], 31.9 [TMP(H) Me], 30.3 [ $\text{CH}_2\text{CHMe}_2$ ], 29.8 [ $\text{CH}_2\text{CHMe}_2$ ], 28.6 [ $\text{CH}_2\text{CHMe}_2$ ], 27.7 [ $\text{CH}_2\text{CHMe}_2$ ], 18.6 [TMP  $\gamma$ ], 18.05 ppm [TMP(H)  $\gamma$ ].

**$^7\text{Li}$  NMR ( $\text{C}_6\text{D}_6$ , 155.46 MHz, 300K)**  $\delta$  = 2.30 ppm.

### 5.6.8 Synthesis of $\{[\text{Fe}(\text{C}_5\text{H}_4)_2]_2\{\text{Na}_2\text{Zn}_2(\text{}^t\text{Bu})_2\cdot(\text{THF})_6\}$ 5.8

The sodium zincate  $[(\text{TMEDA})\text{Na}(\mu\text{-TMP})(\mu\text{-}^t\text{Bu})\text{Zn}(\text{}^t\text{Bu})]$  was first prepared according to the literature procedure <sup>[54]</sup> and then 1 mmol (0.46 g) of it was dissolved in 10 mL of hexane. Ferrocene (0.186 g, 1 mmol) was then added followed by gentle heating to create a transparent orange solution. In a separate Schlenk flask the lithium aluminate “ $\text{THF}\cdot\text{Li}(\text{TMP})_2\text{Al}(\text{}^t\text{Bu})_2$ ” mixture (1 mmol) was prepared in hexane solution according to the literature method <sup>[66]</sup> before being added to the sodium zincate/ferrocene mixture. The orange solution was left to stir for 15 minutes before the flask was placed in the freezer. After a couple of days a crop of small orange crystals had formed.

## 5.7 Bibliography

- [1] R. E. Mulvey, *Acc. Chem. Res.* **2009**, *42*, 743-755.
- [2] R. E. Mulvey, *Dalton Trans.* **2013**, *42*, 6676-6693.
- [3] R. E. Mulvey, *Organometallics* **2006**, *25*, 1060-1075.
- [4] R. E. Mulvey, F. Mongin, M. Uchiyama, Y. Kondo, *Angew. Chem. Int. Ed.* **2007**, *46*, 3802-3824.
- [5] The Nobel Prize in Chemistry was awarded to Georg Wittig and Herbert C. Brown in 1979, [http://www.nobelprize.org/nobel\\_prizes/chemistry/laureates/1979/](http://www.nobelprize.org/nobel_prizes/chemistry/laureates/1979/), accessed May 2015.
- [6] G. Wittig, F. J. Meyer, G. Lange, *Justus Liebigs Ann. Chem.* **1951**, *571*, 167-201.
- [7] B. Haag, M. Mosrin, H. Ila, V. Malakhov, P. Knochel, *Angew. Chem. Int. Ed.* **2011**, *50*, 9794-9824.
- [8] A. Harrison-Marchand, F. Mongin, *Chem. Rev.* **2013**, *113*, 7470-7562.
- [9] F. Mongin, A. Harrison-Marchand, *Chem. Rev.* **2013**, *113*, 7563-7727.
- [10] Y. Kondo, J. V. Morey, J. C. Morgan, H. Naka, D. Nobuto, P. R. Raithby, M. Uchiyama, A. E. H. Wheatley, *J. Am. Chem. Soc.* **2007**, *129*, 12734-12738.
- [11] H. Naka, J. V. Morey, J. Haywood, D. J. Eisler, M. McPartlin, F. Garcia, H. Kudo, Y. Kondo, M. Uchiyama, A. E. H. Wheatley, *J. Am. Chem. Soc.* **2008**, *130*, 16193-16200.
- [12] A. E. H. Wheatley, *New. J. Chem.* **2004**, *28*, 435-443.
- [13] P. J. Harford, A. J. Peel, F. Chevallier, R. Takita, F. Mongin, M. Uchiyama, A. E. H. Wheatley, *Dalton Trans.* **2014**, *43*, 14181-14203.
- [14] M. Uchiyama, C. Wang, *Top. Organomet. Chem.* **2014**, *47*, 159-202.
- [15] Y. Kondo, M. Shilai, T. Sakamoto, M. Uchiyama, *J. Am. Chem. Soc.* **1999**, *121*, 3539-3540.
- [16] R. E. Mulvey, S. D. Robertson, *Top. Organomet. Chem.* **2013**, *45*, 103-140.
- [17] R. E. Mulvey, S. D. Robertson, *Top. Organomet. Chem.* **2014**, *47*, 129-158.
- [18] J. Clayden, *Organolithiums: Selectivity for Synthesis*, Pergamon, Elsevier Science Ltd, Oxford, **2002**.
- [19] A. J. Martinez-Martinez, A. R. Kennedy, R. E. Mulvey, C. T. O'Hara, *Science* **2014**, *346*, 834-838.
- [20] A. J. Martinez-Martinez, D. R. Armstrong, B. Conway, B. J. Fleming, J. Klett, A. R. Kennedy, R. E. Mulvey, S. D. Robertson, C. T. O'Hara, *Chem. Sci.* **2014**, *5*, 771-781.
- [21] V. L. Blair, L. M. Carella, W. Clegg, B. Conway, R. W. Harrington, L. M. Hogg, J. Klett, R. E. Mulvey, E. Rentschler, L. Russo, *Angew. Chem. Int. Ed.* **2008**, *47*, 6208-6211.
- [22] R. E. Mulvey, *Chem. Commun.* **2001**, 1049-1056.
- [23] W. Clegg, K. W. Henderson, A. R. Kennedy, R. E. Mulvey, C. T. O'Hara, R. B. Rowlings, D. M. Tooke, *Angew. Chem. Int. Ed.* **2001**, *40*, 3902-3905.
- [24] P. C. Andrikopolous, D. R. Armstrong, W. Clegg, C. J. Gilfillan, E. Hevia, A. R. Kennedy, R. E. Mulvey, C. T. O'Hara, J. A. Parkinson, D. M. Tooke, *J. Am. Chem. Soc.* **2004**, *126*, 11612-11620.

- [25] K. W. Henderson, A. R. Kennedy, R. E. Mulvey, C. T. O'Hara, R. B. Rowlings, *Chem. Commun.* **2001**, 1678-1670.
- [26] H. R. Barley, W. Clegg, S. H. Dale, E. Hevia, G. W. Honeyman, A. R. Kennedy, R. E. Mulvey, *Angew. Chem. Int. Ed.* **2005**, *44*, 6018-6021.
- [27] A. S. Perucha, J. Heilmann-Brohl, M. Bolte, H.-W. Lerner, M. Wagner, *Organometallics* **2008**, *28*, 6170-6177.
- [28] N. Seidel, K. Jacob, P. Zanello, M. Fontani, *J. Organomet. Chem.* **2001**, *620*, 243-248.
- [29] E. Hevia, A. R. Kennedy, M. D. McCall, *Dalton Trans.* **2012**, *41*, 98-103.
- [30] W. Clegg, B. Conway, P. Garcia-Alvarez, A. R. Kennedy, J. Klett, R. E. Mulvey, L. Russo, *Dalton Trans.* **2010**, *39*, 62-65.
- [31] B. Wrackmeyer, E. V. Klimkina, T. Ackermann, W. Milius, *Inorg. Chem. Commun.* **2007**, *10*, 743-747.
- [32] R. D. Rogers, W. J. Cook, J. L. Atwood, *Inorg. Chem.* **1979**, *18*, 279-282.
- [33] H. Braunschweig, G. K. B. Clentsmith, S. Hess, T. Kupfer, K. Radacki, *Inorg. Chim. Acta* **2007**, *360*, 1274-1277.
- [34] B. Wrackmeyer, E. V. Klimkina, W. Milius, *Eur. J. Inorg. Chem.* **2009**, 3163-3171.
- [35] K. Knabel, I. Krossing, H. Nöth, H. Schwenk-Kircher, M. Schmidt-Amelunxen, T. Seifert, *Eur. J. Inorg. Chem.* **1998**, 1095-1114.
- [36] J. A. Schachner, C. L. Lund, J. W. Quail, J. Müller, *Acta Crystallogr.* **2005**, *E61*, m682-m684.
- [37] B. Wrackmeyer, E. V. Klimkina, W. Milius, *Eur. J. Inorg. Chem.* **2009**, 3155-3162.
- [38] C. L. Lund, J. A. Schachner, J. W. Quail, J. Müller, *Organometallics* **2006**, *25*, 5817-5823.
- [39] J. A. Schachner, C. L. Lund, J. W. Quail, J. Müller, *Organometallics* **2005**, *24*, 785-787.
- [40] H. Braunschweig, C. Burschka, G. K. B. Clentsmith, T. Kupfer, K. Radacki, *Inorg. Chem.* **2005**, *44*, 4906-4908.
- [41] M. F. Lappert, D.-S. Liu, *J. Organomet. Chem.* **1995**, *500*, 203-217.
- [42] M. Lappert, P. Power, A. Protchenko, A. Seeber, *Metal Amide Chemistry*, John Wiley & Sons Ltd, Hoboken, **2008**.
- [43] C. F. Caro, M. F. Lappert, P. G. Merle, *Coord. Chem. Rev.* **2001**, *219-221*, 605-663.
- [44] P. M. Druce, B. M. Kingston, M. F. Lappert, T. R. Spalding, R. C. Srivastava, *J. Chem. Soc. (A)* **1969**, 2106-2110.
- [45] P. B. Hitchcock, M. F. Lappert, C. R. C. Milne, *J. Chem. Soc. Dalton Trans.* **1981**, 180-186.
- [46] M. F. Lappert, C. J. Pickett, P. I. Riley, P. I. W. Yarrow, *J. Chem. Soc. Dalton Trans.* **1981**, 805-813.
- [47] A. F. Halasa, D. P. Tate, *J. Organomet. Chem.* **1970**, *24*, 769-773.
- [48] *Science of Synthesis: Houben-Weyl Methods of Molecular Transformations, Vol. 1*, Georg Thieme Verlag, Stuttgart, **2001**.
- [49] R. Sun, L. Wang, H. Yu, Z. ul-Abdin, Y. Chen, J. Huang, R. Tong, *Organometallics* **2014**, *33*, 4560-4573.

- [50] M. F. R. Fouda, M. M. Abd-Elzaher, R. A. Abdelsamaia, A. A. Labib, *Appl. Organomet. Chem.* **2007**, *21*, 613-625.
- [51] D. R. van Staveren, N. Metzler-Nolte, *Chem. Rev.* **2004**, *104*, 5931-5986.
- [52] L.-X. Dai, T. Tu, S.-L. You, W.-P. Deng, X.-L. Hou, *Acc. Chem. Res.* **2003**, *36*, 659-667.
- [53] K. Heinze, H. Lang, *Organometallics* **2013**, *32*, 5623-5625.
- [54] P. C. Andrikopoulos, D. R. Armstrong, H. R. L. Barley, W. Clegg, S. H. Dale, E. Hevia, G. W. Honeyman, A. R. Kennedy, R. E. Mulvey, *J. Am. Chem. Soc.* **2005**, *127*, 6184-6185.
- [55] L. Yang, D. R. Powell, R. P. Houser, *Dalton Trans.* **2007**, 955-964.
- [56] J. J. Morris, B. C. Noll, G. W. Honeyman, C. T. O'Hara, A. R. Kennedy, R. E. Mulvey, K. W. Henderson, *Chem. Eur. J.* **2007**, *13*, 4418-4432.
- [57] R. E. Dinnebier, U. Behrens, F. Olbrich, *Organometallics* **1997**, *16*, 3855-3858.
- [58] M. L. Cole, C. Jones, P. C. Junk, *J. Chem. Soc. Dalton Trans.* **2002**, 896-905.
- [59] C. M. Widdifield, J. A. Tang, C. L. B. Macdonald, R. W. Schurko, *Magn. Reson. Chem.* **2007**, *45*, S116-S128.
- [60] J. Hey, D. M. Andrada, R. Michel, R. A. Mata, D. Stalke, *Angew. Chem. Int. Ed.* **2013**, *52*, 10365-10369.
- [61] T. Aoyagi, H. M. M. Shearer, K. Wade, G. Whitehead, *J. Chem. Soc. Chem. Commun.* **1976**, 164-165.
- [62] M. G. Davidson, D. Stalke, D. S. Wright, *Angew. Chem. Int. Ed.* **1992**, *31*, 1226-1227.
- [63] A. Reichert, J. Schmidt, M. Bolte, M. Wagner, H.-W. Lerner, *Z. Anorg. Allg. Chem.* **2013**, *639*, 1083-1086.
- [64] B. Conway, E. Hevia, J. Garcia-Alvarez, D. V. Graham, A. R. Kennedy, R. E. Mulvey, *Chem. Commun.* **2007**, 5241-5243.
- [65] B. Conway, J. Garcia-Alvarez, E. Hevia, A. R. Kennedy, R. E. Mulvey, S. D. Robertson, *Organometallics* **2009**, *17*, 6725-6730.
- [66] E. Crosbie, P. Garcia-Alvarez, A. R. Kennedy, J. Klett, R. E. Mulvey, S. D. Robertson, *Angew. Chem. Int. Ed.* **2010**, *49*, 9388-9391.
- [67] R. E. Mulvey, D. R. Armstrong, B. Conway, E. Crosbie, A. R. Kennedy, S. D. Robertson, *Inorg. Chem.* **2011**, *50*, 12241-12251.
- [68] B. Conway, E. Crosbie, A. R. Kennedy, R. E. Mulvey, S. D. Robertson, *Chem. Commun.* **2012**, *48*, 4674-4676.
- [69] E. Crosbie, A. R. Kennedy, R. E. Mulvey, S. D. Robertson, *Dalton Trans.* **2012**, *41*, 1832-1839.
- [70] R. Campbell, E. Crosbie, A. R. Kennedy, R. E. Mulvey, R. A. Naismith, S. D. Robertson, *Aust. J. Chem.* **2013**, *66*, 1189-1201.
- [71] D. R. Armstrong, E. Crosbie, E. Hevia, R. E. Mulvey, D. L. Ramsay, S. D. Robertson, *Chem. Sci.* **2014**, *5*, 3031-3045.
- [72] D. W. Stephan, *Acc. Chem. Res.* **2015**, *48*, 306-316.
- [73] F. A. Tsao, D. W. Stephan, *Dalton Trans.* **2015**, *44*, 71-74.
- [74] T. Mahdi, D. W. Stephan, *J. Am. Chem. Soc.* **2014**, *136*, 15809-15812.
- [75] D. W. Stephan, *Org. Biomol. Chem.* **2008**, *6*, 1535-1539.
- [76] G. Dayaker, A. Sreeshailam, F. Chevallier, T. Roisnel, P. Radha Krishna, F. Mongin, *Chem. Commun.* **2010**, *46*, 2862-2864.

- [77] D. R. Armstrong, A. R. Kennedy, R. E. Mulvey, J. A. Parkinson, S. D. Robertson, *Chem. Sci.* **2012**, *3*, 2700-2707.
- [78] E. Hevia, G. W. Honeyman, A. R. Kennedy, R. E. Mulvey, *J. Am. Chem. Soc.* **2005**, *127*, 13106-13107.
- [79] U. Braun, T. Haberer, H. Nöth, *Eur. J. Inorg. Chem.* **2004**, 3629-3643.
- [80] J. Garcia-Alvarez, E. Hevia, A. R. Kennedy, J. Klett, R. E. Mulvey, *Chem. Commun.* **2007**, 2402-2404.
- [81] D. R. Armstrong, A. M. Drummond, L. Balloch, D. V. Graham, E. Hevia, A. R. Kennedy, *Organometallics* **2008**, *27*, 5860-5866.
- [82] D. R. Armstrong, A. R. Kennedy, R. E. Mulvey, R. B. Rowlings, *Angew. Chem. Int. Ed.* **1999**, *38*, 131-133.
- [83] E. Hevia, D. J. Gallagher, A. R. Kennedy, R. E. Mulvey, C. T. O'Hara, C. Talmard, *Chem. Commun.* **2004**, 2422-2423.
- [84] P. C. Andrikopoulos, D. R. Armstrong, D. V. Graham, E. Hevia, A. R. Kennedy, R. E. Mulvey, C. T. O'Hara, C. Talmard, *Angew. Chem. Int. Ed.* **2005**, *44*, 3459-3462.
- [85] D. R. Armstrong, W. Clegg, S. H. Dale, D. V. Graham, E. Hevia, L. M. Hogg, G. W. Honeyman, A. R. Kennedy, R. E. Mulvey, *Chem. Commun.* **2007**, 598-600.
- [86] A. A. Fyfe, A. R. Kennedy, J. Klett, R. E. Mulvey, *Angew. Chem. Int. Ed.* **2011**, *50*, 7776-7780.
- [87] M. Uchiyama, Y. Matsumoto, D. Nobuto, T. Furuyama, K. Yamaguchi, K. Morokuma, *J. Am. Chem. Soc.* **2006**, *128*, 8748-8750.
- [88] W. Clegg, B. Conway, E. Hevia, M. D. McCall, L. Russo, R. E. Mulvey, *J. Am. Chem. Soc.* **2009**, *131*, 2375-2384.
- [89] D. R. Armstrong, J. Garcia-Alvarez, D. V. Graham, G. W. Honeyman, E. Hevia, A. R. Kennedy, R. E. Mulvey, *Chem. Eur. J.* **2009**, *15*, 3800-3807.
- [90] D. R. Armstrong, V. L. Blair, W. Clegg, S. H. Dale, J. Garcia-Alvarez, G. W. Honeyman, E. Hevia, R. E. Mulvey, L. Russo, *J. Am. Chem. Soc.* **2010**, *132*, 9480-9487.

## **Chapter 6**

### **General Conclusions**

## 6.1 General Conclusions

While organometallic chemistry may still slightly be in the shadows of organic and inorganic chemistry, gradually it is moving further into the spotlight with researchers and industry alike taking notice of the vast untapped potential this field still has to offer. To date there have been many significant achievements in organometallic chemistry, most notably studies on organometallic catalysts for use in alkene metathesis reactions,<sup>[1]</sup> and palladium catalysed cross-coupling reactions,<sup>[2]</sup> both of which provided their pioneers with Nobel Prizes.

Monometallic reagents have dominated the field of organometallic chemistry for 50 years or more, with industry widely utilising organolithium reagents in particular for a variety of processes, including most notably the synthesis of pharmaceutical compounds. Professor Collum (Cornell University, USA), a world authority in the kinetics of organolithium compounds (a particularly challenging topic intellectually), recently acknowledged the scope of such reagents by intimating that “well over 95% of natural products syntheses rely upon lithium-based reagents in one form or another.”<sup>[3]</sup> Due to significant ionic character, organolithium reagents in particular though have a tendency to aggregate, leading to a range of possible oligomers both in the solution state (the most important as that is where they are utilised) and in the solid state. It is of course extremely beneficial to know the structure of reagents that are employed in reactions, especially if those reactions are shape selective in nature. Contributing to this theme, Chapter 2 reveals a new oligomer of the commonly used organolithium reagent LiTMP in the cyclotrimer (LiTMP)<sub>3</sub>. LiTMP was first characterised in 1983, so to find a new polymorph of it after such a long time lag begs the question, how many other important organoalkali metal reagents have hidden polymorphic forms?

While monometallic reagents have been successfully utilised for many years, the disadvantages and limitations associated with them have allowed the field of bimetallic chemistry to flourish, with many renowned research groups around the world now taking to studying and designing new bimetallic reagents, most

commonly in metallation chemistry. Such multicomponent systems, that combine an alkali metal with a softer less electropositive metal within a charge-balancing ligand set, frequently offer improved reactivity over their monometallic counterparts and in some cases are capable of producing novel regioselectivities. The increasing demand for such bimetallic reagents is reflected in their recent commercial availability from major chemical suppliers such as Sigma-Aldrich; from which the turbo-Grignard reagent  $t\text{-PrMgCl}\cdot\text{LiCl}$  can be purchased by the bottle. However, to gain a full understanding of the synergy at work in these bimetallic systems requires detailed knowledge of both their structures in solution and their reaction mechanisms. As outlined in Chapter 3, the solution composition and reaction mechanism of two of the main aluminium based “ate” systems were therefore studied and surprisingly revealed that their metallating actions were two-step processes whereby the reactions were not direct aluminations as previously thought but actually lithiation – trans-metal-trapping reactions. This knowledge can then aid reagent design and optimisation of reaction yields. Moreover, with judicious choice of metal-ligand partnerships, this new concept of trans-metal-trapping promises to greatly expand in the future.

An intriguing feature of these second generation reagents is the prospect of performing polymetallations, enabling substrates to be subsequently selectively functionalised in several positions. Studies have already shown that certain bimetallic systems can execute such polymetallation reactions, for example with ferrocene, yielding up to tetra-metallated products.<sup>[4]</sup> Interestingly, novel regioselectivities can also be achieved during such polymetallations, with recent examples being the *ortho-meta'* and *meta-meta'* orientated deprotonations of aromatic substrates, in which metallation of the *ortho* site is usually the only option.<sup>[5]</sup> Adding to this literature, Chapter 5 discloses two further bimetallic reagents that are capable of performing multi-deprotonations of ferrocene. Most intriguingly, there is also suggestion of a tetra-zincated ferrocene compound, which would be the first example of a zinc reagent having cleaved four C-H bonds in the one reaction to generate the tetra-zincated product.



Currently, a major area of activity is small molecule activation which makes a significant impact in many sectors, including medicine and catalysis.<sup>[6]</sup> Bimetallic systems containing multiple Lewis-acidic and Lewis-basic sites are capable of performing 'cleave and capture' chemistry where the cleavage of a bond within a substrate, including especially relatively strong and inert C-H bonds, is followed by the capture of the resultant anion within the bimetallic framework. As discussed in Chapter 4, the small NMe<sub>2</sub> fragment cleaved from the parent amine could successfully be captured within a range of bimetallic systems. This cleave and capture ability could therefore have the potential for the capture and subsequent release of small molecules, catapulting bimetallic systems into the field of small molecule activation.

The future of bimetallic and multimetallic chemistry in general therefore looks extremely prosperous.

## 6.2 Bibliography

- [1] The Nobel Prize in Chemistry was awarded to Yves Chauvin, Robert H. Grubbs and Richard R. Schrock in 2005, [http://www.nobelprize.org/nobel\\_prizes/chemistry/laureates/2005/](http://www.nobelprize.org/nobel_prizes/chemistry/laureates/2005/), accessed September 2015.
- [2] The Nobel Prize in Chemistry was awarded to Richard F. Heck, Ei-ichi Negishi and Akira Suzuki in 2010, [http://www.nobelprize.org/nobel\\_prizes/chemistry/laureates/2010/](http://www.nobelprize.org/nobel_prizes/chemistry/laureates/2010/), accessed September 2015.
- [3] D. B. Collum, *Acc. Chem. Res.* **1993**, *26*, 227-234.
- [4] W. Clegg, K. W. Henderson, A. R. Kennedy, R. E. Mulvey, C. T. O'Hara, R. B. Rowlings, D. M. Tooke, *Angew. Chem. Int. Ed.* **2001**, *40*, 3902-3905.
- [5] A. J. Martinez-Martinez, A. R. Kennedy, R. E. Mulvey, C. T. O'Hara, *Science* **2014**, *346*, 834-837.
- [6] W. Macyk, A. A. Franke, G. Y. Stochel, *Coord. Chem. Rev.* **2005**, *249*, 2437-2457.

## **Chapter 7**

### **General Experimental Techniques**

## 7.1 Schlenk Techniques

Inert atmosphere techniques were used routinely throughout this project. This is because nearly all of the metal-based reagents and products handled within this project are air- and moisture- sensitive. Some of these compounds are even pyrophoric such as the branched alkyl reagent *tert*-butyllithium. Consequently, the use of standard Schlenk techniques was mandatory for all practical work (including analytical preparations), allowing for reactions and manipulations to be carried out under a dry, inert atmosphere. A Schlenk line (Figure 7.1) possessing two independent pathways – one connected to a high vacuum pump and the other connected to a supply of dry, oxygen-free argon gas – was utilised on the bench. The line incorporates five separate ports allowing for Schlenk apparatus (most commonly a Schlenk tube) to be connected. Each port contains a double tap (coated with high vacuum grease to ensure an effective seal) which permits the application of either vacuum or argon gas to the apparatus.



Figure 7.1. A typical laboratory Schlenk line in use.

As a prelude to starting reactions it is necessary to evacuate the apparatus, then refill it with argon to ensure an air-free environment (note that s-block organometallic compounds are thermodynamically unstable with respect to dioxygen). Standard practice is to repeat this process in triplicate. To try and prevent air from entering the system and causing compound degradation, a positive pressure of argon is always maintained while adding solvents and reagents to the apparatus. However, this constant supply of gas requires Dreschel bottles to be directly connected to the line preventing any pressure build-up within the system. Finally, gaseous products and solvent vapours are prevented from entering and potentially damaging the vacuum pump by way of a condensing solvent trap, cooled to  $-196^{\circ}\text{C}$  by a liquid nitrogen jacket.

## 7.2 Glove Box

All solid reagents and products have to be stored and handled under an inert atmosphere; thus this necessitated the employment of an argon-filled glove box with a gas recirculation and purification system (Figure 7.2).

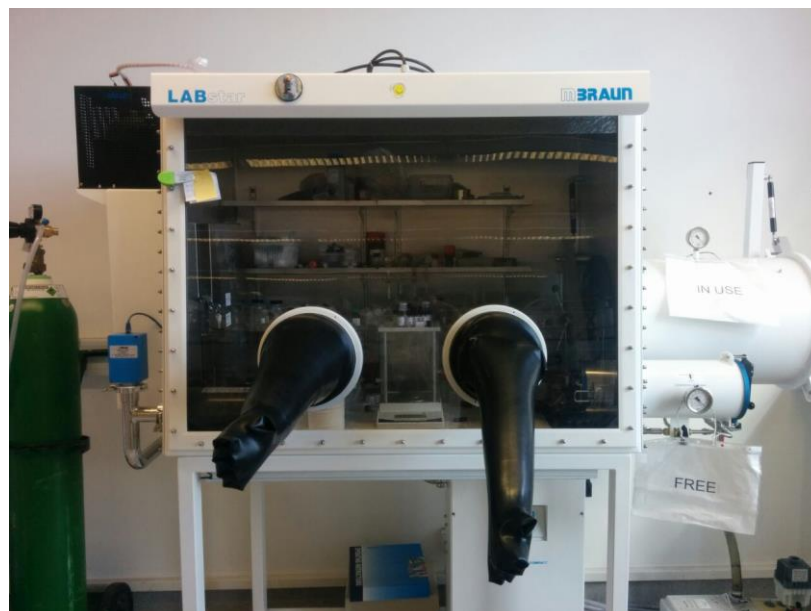


Figure 7.2. A typical research glove box fitted with an argon gas cylinder.

Purchased commercially from MBraun, the glove box is a sealed argon-filled environment connected to both a dry argon gas supply and high vacuum pump, akin to the set-up in the aforementioned Schlenk line. The box contains a large transparent viewing window making the contents visible to users, who wear the attached pair of neoprene gloves, which facilitate manipulation inside the box without contaminating the dry atmosphere. Materials and chemicals can be entered into or removed from the box via a chamber attached to the outside. The chamber has a door on the outside allowing materials to be placed inside and once this door is sealed the chamber can then be independently evacuated and refilled with argon gas to expel the air present. Following repetition of this process three times (to ensure as much as possible that no or only negligible quantities of air and moisture are present), the inside door of the chamber can then be opened from within the glove box allowing the materials to be transferred inside. The recirculating atmosphere within the box is constantly cleaned over a “scrubber”, which removes any traces of air or water contamination that may be present, with the box also being regenerated as required to ensure the levels of air and water remain low.

### 7.3 Solvent Purification

As a consequence of the highly sensitive nature of the metal reactants and products to air and moisture, all solvents used within this project (commonly hexane, THF, toluene and diethyl ether) had to be dried thoroughly and degassed prior to use to ensure as far as possible that no water or oxygen was introduced inadvertently into reaction solutions. Hence, the solvents were distilled under a stream of nitrogen and in the presence of sodium metal and benzophenone.<sup>[1]</sup> This mixture was used as it acts as a highly effective self-indicator for the presence of oxygen and water. The elemental sodium reacts with the benzophenone to produce a ketyl radical that has an intensely deep blue colour, hence the solvent itself appears deep blue in colour. This ketyl species is extremely reactive towards both oxygen and water and in the

presence of either, the radical loses its deep blue colour producing yellow or colourless products instead, that is the blue colour fades away from the solution. Hence, providing a straightforward method of ensuring the solvents are dry at all times using just the naked eye. Subsequently the distilled solvents were collected into a nitrogen-filled sealed flask fitted with a Subaseal® to keep them dry by protecting them from the atmosphere. A glass syringe and needle, which had been previously flushed out with argon, was then used to transfer the dried solvent to the relevant reaction vessel.

## 7.4 NMR Solvent Purification

Specialist deuterated solvents utilised for NMR spectroscopic purposes (such as  $d_6$ -benzene,  $d_{12}$ -cyclohexane and  $d_8$ -THF) were similarly dried and degassed prior to use. Molecular sieves (4 Å) were activated using microwave radiation and added to an ampoule fitted with a J Young valve. The solvent was subsequently introduced to the argon filled ampoule and then degassed using the common freeze-vacuum-thaw method.<sup>[1]</sup> Liquid nitrogen was used for freezing purposes and the whole degassing process was performed in triplicate.

## 7.5 Purification of Hygroscopic Liquids

Some of the reagents used in this project (for example, the starting amines such as TMEDA and DMPEA) are hygroscopic, which meant they had to be dried prior to employment in a reaction. Liquid reagents were first distilled in the presence of a desiccant ( $\text{CaH}_2$ ) for several hours and then stored over activated 4 Å molecular sieves in a flask fitted with a Subaseal®.

## 7.6 Commercial Reagents Used

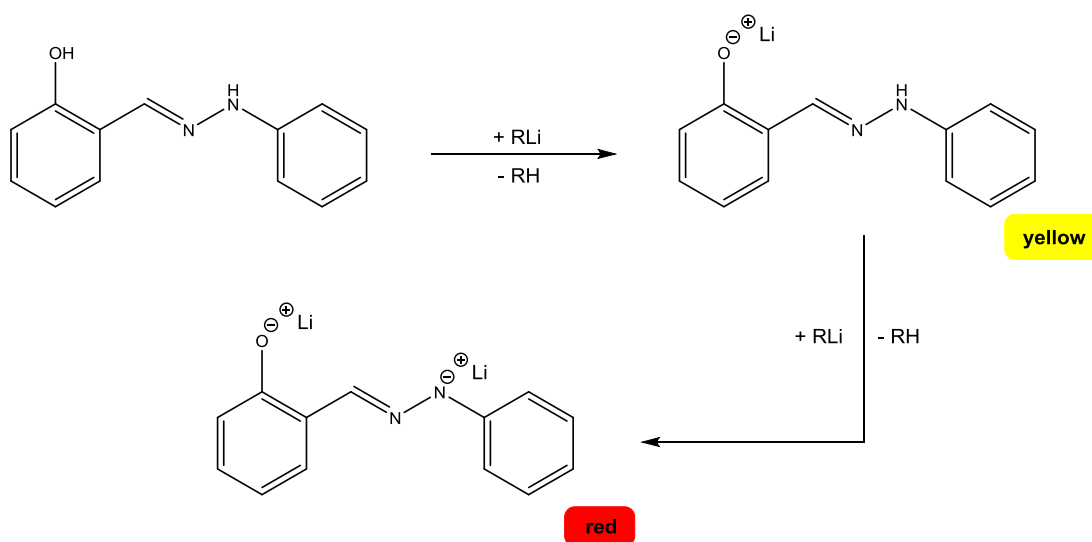
Most of the reagents used in this project were purchased from Sigma-Aldrich. Exceptions were NaO<sup>t</sup>Bu and TMEDA supplied by Alfa Aesar while the bulky amine TMP(H) was supplied by Acros Organics.

## 7.7 Standardisation of Organolithium Reagents

Though they are supplied with molarities, commercial alkyllithium reagents, such as <sup>n</sup>BuLi and <sup>t</sup>BuLi, which are sold in hexane and pentane solutions respectively, had to be standardised before their use in reactions. The reason for this standardisation is that the concentration of these reagents can vary quite substantially over time due to evaporation of the solvent and/or unintentional reaction with air. It is therefore common practice for these chemicals to be standardised in order to confirm the molarity of the solution and to ensure exact correct stoichiometries are employed in reactions as organometallic reactions, especially of lithium examples, are highly sensitive to stoichiometry.

This standardisation procedure outlined below was performed using salicylaldehyde phenylhydrazone as a visual indicator:<sup>[2]</sup> a yellow solution containing 0.6 g of the indicator dissolved in 10 mL of THF was titrated against the organolithium reagent in question until the solution colour changed to a persistent red. On reaction with one equivalent of the organolithium reagent, the indicator becomes a yellow monoanion. However a dianion is generated on the addition of one more equivalent of the organolithium reagent, which accounts for the red colour (Scheme 7.1).





Scheme 7.1. Standardisation reaction sequence for alkyllithium reagents using salicylaldehyde phenylhydrazone as the indicator.

The molarity of the organolithium reagent was then calculated based on the volume of alkyllithium reagent required during the titration using the formula shown in equation 6.1.

$$\text{Molarity of RLi} = (X/Y) \times 1000 \quad (6.1)$$

[Where X = number of moles of salicylaldehyde phenylhydrazone used and Y = volume of RLi (mL) necessary to produce a persistent red colour.]

## 7.8 Preparation of Common Starting Materials

### 7.8.1 Preparation and Isolation of <sup>n</sup>BuNa<sup>[3]</sup>

*n*-Butylsodium, <sup>n</sup>BuNa was synthesised by the metathesis reaction between NaO<sup>t</sup>Bu and <sup>n</sup>BuLi. Firstly, NaO<sup>t</sup>Bu (3.84 g, 40 mmol) was weighed into a Schlenk tube inside the glove box before being transferred to the bench where dried hexane (50 mL) was introduced. The resultant suspension was cooled to 0°C by surrounding the Schlenk tube with an ice bath at which point <sup>n</sup>BuLi (25 mL, 1.6

M, 40 mmol) was slowly added via syringe, inducing the precipitation of a white solid. The ice bath was then removed and the suspension left to stir overnight on the bench. The following day the white solid was collected by filtration and washed with dry hexane in 3 x 20 mL aliquots. Next the washed solid was dried *in vacuo* for one hour prior to isolation inside the glove box, where it was stored until required (typical yield: 2.4 g, 75%). Caution: it should be noted that <sup>n</sup>BuNa is wickedly pyrophoric.

### 7.8.2 Preparation and Isolation of <sup>t</sup>Bu<sub>2</sub>Zn<sup>[4]</sup>

Solid zinc chloride, ZnCl<sub>2</sub> (5.45 g, 40 mmol), dried *in vacuo* beforehand, was weighed into a Schlenk flask in the glove box before being transferred to the bench and dissolved in dried diethyl ether (80 mL). This solution was cooled to 0°C in an ice bath and two molar equivalents of <sup>t</sup>BuLi (48 mL, 1.7 M, 80 mmol) was slowly introduced via syringe to produce a white suspension. Following removal of the ice bath, the flask was covered with a protective black plastic sheet to shield the light-sensitive alkylzinc compound from the light. The solution was allowed to stir for 2-3 hours before being filtered over Celite and glass wool to remove the solid lithium chloride by-product. Solvent was subsequently removed from the filtrate *in vacuo* until approximately only 10 mL remained. The colourless solution was then transferred to the (previously flushed) sublimation apparatus *via* cannula where the remaining solvent was removed under vacuum. Following complete removal of the solvent, chilled *iso*-propanol was introduced to the cold finger and the temperature kept constant in the range -20°C to -30°C throughout the sublimation process. Once the sublimation was complete the apparatus was transferred to the glove box where the purified <sup>t</sup>Bu<sub>2</sub>Zn was isolated, weighed and transferred into a clean, dry Schlenk flask (typical yield: 5.0 g, 69%). The flask was removed from the glove box and the <sup>t</sup>Bu<sub>2</sub>Zn was dissolved in a solvent (commonly hexane was employed) and stored in the freezer at -30°C until needed for a reaction. Caution: it should be noted that <sup>t</sup>Bu<sub>2</sub>Zn is also pyrophoric.

## 7.9 Instrumentation for Compound Characterisation

### 7.9.1 Nuclear Magnetic Resonance (NMR) Spectroscopy

All  $^1\text{H}$  NMR spectra were recorded on a Brüker AV3, AV400 or DRX 500 spectrometer operating at 400.03, 400.13 or 500.13 MHz. For recording proton decoupled  $^{13}\text{C}$  NMR spectra, the same three instruments were used but at operating frequencies of 100.62, 100.60 and 125.77 MHz respectively. All chemical shifts are quoted relative to tetramethylsilane at 0.00 ppm. Finally,  $^7\text{Li}$  spectra were recorded at 155.50 MHz and referenced against LiCl in  $\text{D}_2\text{O}$  at 0.00 ppm, while  $^{27}\text{Al}$  spectra were recorded at 104.25 MHz and referenced against  $\text{AlCl}_3$  in  $\text{D}_2\text{O}$  at 0.00 ppm. Correlations between H atoms and C atoms were obtained through COSY (correlation spectroscopy) and HSQC (heteronuclear single quantum correlation)<sup>[5]</sup> NMR spectroscopic methods. NMR abbreviations are as follows: s – singlet; d – doublet; t – triplet; q – quartet; m – multiplet and br – broad resonance.

The Diffusion-Ordered Spectroscopy (DOSY) NMR experiments were performed on a Brüker AV400 NMR spectrometer operating at 400.13 MHz for proton resonance under TopSpin (version 2.0, Brüker Biospin, Karlsruhe). DOSY plots were generated by use of the DOSY processing module of TopSpin with parameters optimised empirically to find the best quality data for presentation purposes.

### 7.9.2 Elemental Microanalysis

Elemental (C, H, N) analysis was performed on a Perkin Elmer 2400 elemental analyser and used to obtain percentage values of the elemental composition of some of the new compounds synthesised during the course of this project. Samples for microanalysis were made up in the aforementioned argon-filled glove box and sealed in an air-tight box to avoid decomposition during transportation. It should be stressed that due to the extreme air- and moisture-

sensitivity of the synthesised compounds it was not always possible to obtain reliable microanalysis results despite several attempts.

## 7.10 X-Ray Crystallographic Studies

Single crystal X-ray diffraction data were recorded on either an Oxford Diffraction Xcalibur E or Oxford Diffraction Gemini S diffractometer using graphite-monochromatic MoK $\alpha$  or CuK $\alpha$  radiation ( $\lambda = 0.71073$  and  $1.54180$  Å respectively). The structures were solved by direct methods (SHELX-97) and refined on all unique  $F^2$  values (SHELX).<sup>[6]</sup>

## 7.11 Bibliography

- [1] D. F. Shriver, M. A. Drezdson, *The Manipulation of Air-Sensitive Compounds*, 2nd ed., Wiley, New York, **1986**.
- [2] B. E. Love, E. G. Jones, *J. Org. Chem.* **1999**, *64*, 3755-3756.
- [3] C. Schade, W. Bauer, P. V. Schleyer, *J. Organomet. Chem.* **1985**, *295*, C25-C28.
- [4] P. C. Andrikopoulos, D. R. Armstrong, H. R. L. Barley, W. Clegg, S. H. Dale, E. Hevia, G. W. Honeyman, A. R. Kennedy, R. E. Mulvey, *J. Am. Chem. Soc.* **2005**, *127*, 6184-6185.
- [5] D. Williams, I. Fleming, *Spectroscopic Methods in Organic Chemistry*, 6th ed., McGraw-Hill, London, **2008**.
- [6] G. M. Sheldrick, *Acta Crystallogr. Sect. A* **2007**, *64*, 112-122.